Projection of urban settlement in eco-sensitive areas and its impact on watershed hydrology

Thesis
submitted in partial fulfilment of the requirements
of the degree of

DOCTOR OF PHILOSOPHY

by

Sagarika Patowary

Department of Civil Engineering
Indian Institute of Technology Guwahati
Assam-781039, India

July 2018

Dedicated to My Family

Prof. A. K. Sarma
B.P.Chaliha Chair Professor
For Water Resources

Indian Institute of Technology Guwahati,
Guwahati-781039

Phones: 0361- 2582409 (O)
0361- 2584449 (O)
0361- 2584409 (R)
09435732225 (M)
Fax: 0361- 2582440
E-mail: aks@iitg.ernet.in

DEPARTMENT OF CIVIL ENGINEERING

CERTIFICATE

This is to certify that the thesis entitled "**Projection of urban settlement in eco-sensitive areas and its impact on watershed hydrology**" submitted by Ms. Sagarika Patowary (Roll Number 146104016) to the Indian Institute of Technology Guwahati, for the award of the degree of Doctor of Philosophy in Civil Engineering is a record of bonafide research work carried out under my supervision and guidance. The results contained in this thesis have not been submitted in part or full to any other University or Institute for award of any degree or diploma.

IT Guwahati
17 July 2018

(Arup Kumar Sarma)
Department of Civil Engineering
Indian Institute of Technology Guwahati
Guwahati-781039

STATEMENT

I, Sagarika Patowary, declare that the work in the thesis entitled "**Projection of urban settlement in eco-sensitive areas and its impact on watershed hydrology**" has been carried out by me under the supervision of Prof. Arup Kumar Sarma of Civil Engineering Department, Indian Institute of Technology Guwahati. This work has not been submitted elsewhere for the award of any degree. All the assistance received in preparing this thesis and sources have been acknowledged.

IIT Guwahati
17 July 2018

(Sagarika Patowary)
(Roll No: 146104016)
Research Scholar
Department of Civil Engineering
Indian Institute of Technology Guwahati
Guwahati-781039

ACKNOWLEDGEMENTS

I would like to express my deep feeling of appreciation to my thesis supervisors Dr. Arup Kumar Sarma, Professor, Department of Civil Engineering, IIT Guwahati for his stimulation, invaluable guidance and constant support during this work. I am intensely indebted to him for his technical and moral encouragement during the difficult times. I also admire his patient explanation of the concepts and basic principles. I consider it as a great opportunity to work under him and to learn from his research skill.

I am earnestly obliged to the chairman of my Doctoral Committee, Prof. Subashisa Dutta, Professor, Civil Engineering Department, IIT Guwahati, for his useful suggestions and timely help during the entire period of this research work. I am also appreciative to the members of the Doctoral Committee Dr. Sreeja P., Associate Professor, Civil Engineering Department, IIT Guwahati, and Dr. Bimlesh Kumar, Associate Professor, Civil Engineering Department, IIT Guwahati, for every valuable suggestion and encouragement at different phases of the research work.

I would like to acknowledge all the Faculty members of Water Resources Engineering and Management, IIT Guwahati for their keen interest and suggestions. I express my sincere thanks to the staff members of the Civil Engineering Department, IIT Guwahati.

I would like to extend my gratefulness to the authorities of different government offices in Guwahati like GMDA, ASTEC, GMC, RMC, Soil Conservation Department for their kind help and support during the data collection phase of this thesis work. Also, I would like to express my gratitude to Mr. P. K. Sarma for his assistance in the data collection period of this work.

Thanks are also due to Jayshree Hazarika, Bandita Barman, Tapash Ranjan Das, Suman Kumar Padhee, Laveti NV Satish, Juna Devi, Raktim Choudhury, Jimmy Khaklari, Dipima Sarma and all my friends and well wishers who at the various stages of this work have generously extended their support for completion of this work. My special thanks go to Dr. Banasri Sarma for her invaluable suggestions at different phases of the research work.

Most importantly, I would also like to offer my love, high regard and respect for my parents and other family members for showering their blessing and helping me to reach where I am. I would also like to thank my husband, Bhaskar for his constant support and co-operation during this research work.

Lastly, I thank God whose blessing has made this research work possible.

Sagarika Patowary

Abstract

Urbanization is an inevitable component of economic growth. However, hasty and unplanned expansion of an urban area into its eco-sensitive areas like hills, wetlands, and forests is a key concern, mainly in developing countries. By understanding the process and causes of such unplanned urban expansion, the urban settlement projection in those areas is of paramount importance for framing sustainable urban development policies. This study presents a modelling concept named as the model for Assessment of Settlements in Eco-sensitive Area (ASEA) that relates urban settlement in such eco-sensitive areas with potential socio-economic, demographic and geographical factors. The model is applied to an Indian city Guwahati, which is experiencing serious environmental degradation due to unplanned urban settlement in its eco-sensitive hilly areas. Projection of urban settlement in hills of Guwahati city has been performed by using this model deriving the input model parameters concerning the master plan of the city. Urban flash flood and the blockage of drainage system by sediment brought down from the inhabited hills of Guwahati city are two major urban related concerns of today's Guwahati city. The projected Landuse Land Cover (LULC) map of the hills of Guwahati city has been utilized in watershed-hydrological impact analysis of the projected urban settlement increment. Estimates of future peak runoff generation from the hilly watershed indicate that urban flash flood problem is going to be worsened in future in Guwahati city. Apart from this, the present study emphasizes the need for consideration of soil loss from the steep hill cuts associated with urban settlement in a hilly area through the introduction of a new factor called "Hill Cut Factor". Because, in ortho-rectified images, instead of the actual area only the projected area of these steep hill cuts is visible, which leads to underestimation of soil loss from an urban hilly watershed. In comparison to the peak runoff, the soil loss from hilly watersheds of Guwahati city was found more sensitive to urban settlement increment. This type of the future scenarios of landscape and hydrology developed by using future socio-economic and, demographic conditions derived from the master plan of a city provides an opportunity to reexamine the master plan. Finally, to bring the peak runoff and sediment loss from hilly watersheds within a permissible limit, the optimal allocation of ecological management practices has been suggested with the fulfilment of their suitability and applicability criteria at a minimum possible cost.

Keywords: Eco-sensitive area, urban settlement, watershed hydrology, future projection, peak runoff, sediment loss, optimal ecological management practices.

Table of Contents

List of Figures

Figure number and caption **Page No.**

List of Tables

List of Notation

A = Area of watershed.

A_0 = Areas with no likelihood of having urban settlement.

A_c = Impervious area in the watershed (m^2).

A_{ch} = Impervious area (actual) in the hilly area of the watershed (m^2).

A_{cp} = Impervious area in the plain area of the watershed (m^2).

A_f = Free space availability in area of influence (AOI).

A_{huc} = Settlement area having no imperviousness in the hilly area of the watershed (m^2).

A_i = AOI of eco-sensitive area.

a_i = Percent of total steep hill cut area covered by the i^{th} type of surface cover.

A_{Lm} = Area of m type of natural land covers in the watershed (m^2).

A_{LSHl} = Area of l^{th} type of existing surface covers of the steep hill cuts associated with urban settlements in the hilly area of the watershed (m^2).

A_n = Net AOI where urban settlement is possible.

A_{puc} = Settlement area having no imperviousness.

A_{shuc} = Area of bare steep hill cuts associated with urban settlements in the hilly area of the watershed (m^2).

A_{us} = Urban settlement area in AOI.

C_{add} = Cover management factor for hill cut area not visible in satellite image.

C_c = Cover management factor for impervious area.

C_{EHj} = Cover management factor for j^{th} type of EMPs applied in the settlement area of the hilly portion of the watershed.

C_{Epi} = Cover management factor for i^{th} type of EMPs applied in the plain area of the watershed.

C_{ESHk} = Cover management factor for k^{th} type of EMPs applied to the bare steep hill cuts associated with urban settlements in the hilly area of the watershed.

C_g = Cover management factor for urban settlement located in plain areas.

C_{hu} = Cover management factor for urban settlement in hill.

C_{Lm} = Cover management factor for m type of natural land cover in the watershed.

C_{LSHl} = Cover management factor for l^{th} type of existing surface covers of the steep hill cuts associated with urban settlements in the hilly area of the watershed.

C_u = Cover management factor for visible urban settlement area of hills in the satellite image.

C_u = Commercial unit density in AOI.

Cu_c = Cover management factor for settlement area not having imperviousness.

D = Equivalent diameter of a circular basin having area equal to A.

E = Total storm kinetic energy in MJ/ha.

e_r = Rainfall energy per unit depth of rainfall per unit area for the rth increment of divisions of the storm hydrograph (MJ $ha^{-1}mm^{-1}$).

E_{us} = Amount of urban settlement in the eco-sensitive area.

F = Favouring index.

F_P = Pond and swamp adjustment factor.

G_1 = Average slope of hill.

G_2 = Average elevation of hill.

G_i = i^{th} type of Geographical condition of an eco-sensitive area.

h = Vertical projection of steep hill cut.

I_{30} = Maximum 30 minutes rainfall intensity.

H_f = Hill cut factor

i_r = Rainfall intensity for r^{th} increment of divisions of the storm hydrograph.

K = Conveyance factor.

K = Soil erodibility factor (t h MJ^{-1} mm^{-1}).

L = Slope length factor.

L_c = Length of the longest flow channel.

L_v = Land value in AOI.

m = Horizontal projection of steep hill cut.

P = Support and conservation practices factor.

P_{24} = Daily rainfall (mm).

p_c = Maximum allowable percent coverage of a plot of land.

P_t = Rainfall depth at t-hr duration (mm).

Q_d = Runoff depth (in)

Q_{max} = Maximum peak runoff allowed from the watershed (m^3/s).

Q_{min} = Minimum peak runoff required from the watershed (m^3/s).

q_u = Unit peak discharge (csm/in).

R = Rainfall-runoff erosivity factor (MJ mm ha^{-1} $h^{-1}year^{-1}$).

R^2 = Nash–Sutcliffe efficiency.

R_{Cc} = Runoff co-efficient for m type of natural land cover in the watershed.

R_{Cc} = Runoff co-efficient for impervious area.

R_{CEHj} = Runoff co-efficient for j^{th} type of EMPs applied in the settlement area of the hilly portion of the watershed.

R_{CEPi} = Runoff co-efficient for i^{th} type of EMPs applied in the plain area of the watershed.

R_{Cuc} = Runoff co-efficient for settlement area having no imperviousness.

S = Slope steepness factor.

S = Slope of the flow path.

S_c = Slope of the longest flow channel.

t = Duration of rainfall (hr).

T_c = Time of concentration of watershed.

T_{fi} = Time of flow through the channel (min) from outlet of i^{th} sub-watershed to final outlet of the watershed (min).

T_{ti} = Total time to reach discharge from the most remote point of i^{th} sub-watershed to final outlet of the watershed (min).

U_{sh} = Urban settlement area in the hilly area derived from satellite image (m^2).

U_{sp} = Urban settlement in plain area of the watershed (m^2).

U_{sw} = Urban settlement in the watershed (m^2).

W_i =Weight applied to the i^{th} component of 'F'.

β = Average hill cut angle.

Δt_r = Duration of r^{th} increment in h (hour).

ΔV_r = Depth of rain falling in the r^{th} increment.

θ = Average slope of hill.

Abbreviation

ANN	Artificial Neural Networks
AOI	Area of Influence
ARSAC	Assam Remote Sensing Application Centre
ASEA	Assessment of Settlements in Eco-sensitive Area
CART	Categorical Regression Tree
CCL	Connecticut's Changing Landscape
DCIA	Directly Connected Imperious Area
DCP	Data Collection Platform
DEM	Digital Elevation Model
DLS	Dynamic Landuse System
DORS	Distributed Object-oriented Rainfall and runoff Simulation
DWS	Disaster Warning System
EIA	Effective Impervious Area
EMP	Ecological Management Practices
ERDAS	Earth Resources Data Analysis System
ESA	Eco-sensitive area
ETIS	Estimation Tool for Impervious Surfaces
FCC	False Colour Composite
GIS	Geographical Information System
GMA	Guwahati Metropolitan Area
GMCA	Guwahati Municipal Corporation Area
GMDA	Guwahati Metropolitan Development Authority
GPS	Global Positioning System
GUFIM	GIS-based urban flood inundation model

HSPF	Hydrologic Simulation Program Fortran
IDF	Intensity-Duration-Frequency
IFMOP	Inexact-Fuzzy Multi-Objective Linear Programming
IGAS	Integrated GIS-based Analysis System
ILWIS	Integrated Land and Water Information System
IMD	Indian Meteorological Department
ISAT	Impervious Surface Analysis Tool
LULC	Land Use Land Cover
LISS	Linear Imaging Self Scanning Sensor
MDS	Multiple Data Source
MMF	Morgan–Morgan–Finney
MSL	Mean Sea Level
MUSLE	Modified Universal Soil Loss Equation
NDVI	Normalized Difference Vegetation Index
NDWI	Normalized Difference Water Index
NLCD	National Land Cover Data
NSE	Nash–Sutcliffe efficiency
OPTEMP-CSMO	OPTimal EMP model considering Carbon Sequestration with Multi-Objective optimization
OPTEMP-LS	Optimal EMP model with Linear programming for Single ownership
RDBMS	Relational Database Management System
RMC	Regional Meteorological Centre
RMSE	Root Mean Square Error
RS	Remote Sensing
RUSLE	Revised Universal Soil Loss Equation
RWH	Rainwater Harvesting System

SCSCN	Soil Conservation Service curve number
SERGoM	Spatially Explicit Regional Growth Model
SOI	Survey of India
SRES	Special Report on Emission Scenario
SRTM	Shuttle Radar Topography Mission
TIA	Total Impervious Area
TSS	Total Suspended Solids
USLE	Universal Soil Loss Equation
VFS	Vegetative Filter Strips
WaSSI	Water Supply Stress Index

Chapter-1

Introduction

1.1 General

According to Lu et al. (2017) the process of urbanization or urban transition can be defined as "A shift in a population from one that is dispersed across small rural settlements in which agriculture is the dominant economic activity towards one where the population is concentrated in larger, dense urban settlements characterised by industrial and service activities." Urbanization is growing at a very disquieting rate across the world. Sustainable urban development focuses on strategies to maintain the desirable balance between social, economic and ecological systems. The rapid unplanned urbanization, witnessed in the recent time, particularly in developing countries, raises concerns regarding sustainable development (Brockerhoff 2000). For the first time in 2007, world's urban population went above the world's rural population. In 2014, almost 54% of the total population was urban whereas in 1950 it was only 30% (UNDESA/ PD 2014). In 2010, against 46 and 78% of urbanization in developing and developed countries, respectively, urban population in developing countries was 2.6 billion, whereas in developed it was only 96 million (UNDESA/ PD 2012; Cobbinah et al. 2015). This indicated inferior economic growth in comparison with urban population growth in developing countries (United Nations 2013b). Only three countries- India, China and Nigeria are projected to contribute 37% of the total growth of world's urban population within the period from 2014 to 2050. According to the census (2011), India is the second highest populated country and 31.16% of its total population is in urban area. The total number of metropolitan cities (population 1 million and above) in India has increased from 23 in 1991 to 35 in 2001 and on to 53 by 2011. Number of towns increased from 2657 in 1961 to 7935 in 2011 in India. Rural to urban migration is the main reason for this high growth of urban population in developing countries (United Nations 2001). This increase in urbanization is constantly contributing to increasing housing density, conversion of wetland, forest etc. to residential area or commercial area, increase of highways, roads, parking lots etc. due to which, the amount of impervious surface is increasing day by day (Arnold and Gibbons 1996; Shuster et al. 2005). This significantly increases the amount and velocity of runoff entering natural streams or rivers (Ng and Marsalek 1989; Kang et al. 1998; Bird et al. 2002). Thus it intensifies the urban flash flood problem. At the same time, water absorbing capacity of the landscape decreases which ultimately leads to a decrease in base flow (Klein 1979; Kauffman et al. 2009; Barron et al. 2013). Groundwater table itself is not only a source of water but also the supporting system for surface water (natural streams, rivers etc.) to maintain a minimum flow during the dry period. Again, increase in imperviousness also affects the water quality by transporting the accumulated pollutants more easily to local waterways (EPA 2004). Similarly, under the impact of high-intensity rainfall as well as high runoff volume, surface erosion by water is being exacerbated due to the removal of natural vegetative covers resulting from urban settlements (Aswathy and Sindhu 2013). As a consequence of the sedimentation, the drainage capacity of flow channels decreases resulting in increase in frequency of urban flash flood hazard. This also increases the maintenance cost of the drainage system (Fernandez et al. 2003). In addition to the sediment deposition on river banks or into the reservoirs, some percent of sediments carried by rivers are transported to the sea. Fine sediments adversely affect water quality and the balance of aquatic ecosystem (Nelson and Booth 2002). All these points exclusively indicate that the future of the natural environment is mainly depending upon the way through which the urbanization prospect will be directed.

1.2 Motivation for the study

Apart from the various hydrological adverse effect of urban settlement as mentioned above, the scarcity of space required to settle the constantly increasing urban population is a serious challenge associated with urbanization. In most of the developing countries, the nature conservation and protection policies are only encouraged, but not followed strictly. Consequently, newly migrating people are encroaching eco-sensitive areas like hills, water bodies, wetlands or forests located within and near an urban area although these areas are incompatible for living compared to plain urban areas (Ichimura 2003; Amoako and Cobbinah 2011). ‘‘Eco-sensitive area’’ (ESA) may have variable meaning referring not only ecologically sensitive areas but also ecologically significant areas for their ecological, biological, cultural, economic and historical values (Gadgil et al. 2011). These areas are protected by government regulations. In this study, areas or regions such as hills, water bodies, wetlands or forests, located near or within an urban area, have been specified as ‘‘eco-sensitive area (ESA)’’, as they are very sensitive to mild disruption from outside and hence need to be conserved. Although urbanization is inevietable for nation's development, its rapid, unguided and unplanned growth is causing constant interruption and encroachment to urban greenery (Cobbinah and Darkwah 2016). Destruction of urban greenery may also create an additional stress on neighbouring location which can be even more ecologically sensitive (Ichimura 2003). Evidence of degradation of eco-sensitive areas due to human disruption is found all over the world including the most developed areas like Europe and USA (European Environment Agency 2002; McDonald et al. 2010). Just because of urban expansion, 50% of the wetland area in Dhaka city (Bangladesh) has reduced within a period of 1968–2001 (Sultana et al. 2009). Forests located within or outskirt of many African cities such as Lilongwe, Lagos, Nairobi, Kumasi, Addis Ababa have also been the victim of rapid urban growth (Darkwah and Cobbinah 2014). Similarly, wetland area in Bangalore city of India has reduced from 321 ha in 1973 to 87 ha in 2007 (Ramachandra and Mujumdar 2009). If this continues, the imbalance of ecosystem is guaranteed in near future and it accentuates the need for proper management plan to tackle the future situations that may arise due to increase in urban settlement in eco-sensitive areas. However, for better management purpose, the future projection is vital and it is quite challenging as well as uncertain since it is highly dependent on future policies implementation and also on the changing human attitude. In general, the management planning is done based on assumption that the same 'as usual' scene will prevail in future. Many studies have been performed focusing on the optimal land cover combination for controlling the adverse impacts of landscape degradation (Guldmann 1986; Gabriel et al. 2006; Sadeghi et al. 2009). These management practices will be more effective if those are applied taking into account of the future urban settlement in eco-sensitive areas. Such needs have motivated this research work to visualize the urban-induced future LULC and hydrological scenarios of the eco-sensitive area in a more detailed way.

1.3 Broad objectives of the study

1. To analyse the urban settlement process in the eco-sensitive areas of developing countries in view of its future expansion.
2. To evaluate the impact of the projected urban settlement scenario on the watershed hydrology.

3. To use the projected scenario of watershed hydrology for suggesting best possible watershed management plans.

1.4 Organization of the thesis

In addition to the basic introduction, motivation and the broad objectives of this research, a synoptic view of the organization of rest of the chapters of the thesis is also presented in Chapter-1. The overview of the study is presented in Fig. 1.1

Chapter-2 gives a systematic and detailed review of the previous works on the research area to have up-to-date knowledge on various themes relevant to this study. This is followed by a critical assessment of the literature stating the necessity for further research. Finally, the scope of present work has been stated clearly mentioning the goal of this research.

Chapter-3 introduces a general modelling concept for indirect assessment of urban settlement in eco-sensitive areas. To demonstrate the utility of the model, a case study has been performed. A thorough description of the study area and the data requirement for the model development has also been included in this chapter.

Chapter-4 presents the projection of urban settlement in the study area including the generation of various types of future data, required for projection. This is followed by the preparation of future Land Use Land Cover (LULC) maps of the study area.

In Chapter-5, the effect of increased urban settlement on peak runoff generation has been studied by using the future LULC maps. Consequently, watershed delineation and determination of the input parameters for runoff calculation have been performed in this chapter. Apart from this, runoff maps have also been prepared for the watersheds of the study area.

Chapter-6 essentially assesses and quantifies the impact of the urban settlement on sediment loss. In this chapter, an attempt is made to estimate the soil loss from the study area areas in a more appropriate way. Finally, soil loss vulnerability map showing the pixel-based value of the soil loss rate of the watersheds are presented.

In Chapter-7, an effort is made to manage the projected alterations in peak runoff and sediment yield as a consequence of increasing urban settlement in the study area. An optimization model has been used to select the optimal combination of ecological management practices with a minimum cost to bring the peak runoff and sediment runoff value within a desirable limit.

Finally, Chapter-8 gives a summary and conclusion of the research work performed. The limitation and future scope of the research have also been described here.

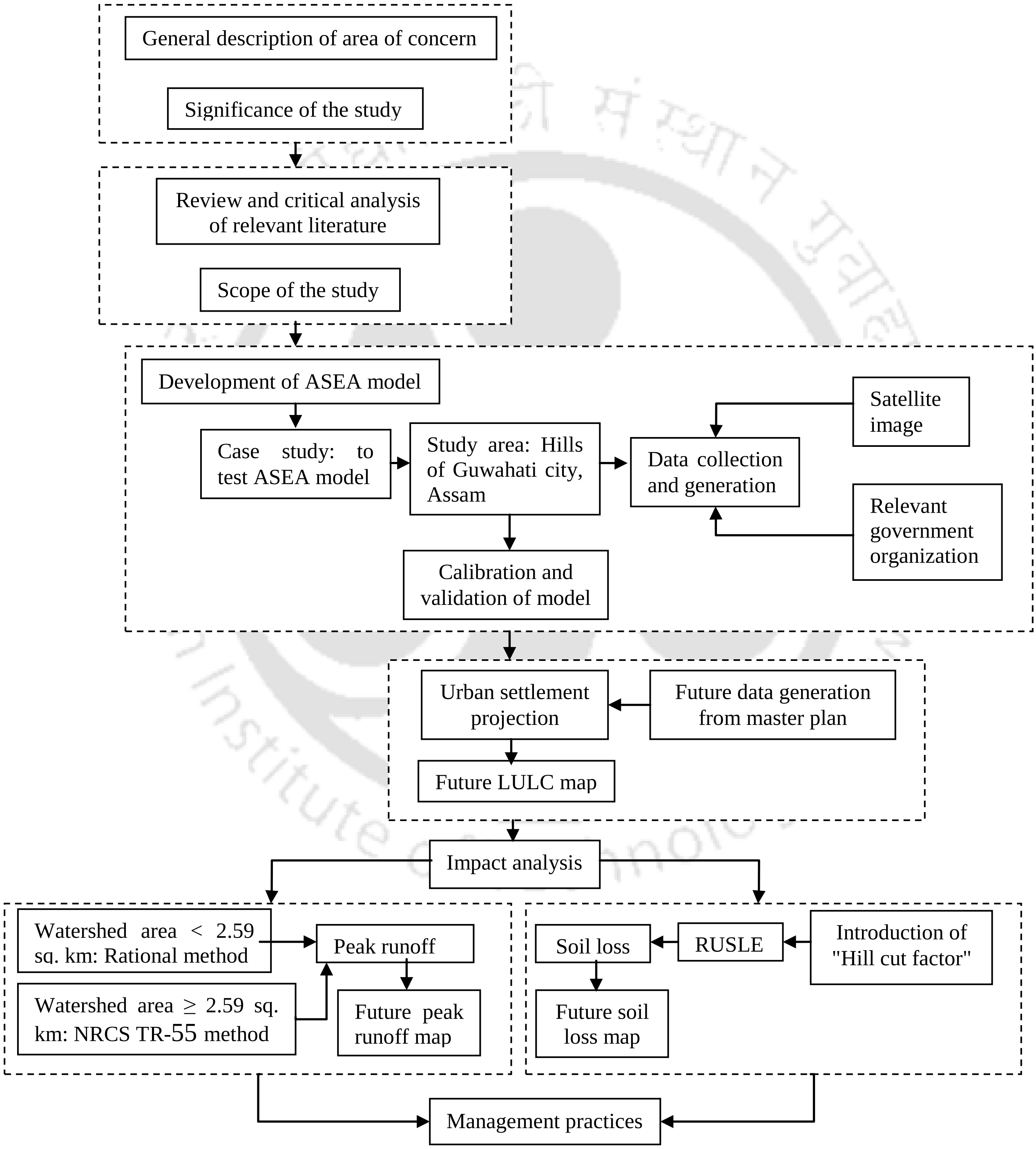

Fig. 1.1: Overview of the study

Chapter-2

Literature review

2.1 Introduction

Due to the relentlessly increasing adverse impacts of urban settlement on various aspects of watersheds such as hydrological, biological, physical, water quality, the urban settlement related studies are drawing continuous attention of researchers from different disciplines. The objective of this literature review is to give a critical summary of available research relevant to this study and those have been categorised as given below:

- Determination and projection of urban settlement/impervious area.
- Effect of urban settlement on hydrology.
- Sediment yield models and its application on impact analysis of land use land cover change on soil erosion.
- Management practices/techniques for controlling sediment and runoff
- Role of remote sensing (RS) and Geographical Information System (GIS) in the hydrological study.

Finally, a critique of the reviewed literature has been appraised to figure out their usefulness, strengths and research gaps.

2.2 Determination and projection of urban settlement/impervious area

There are numerous past and ongoing research ventures on determination and projection of urban settlement or impervious surfaces. A brief review of the previous works reported on it is presented below:

According to Martens (1968), percent of impervious cover is a measure of urban development in an area. He used a sampling process for determining the percentage of imperious cover of watershed directly from the map. A transparent grid was superimposed over a detailed topographic map of the study area, Charlotte, North Carolina, US. Percentages of the impervious area were estimated by counting the number of intersections that overlay manmade impervious areas.

According to Stankowski (1972), population density, an indirect indicator of urbanization, can be used as the only independent variable to estimate the proportion of impervious area resulting from different degrees of urban and suburban development. The impervious cover was quantified based on its correlations with population density in different urban and suburban land-use categories. The land use and population density data of New Jersey were used for illustration of the method and a set of empirical relations were developed between the percent of imperviousness and the population density, which can be used for determination of percent imperviousness in New Jersey in past, present and future.

Graham et al. (1974) developed empirical equations using demographic data for the estimation of percent imperviousness for Maryland, USA. Using imperviousness as the dependent variable, an asymptotic regression analysis was performed individually with population density, housing density and employment density as independent variables. Housing density was found as the best independent variable for the estimation of impervious cover. For developing the empirical equations, the required data of imperviousness was derived from colour infrared aerial photography.

Alley and Veenhuis (1983) discussed different methods of estimating total impervious area (TIA). According to them, effective impervious area (EIA), which can be estimated by field surveys along with aerial photographs or by relating EIA to the minimum ratio of runoff/rainfall measured for small storms, should be used in the rainfall-runoff model in order to avoid the overestimation of runoff. It has been emphasized that a relationship between EIA and TIA can be determined if the known values of ratio of EIA and TIA can be expressed as a function of land uses.

Laenen (1983) calculated the EIA by using the optimal fitting technique with the USGS digital rainfall-runoff model. All other parameters were set to the values computed from either regional data or graphical analysis. Verification of the estimation was accomplished by a field survey of the effective impervious area in the gauged sites of four basins. Finally, an empirical equation for EIA was derived in terms of mapped impervious area of metropolitan areas of Salem and Portland.

Boyd et al. (1993) examined rainfall-runoff depth for 763 storms on 26 urban basins located in 12 countries in Australia. The effective impervious fraction was determined by carrying a least square linear regression analysis to fit the rainfall-runoff data of several numbers of storms. It was found that when the runoff versus rainfall graph is a straight line, all the runoff generated from the basin is impervious runoff. Again, the effective impervious fraction obtained from regression analysis was found to be more close to the directly connected impervious fraction determined from map than the total impervious fraction.

Sutherland (1995) developed a set of empirical equations for EIA based on the USGS calibrated values of EIA from a rainfall-runoff model for over 40 watersheds throughout the metropolitan areas of Portland and Salem, Oregon. EIA has been expressed in terms of TIA, which has been determined from the basin maps. The basin conditions, for which the basin empirical equations were developed, are average connected basins, highly connected basins, totally connected basins, less disconnected basins and extremely disconnected basins. For considering all these basin conditions, these equations provide reasonable estimates of EIA over the entire range of TIA.

Clarke and Gaydos (1998) developed a cellular automata model called spatially explicit urban land cover change model (SLEUTH) for modelling and projecting the future urban as well as multiple land use land cover (LULC) change. Inputs, required for SLEUTH model were a slope layer, a transportation layer reflecting primary roads, and exclusion-attraction layer describing areas that will either attract or exclude development. SLEUTH is composed of four growth rules to simulate the urban growth: spontaneous growth rule, new spreading centre growth rule, Edge growth rule and the road influenced growth rules.

Ji and Jensen (1999) emphasized the use of sub-pixel analysis technique and layered classification process for quantifying and determining the type of imperviousness within pixels of satellite images. The sub-pixel analysis is based on the idea of removing background spectra from the total radiance of a pixel and testing the residual spectrum against the signature spectrum. This enables the determination of the type of impervious cover within a pixel. To cope with the extreme spectral diversity within a pixel, the layered classification system is used. When some spectral values (which occur with low probability) are not known within a pixel then those values are determined by subtracting spectral values of different material cover types, one at a time. After subtracting, if there exists some spectral value then it indicates that the unknown spectral value is not of that material cover. Thus, the iteration technique was carried till the subtraction results zero. To evaluate the bias and accuracy of the classification, Spearmen rank correlation analysis was used.

Sleavin et al. (2000) developed parcel size and zoning specific percent impervious surface coefficients and land cover specific percent impervious surface coefficients. Data required for the first set of coefficients were digitized from 1:2400 aerial photographs using stereographic techniques. The second set of coefficients is based on Thematic Mapper satellite-derived land cover data. GIS software was used to convert the data into a useable format and perform overlay analyses. A Relational Database Management System (RDBMS) was employed to analyze the data and produce summary statistics. The mean of the percent imperviousness coefficients of a particular group of zone or parcel was used to predict the imperviousness of similar group of another city. On the other hand, land cover specific percent impervious surface coefficients were used to determine total town imperviousness.

Bird et al. (2002) used DOQQ analysis technique for subwatershed and two other approaches- multiple data source (MDS) approach and NLCD approach (with ATTILA tool) for large watersheds to determine the percent imperviousness in Georgia. In the DOQQ analysis technique, the point-sampling method on a 200 m regular grid was used to evaluate the impervious area. In MDS approach, the population density, commercial/industrial, quarrying/mining land-cover and highway coverage data were combined to estimate the impervious cover. Again, in the NLCD approach, simple class-based imperviousness assumptions were applied to the National Land Cover Data using the ATTILA landscape.

Lee and Heaney (2003) quantified the urban imperviousness of a 5.81 ha residential area in Boulder, Colorado in a very detailed way by using Geographic information system (GIS) and field investigations. The analysis was done in five levels of accuracy to most accurate estimation. The levels were classified by the detail of applying GIS and field investigations. The analysis showed that transportation-related imperviousness plays an important role in producing runoff. The transportation-related imperviousness comprises 97.2% of the directly connected imperious area (DCIA).

Chabaeva et al. (2004) developed an impervious estimation model by relating percent imperviousness with land use and population. The required data of imperviousness was taken from high-resolution planimetric data of building and transportation features of Connecticut, Massachusetts, and New York. Census Population data were collected for the more than 100 tracts covering these towns. The total area of each tract, the percent imperviousness of each tract, the area of each land cover category within each tract and the impervious surface coefficients were calculated. The JMP Statistical Discover Software was used to create a regression model. This regression model generated a set of coefficient that predicts percent imperviousness as a function of population density and percent coverage of the land use types.

Theobald (2005) developed a simulation model called Spatially Explicit Regional Growth Model (SERGoM) to forecast future housing density patterns based on county-level population projections. SERGOM is basically a supply–demand–allocation based model. It assumes that new housing units are developed in an area in order to meet the housing demand of the increased population. The spatial distribution of the housing density was done based on travel time from a location along the main roads and highways to the nearest urban core. According to this SERGoM model, in conterminous US, the urban and suburban housing densities will expand to 2.2% by 2020 and exurban housing densities will grow up to 14.3%.

Exum et al. (2005) used multiple data source (MDS) method for estimating and projecting impervious cover resulted from human settlement in eight southeastern United States. At first, the various methods of estimating impervious cover such as satellite imagery, NLCD only method, population density - imperviousness relationship methods etc are analysed and tested. The MDS technique was found to provide a more reliable method for projecting the change in impervious cover over time based on future population projection.

Han and Burian (2009) presented a two-step method by using multispectral satellite imagery and geographic information system in order to estimate the effective impervious area (EIA) of a watershed. In the first step, fine-scale multispectral imagery is classified to land cover classes to determine TIA and the second step carried out in GIS to overlay the impervious surface coverage geospatially over a fine-scale digital elevation model (DEM). This enables to trace the water flow path until it reaches the drainage system or passes over a pervious area. Thus an area can be designated either as effective or non-effective impervious cover.

Theobald et al. (2009) developed a statistical relationship between the housing density and impervious surface which can be used both to determine the current impervious area and also to project the future imperviousness. For developing the statistical relationship, the NLCD 2001 Percent Urban Imperviousness dataset of US was used as dependent variable and the independent variable housing density data was developed from SERGoM (Theobald 2005). A relationship between these two variables was obtained from Categorical Regression Tree (CART) model by using cross-validation (CV) tree function. To forecast likely imperviousness in the future, the housing density for 2030 from SERGoM was input into the CaRT model and generated a predicted map of imperviousness in 2030 by using ArcGIS.

Chabaeva et al. (2009) examined the accuracy of several analytical techniques and different data types for estimating urban settlements and compared them against photogrammetrically derived calibration and validation data from high resolution digital planimetric datasets for 52 towns in Connecticut and New York. Six IS estimation methods were examined: 1) NLCD 2001 impervious surface layer; 2) CCL (Connecticut's Changing Landscape) 2002 impervious surface layer; 3) land cover specific coefficients applied to NLCD 2001 land cover and modelled with the ISAT (Impervious Surface Analysis Tool); 4) land cover specific coefficients applied to CCL 2002 land cover and modelled with the ISAT; 5) population density and land cover-based regression model ETIS (Estimation Tool for Impervious Surfaces), using US Census Bureau population applied to NLCD 2001 land cover; and 6) population density and land cover-based regression model ETIS, using US Census Bureau population applied to CCL 2002 land cover. Out of these six techniques, the last one that is ETIS was found to be given the highest accuracy of estimates.

Beighley et al. (2009) studied on the effect of estimation of urban cover by using manual digitization of high resolution aerial photograph and automated interpretation of medium resolution satellite data on simulated peak discharges in Mission Creek watershed of California. HEC-HMS was used in runoff modelling. By using manual digitization, imperviousness was found as 22.5% whereas, from automated image classification it was obtained as 14.5%. The difference between the results of these two methods is high for areas having high and low-density urban settlements. Overall, the two methods result in different peak discharges. However, none of them consistently gave discharges less than the flood frequency based discharges.

Bierwagen et al. (2010) developed a gravity model of domestic migration which can be used in forecasting the populations by a cohort-component population-growth model which in turn used to derive the future housing density. These housing units are distributed by SERGoM to 1 ha areas based on past land-use patterns and travel time along roads from urban areas. The population growth scenarios were based on the four main SRES (Special Report on Emission Scenario) storylines- A1, A2, B1, B2. Parameters in SERGoM that influence the growth patterns (i.e., compact vs. dispersed) were also modified to be consistent with the SRES storylines. Out of these four storylines, A2 scenario found to be displayed the highest population growth rate, business-as-usual dispersed development pattern, largest changes in urban and suburban housing density classes, greater conversion of other land-cover classes, and an increased percentage of impervious surface cover by 2100.

Sahoo and Sreeja (2011) used analysis of the low-resolution satellite imageries employing remote sensing technique for quantifying total and effective imperviousness of an urban city of North East India. Two indirect methods and a semi-automated direct method were used to determine the effective impervious area of the study area.

Dhorde et al. (2012) developed a multiple regression based model in order to determine urban impervious surfaces using sample points. The moderate resolution data from Landsat TM and IRS P6 LISS-III were used to develop the model to identify impervious surfaces at pixel level. A regression equation was obtained expressing percent imperviousness in terms of band values, NDVI, Tasselled Cap values, slope, elevation, and population density. Impervious surfaces were extracted village wise and impervious surface coefficients were calculated for the entire study area, Bhima basin, India.

Weng (2012) presented a review of various remote sensing methods to identify and quantify the impervious surfaces in urban areas. The major approaches included were pixel-based; sub-pixel based object-oriented algorithms, and artificial neural networks (ANN). The impacts of spatial, geometric, spectral, and temporal resolutions on the estimation and mapping have also been discussed. The advantages and disadvantages of all the methods and their circumstances of applications were discussed and finally, the various emerging trends in image processing techniques and the data analysis methods which will help the remote sensing of impervious surfaces in the future have been mentioned.

Dams et al. (2013) estimated urban land cover by the use of medium resolution remote sensing data in the north of Belgium. The training data for the study area were obtained by overlaying a high-resolution image with Landsat TM image acquired in 1986 (historical) and a Landsat ETM+ of 2003 (recent) imagery. Historical medium resolution pixels for which the impervious surface cover has changed were filtered out by a temporal filtering technique. The urban pixels which were common in all the three images were only considered such that the linear regression model can also be applied to the historical image to get the impervious fraction of each urban pixel. The linear regression model was calibrated relating the spectral information of the medium resolution images with the impervious fraction, obtained from the high-resolution images, of the corresponding pixels. The obtained regression coefficients were used to extrapolate the impervious fraction estimation over the whole medium resolution image. The change in impervious cover between 1986 and 2003 was used to evaluate the impact of urbanization on the vertical water balance and groundwater system.

Miller and Grebby (2014) presented two methods for mapping the urban extent and estimating the impervious cover in an area of South England for the period 1960-2010. For both methods, the historical topographic maps were converted to representative binary maps of impervious and pervious pixels. In the first method, fractional impervious surfaces for the six catchments of the study area were determined by calibrating fractional impervious surface maps. The second method is based on the generation of urban land use maps by aggregating the binary maps to larger grid cells and the imperviousness was determined by calculating the index of urban extent. The fractional impervious surface areas estimated from aerial photographs were used as referenced data for validation of the two methods.

Liu and Gu (2017) used a hybrid process comprising spectral-spatial feature sparse representation (SS-SR) and post-processing to improve the accuracy in determination of urban imperviousness from hyperspectral images by minimizing the misunderstanding between impervious surface and bare land. To test the usefulness of the process, four sets of hyperspectral data were applied to estimate the impervious area. Inspite of its more accurate estimation, the method was found to be very time-consuming.

2.3 Effects of urbanization on land use land cover change

Urbanization is leading to intense environmental alterations. To cope with these alterations, it is necessary to understand the process of urban-induced landuse land cover change. Some of the past studies on this aspect are given below:

Xu et al. (2000) used Landsat TM satellite data along with socio-economic information collected from the Fuqing Bureau of Statistics to determine the impact of urbanization on LULC changes in Fuqing City, China. It was found that in the study period from 1991 to 1996; mainly arable lands were converted to urban land covers. Again, in this period, the annual deforestation rate was obtained as 3.9%. The rapid economic growth, transportation system and the topographic condition of the city were found as the most important influencing factors of this spatial expansion of the city.

Mundia and Aniya (2006) compiled Landsat data, aerial photographs, and topographical maps over a period 1976 to 2000 to interpret the LULC change dynamics of Nairobi city, Kenya. It was observed due to the urban expansion there is a substantial decrease in forest land cover. On the other hand, to meet the demand of the increasing urban population, the agricultural landuse was also found to increase.

Weng (2007) integrated urban gradient paradigm and landscape pattern matrix to analyse the effect of urbanization on the change in landscapes of Dane County, USA. Landscape metrix measures landscape patterns and provides the differentiation between different landuse planning scenarios. Gradient analysis systematically evaluates the effects of urbanization on landscape patterns with some additional insights into urban landuse planning. The study reveals that the core city area expands outward in a contiguous way, where rural areas experience scattered settlements. Again, the rate of change in landscape in already developed core urban area is less in comparison to that in urban fringes.

Deng et al. (2009) used SPOT images along with spatial metrics in order to evaluate the change in landscape characteristic as a result of rapid urbanization in Hangzhou, China. FRAGSTATS software was applied to derive spatial metrics. It was found that 88.66% of the total change in landscape occurred in a period of 10 years is only due to the transformation of non-urban area to urban area. In this transformation, mainly agricultural land and water bodies were affected.

Mohan et al. (2011) studied the spatial expansion of an Indian city Delhi emphasizing the impact of hasty urbanization on LULC change. They used multi-spectral satellite data and topographical map to extract landscape data over a period from 1997 to 2008. It was observed that in this period built-up area increased by 17%. In 1997, agricultural lands were the most prevailing land cover. In 2008, the low density built up area took this position. Finally, a statistical study was also performed for determining the relation between LULC change and different growth parameters.

Sajjad and Iqbal (2012) studied the LULC dynamics of Dudhganga watershed of Kashmir Valley in India, under the impact of urban expansion by using Landsat thematic map of 1991 and 2010. Two parameters- land consumption ratio (LCR) and land absorption coefficient (LAC) were calculated for assessing the expansion pattern urban landscape with the increase in urban population. Results revealed a considerable increase in built-up area with a drastic reduction in agricultural landcover. LCR and LAC values showed that the rate of spatial expansion of urban coverage is lower than the rate the urban population growth. This indicates an increase in population density in the existing urban area.

Su et al. (2014) determined the main urbanization factors that influence the agricultural landscape pattern in China. For this purpose, they used remote sensing, GIS, spatial landscape metric analysis, and spatial error and lag regression analysis It was found that the relationship between urbanization and agricultural landscape pattern is greatly variable. The expansion intensity index (EII), which measures the dynamics of expansion of built-up land area in an ecoregion, is the most influential urbanization indicator describing the changes in agricultural landscape pattern at ecoregion-level. Again, demographic factors like non-agricultural population proportion (NAPP) were found to have no significant influence on agricultural landscape dynamics.

Long et al. (2014) analyzed the land use changes in a new developing area of China in a period of 1985 to 2010 by determining the consequent changes in ecosystem services value (ESV) with the help of remote sensing and geographic information system (GIS) technology. It was found that due to the conversion of agricultural land and water body into urban cover, the ESV of the study area reduced by 25.9%.

2.4 Impact assessment of urban settlement on hydrology

The two important components of hydrology, surface and groundwater, both may be affected by the expansion of urban settlement. Till date, numerous studies have been carried out to study the impact of imperviousness on hydrology. Some of those are presented below:

Brun and Band (2000) investigated the impact of impervious surface on runoff ratio and base flow in a watershed Baltimore, USA by coupling "Hydrologic Simulation Program Fortran" (HSPF) with "GIS". The relationships between rainfall-runoff ratio and base flow versus percent impervious cover and percent soil saturation were analysed. It was found that the runoff ratio does not change dramatically till the imperviousness crosses a threshold value (18%). Again, base flow declines as percent impervious cover increases for any percent soil saturation. At 100% soil saturation, base flow ranges from 13 mm per week at 0% impervious cover to 3.5 mm per week near 100% impervious cover.

Megic et al. (2004) evaluated the impact of urbanization (impervious cover) on water availability for groundwater based water supply in Florida. The net groundwater recharge was calculated by using water balance equation with consideration of the constant precipitation but the changing values of the evapotranspiration, groundwater inflow/outflow, surface runoff and artificial recharge under the impact of imperviousness. In the study area, it was found that there is an increase in net recharge as more amount of stormwater runoff generated as result of the increase in urban cover, can be directly recharged to the Floridan aquifer.

Burns et al. (2005) studied the effect of urban cover on hydrologic processes in high density, medium density and undeveloped area individually. It was done by direct measurement of the rainfall, stream discharge and groundwater levels at wells in every catchment. The mean residence time of stream water was calculated from measurements in precipitation and base flow for every type of catchments. It was found that the peak runoff increases and the mean residence time decrease with the suburban development.

Kauffman et al. (2009) examined how the base flow is affected by impervious covers by plotting stream base flow data against impervious covers of 19 watersheds ranging from heavily forested to highly urbanized in White Clay Creek watershed, part of the Christina River Basin in northern Delaware. The impervious surface was quantified by GIS mapping and base flows were estimated by using stream velocity and cross-sectional areas of streams. A good correlation was found between the base flow and imperviousness indicating that base flow decreases with the increase in impervious cover in watersheds. This decrease in base flow may result in drinking water scarcity especially during drought for the study areas.

Menzel et al. (2009) showed how the stream base-flow is affected by land use and land cover change in Jordan river region. The LandSHIFT.R model was used to simulate and to generate the land use and land cover change distribution maps for the two scenarios- the "Poverty & Peace" and the "Modest Hopes". These maps were input to the hydrological model "Train" in order to simulate the water availability for the considered scenarios. It was found that for both scenarios though there is an average increase in surface water availability in the urban areas due to the high volume of simulated surface runoff, there will be a shortage of drinking water, especially in dry periods. Again, the 'Modest Hopes' shows the increase of irrigation water demand.

Flinker (2010) reported the hydrological, physical, biological and chemical impacts of impervious surface on a watershed. The "Impervious Cover Model" was used to determine the impact of impervious cover on the present as well as the future stream health. It was mentioned that under natural condition, in general, 10% of rainfall becomes runoff, 50% is absorbed by the ground and the rest 40% is taken by trees and evapo-transpirated to the atmosphere. Again, for a highly impervious surface (75%-100% imperviousness), the absorption of water by ground may reduce to 15% and the runoff may increase up to 55%.

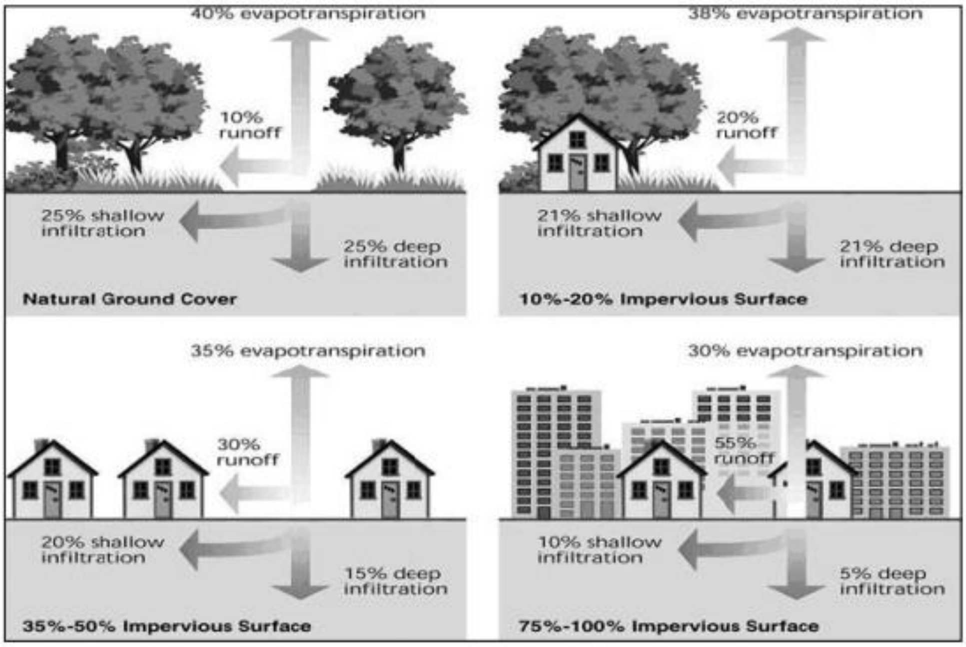

Fig. 2.1: Changes in site hydrology with increasing impervious cover (US EPA) (Flincker, 2010)

Caldwell et al. (2012) performed a study to quantify the impacts LULC change, water withdrawals, and climate change on river flows in the conterminous US by using integrated Water Supply Stress Index (WaSSI) monthly water balance and flow routing model. It was found that in comparison to 1981–2000 flows without impervious cover, 2010 levels of impervious cover (1.3 % of the total land area) increases the mean annual river flow by 9.9%. Again, compared to no water withdrawals, 2005 withdrawals decreased the mean annual river flows by 1.4 %. In 2060, for the Low and High growth emission scenarios, the combined effect of impervious, population, and climate change, showed a mean decrease in river flow by 11.8% and 11.0%, respectively.

Wagner et al. (2013) analyzed the impact of land cover and land use change on runoff and evaporation for Mula and Mutha rivers catchment upstream of Pune. Three multi-temporal land use scenarios were prepared from multispectral satellite data of three different sensors. SWAT model has been used to assess the impact of land use change on water resources. It was found that due to the increased impervious surface, there is an increase in water yield (+ 7.6%), which can be balanced by the decrease in water yield due to the increase in cropland in some areas of Pune.

Barron et al. (2013) used a coupled surface water–groundwater model (MODHMS) to examine the impacts of urbanization on catchment water balance. This result indicates that depending upon the amount of groundwater abstracted, a 10% increase in imperviousness leads to an increase in discharge by 13% to 33%. Again, infiltration reduced from 70% to less than 20% after urbanization. This shows that increase in imperviousness increases the water availability which can be used for water supply.

Zhou et al. (2014) used distributed object-oriented rainfall and runoff simulation (DORS) model to simulate the discharge, runoff, base flow etc. in Rhode Island, US. From the simulated data, discharge per unit area and the ratio of runoff to base flow (response variables) are correlated to a set of watershed characteristics including the percentage of IS, distance from IS to stream, and stream density in 20 study watersheds by using ordinary least square, spatial lag and spatial error regression models. The results show that the study watershed with 11 % impervious surface, the magnitude of the peak discharge is almost doubled compared to the simulated discharge without impervious surface. Similarly, the magnitude of peak ratio of runoff to base flow is twice of that from the simulation without IS.

Gwenzi and Nyamadzawo (2014) performed a review on the impact of urbanization and urban roof water harvesting on hydrologic processes in water-limited catchments. It was mentioned that impervious surface causes urban heat island effect due to which there is an alteration in atmospheric water demand, frequency and magnitude of high-intensity rainfall (summer time). Evaporation and ground-water recharge also decline for low soil moisture availability, especially in water limited area. It was suggested that by adopting roof water harvesting, some percentage of water shortage and surface runoff generation can be reduced.

Li et al. (2015) presented how water utilization ratio can be related to land use changes in the upper and middle reaches of the Heihe River Basin, China. The generation time and also the magnitude of peak runoff decreases with the increase of forest or vegetated area. As a result, water yield will decrease and hence there is an increase in water utilization ratio. To simulate spatial land use patterns, the Dynamic Landuse System (DLS) was used for three different land used scenarios based on low, medium and high utilization ratio. After that, SWAT model was used to simulate surface runoff and water yield changes in response to the impacts of land use changes.

2.5 Sediment yield models and their application on impact analysis of land use land cover change on soil erosion

Soil erosion is a major global environmental hazard. In India, 130 million hectares of land i.e. 45% of the total geographical area is having serious soil erosion (Kothyari 1996; Ganasri and Ramesh 2016). Approximately 5,334 Mt of soil is detached yearly; of which 29% is transported by rivers into the sea and 10% is settled down in reservoirs reducing the storage capacity (Narayana and Babu 1983). On the other hand, nature requires a period of 200–400 years to form a topsoil layer of 1 cm depth (Singh and Phadke 2006). Effect of soil loss can be categorised into two types: on-site and off-site effects (Morgan 2009). On-site effect mainly deals soil quality and health including its structure, organic content, moisture content, fertility etc. and the off-site effect includes the sedimentation in watercourses and reservoirs, increase in downstream flood, disturbance in downstream eco-system etc., which are mainly caused by the movement of the sediments to downstream. Due to its multi-dimensional side effects, soil loss information is becoming a basic need for management purpose. However, the field observation of soil loss is very time consuming and by this method it also not possible to evaluate the effect of climate change and LULC change on soil loss over a long time (Morgan 2009, Syahli 2015). Hence, numerous models are available for estimation of soil surface erosion. These models mainly are of two types- empirical model and physical model (Bhattarai and Dutta 2007).

Wischmeier and Smith (1961) developed the Universal Soil Loss Equation (USLE), which is one of the most extensively used empirical soil loss estimation models. This is a plot-scale model which considers numbers of factors like topographical condition and soil characteristics of watersheds, local rainfall pattern, land use land cover type or land management practices to calculate long-term average annual soil loss (Smith 1999). Many watershed models like CREAMS (Knisel 1980), ANSWERS (Beasley et al. 1980), EPIC (Williams et al. 1984), GWLF (Haith and Shoemaker 1987), AGNPS (Young et al. 1989), SWAT (Arnold et al. 1998), SEDD (Ferro and Porto 2000) estimates soil loss based on USLE. One limitation of USLE is that it is basically applicable to small sized watershed having negligible gully and channel erosion (Simanton et al. 1980). MUSLE (Modified Universal Soil Loss Equation; Williams 1975) and RUSLE (Revised Universal Soil Loss Equation; Renard et al. 1991) are the upgraded version of USLE. Initially USLE model was valid only for cropland having a mild slope. RUSLE, resulted from revised estimation of different input parameters has expanded the area of applicability of USLE to different land use types with a variable range of slopes (Gelagay and Minale 2016). Similarly, MUSLE was improved by substituting the rainfall erosivity factor with runoff factor which makes the soil loss estimation better as runoff depends on both the antecedent moisture content and the rainfall intensity (Zhang et al. 2009). MUSLE can estimate the soil loss resulting from a single event where both RUSLE and USLE estimate the long-term average annual soil loss (Lim et al. 2005). Morgan et al. (1984) developed a field scale model called MMF (Morgan–Morgan–Finney) model, which can be applied to hill slope areas. The model is simple and input data requirement also less providing a better physical base than USLE (Morgan 2001, Bayramov et al. 2013). It calculates the soil loss in two phases (Morgan 1984). First one is the water phase which calculates the kinetic energy of rainfall and volume of overland flow. The sediment phase i.e. the second one takes account of the rate of detachment due to the impact (kinetic energy) of raindrops and the transportation capacity of the overland flow. Morgan (2001) revised the MMF model to consider the effect of the plant canopy height and leaf drainage and the flow on soil particle detachment. It was again modified by Morgan and Duzant (2008) to take account of the effect of the plant and vegetation properties on soil loss. The main limitation of MMF model is that the model validation for non-agricultural land is very few and the model is highly sensitive to the variation of slope steepness (Ghosh and Guchhait 2012). In addition to these empirical models, WEPP (Nearing et al. 1989), LISEM (De Roo et al. 1996), EUROSEM (Morgan et al. 1998) etc. are some widely used physical models for estimation of soil surface erosion. Though these models are based on real processes and they are capable of giving spatial and temporal variation of soil loss data, they contain a large numbers of input parameters with extensive computation. Also, simulation of these models for a specific area requires observe sediment loss data which is not available for ungauged watersheds (Beven 1990, Bhattarai and Dutta 2007). Tyagi et al. (2008) developed an event-based temporally distributed model based on USLE and SCS-CN method.

Though soil surface erosion is a natural process, it has been being exacerbated by anthropogenic activities (De Graaff 1996). He (2003) studied the effect of LULC change on runoff, sediment, and nutrient yields by using GIS-based AGNPS model. The simulation shows that higher rate in the urban expansion will lead to increase in discharge and sediment yield in Dowagiac River watershed, US. According to Morgan (2009), vegetation cover protects the soil surface from the direct impact of raindrops causing soil loss to decrease. Soil erosion rate has a stronger relationship with LULC change than that with the variability in rainfall or slope (Kosmas et al. 1997). Table 2.1 (Morgan 2009) shows how the soil loss rate responds to land covers in different countries. Research is going on the evaluation of the relation between sediment loss and the change in land use land cover in an area. Sharma and Tiwari (2011) used USLE model to carry the same impact study in Maithon reservoir catchment of India in a period of 1989 to 2004. It was found that mainly the flat portion of the watershed which is experiencing the rapid deforestation and construction has the increasing soil erosion risk. Similarly, Yuksel et al. (2007) calculated total sediment loss from a dam watershed in Kahramanmaras region (Turkey) by using GeoWEPP (GIS-based WEPP) model which is capable of giving both the spatial and temporal variation scenario of soil loss. The model was found as a fast tool of sediment loss estimation from large watersheds but with high accuracy. Regmi and Saha (2015) used revised MMF model in GIS platform to determine the present and future increasing erosion risk in Phewa Lake watershed of Nepal. From 1995 to 2010, mainly in open forest, scrub and wasteland, the average soil loss rate was found to increase due to the increased farming practice, deforestation and urban expansion. Similar to Sharma and Tiwari (2011), Lech-hab et al. (2015) also used USLE model in GIS platform to analyse the impact of degradation of vegetation cover due to the expansion of urban and agricultural land on soil erosion from Kalaya Watershed of North Western Morocco. An increase in average soil loss rate was observed from this estimation.

Table 2.1: Annual soil loss rate (t ha^{-1}) for different land covers (Morgan 2009)

Country	Natural	Cultivated	Bare soil
China	0.1-2	150-200	280-360
USA	0.03-3	5-170	4-9
Australia	0.0-64	0.1-150	44-87
Ivory Coast	0.03-0.2	0.1-90	10-750
Nigeria	0.5-1	0.1-35	3-150
India	0.5-5	0.3-40	10-185
Ethiopia	1-5	8-42	5-70
Belgium	0.1-0.5	3-30	7-82
UK	0.1-0.5	0.1-20	10-200

2.6 Management practices/techniques for controlling sediment and runoff

Extensive erosion and peak runoff due to urbanization is a serious global urban issue (Sarma et al. 2015). Researchers are providing key inputs into sustainable watershed management practices to control these adverse hydrological hazards. Some past research studies on this aspect are given below:

Wenger (1999) reviewed the formulae for riparian vegetative buffer delineation, which are very effective in entrapping sediments and nutrients from surface runoff before reaching the aquatic ecosystem. In general, though buffers of width 4.6 m (15 ft) are reasonably useful, wider buffers are suggested for steeper slopes. These buffer zones also help in maintaining the biodiversity.

Shammaa and Zhu (2001) summarise different techniques to cope with stormwater, which is the key carrier of total suspended solids (TSS). Basically, three types of techniques: infiltration, filtration and detention, and their application criteria, advantages, disadvantages were explained. Infiltration strategy contains infiltration trenches, infiltration basins and permeable pavements. Though porous pavements can infiltrate 90% of the annual rainwater to groundwater (Schueler et al. 1992), it often fails due to clogging. Under filtration strategy, which is basically ideal for removing TSS and pollutants, the filter strips, grassed swales and media filters were described. Among these three techniques, sand filter (media filter) has the highest TSS retaining capacity though this technique is not applicable for a large watershed. Again, the detention techniques comprising dry ponds, wet ponds and constructed wetlands are the most widely adopted practices for stormwater management. These three detention techniques can have TSS removal rate up to 60% (Shammaa and Zhr 2002), 90% (EPA 1983) and 93% (Barrett 1999), respectively, if designed adequately. Additionally, it was also mentioned that Polymer-assisted detention ponds can eliminate 95-99% of TSS (Minton and Benedict 1999).

Taebi and Droste (2004) tested the effectiveness of the urban runoff quality control system and the advanced wastewater treatment system for controlling polluted runoff releases in the city of Isfahan, Iran, which contains ten urban catchments. Results revealed that in low precipitation area, advanced treatment is a better option. Whereas, in high precipitation areas, urban runoff quality control system such as detention ponds are more useful for suspended solids and oxygen-demanding matter control, and that advanced wastewater treatment system is more efficient for controlling nutrient.

Wang et al. (2004) integrated GIS and optimization technique in order to develop an inexact-fuzzy multi-objective linear programming (IFMOP) model for having land use planning based on economic, ecological and land suitability of a basin. An optimization model was applied to the Lake Erhai basin of China under the consideration of four different environmental-cost effective conditions. These were shaped in a view of maintaining the water quality and ecological balance in the lake as well as the regional development through efficient tourism development. Results show that forest area should be increased to improve the water quality of the lake.

Gharabaghi et al. (2006) determined the how the efficiency of Vegetative filter strips (VFS) in eliminating contaminants from runoff depends on grass type, filter strip width, flow rate and the concentration and size of inflow sediment by conducting some field experiments. Results showed that with the increase of filter strip width from 2.5 to 20 m, the efficiency of VFS increased from 50% to 98%. Again, most of the aggregates of diameter greater than 40 μm were screened within the first 5 metres of the strip.

Liu et al. (2007) used integrated GIS-based analysis system (IGAS) for addressing land-use management strategy in lake areas of urban fringes maintaining an ecological balance. IGAS contains four subsystems- land use suitability assessment, demand analysis, land evaluation analysis and land allocation. Multi-criteria analysis was used in GIS platform for land suitability assessment. Again, cost approximation and hypothetical development methods were used land evaluation. The case study was carried out in the Hanyang Lake area in the urban fringe of Wuhan City, China by modelling the potential land-use changes from 2006 to 2020.

Shiono et al. (2008) developed a numerical model in order to simulate the reddish sediment flow in centipede grass strip used for reduction of sediment runoff. The numerical model was based on the energy conservation equation for steady non-uniform flow and the continuity equation for sediment. The model was verified with experimental data conducted at the Arashiyama field site of Okinawa Island. The sensitivity analysis of the model showed that the grass strip width and the discharge have a great influence on the sediment removal efficiency.

Ibrahim (2009) documented how the Gadarif City of Central Sudan managed the seasonal flood as well as the scarcity of drinking water by implementing the rainwater harvesting system of constructing two small dams in a river. Construction of these dams increased the groundwater recharge due to which groundwater table raised by a few meters. Additionally, this also created a good ecologically balanced environment for vegetation growth upstream the dam.

Sarma et al. (2013) developed OPTEMP-CSMO (OPTimal EMP model considering Carbon Sequestration with Multi-Objective optimization) model to determine the best combination of Ecological Management Practices (EMPs) with an aim to maximize the carbon sequestration and to minimize the cost. The model was applied to a micro hilly watershed located in Guwahati city of Assam. EMPs used for the study area were- grass, shrubs and forests.

Mekonnen et al. (2015) determined the sediment trapping efficiency of small dams constructed for the purpose of sediment storage at the outlet of eight sub-watersheds in the Amhara Regional State of Ethiopia. Dams were constructed by using either gabions or stones. It was found that though both types of dams were good as offsite structural measures, gabions dams were more efficient in sediment trapping than those made from stone. However, construction costs of both of them were quite high, which were not affordable by small-scale farmers.

Sarma et al. (2015) presented Optimal EMP Model with Linear Programming for Single Ownership (OPTEMP-LS) model to determine the best combination of the ecological management practices (EMPs) at the minimum cost in a micro hilly watershed of India such that it produces the sediment and peak flow within a controllable limit. For calculating the sediment yield and peak discharge in the model, the Revised Universal Soil Loss Equation (RUSLE) and the Rational Method were used. Sensitivity analyses of the model parameters showed that the total EMP cost is highly responsive to rainfall intensity of the watershed.

2.7 Role of remote Sensing and Geographical Information System in hydrological study

Remote sensing (RS) is the science of getting information of the earth surface without coming in physical contact with it (Sharma et al. 2015). Information about any object is acquired by using a sensor which receives electromagnetic energy reflected, emitted or released by the object. On the other hand, Geographic information system (GIS) is a computer-based system dealing with the storing, manipulating, interpreting and retrieving or processing of the spatial geographic data. Nowadays, without the ease of RS and GIS, it is not possible to carry a hydrological study, which will be time-efficient, economical and also dynamic at the same time. Hence, water resources engineers and researchers are utilizing the RS and GIS advantageously in hydrological information extraction. Some of the previous works dealing with the use of RS and GIS techniques in the hydrological analysis are given below:

According Moore et al. (1991) topographical information, which is the basic data for solving water resources and biological issues, can be derived from digital elevation model (DEM). Mentioning the usefulness of GIS for manipulating, storing, and accessing the topographical information, the researchers reviewed the various available digital elevation data and its accuracy and how the topography of an area can be digitally represented for hydrological, geomorphological, and biological applications.

Jayaraman et al. (1997) emphasized the role of space technology including RS and GIS in analysing and managing the vulnerability of various natural disasters like Cyclones, Floods, earthquakes, volcanoes etc. They presented a number of successful cases of reduction of losses due to the natural disasters by using space technology around the world. Disaster warning system (DWS), satellite-based global positioning system (GPS), data collection platform (DCP), and emergency terminals etc. can be widely applied for flood forecasting, geological changes monitoring etc.

Gangodagamage and Aggarwal (2001) developed a hydrological model for Bata river basin of India based on SCS curve number, unit hydrograph methods and Muskingum hydrological routing method. Survey of India (SOI) toposheets, field data, LISS III multi-temporal satellite image data and IRS pan data were used for acquiring the required information. Spatially distributed values of topographical parameters were derived with the help of RS and GIS. The developed distributed hydrological model was capable of producing a good estimate of runoff from the basin.

Melesse and Shih (2002) determined the spatially distributed runoff depth in a sub-basin of Kissimmee River in south Florida. for three different years by using US

Department of Agriculture, Natural Resources Conservation Service Curve Number (USDA-NRCS-CN) method. Various types of spatial data like the land cover or topographical characteristics of the basin were extracted from Landsat images in GIS. It was found that as a result of the Kissimmee River restoration work, the wetland and water body area in 2000 were more than those in 1980 and 1990.

Anbazhagan et al. (2005) selected the artificial recharge potential area in Aliyar basin of Tamil Nadu, India based on the amount of runoff generation, aquifer size, suitable areas and groundwater level in different watersheds of the basin. Soil Conservation Service curve number (SCSCN) method was used for runoff calculation. The weighted curve number for every watershed was achieved by spatial analysis of LULC and hydrological soil group in GIS software. Finally, watersheds were prioritized on the basis of its groundwater condition for the purpose artificial recharge planning.

Jain et al. (2005) applied satellite data of just ahead and after the flood to demarcate flood inundated areas in Koa catchment, Bihar. For this purpose, IRS-1C LISS III, Landsat TM data were used. Various types of image processing techniques like density slicing, Tasseled Cap Transformation and Normalized Difference Water Index (NDWI) were carried out in the Earth Resources Data Analysis System (ERDAS) and Integrated Land and Water Information System (ILWIS) software. Another flood map was also prepared based on river gauge data by using DEM. Among all these methods, NDWI is found as the best method for mapping of flood-prone areas.

Cheng et al. (2006) introduced a regionalization technique for the determination of runoff and applied this methodology to an ungauged drainage basin in Greater Toronto Area, Canada. At first, the model parameters values were statistically calibrated by using observed rainfall-runoff data of a gauged basin in the same area. Then, regression analysis was carried out between the model parameters and different land cover types in the drainage basins. The resulted regression model was used for calculating the model parameters for the ungauged basin and hence to predict the runoff values in the same basin by inputting precipitation data to the rainfall-runoff model. The model implementation was performed in GIS environment and finally, a map was produced showing the runoff volumes in the study area.

De Winnaar et al. (2007) identified the potential runoff harvesting sites in GIS platform by understanding the spatial diversity in topographical parameters in Potshini catchment of South Africa. To determine the potential runoff generation area, slope and SCS curve numbers maps were combined. Whereas, suitable runoff harvesting sites were determined based on the amount of runoff and need of runoff harvesting from the socio-economic point of view and distance from the residential areas and croplands. It was found that 17% of the study catchment area has a high potential for surface runoff generation and 18% is having the suitability for runoff harvesting.

Ramlal and Baban (2008) presented some flood and watershed management strategies in Caparo River Basin of West Indies based on the estimation of the soil erosion from the river basin and the morphological characteristics of the river in GIS environment. For calculating the soil loss, RUSLE model was used and a morphological study was done based on river field survey and collected data. It was mentioned that the flood problem in the study basin can be mitigated to a large extent by implementing the watershed management plan, land acquisition plan and also by increasing the conveyance capacity of the river through flood control works.

Bahadur (2009) prepared soil erosion risk map by using remote sensing and GIS in Upper Nam Wa Watershed in Thailand. The watershed was divided into grid cells of homogeneous hydrological, topographical, and geographical characteristics. Raster maps of all the parameters of universal soil loss equation (USLE) were prepared in GIS and used to calculate the soil erosion in every cell. Cells having shifting cultivation were found to have the highest rate of soil erosion.

Chen et al. (2009) used a GIS-based urban flood inundation model (GUFIM) in order to a get flood inundation map of the campus of University of Memphis in Memphis, Tennesseean. The model comprises two components: (i) a storm–runoff model which gives surface runoff by using Green–Ampt equations and (ii) a flat water model which produces a grid-based map of flood inundation depths by using the output of the storm-runoff model as input to it. GUFIM was found to be useful for giving accurate results with reasonable requirements of inputs and hardware.

Santillan et al. (2012) integrated RS, GIS and hydrologic models to determine the effect of LULC change on increase in runoff and sediment yield from Taguibo watershed in

Philippines. LULC change detection was carried out by using Landsat and ETM+ satellite data. Rainfall-runoff modelling was done by using SCSCN method and soil loss was calculated by modified universal soil loss equation (MUSLE).

Singh et al. (2017) used GIS-based multi-criteria decision analysis for identification and prioritization of rainwater harvesting sites in order to meet the water supply demand in upper Damodar River basin of West Bengal, India. For mapping rainwater harvesting potential, weighted thematic maps of runoff coefficient, slope and drainage density and they were combined linearly in GIS environment. On the other hand, rainwater harvesting demand areas were identified by combining the weighted thematic maps of water requirement, groundwater table fluctuations and the post-monsoon groundwater table.

2.8 Critical appraisal of literature review

From the literature review, it is clear that several approaches are available for quantification of impervious cover or built-up area in a place. Historically, many studies have used population density to estimate urban settlement (Stankowski 1972; Chabaeva et al. 2004). On the other hand, Graham et al. (1974) found housing density as the best parameter for giving a good estimate of urban settlement in comparison with population density and employment density. These empirical relationships are useful tools for the urban planners and decision makers as those can be used for future projection of the same (Graham et al. 1974). Urban settlement can also be projected by using spatially explicit regional growth model (SERGOM) (Theobald 2005; Theobald et al. 2009; Bierwagen et al. 2010) and multiple data source method (MDS) (Bird et al. 2002; Exum et al. 2005). Where SERGOM relates future housing density to impervious cover, MDS method considers that imperviousness is generated not only for residential development but also for construction of roads, commercial/industrial buildings. Hence, in this method, for projection of impervious area in a city, future residential as well as commercial, industrial and transportation-related developments have been included. Use of satellite imagery derived from remote sensing in estimation of impervious surface (Ji and Jensen 1999; Han and Burian 2009; Weng 2012; Sahoo and Sreeja 2011; Dams et al. 2013; Dhorde et al. 2012) can be said as a milestone towards cost-effectiveness and swiftness. From the accuracy point of view, although impervious surface measurement by the traditional ground survey is the best method (Lee and

Heaney 2003), this is very labour intensive and not applicable to the large and remote area. Again, cellular automata models like SLEUTH (Clarke and Gaydos 1998), CLUE and CLUE-S (Veldkamp and Fresco 1996; Verburg et al. 2002) have also been used for modelling and projecting the future urban as well as multiple land use land cover (LULC) change. Despite the extensive use of these cellular automata models for prediction of LULC change at regional scale, they are less accurate for predicting local level LULC change, e.g. prediction of urban development around National Parks (Otis 2012). Again, a few studies (Alley and Veenhuis 1983; Laenen 1983; Boyd et al. 1993; Sutherland 1995; Han and Burian 2009; Sahoo and Sreeja 2011) have been done on the estimation of EIA. EIA is the impervious area in the catchment that is directly connected to stream channels. It means that impervious area draining water to a pervious area is not considered as effective in runoff generation. For accurate estimation of runoff generation from a catchment, it is very important to determine EIA since TIA overestimates the runoff. In some previous studies, EIA has also been estimated by relating it to rainfall- runoff ratio (Laenen 1983; Boyd et al., 1993). However, this approach requires observed rainfall-runoff data from the watershed. Again, the method can be sensitive to errors in rainfall-runoff measurements and also the method is not appropriate to basins with moderate to low permeable soil (Alley and Veenhuis 1983). Hence, all these past works undoubtedly show the research advances in indirect estimation and projection of urban settlement in general in a city. However, high rate of environmental degradation due to the continuous diminishment of urban forests and wetlands demands further research on modelling of urban settlement in eco-sensitive areas located within or near a city, interpreting its relationship with various factors of urbanization.

The reviewed literature gives an idea of the impact of impervious cover on hydrology. With the increase of imperviousness in an area, the groundwater recharge, stream base flow, evapotranspiration decrease and surface runoff increases. Although assessment of these impacts can be carried out by direct measurements of the rainfall and discharge at streams and the groundwater levels at wells (Burns et al. 2005), this method is quite time-consuming and labour intensive. Through the use of some assumptions, mathematical models and various empirical equations have been developed to determine the amount of runoff resulted from rainfall. Despite the fact that they are not capable of exactly replicating the complex conversion process from rainfall to runoff, with some limitations or approximations, these models and empirical equations are capable of giving reasonably good results. It is also true that more the availability of input data to a model better the results of the model. As mentioned in the literature review, a numbers of hydrological models such as HSPF (Brun and Band 2000), SWAT (Goetz et al. 2011; Wagner et al. 2013; Li et al. 2015), MODHMS (Barron et al. 2013) etc. have been used for evaluating the impact of impervious cover on hydrology. Calibration of parameters of these models requires historical data of rainfall and runoff of the study area. As a result, these models are not directly applicable to ungauged basin having no historical observed runoff data. However, through the use of regionalization techniques, these hydrological models have been applied to a number of ungauged watersheds. Mainly two ideas are applied in regionalizing the model parameters (Merz et al. 2006). One is based on the assumption that neighbouring catchments have similar hydrologic behaviours (Mosely 1981). This is called geographical regionalization (Vandewiele and Elias 1995). In this technique, model parameters derived from a gauged basin are applied to a nearby ungauged basin. This idea is not very useful as the neighbouring catchments can also be vastly dissimilar in hydrological characteristics (Beven 2000; Piman and Babel 2013). Another idea of regionalization is based on the similarity of catchments attributes (catchment dimensions, vegetation type etc.) and climate variables (mean annual rainfall, temperature etc.) (Acreman and Sinclair 1986; Post et al. 1998). Yet, this concept was not too successful as most of the catchment characteristics are measured at only land surface whereas the total runoff resulted from precipitation is highly dependent on the sub-surface condition of the catchment (Merz et al. 2006). Additionally, it is not an easy task to find a homogeneous gauged catchment which has similar hydrologic or catchment characteristics with those of the ungauged catchment. In spite of all these complex techniques used for determination of runoff from an ungauged watershed, Rational Method (Kuichling 1889) which is one of the most widely used methods can be applied to determine the peak runoff generated from a watershed. This Rational Method is quite simple and gives the peak surface runoff without using any observed runoff data. Hence, in this study, for evaluating the impact of urbanization on runoff generation from ungauged watersheds, Rational Method has been used.

The synoptic review of the sediment yield models implies that process-based physical soil loss estimation models are a little bit complex and are not applicable in absence of observed soil loss data. Among the available empirical models, USLE/RUSLE methods are found to have ample application in analysing the sediment yield characteristics from different types of LULC (Sarma 2011). Use of remote sensing and GIS techniques in USLE/RUSLE model is another milestone in the history of soil loss estimation. Researchers from different parts of the world have extensively used GIS techniques to measure the amount of soil loss from a watershed (Fistikoglu and Harmancioglu 2002, Dabral et al. 2008, Panday et al. 2007, Biswas and Pani 2015). The soil erosion map derived by using GIS tools helps to identify the erosion-prone areas, which basically acts as a key input into the sustainable watershed management practices. For the current research work, based on the simplicity of input data requirement, GIS-based RUSLE is found to be appropriate to apply. Presently, urban planners are giving more interest on sediment yield control by using ecological management practices (EMP) like grass, forest, gardens, detention ponds etc. (Sarma 2011). The effectiveness of these practices is well dependent on geological, topographic and climatic conditions of the watershed. The literature review revealed that with the ease of RS and GIS along with the use of optimization techniques, a few studies have determined the optimum combination of different ecological land covers for controlling runoff and sediments from hilly watersheds (Sarma et al. 2013; Sarma et al. 2015). However, in developing countries like India, urban settlements are expanding to hilly areas in a very unplanned and unscientific way. Hence, in-depth research is required to precisely estimate the soil loss from hilly watersheds and based on those estimations, best management practices should be implemented.

2.9 Scope of the work

The eco-friendly urban planning and design, the ideal aim of the urban planners, requires urban settlement projection in eco-sensitive areas. The reviewed literature reveals that very few works have been reported on the analysis of causes of urban expansion to eco-sensitive areas and its future projection, especially in developing countries. Therefore, an intense research is urgently required to fill this research gap. Again, there exists limitted research evaluating the impact of future urban settlement on hydrology. Based on these needs, the scope of the research work have been defined as –

I. To get insight into the actual processes that compel people to settle in eco-sensitive areas despite the fact that these areas are not well-suited for residential purpose and hence, to introduce a model for indirect quantification of urban settlement in an eco-sensitive area by using a wide range of influencing factors.

II. To perform a case study to test and describe the practical efficiency/usefulness of the developed model and to apply the developed model for the projection of urban settlement in eco-sensitive areas of the city considered for the case study.

III. To generate future land use land cover (LULC) maps of the eco-sensitive areas by spatially allocating the projected urban settlement in GIS platform.

IV. To determine the impact of the projected urban settlement on watershed hydrology. For the impact analysis, basically, two hydrological components have been chosen- (a) peak runoff (b) soil loss. This study investigates a promising step towards the precise estimation soil loss from urban hilly watersheds in GIS-platform.

V. Finally, to propose an optimal combination of ecological management practices (EMP) to mitigate the adverse effects of urbanization on sediment and water yield from the study area.

Chapter-3

Model development for indirect quantification of urban settlement in eco-sensitive area

3.1 Introduction

According to Preston (1979), demographic, economic and political situation of a city strongly influences its expansion. Jedwab et al. (2015) also state that for developing countries (with low economic growth) demography plays the prime role in urban expansion. This chapter presents a modelling approach of quantifying urban settlement in eco-sensitive areas by deriving its statistical relation with relevant socio-economic, demographic and geographical factors. The model has been referred as the model for Assessment of Settlements in Eco-sensitive Area (ASEA). The basic assumption of this model is—‘‘Urban expansion into an eco-sensitive area present in a city depends on the demographic and socio-economic condition of the city’’. The proposed modelling approach is more relevant to developing countries where eco-sensitive areas are not strictly conserved.

3.2 Model Development

Activities and demographic characteristic of a plain urban area, located in close proximity to a particular type of eco-sensitive area, influence the habitation growth in that eco-sensitive area. This influencing plain urban area located adjacent to the eco-sensitive area is termed as ‘‘area of influence’’ (AOI) of that eco-sensitive area. Green hills, forests, and wetlands are the most commonly found eco-sensitive areas in and around a city. Though the proposed modelling concept can be applied to any type of eco-sensitive area, the potential driving factors considered for a particular type of eco-sensitive area may not be relevant to another type of eco-sensitive area. If the social and geographical condition of a city is almost uniform, allotment of AOI for an eco-sensitive area can be done by Euclidian allocation, where every cell in the image of the study area is assigned to an eco-sensitive area which is closest to that cell. Otherwise, it should be allotted giving due emphasis on geographical and social uniformity extent. Potential factors considered in the proposed ASEA model are given below:

(a) Free space availability in AOI (A_f): Due to the availability of more resources and facilities, people prefer to settle in a plain urban area, which is ideal for residential purpose. Gradually, as the plain plots of land become scarce in the main city area, the city starts to expand both in the outward direction and to the eco-sensitive areas located in the city (Rahman et al. 2008; Sultana et al. 2009; Ajibola et al. 2012). From this view, low availability of free space in AOI is considered as an indicator of increasing urban settlement in the corresponding eco-sensitive area. A_f can be considered as a demographic factor since it depends on urban population growth. However, this free space excludes areas (A_0) with no likelihood of having urban settlement, e.g. river, lake, wildlife sanctuary, zoo, park, playground (Clarke and Gaydos 1998). Hence, A_f is expressed as,

$$A_f \text{ (in \% of } A_n) = \frac{(A_i - A_0) - A_{us}}{A_n} \times 100\% = \frac{A_n - A_{us}}{A_n} \times 100\% \qquad (3.1)$$

where,

A_i = AOI of the eco-sensitive area.

A_0 = Areas with no likelihood of having urban settlement.

A_n = Net AOI where urban settlement is possible $= A_i - A_0$

A_{us} = Urban settlement area in A_i.

(b) Commercial unit density in AOI (C_u): Commercial growth which can be measured in terms of clear count of shops or local markets is one of the major signs of urbanization. People are attracted towards an area having better facilities added by commercial development in that area (Preston 1979). Consequently, the growth of C_u (numbers of commercial units or shops per unit area) forces to increase urban settlement in the corresponding eco-sensitive area. Here, C_u can be considered as socio-economic as well as a demographic factor since its growth is governed by both size of population (local needs or demands) and the socio-economic status of the society.

(c) Land value in AOI (L_v): Land value is an important factor influencing urban sprawl (Amoateng et al. 2013; Oueslati et al. 2014). In general, land value is a function of various factors like geographical location of the area, accessibility to various facilities like shopping, school, parks and playgrounds and increasing demand of plot with population growth. Hence, L_v is affected by the geographical, socioeconomic and demographic characteristic of the area. In developing countries, plain urban areas are having high land values which are not affordable by low-moderate income group of people (Sarma et al. 2015). Due to the lack of strict regulation of the protection acts, these people encroach on the eco-sensitive areas causing unauthorized settlement in those prohibited lands.

(d) Geographical condition of the eco-sensitive area (G_i): The geographical condition or the site quality determines the developmental potential in an area (Lee 1979). As for example, average slope and average elevation in case of a hill and water depth in case of a wetland may affect the extent of urban settlement in that hill or wetland. Here, the subscript ‘‘i’’ in G_i indicates the type of the geographical parameter. Every type can be considered as an individual factor in the model.

(e) Favouring index (F): Apart from the above-mentioned factors, some additional factors like educational facilities, tourism activities, economic activities and location of the eco-sensitive area also favour urban growth in an eco-sensitive area. A favouring index F has been introduced to indicate combined effect of all such factors. The capability of these components to pull urban population is incorporated in computing ‘‘F’’ in terms of some weights. Available literature or data on the contribution of these components to increasing urban settlement in the study area can help to determine the weights. Otherwise, these can also be determined by expert weighting approach (Goetz et al. 2011), i.e. applying weight based on the opinion of experienced urban planners and other stakeholders having in-depth knowledge on urban growth of the study area. Finally, ‘‘F’’ for every eco-sensitive area is calculated as the average of the weights given to all of these components, i.e.

$$F = \frac{\sum_{i=1}^{4} W_i}{4} \tag{3.2}$$

where,

$i = 1, 2, 3, 4$ are the components of 'F'.

W_i = Weight applied to the i^{th} component of 'F'.

Details of the components of F are given below:

i. **Educational facilities in AOI:** In developing countries, rural-urban migration for education is playing a key role in increasing urban population (Ichimura 2003; Acharjee et al. 2013). For easy access, people prefer to settle in a place located in the proximity of an educational institute. Moreover, with the establishment of a new university or college in an area, construction of hostels, staff quarters, etc., contributes to increment of urban settlement in that area. From this viewpoint, the educational facility in an AOI, which improves the socio-economic condition of a place by improving the personal proficiencies, livelihood, social awareness, people's involvement in socio-economic activities, is considered as a favouring factor for urban settlement. Weight is assigned based on how many numbers of higher educational institutes are present in an AOI.

ii. **Tourist places in AOI**: Tourist places can be considered as a socio-economic factor influencing urban settlement in an area, as it can improve the socio-economic condition of an area by producing opportunities for businesses and employment and also by influencing the lifestyle and culture (Liu et al. 2015). Additionally, due to the presence of such a tourist place, the special development plan is taken for that area to provide more facilities to tourists, which, in turn, attracts more people to settle in that place (Dumitru 2012). Weight for tourist place is given based on its degree of importance and also on the basis of numbers of tourist places within an AOI.

iii. **Economically active places in AOI:** Urbanization and economic development are the two sides of the same coin. Economic development acts as the pull factor in rural-urban migration (Henderson 2003; Jedwab et al. 2015). Here, economically active places indicate city-level places for small-scale industry, major industry, construction, trade and commerce, transportation, communication, etc. These are the sources of job/ income opportunities for all economic groups of people, and hence, urban settlement increases in the nearby area. Weight for this factor is assigned depending on how many prominent economically active areas are lying in the AOI of an eco-sensitive area.

iv. **Location of the eco-sensitive area with respect to the city centre:** Eco-sensitive areas, which are located in core city area, become the very early victims of urban settlement (Tan et al. 2013; Mensah 2014). Therefore, the location of the eco-sensitive area with respect to core city area has been considered as urban settlement favouring factor and some weight is assigned to an eco-sensitive area based on the percentage of AOI lying within the heart of the city.

Considering all the above-mentioned factors, the proposed ASEA model can be expressed as:

$$E_{us} = f(A_f, C_u, L_v, G_i, F) \qquad (3.3)$$

Here, E_{us} is the amount of urban settlement in the eco-sensitive area (in % of area). The model structure is presented in Fig. 3.1. For modelling urban development in an eco-sensitive area of a particular city, one essential task is to check whether and how the urban settlement in an eco-sensitive area is influenced by every individual factor (independent variable). The efficiency of the ASEA model also depends on the availability of data. More the dataset, better will be the model. Therefore, availability of historical data series is desired. In the absence of a historical record, which is very common in developing countries, data set of similar type of eco-sensitive areas can also be used for developing the model.

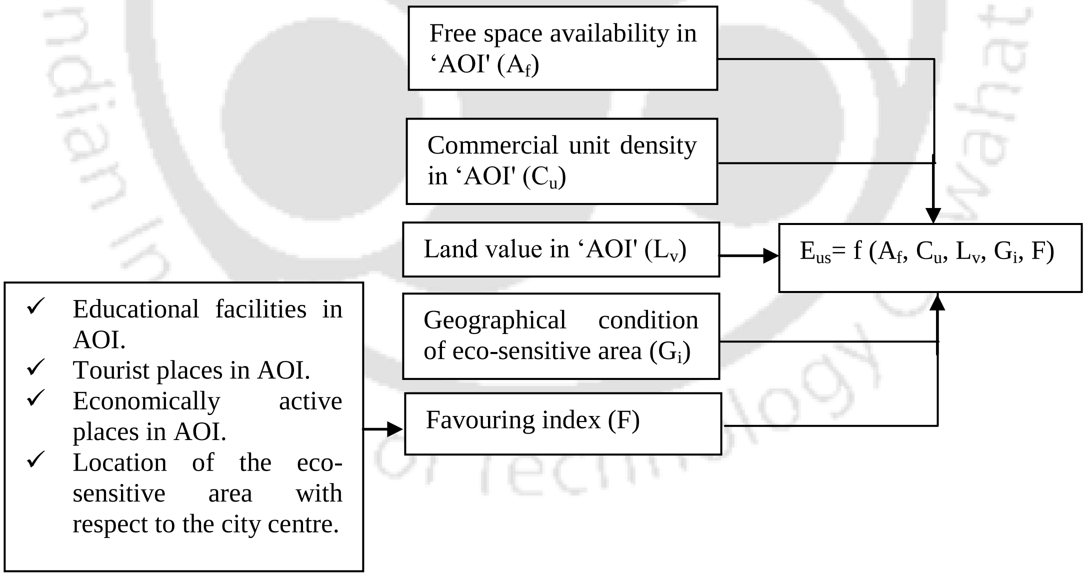

Fig. 3.1: ASEA model structure

3.2 Case study

3.2.1 Description of the study area

Guwahati, the gateway to the North-East India is one of the fastest growing cities in India. It is located in Kamrup district of state Assam. It is situated between the mighty Brahmaputra and the Shillong plateau with geographic coordinates from 26° 4' 45" to 26° 13' 25" North Latitude and from 91° 34' 25" and 91° 52' 00" East Longitude. The city is surrounded by hills, except a little portion where the Bharalu, a tributary of the Brahmaputra confluences with the Brahmaputra. In the west side of the city there is Nilachal Hill on the southern banks of the Brahmaputra, to the north there is Chitrachal Hill and to the south Narakasur Hill is situated. To the south-west of the city, there is Dipor Bil, one of the largest lakes in the Brahmaputra valley of Lower Assam. The topography of the city is undulating comprising plains and hills. Elevation of its plain area ranges from 49.5 to 55.5 m above mean sea level (MSL), and elevation of its hilly area goes up to 327 m. Guwahati has a humid subtropical climate with an average annual temperature 24.2°C and the average annual rainfall 1600 mm. Guwahati is the main centre of economic activity in the entire North-East region. Desai et al. (2014) said: ‘‘Being a primary city in a region with low economic growth, an agrarian crisis and ecological degradation, and ethnic conflicts and insurgency movements, Guwahati became a magnet for migrants from surrounding regions’’. According to the census of India—2001, due to various types of migrations like intra-district (35.9%), inter-district (43%), interstate (19.6%) and cross-borders (1.5%), total migrated population of Guwahati city is 378,657. Again, 30.2% of these migrants are moving into Guwahati for livelihood (business and employment). Next major reason is the family movement (16.9%). Demographically, Guwahati is one of the most dynamic cities in India having an exponential population growth. Establishment of Gauhati University (1948), North-East Frontier Railway Headquarters (1958), engineering college, medical college, oil refinery (1962), construction of the Saraighat Bridge (1964), etc., became the reason of the initial significant importance of Guwahati city in the entire North-East India. Fig. 3.2 shows decadal population data of Guwahati Municipal Corporation Area (GMCA) from 1901 to 2011. Historically, the increase in population is mainly observed in two stages—1951 to 1961, associated with post-independence migration from East Pakistan (Bangladesh) and 1971 to 1991, associated with the shifting of the capital of Assam from Shillong to Guwahati (Dispur) in 1971.

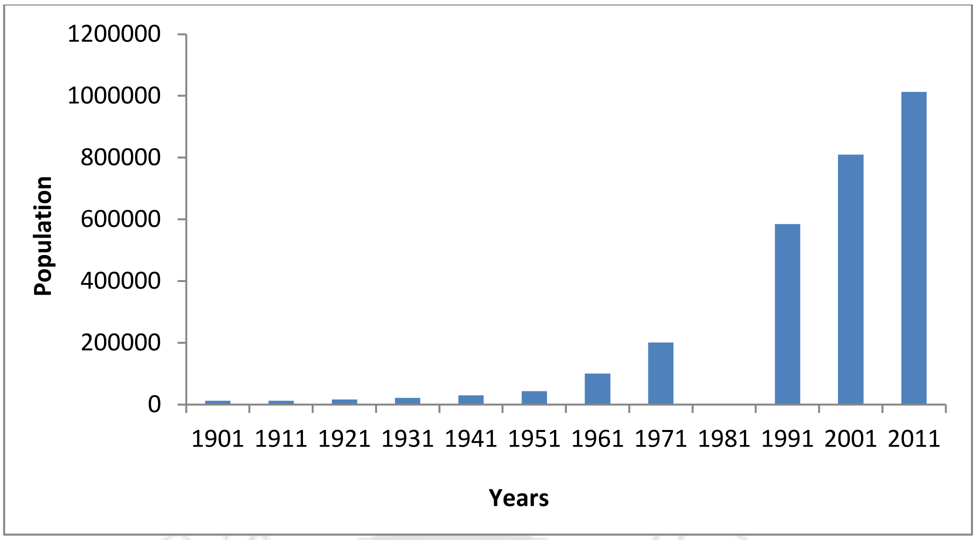

Fig. 3.2: Population in GMCA (Data source: Census of India; no Census could be conducted in Guwahati in 1981)

According to Hussain and Phanjoubham (2007), construction of administrative and residential blocks resulted from shifting of the capital in 1971 has displaced about 1 lakh people from plain areas, most of whom moved to the hills of Guwahati city. In the core city area, informal land market constituting informal occupation of government lands and selling of these lands at a very high price is another reason for increasing urban settlement in hills of Guwahati city. Many poor people who were occupying state government land in plain core city area eventually sold out their land and resettled in the hills (Desai et al. 2014). Additionally, the poor migrants coming to Guwahati city either in search of jobs or getting displaced by the devastating flood are also contributing to increasing settlement in hills. The uncontrolled growth of population along with the lack of coordination between different departments related to construction and development of the city, the absence of efficient planning and management policy, the insufficient funding (low budget) and the un-enforcement of municipal regulation has made Guwahati city one of the most unplanned cities in India. The unauthorized and unscientific settlements altering the natural drainage system of the city are adding fuel to this unplanned development of the city. A field survey conducted by Sarma (2011) in hills of Guwahati city reveals that high rate of urban settlement caused by the low-income group of people is leading to deforestation in the hills resulting in massive landslides, soil erosion and urban flash floods in Guwahati city. Due to increased urbanization, dense vegetative cover mostly lying in hills of Guwahati Metropolitan Area (GMA) has degraded with a rate of 4.8% in 2000 to

26.3% in 2009 (Borthakur and Nath 2012). In order to protect these hill lands and other ecological sites, Assam State Government has enacted ‘‘The Assam Hill Land and Ecological Sites (Protection and Management) Act’’ in 2006. According to this act, all the hill lands lying in Guwahati city are included in ‘‘ecological site’’ and have been identified as ‘‘eco-sensitive zone’’ by Guwahati Metropolitan Development Authority (GMDA 2009). However, due to slackness in the enforcement of the act by the administration and also due to some political reasons, encroachment is still going on the hills, degrading the ecological balance of Guwahati (Desai et al. 2014). Hence, it indicates that hills of Guwahati city are ideal for testing the practical applicability of the proposed model.

The location of the study area is shown in Fig. 3.3. It is occupied by all the 60 wards of Guwahati Municipal Corporation (GMC) covering an area of 216 km^2 with approximate geographical coordinates from 26° 5′ to 26° 12′ North Latitude and from 91° 38′ to 91° 51′ East Longitude (in 2013, 60 wards of GMC have been merged to form 31 wards). There are 15 hills under GMCA. These are—(1) University, (2) Fatasil, (3) Kalapahar, (4) Sonaighuli, (5) Sarania, (6) Kharguli, (7) Japorigog, (8) Burhagosain, (9) Khanapara, (10) Garbhanga, (11) Kamakhya, (12) Kahilipara, (13) Betkuchi, (14) Chunsali and (15) Koinadhara (source: http://www.iitg.ac.in/coeiitg/monogram.pdf, as browsed on 26 November 2015). Out of these hills, Burhagosain, Khanapara, Garbhanga and Koinadhara hills are lying partly in the study area.

3.2.2 Data collection and generation required for model development of the study area

For the study area, although historical urban settlement data can be derived from satellite images, the other sets of data like land values, numbers of commercial units, etc., are not available for sufficient numbers of years. On the contrary, due to the availability of all aspects of data in the recent census year 2011, the model has been formed with spatially variable data of the year 2011 with respect to 15 hills of Guwahati city.

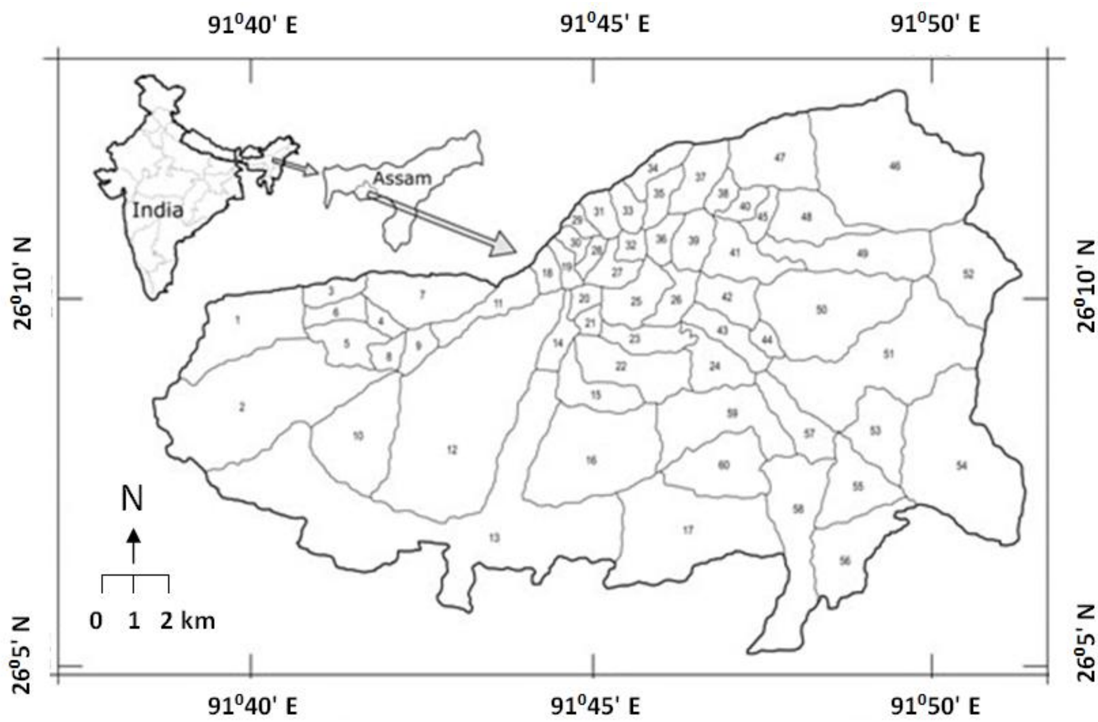

Fig. 3.3: Location of Guwahati city in India (Source: GMC)

3.2.2.1 Determination of urban settlement in hills and free spaces available in AOI

A Linear Imaging Self Scanning Sensor (LISS)-IV satellite image of 5.8 m resolution (capture date: 11 November 2011) was used for this purpose. Processing of the multispectral image has been performed in ERDAS Imagine (2014 version) platform. The image consists of three bands: band 4 (near infrared), band 3 (red) and band 2 (green). These three bands are stacked and a false colour composite is generated in the software where the data collected in band 4, band 3 and band 2 are displayed through the colour red, green and blue, respectively. To have good and distinct visual appearance of the inbuilt geo-referenced image, the brightness and contrast enhancement, atmospheric correction etc. were carried out. Again, the geographic information related tasks such as edition, storage, handling or management of spatial database etc. are executed in ArcGIS-9.3 software. Based on visual interpretations i.e. depending on their unique texture, shape and tone, the urban settlements, hills and various excluding areas like the river, lake, zoo, etc., are outlined from the image in ArcGIS-9.3. Delineated objects were also checked in high-resolution Google Earth view (imagery date: 31 December 2011). Since the study area (GMCA) has no distinct division based on social and geographical condition, the Euclidian allocation has been used to assign AOI to every hill. The location of the hills and their AOI in the LISS-IV image of the study area are shown in Fig. 3.4.

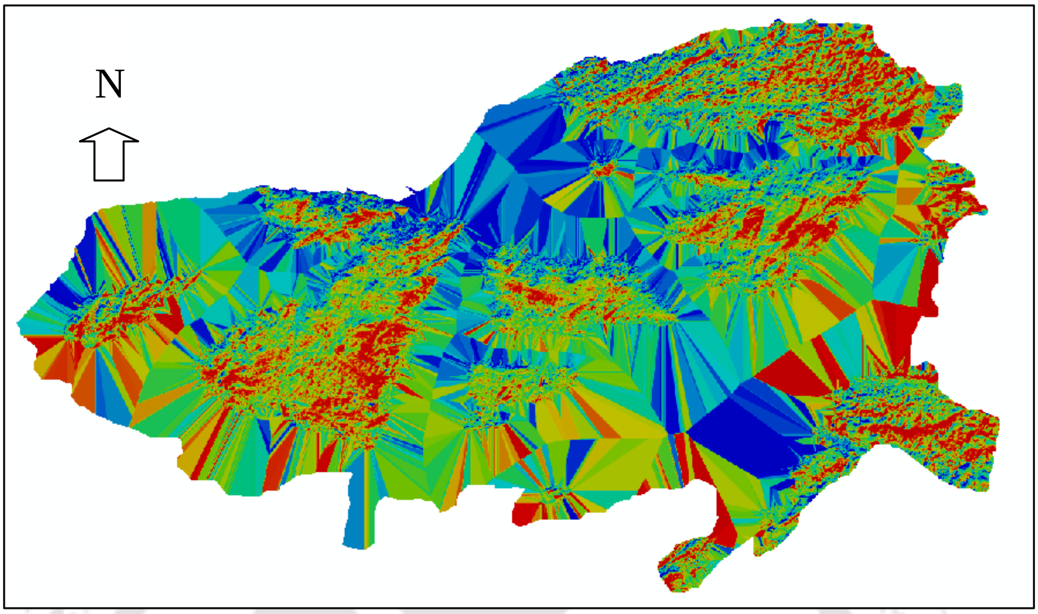

(i)

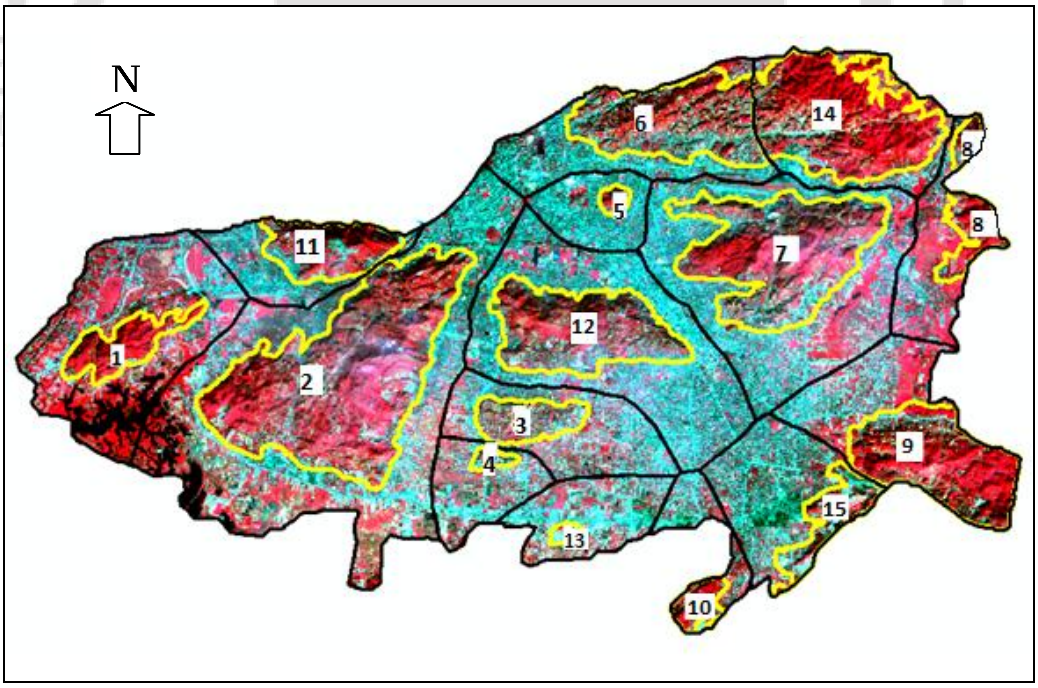

(ii)

Fig. 3.4: (i) Scene of Euclidean allocation (ii) Outlines of the hills (yellow) and AOIs (black line)

Till 2011, 28.43% of total area of Guwahati Municipal Corporation Area (GMCA) was found to have urban settlements. One important point is that out of the total area of Japorigog hill (9.65 sq. km), an area of 1.57 sq. km is covered by state zoo, which does not have the probability of having urban settlements in future. So, for Japorigog hill, urban settlement till 2011 has been expressed in terms of net hill area (excluding state zoo area). Finally, free space available in AOI of every hill is calculated by using Eq. (3.1) and is shown in Table 3.1.

Table 3.1: Urban settlement in hill and free space available in AOI in 2011

Hill ID	Hill name	Hill area (sq. km)	Urban settlement in hill, till 2011 (in % of hill area)	AOI (sq km)	Urban settlement in AOI, till 2011 (sq. km)	Excluding area (sq. km)	Net AOI (sq. km)	[*1]Free space in AOI in 2011 (%), A_f
1	**University**	2.10	7.85	13.34	1.98	2.95	10.39	80.91
2	**Fatasil**	15.91	12.47	22.07	6.51	1.77	20.30	67.93
3	**Kalapahar**	1.98	18.56	6.25	3.12	0.09	6.16	49.30
4	**Sonaighuli**	0.36	16.54	4.08	0.85	0.04	4.04	78.86
5	**Sarania**	0.34	28.31	3.62	2.30	0.10	3.52	34.63
6	**Kharguli**	6.54	25.87	5.26	2.63	0.21	5.05	47.95
7	**Japorigog**	9.65	17.49	13.14	5.97	0.87	12.26	51.35
8	**Burhagosain**	2.01	5.70	4.31	0.80	0.00	4.31	81.41
9	**Khanapara**	6.63	6.44	5.19	1.23	0.07	5.13	76.00
10	**Garbhanga**	0.95	8.21	2.20	0.73	0.04	2.17	66.30
11	**Kamakhya**	3.05	22.63	3.16	1.54	0.05	3.11	50.41
12	**Kahilipara**	6.62	20.91	12.97	8.43	0.34	12.62	33.24
13	**Betkuchi**	0.24	14.36	5.01	1.42	0.23	4.78	70.37
14	**Chunsali**	8.93	6.82	2.69	0.64	0.03	2.66	76.06
15	**Koinadhara**	2.22	14.03	6.93	3.26	0.09	6.84	52.39

[*1]Free space available in 2011 in AOI is expressed in % of net AOI.

3.2.2.2 Calculation of average slope and average elevation of hills

A slope map is prepared from Shuttle Radar Topography Mission (SRTM) Digital Elevation Model (DEM) of 1 arc-second resolution (downloaded from USGS earth explorer) in ArcGIS 9.3. Then, average elevation and slope for every hill are obtained by inputting the DEM and the slope map of the study area to the ‘‘zonal statistics as table tool’’ of ArcGIS 9.3. The DEM and the slope map of the study area are shown in Fig. 3.5 and Fig. 3.6, respectively. The average slope and elevation of individual hill are shown in Table 3.2.

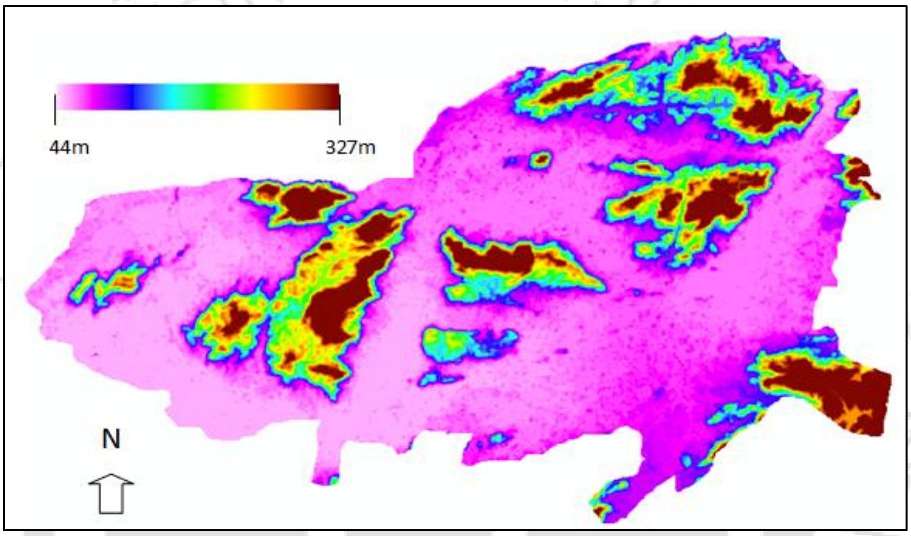

Fig. 3.5: DEM of the study area.

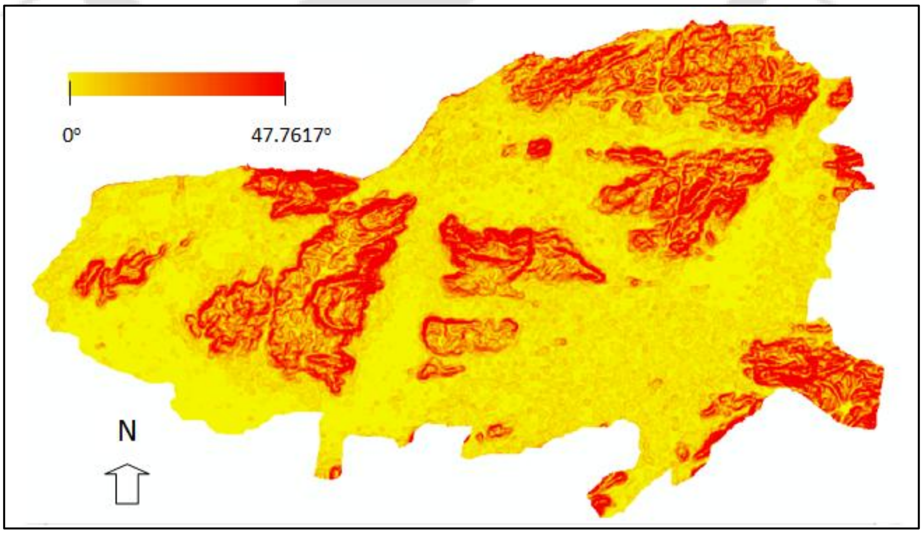

Fig. 3.6: Slope map of the study area

Table 3.2: Average elevation and average slope of hills

Hill ID.	Name of hills	Average slope (degree), G_1	Average elevation (m), G_2
1	University	13.78	90.85
2	Fatasil	12.96	127.72
3	Kalapahar	9.74	90.59
4	Sonaighuli	11.62	77.86
5	Sarania	19.68	99.35
6	Kharguli	10.94	98.91
7	Japorigog	13.76	119.13
8	Burhagosain	13.67	108.01
9	Khanapara	14.11	153.21
10	Garbhanga	10.97	88.60
11	Kamakhya	18.68	137.05
12	Kahilipara	13.12	118.37
13	Betkuchi	10.98	76.81
14	Chunsali	12.84	117.39
15	Koinadhara	10.57	85.03

3.2.2.3 Calculation of commercial unit density in AOI of hill

Numbers of commercial buildings lying in every ward of GMCA for the census year 2011 were collected from Property Tax Division of GMC. Different wards are contributing different amount of areas to AOIs of hills. Hence, numbers of commercial units in every AOI are calculated based on the percentage of ward area shared by an AOI. Fig. 3.7 shows the wards lying in the AOIs of the hills of Guwahati city. The calculated commercial unit densities (numbers of commercial units per unit AOI) are shown in Table 3.3.

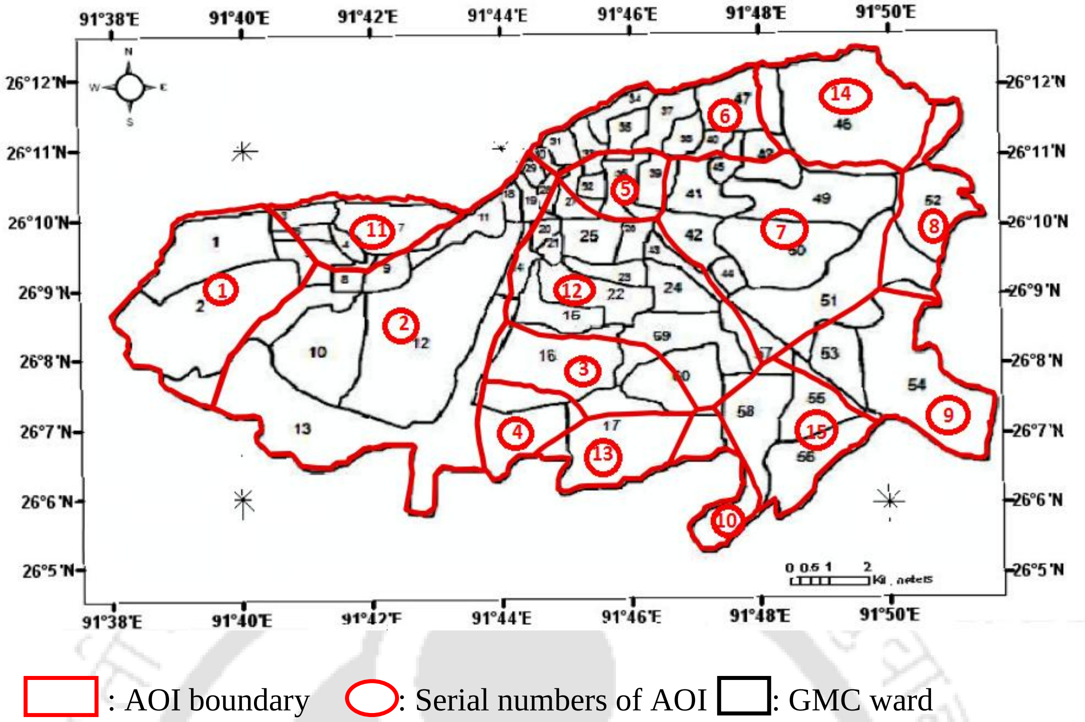

Fig. 3.7: GMC wards lying in areas influence of hills

Table 3.3: Commercial unit density (2011) in AOIs of hills

Hill ID.	Name of hills	Numbers of commercial units (2011)	AOI (sq km)	Commercial unit density (numbers/sq km), C_u
1	**University**	419	13.34	31.39
2	**Fatasil**	3953	22.07	179.09
3	**Kalapahar**	966	6.25	154.55
4	**Sonaighuli**	743	4.08	182.34
5	**Sarania**	851	3.62	234.94
6	**Kharguli**	1956	5.26	371.81
7	**Japorigog**	890	13.14	67.77
8	**Burhagosain**	148	4.31	34.34
9	**Khanapara**	267	5.19	51.35
10	**Garbhanga**	267	2.20	121.26
11	**Kamakhya**	377	3.16	119.34
12	**Kahilipara**	2909	12.97	224.33
13	**Betkuchi**	533	5.01	106.31
14	**Chunsali**	26	2.69	9.49
15	**Koinadhara**	611	6.93	88.24

3.2.2.4 Determination of land value in the AOI of a hill

Lists of land values of Guwahati city for the census year 2011 were collected from Revenue Branch of Kamrup Metropolitan district. In these lists, the land value of a locality within an AOI varies depending on its distance from main roads. An average land value has been determined for every AOI based on area-weighted method. In the official list, land values have been expressed in a unit of 'bigha'. In Assam, 1 bigha is equal to 1340 m^2. Here, the calculated average land values have been expressed in square metre. These are displayed in Table 3.4.

Table 3.4: Land value (2011) in AOIs of hills

Hill ID.	Name of hills	Land Value (Rs/Bigha) (2011)	Land Value (Rs/sq m), L_v
1	University	4167000	3109.70
2	Fatasil	5535750	4131.16
3	Kalapahar	8085000	6033.58
4	Sonaighuli	7000000	5223.88
5	Sarania	15800000	11791.04
6	Kharguli	13965000	10421.64
7	Japorigog	8060000	6014.93
8	Burhagosain	2475000	1847.01
9	Khanapara	4950000	3694.03
10	Garbhanga	6200000	4626.87
11	Kamakhya	12220000	9119.40
12	Kahilipara	11835000	8832.09
13	Betkuchi	6760000	5044.78
14	Chunsali	3200000	2388.06
15	Koinadhara	6720000	5014.93

3.2.2.5 Assignment of favouring index to AOI

Names of the major educational institutes (Govt./provincialised) are taken from Directorate of Higher Education and Directorate of Technical Education, Govt. of Assam. On the other hand, tourist places and economically active areas are obtained from the master plan of Guwahati Metropolitan area-2025 (GMDA 2009). For the study area, no statistical data are available on the contribution of components of favouring index on increasing urban settlement. Hence, an expert opinion survey has been conducted among the urban planners and other stakeholders who are closely related to the city development programs and have knowledge on historical growth of the city. Through this survey, weights to every component of ‘‘F’’ have been applied on a scale of 0–1. Based on their view on the role of every institute of an AOI on increasing settlement in its corresponding hills, experts were asked to categorize the educational institutes into two classes—significant level and average level. AOI of Sarania and Kahilipara hills, having the highest numbers of higher educational institutes (2 significant and 5 average levels), gets the highest weight (=1). Next, AOI of university hill which contains 3 significant institutes acquires the second highest weight (=0.6). Accordingly, weights applied to every average and significant level institute is obtained as 0.12 and 0.2, respectively. Similarly, Kamakhya temple, located on the top of the Kamakhya hill, is the most prominent tourist place in Guwahati, and hence, it gets the highest weight (=1) in the expert opinion survey. Weights to the other tourist places were assigned by experts based on the role of tourist places on providing job/business opportunities and growing developmental activities in the neighbouring area. Depending on the degree of economic activeness, weights have been applied by the experts to these places. On the other hand, weights for the location of the hill with respect to the core city area have been assigned based on the percentage of AOI lying within the core city area. Here, the old municipal area of Guwahati city has been considered as the core city area. Finally, ‘‘F’’ for every hill is calculated by taking the average of the weights given to all of the four components. These values are displayed in Table 3.5.

Table 3.5: Favouring indices for hills of Guwahati city

Hill ID.	Name of hills	Total weight for educational facilities in AOI of hill	Weight for Major tourist places in AOI	Weight indicating present economic activities in AOI	Weight indicating Location of hill in heart of city	Favouring index, F
1	**University**	0.60	0.35	0.00	0.00	0.24
2	**Fatasil**	0.36	0.00	0.40	0.30	0.27
3	**Kalapahar**	0.00	0.00	1.00	0.70	0.43
4	**Sonaighuli**	0.00	0.00	0.30	0.00	0.08
5	**Sarania**	1.00	0.20	1.00	1.00	0.80
6	**Kharguli**	0.40	0.90	0.90	1.00	0.80
7	**Japorigog**	0.00	1.00	0.40	0.30	0.43
8	**Burhagosain**	0.00	0.00	0.00	0.00	0.00
9	**Khanapara**	0.00	0.60	0.00	0.00	0.15
10	**Garbhanga**	0.00	0.30	0.00	0.00	0.08
11	**Kamakhya**	0.24	1.00	1.00	0.80	0.76
12	**Kahilipara**	1.00	0.00	1.00	1.00	0.75
13	**Betkuchi**	0.00	0.00	0.90	0.00	0.23
14	**Chunsali**	0.00	0.00	0.00	0.00	0.00
15	**Koinadhara**	0.40	0.00	0.80	0.00	0.30

3.2.3 Model development for the study area

Calibration and validation are two important parts of model development. Calibration is the process of fixing of the constants and coefficients of a model in such a way that it can replicate the observed data or can produce realistic results. On the other hand, validation is the process of application of the calibrated model and comparison of the model results with a set observed data other than those used for calibration of the model. In this study, the model is calibrated with respect to data of first ten numbers of hills (from Hill ID 1 to 10) and is validated against the remaining five numbers of hills (from Hill ID 11 to 15). For the study area, the independent variables assumed to influence the urban settlement in hills are- (1) average slope of hill (G_1) (2) average elevation of hill (G_2) (3) commercial unit density in AOI of hill (C_u) (4) free space available in AOI of hill (A_f) (5) land value in AOI of hill (L_v) and (6) favouring index (F). Values of the potential influencing factors of urban settlement in hills of Guwahati city are presented in Table 3.6. For better interpretation of variability of these variables, these are normalized (feature scaling) to a range of (1, 10). Before modelling, it is important to check how and whether all these potential factors really influence the urban settlement in the hills of Guwahati city. Therefore, the relation of each of these factors with urban settlements in hills (hill ID from 1 to 10) is analysed by fitting both linear and various non-linear forms of equations. Fig. 3.8 (a)-(f) shows the dependency of hill settlement on each of these factors.

Table 3.6: Values of potential influencing factors of urban settlement in hills of Guwahati city.

Hill ID	Hill name	G_1 (Degree)	G_2 (m)	C_u (numbers/sq km)	A_f (%)	L_v (Rs/sq km)	F
1	**University**	13.78	90.85	31.39	80.91	3109.70	0.24
2	**Fatasil**	12.96	127.72	179.09	67.93	4131.16	0.27
3	**Kalapahar**	9.74	90.59	154.55	49.30	6033.58	0.43
4	**Sonaighuli**	11.62	77.86	182.34	78.86	5223.88	0.08
5	**Sarania**	19.68	99.35	234.94	34.63	11791.04	0.80
6	**Kharguli**	10.94	98.91	371.81	47.95	10421.64	0.80
7	**Japorigog**	13.76	119.13	67.77	51.35	6014.93	0.43
8	**Burhagosain**	13.67	108.01	34.34	81.41	1847.01	0.00
9	**Khanapara**	14.11	153.21	51.35	76.00	3694.03	0.15
10	**Garbhanga**	10.97	88.60	121.26	66.30	4626.87	0.08
11	**Kamakhya**	18.68	137.05	119.34	50.41	9119.40	0.76
12	**Kahilipara**	13.12	118.37	224.33	33.24	8832.09	0.75
13	**Betkuchi**	10.98	76.81	106.31	70.37	5044.78	0.23
14	**Chunsali**	12.84	117.39	9.49	76.06	2388.06	0.00
15	**Koinadhara**	10.57	85.03	88.24	52.39	5014.93	0.30

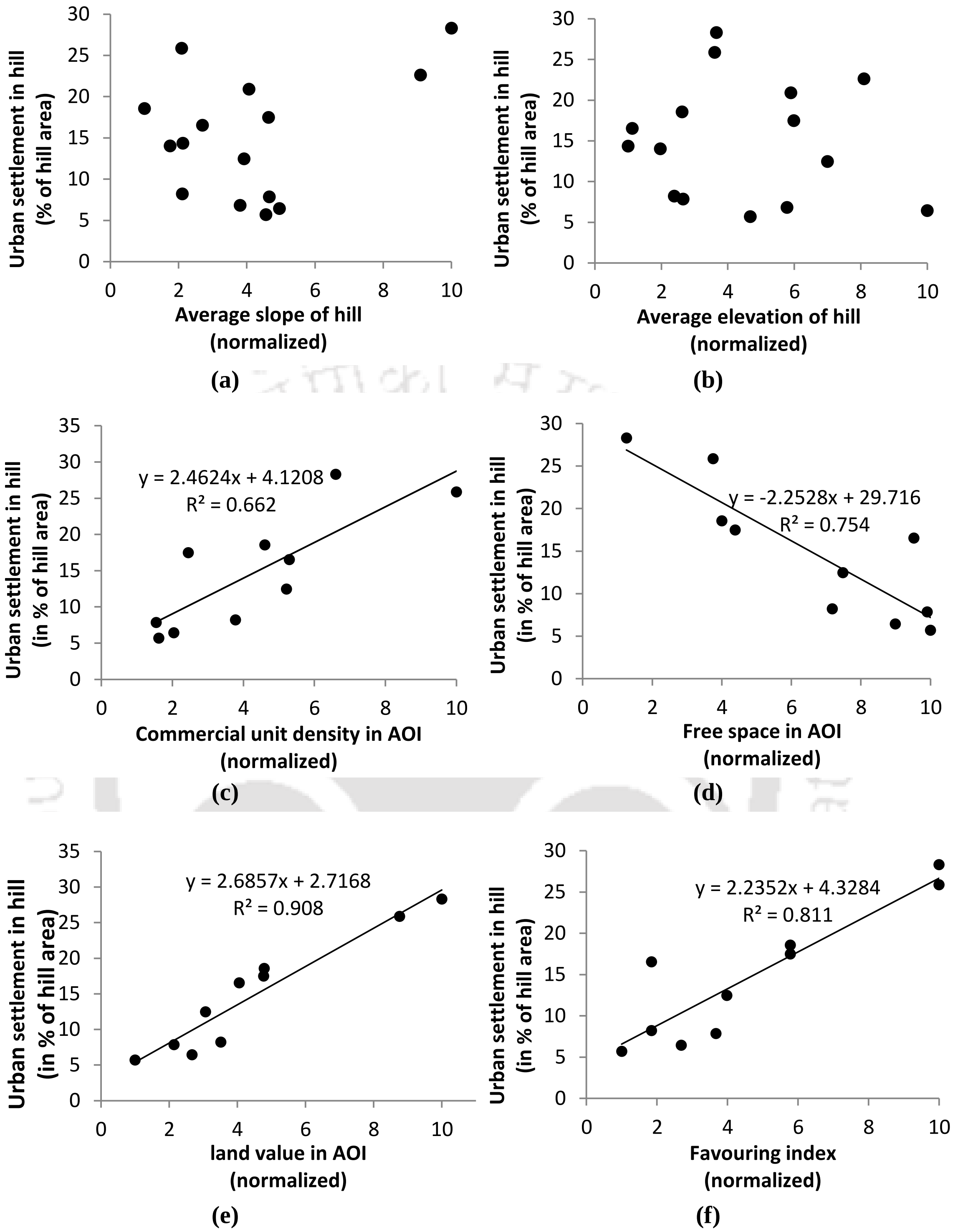

Fig. 3.8: Urban settlement in hill versus- (a) average slope of hill (b) average elevation of hill (c) commercial unit density in AOI (d) available free space in AOI (e) average land value in AOI (f) favouring index.

From Fig. 3.8, it is observed that urban settlement in hills of Guwahati city has no linear or nonlinear relation with average slopes and average elevations of hills. Hence, these two variables are avoided in the model specifically developed for Guwahati city.

Again, all the other four factors are found to have fairly good linear correlations with the urban settlement in hills of Guwahati city. This indicates that other factors being fulfilled, people are ready to compromise with steepness and height of a hill present in the study area. Another probable reason for having poor correlation with the average slope of a hill is that people usually cut the steep portion of a plot of land and make it plain before settling in that plot. On the other hand, land value in AOI of a hill has the best correlation (R^2 = 0.908) with urban settlement in the hill. This is obvious as high land value indicates more facilities in an area. The low-income group of people though gets attracted towards that AOI, cannot afford land in it and hence settle in the nearby hills. The good linear correlations with the variables other than average slope and average elevation indicate that multi-linear regression analysis can be used to develop the proposed model for Guwahati city. Normalized data used for calibration and validation of the model are displayed in Table 3.7. The model can be expressed as,

$$\text{Urban settlement in a hill (in \% of hill area)} = B_0 + B_1C_u + B_2A_f + B_3L_v + B_4F \quad (3.4)$$

where, B_0 is the constant term (intercept) in the model, $B_{1,}$ $B_{2,}$ $B_{3,}$ and B_4 are the coefficients of independent variables C_u, A_f, L_v and F, respectively.

Table 3.7: Data (normalized) used for calibration and validation of the model.

Hill ID	Hill name	C_u (numbers/sq km)	A_f (%)	L_v (Rs/sq km)	F	Observed urban settlement in hill (%)	Computed urban settlement in hill (%)
1	**University**	1.54	9.91	2.14	3.67	7.85	7.81
2	**Fatasil**	5.21	7.48	3.07	3.98	12.47	12.40
3	**Kalapahar**	4.60	4.00	4.79	5.78	18.56	16.85
4	**Sonaighuli**	5.29	9.52	4.06	1.84	16.54	12.65
5	**Sarania**	6.60	1.26	10.00	10.00	28.31	28.51
6	**Kharguli**	10.00	3.75	8.76	10.00	25.87	27.16
7	**Japorigog**	2.45	4.38	4.77	5.78	17.49	15.51
8	**Burhagosain**	1.62	10.00	1.00	1.00	5.70	5.36
9	**Khanapara**	2.04	8.99	2.67	2.69	6.44	9.12
10	**Garbhanga**	3.78	7.18	3.52	1.84	8.21	12.04
11	**Kamakhya**	3.73	4.21	7.58	9.55	22.63	21.64
12	**Kahilipara**	6.34	1.00	7.32	9.44	20.91	24.03
13	**Betkuchi**	3.40	7.94	3.89	3.53	14.36	12.49
14	**Chunsali**	1.00	9.00	1.49	1.00	6.82	6.29
15	**Koinadhara**	2.96	4.58	3.87	4.38	14.03	13.91

3.3 Results and discussion

From calibration, the Nash–Sutcliffe efficiency (NSE = R^2), coefficient of determination and root mean square error (RMSE) are obtained as 0.92, 0.947 and 2.13, respectively. The resulted model with the regression coefficients is,

$$\text{Urban settlement in a hill} = 7.2073 + 0.5264C_u - 0.4535A_f + 1.6209L_v + 0.2191F \quad (3.5)$$
(in % of hill area)

As expected, A_f has negative regression coefficient and all the other three variables C_u, L_v and F have positive regression coefficients. Hence, the signs of resulted regression coefficients match with the real influence of the variables on urban settlement in hills. Fig. 3.9 compares the observed and computed values of the urban settlement obtained from calibration.

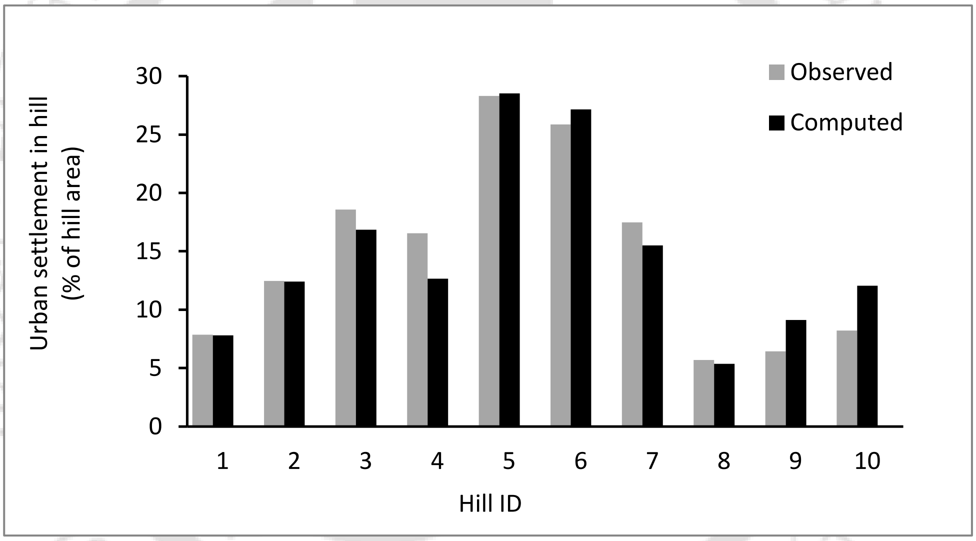

Fig. 3.9: Comparison between observed and computed values of urban settlement in hills (Calibration)

To test the efficiency of the resulted model, Eq. (3.5) is applied to the remaining five hills (Hill ID from 11 to 15) present in Guwahati city. AOI of all these five hills used in validation is of diverse natures, having dissimilar values of C_u, A_f, L_v and F. On validation, the NSE, coefficient of determination and RMSE are obtained as 0.93, 0.938 and 1.7, respectively. Fig. 3.10 indicates that the computed values are in good agreement with the observed values obtained from validation. The magnitudes of errors range from 0.8% (for hill ID 15) to 14.9% (for hill ID 12). Hence, the regression model developed by applying the ASEA model is well validated and is capable of giving a good estimate of urban settlement in hills of Guwahati city.

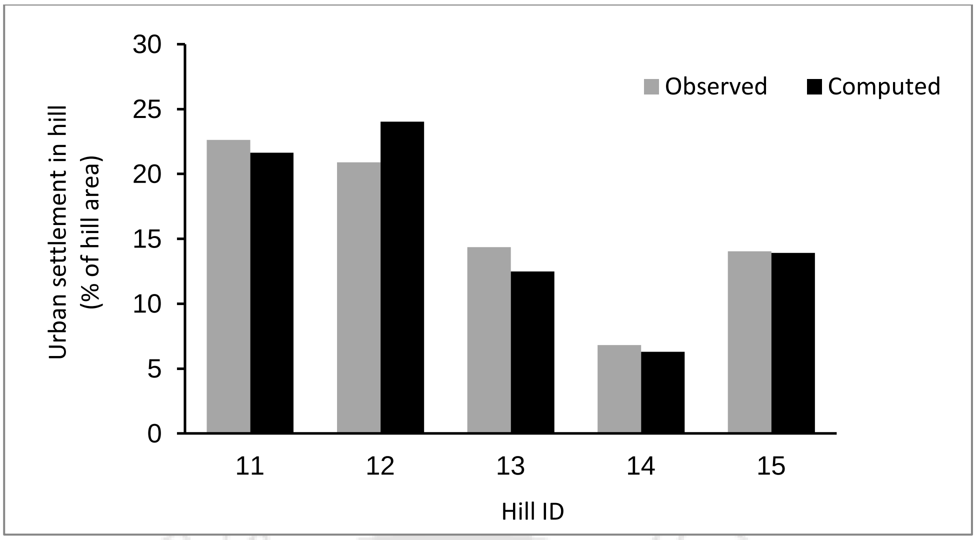

Fig. 3.10: Comparison between observed and computed values of urban settlement in hills (validation)

A sensitivity analysis has also been carried out to investigate how the urban settlements in hills of Guwahati city are sensitive to the variation in every individual explanatory variable. The highest and lowest sensitive hills for every explanatory variable have been identified, and their sensitivities are presented in Fig. 3.11. In addition to this, the average change in the urban settlement in hills of Guwahati city due to the change in values of these individual variables is also displayed in the same figure. It is found that on average, the urban settlement in hills of Guwahati city is most sensitive to land value followed by free space available and commercial unit density in AOI of hills. It is least sensitive to favouring index. This indicates that city development plans should give more importance to outward spatial expansion in plain areas with regulated land value to minimize unauthorized settlement in eco-sensitive hilly areas of Guwahati city. However, agglomeration is an important criterion in this case. City expansion should not be only in residential form but also in commercial, industrial or recreational form with proper land use zoning scheme. A good transportation system is also mandatory. Otherwise, people will not prefer to settle in the outskirt of a city if their daily works are related to old core city area and in that case, encroachment in hills located in main city area will continue as usual. Hence, with this type of analysis, one can identify the most influencing factors that can compel people to settle in eco-sensitive areas of a city in a developing country. Consequently, this type of model can be very useful for environmentalist and urban planner to frame eco-friendly development policy.

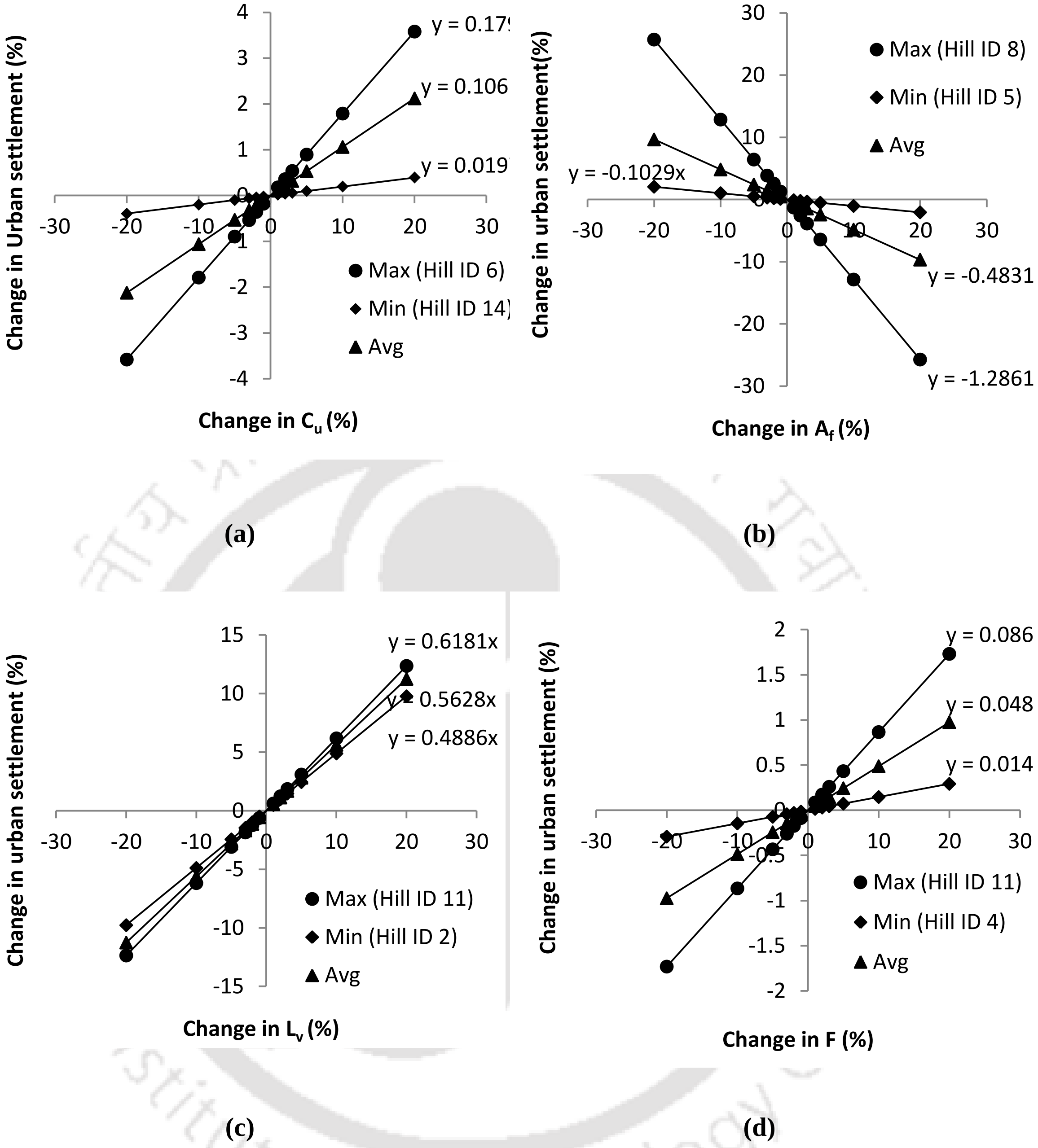

Fig. 3.11: Sensitivity of urban settlement in hills of Guwahati city with respect to variation in explanatory variables (a) commercial unit density, C_u (b) free space available in AOI, A_f (c) land value, L_v and (d) favouring index, F

Despite the linear nature of sensitivity of urban settlement in every hill to the variation in the explanatory variables, the degree of sensitivity is different to different explanatory variables for every hill. Table 3.8 shows the most sensitive explanatory variable for urban settlement in every hill and also the rate of change in the urban settlement in the corresponding hill for per unit change in that explanatory variable. The site-specific model developed for the case study area, is also applicable to hilly areas of a city, of which socio-economic, geographical or urban sprawl pattern or development policies are very similar with those of Guwahati city. Otherwise, the regression coefficients have to be regenerated by proper calibration and validation process with respect to data of that city.

Table 3.8: Hill wise most sensitive explanatory variable and the rate of change in urban settlement for per unit change in that explanatory variable.

Hill ID	1	2	3	4	5	6	7	8	9	10	11	12	13	14	15
Variable	A_f	L_v	L_v	L_v	L_v	L_v	L_v	A_f	A_f	L_v	L_v	L_v	L_v	A_f	L_v
Rate	(-) 0.88	0.49	0.53	0.61	0.61	0.56	0.57	(-) 1.29	(-) 0.71	0.56	0.62	0.54	0.59	(-) 1.03	0.53

Chapter-4

Model application: Projection of urban settlement in hills of Guwahati city

4.1 Introduction

The demographic and socio-economic status of an area is closely related to urban plans and government policies. Again, the success of urban planning and management and the signs of a good urban system are often recognized by its healthy urban greenery (Jim 2004). Hence, it is important to study the influence of urban development plans and future socio-economic or demographic activities in the city on its expansion to eco-sensitive areas.

4.2 Generation of future data

In 2009, GMDA published the "Master Plan for Guwahati Metropolitan Area-2025" with details of plans to be implemented in Guwahati Metropolitan Area (GMA). It includes various developmental strategies to increase or upgrade the city level facilities and to enable the city for handling various socio-economic problems related to increasing urban populations. Total existing area covered by GMA is approximately 262 km^2 (proposed to be increased by 66 km^2). The study area GMCA is also a part of GMA. It is worth mentioning that if slackness in the regulation of nature conservation acts continues in the same way in Guwahati city, the future urban settlement in hills of the city will be mainly influenced by the pattern of future socio-economic or demographic development in the city. Hence, the regression model of Guwahati city, developed by applying the ASEA model in the previous chapter, can be used for indirect assessment of future urban settlement in hills of Guwahati city. Future values of various input variables of ASEA model have been derived from the "Master Plan for Guwahati Metropolitan Area-2025" (GMDA 2009). The methodology adopted for determining these input values is briefly presented below.

4.2.1 Determination of future commercial unit density (C_u) in AOIs

The commercial development in an area has a good correlation with the population growth (Exum et al. 2005). Therefore, the future values of commercial units in the plain urban area can be calculated by developing some relation between this parameter and population growths. However, for Guwahati city, to generate such relation, ward-wise data for commercial development and population growth are not sufficiently available for the historical period. As a result, assuming the relation "numbers of commercial unit vs. population" is of linear nature, it is considered that the ratio of the commercial unit and urban coverage area to the population, calculated based on the available data of the year 2011, will remain same in future in the study area.

The ward-wise projected population in the study area for the year 2025 has been obtained from the map of "Population Distribution in GMA - 2025" (GMDA 2009). The same for the years 2001 and 2011 have been collected from Directorate of Census Operations, Assam. The ward-wise populations of the study area for the years 2001, 2011 and 2025 (projected) are shown in Table A.1 (Appendix A). From 2001 to 2011, the percent decadal growth is 25.02% and from 2011 to 2025 (Projected), it is 23.59%. This indicates that population growth in the past is similar to that in the future decade with a marginally decreasing growth rate with time, which is an acceptable trend. The population in an AOI of a hill has been estimated by summing up the ward populations based on the percentage of ward areas shared by the AOI. Again, despite an overall growth in the total projected population of GMCA in 2025, an under-projection of populations has been observed in 18 GMC wards. Since every AOI comprises several wards, an overall increase in population in every AOI has resulted except in AOIs of University and Chunsali hills. In these two AOIs, the under- projection of populations (2025) of wards 1 and 46 are causing this decrease in populations. So, populations in these two wards have been projected by applying the annual growth rate (from 2011 to 2025) of the city population to their census population (2011). Table A.2 to Table A.17 (in Appendix A) show the determination of population for every AOI. Finally, future commercial unit densities in the AOIs of hills in 2025 are shown in Table 4.1.

4.2.2 Determination of free space (A_f) to be available in 2025 in AOI of hill

Urban coverage and population growth in an area are strongly correlated (Stankowski 1972; Chabaeva et al. 2004). Therefore, similar to the future commercial unit density, the future urban settlement in the AOIs of hills of Guwahati city has been projected by assuming that the per capita urban settlement will remain same in future. Finally, free spaces available in AOI in 2025 have been calculated by using Eq. (3.1). These are shown in Table 4.2.

Table 4.1: Commercial unit density to be developed till 2025 in AOI of hill

Hill ID.	Hill name	Numbers of Commercial units in AOI in 2025	AOI (Sq km)	Commercial unit density in 2025 (numbers/sq km), C_u
1	University	606	13.34	45.42
2	Fatasil	5073	22.07	229.86
3	Kalapahar	1744	6.25	279.04
4	Sonaighuli	959	4.08	235.23
5	Sarania	1036	3.62	285.74
6	Kharguli	2154	5.26	409.58
7	Japorigog	1485	13.14	113.04
8	Burhagosain	371	4.31	86.07
9	Khanapara	458	5.19	88.21
10	Garbhanga	645	2.20	292.84
11	Kamakhya	387	3.16	122.52
12	Kahilipara	3984	12.97	307.25
13	Betkuchi	1488	5.01	297.06
14	Chunsali	33	2.69	12.44
15	Koinadhara	1007	6.93	145.38

Table 4.2: Free spaces to be available in AOIs of hills in 2025.

Sr. no.	Hills	Per capita urban settlement in 2011 (sq. m/person)	Urban settlement in AOI in 2025 (sq. km)	*2Free space available in AOI in 2025 (%), A_f
1	University	23.10	2.87	72.38
2	Fatasil	69.04	8.36	58.84
3	Kalapahar	83.89	5.64	8.46
4	Sonaighuli	45.18	1.10	72.73
5	Sarania	50.75	2.80	20.49
6	Kharguli	58.19	2.89	42.66
7	Japorigog	71.78	9.95	18.86
8	Burhagosain	51.37	2.01	53.42
9	Khanapara	49.91	2.11	58.76
10	Garbhanga	50.69	1.76	18.61
11	Kamakhya	38.31	1.58	49.09
12	Kahilipara	65.50	11.54	8.56
13	Betkuchi	180.79	3.96	17.19
14	Chunsali	105.39	0.84	68.63
15	Koinadhara	84.10	5.37	21.56

*2Free space, available in 2011 in 'area of influence' has been expressed in terms of percent of net AOI.

4.2.3 Projection of favouring index (F) to 2025

For Guwahati City, the values of weights for every component of F in the ASEA model are given in a range of 0-1. Here, additional educational institutes to be developed in the AOIs of hills by 2025 are taken by referring map of the master plan showing proposed educational institutes (GMDA 2009). As numbers of historical tourist places will not change with time in this relatively short period, i.e., by 2025, the weights assigned to historical places present in AOIs of hills will remain same. However, the master plan of Guwahati city proposes to increase the recreational park ambitiously to cover an area of 5299 ha from its present area of 114 ha. Based on the population to be served, these recreational areas are categorised into different levels, such as city level, district level, community level, neighbourhood level and housing area level. It is expected that the higher level parks and play areas will serve as a tourist attraction and thus will attract more people. So, weights are assigned to the city, district and community level park and play areas accordingly. The locations of these proposed play and park areas are given in the "Map of Proposed Recreational Facilities" (GMDA 2009). Similarly, to determine the future economically active areas in AOIs, "Map of Proposed Major Activities" (GMDA 2009) has been referred. Weights are applied to this factor based on the amount of proposed economically active areas present in an AOI. Again, weight for the component "location of the hill with respect to city centre" for a hill is given depending on the amount of proposed area for composite use [Map of "Land use Zoning Plan", (GMDA 2009)] lying in the AOI of that hill. Composite use comprises of commercial, industrial, residential, public and semi-public uses (GMDA 2009). Since these areas are going to be used for mixed-use development; those have been considered as core urban area to be developed till 2025. Finally, favouring index for every AOI is calculated as the average of the weights given to all of the four components. These are shown in Table 4.3.

Table 4.3: Projected favouring indices (F) to 2025

Hill ID.	Name of hills	F (2025)	Hill ID.	Name of hills	F (2025)	Hill ID.	Name of hills	F (2025)
1	University	0.62	6	Kharguli	0.83	11	Kamakhya	0.81
2	Fatasil	0.65	7	Japorigog	0.62	12	Kahilipara	0.75
3	Kalapahar	0.68	8	Burhagosain	0.33	13	Betkuchi	0.53
4	Sonaighuli	0.56	9	Khanapara	0.66	14	Chunsali	0.20
5	Sarania	0.80	10	Garbhanga	0.45	15	Koinadhara	0.66

4.2.4 Projection of average land values (L_v) to 2025 in AOIs of hills

Determining future land value in Guwahati city is challenging, as no systematic record of past land value is available for the city. Several studies have highlighted the factors on which valuation of land depends (Topcu and Kubat 2009; Kolowe 2014; Kok et al. 2014). Ezra (2006) stated that accessibility of plots to the major locations or roads is a significant factor influencing land valuation. According to Topcu and Kubat (2009), the value of a plot of land not only depends on its structural condition but also on the physical and physiological characteristics defined by the other urban and spatial assets in its neighbourhood. They mentioned that factors like educational facilities, recreation places, trade centres, transport services and the distance from the sea are useful factors in determining the land values in an area. Favouring index F of ASEA model includes factors like educational facilities, tourism or recreational activities, economic activities and proximity to city centre, and therefore can be used as a determinant of land value. To ascertain this dependency, data of 2011 of the study area was analysed and, as expected a good correlation was observed (R^2= 0.88) between the average land value (L_v) in AOI and favouring Index (F). The price of land is a vital sign of the facilities and the economic value of a particular location (Kok et al. 2014). Hence, to project the future land values in AOI of hills, it is assumed that the ratio of the average land value in 2025 to that in 2011 in an AOI is equal to the ratio of the favouring index in 2025 to that in 2011. The ratios of the favouring indices have been classified in some ranges and to be in the conservative side, the upper limits of these ranges are used for determining future land value from the land value of 2011. The multiplication factors of land values against the ratios of favouring index are shown in Table 4.4. The projected land values are shown in Table 4.5.

Table 4.4: Multiplication factors to be applied to the land values in 2011 in AOI of hill

Range of ratio [=Favouring index (2025)/favouring index (2011)]	**Multiplication factor to be applied to the land values in 2011**
[1,1.5]	1.5
]1.5,2]	2
]2,2.5]	2.5
]2.5,3]	3
]3,3.5]	3.5
>3.5	4

Table 4.5: Projected land values (L_v) in 2025 in AOI

Hill ID.	Name of hills	Average land value in AOI (2011) (per sq. m)	Ratio [=Favouring index (2025)/ favouring index (2011)]	Multiplication factor	Average Land value in AOI (2025), (L_v) (per sq. m)
1	**University**	3109.70	2.16	2.5	7,774
2	**Fatasil**	4131.16	2.09	2.5	10,328
3	**Kalapahar**	6033.58	1.49	1.5	9,050
4	**Sonaighuli**	5223.88	3.96	4	20,896
5	**Sarania**	11791.04	1.00	1.5	17,687
6	**Kharguli**	10421.64	1.03	1.5	15,632
7	**Japorigog**	6014.93	1.37	1.5	9,022
8	**Burhagosain**	1847.01	4.68	4	7,388
9	**Khanapara**	3694.03	3.15	3.5	12,929
10	**Garbhanga**	4626.87	3.29	3.5	16,194
11	**Kamakhya**	9119.40	1.06	1.5	13,679
12	**Kahilipara**	8832.09	1.00	1.5	13,248
13	**Betkuchi**	5044.78	1.97	2	10,090
14	**Chunsali**	2388.06	3.25	3.5	8,358
15	**Koinadhara**	5014.93	1.92	2	10,030

4.3 Results of urban settlement projection

Values of all the four factors (independent variables) - C_u, A_f, L_v, and F are scaled to the same range (1, 10), to which data were normalized during the application of the ASEA model in Guwahati city (in section 3.2.3). These values have been input to Eq. (3.5). The values of the four input variables and the resulted urban settlements (in % of hill area) in 15 hills of Guwahati city are shown in Table 4.6.

Table 4.6: Input variables (normalized) and projected urban settlements in hills of Guwahati city

Hill ID.	Name of hills	C_u (2025)	A_f (2025)	L_v (2025)	F (2025)	Urban settlement in hills till 2025 (in % of hill area)	urban settlement in hills till 2011 (in % of hill area)	Increase in urban settlement area from 2011 to 2025 (sq km)	Increase in urban settlement from 2011 to 2025 (in % of hill area)	Change in urban settlement UA in 2025 with respect to that in 2011 (%)
1	**University**	1.89	8.31	6.36	7.95	16.49	7.85	0.18	8.64	109.99
2	**Fatasil**	6.47	5.78	8.68	8.34	23.88	12.47	1.82	11.42	91.59
3	**Kalapahar**	7.70	-3.63	7.52	8.62	26.98	18.56	0.17	8.42	45.36
4	**Sonaighuli**	6.61	8.38	18.24	7.30	38.05	16.54	0.08	21.52	130.11
5	**Sarania**	7.86	-1.38	15.34	10.00	39.02	28.31	0.04	10.72	37.86
6	**Kharguli**	10.94	2.76	13.48	10.28	35.81	25.87	0.65	9.94	38.42
7	**Japorigog**	3.57	-1.69	7.49	7.95	23.74	17.49	0.71	6.26	49.88
8	**Burhagosain**	2.90	4.77	6.02	4.68	17.35	5.70	0.23	11.65	204.62
9	**Khanapara**	2.96	5.77	11.03	8.45	25.88	6.44	1.29	19.44	302.10
10	**Garbhanga**	8.04	-1.73	13.99	6.06	36.22	8.21	0.27	28.01	341.05
11	**Kamakhya**	3.81	3.96	11.71	10.11	28.61	22.63	0.18	5.98	26.45
12	**Kahilipara**	8.40	-3.61	11.32	9.44	33.68	20.91	0.85	12.77	61.09
13	**Betkuchi**	8.14	-2.00	8.46	6.96	27.64	14.36	0.03	13.28	92.53
14	**Chunsali**	1.07	7.61	6.89	3.25	16.21	6.82	0.84	9.38	137.46
15	**Koinadhara**	4.38	-1.18	8.41	8.40	25.51	14.03	0.26	11.48	81.86

As per the model projections, the rate of change in the urban settlement in 2025 will be highest in hills like Garbhanga and Khanapara lying in the southern part of the city. According to GMDA (2009), in 2025, Guwahati city will shift towards the south and the urban development activities will be more pronounced in the area along the NH-37 highway. Model results are reflecting this shifting of the city. It is noticed that the majority of hills located in the southern part of the city like Garbhanga, Khanapara, Sonaighuli, Betkuchi are having relatively a higher rate of increment in urban settlements from 2011 to 2025. In 2011, the average urban settlement in hills of Guwahati city was 14.33% (in % of hill area), whereas in 2025 it is going to be 25.45%. Fig. 4.1 compares the urban settlements in hills of Guwahati city between the two time periods i.e. 2011 and 2025. From this figure, it is observed that in 2011, hills having a higher amount of urban settlements (in % of hill area) are Sarania, Kharguli and Kamakhya hills, whereas, in 2025, these are in Sarania, Sonaighuli, and Garbhanga hills. Till 2011, the lowest urban settlement was observed in Burhagosain hill. On the contrary, in 2025, it is the Chunsali hill, which will have the lowest amount of urban settlement (in % of hill area), although the rate of increase in the urban settlement is highest in this hill.

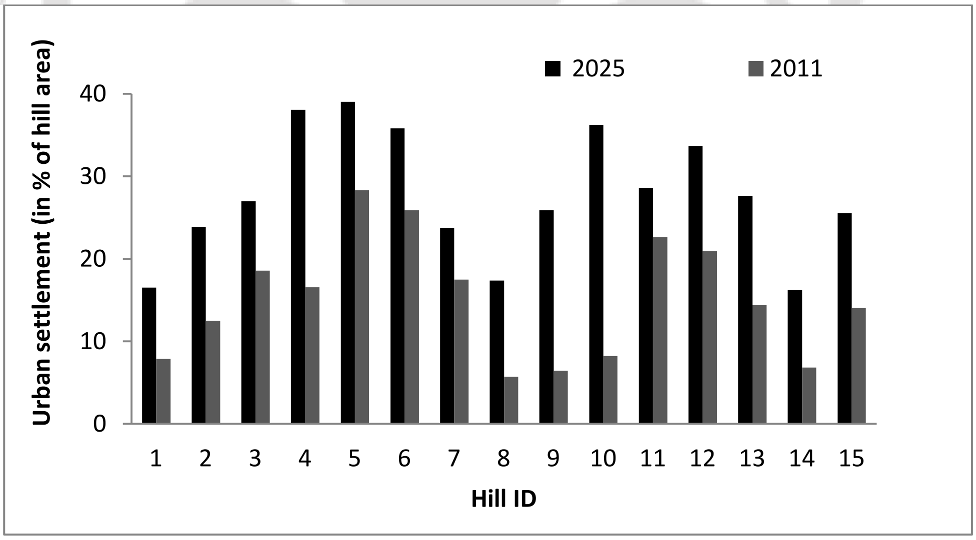

Fig. 4.1: Comparison of urban settlements in hills of Guwahati in 2025 (projected) and 2011

4.4 Preparation of future LULC map for hills of Guwahati city

After projecting the amounts of future urban settlement in hills, another important task is to spatially distribute the projected increment of urban settlement within the hills. In the case of hills, it is generally witnessed that people prefer to settle near the hill boundary where elevation is relatively low. Based on this fact, spatial allocation of projected urban settlements in a hill was done from the lower elevation to the higher elevation area of the hill. To do this, all the hills are subdivided into grids of size 30m×30m by using the fishnet tool of ArcGIS. The grid-wise average elevation of a hill is extracted against every grid ID by combining the shapefile of DEM (Shuttle Radar Topography Mission (SRTM) DEM of 1 arc-second resolution) of the hill with its fishnet file. The increment of urban settlement area (in square m) from 2011 to 2025 of every hill is expressed in terms of numbers grids of size 30m×30m. Finally, the non-urbanized hilly area in the LULC map (2011) of the hill is found out, where the newly urbanized grids (from 2011 to 2015) are assigned in an order of lower elevation to high elevation of grids. The detailed step by step procedure of spatial distribution of projected urban settlement in ArcGIS is given in Fig. 4.2.

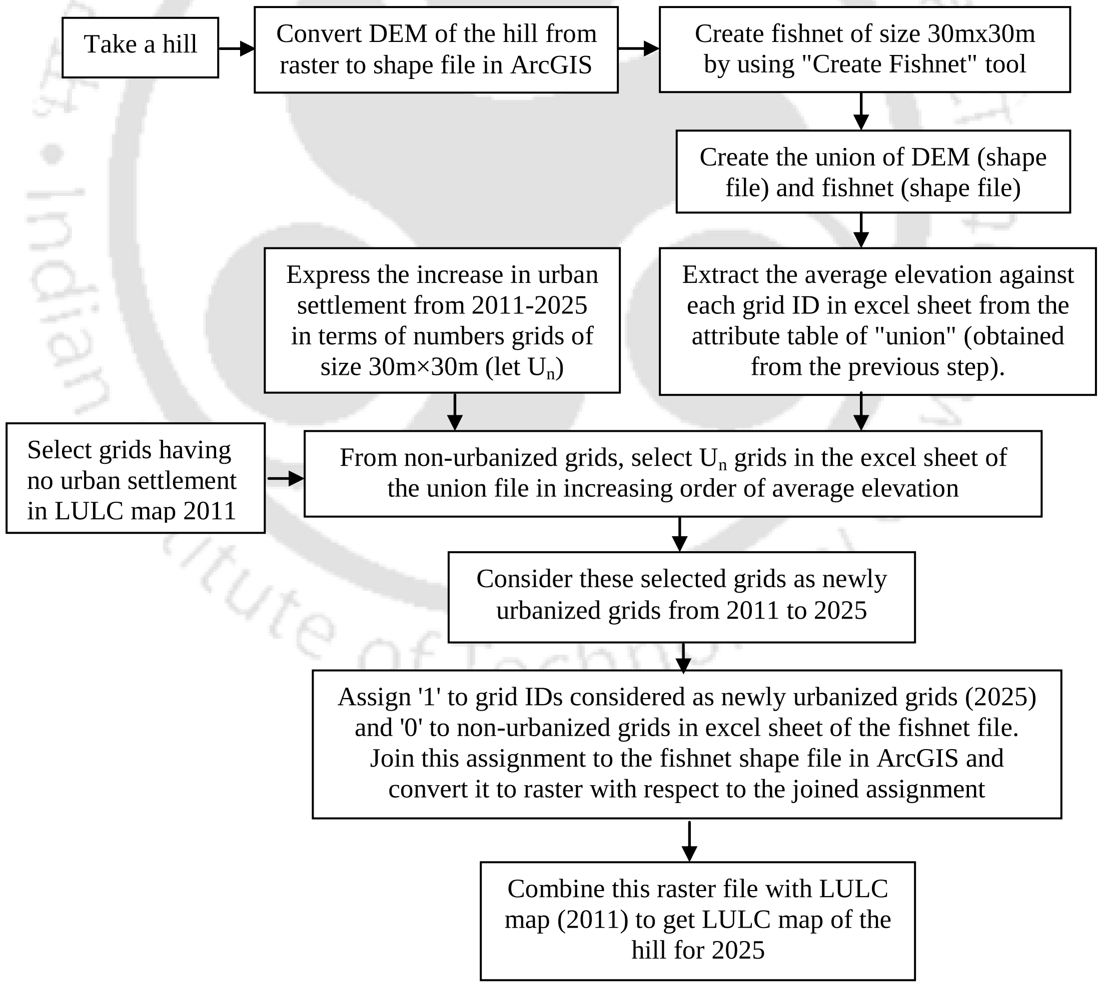

Fig. 4.2: Flow chart of preparation of future LULC map for hills of Guwahati city

In order to study the recent change in LULC of hills of Guwahati, LULC map has also been prepared for the year 2015 by digitizing a LISS IV satellite image of capture date 4 December 2015. Fig. 4.3 shows the LULC maps of hills of Guwahati city for the years 2011, 2015 and 2025 (projected). Table 4.7 shows the quantity of LULCs (in sq. km) of 15 hills of Guwahati city in 2011, 2015 and 2025. From this table, it is clear that in all hills except Sarania (Hill ID: 5) and Kamakhya hill (Hill ID: 11), mainly scrublands are going to be converted to urban settlement. On the other hand, in Sarania and Kamakhya hills mostly forest areas are going to be degraded due to increase in urban settlement. In 2011, the average urban settlement in hills of Guwahati city was 14.33% (in % of hill area); in 2015 it was 16.97% and in 2025 it is to be 25.45%. That means, from 2011 to 2015, urban settlements have increased by 2.64% of total hill area whereas from 2015 to 2025 it will increase by 8.48%.

4.4 Conclusions

This chapter has revealed the fact that implementation of the master plan in Guwahati city may cause further degradation of the ecological balance in its hilly areas if the nature conversation law is not implemented in the city for some socio-economic and demographic constraints. This fact, though well understood, is generally overlooked in the planning process. Thus, the planned city area always experiences multiple natural hazards like urban flood, landslide and water pollution originated due to unplanned or unauthorised settlement in its surrounding eco-sensitive hills. Having an idea about the future possible settlement in the eco-sensitive areas can always help in the better future planning of the prime city area. Knowledge of the potential settlement in the hilly areas can help the concerned authorities to plan settlement in those areas more scientifically to reduce adverse impacts of unplanned settlement.

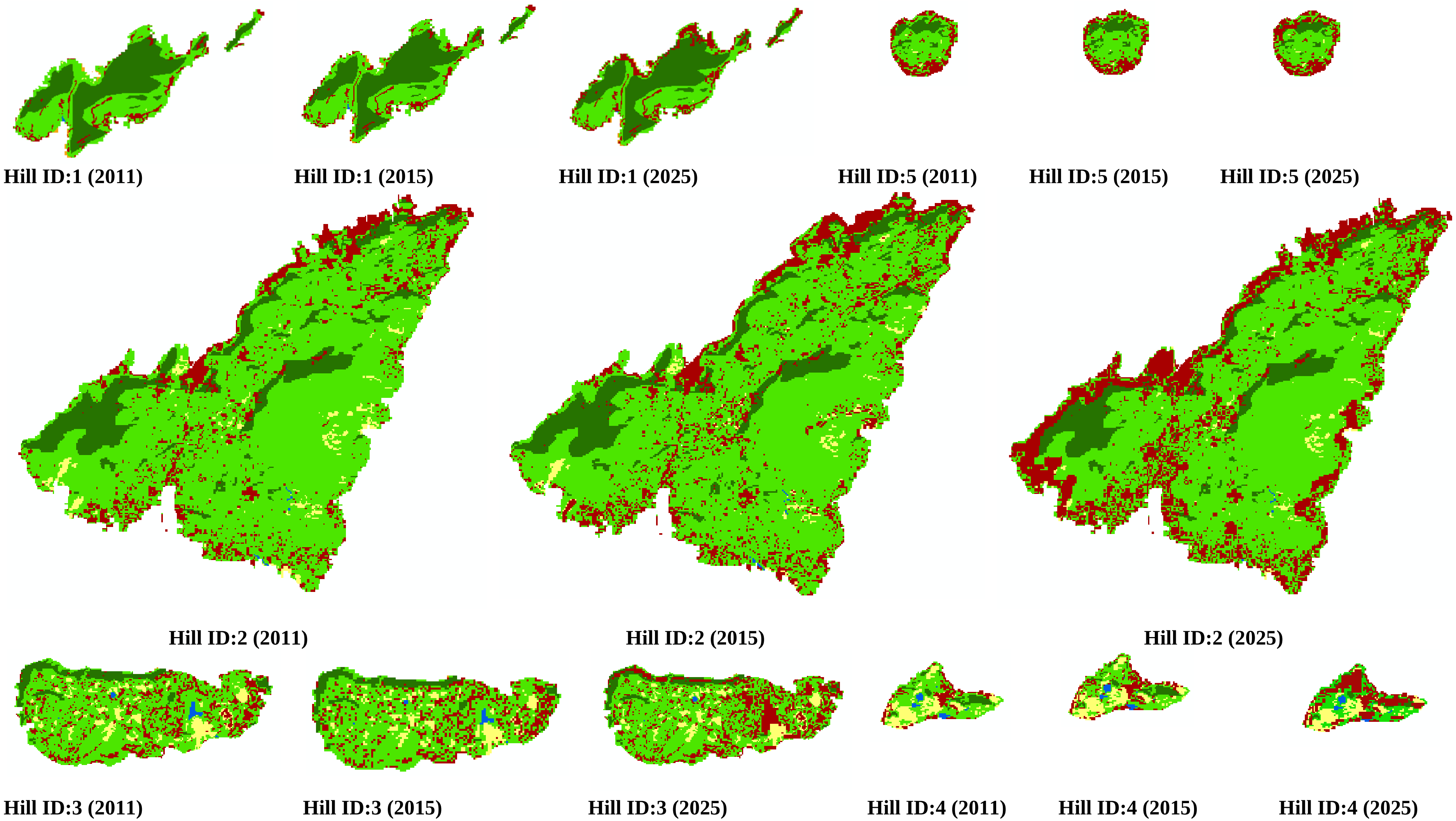

Fig. 4.3 (a): LULC maps of hills of Guwahati city (Hill ID: 1 to 5; 1: 80000)

: Scrub land : Forest : Marshy land : Bare land : Water bodies : Urban settlement

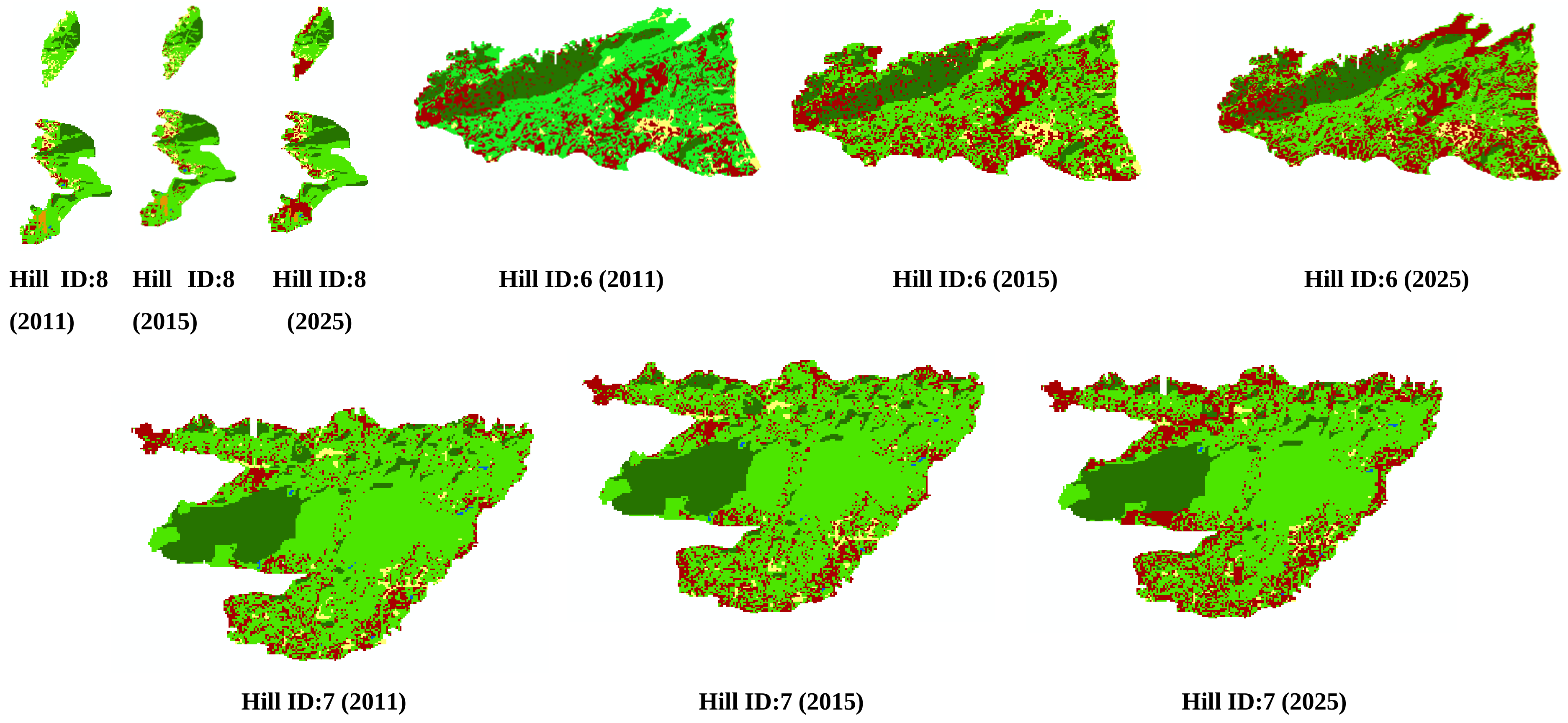

Fig. 4.3 (b): LULC maps of hills of Guwahati city (Hill ID: 6 to 8; Scale= 1: 80000)

: Scrub land : Forest : Marshy land : Bare land : Water bodies : Urban settlement

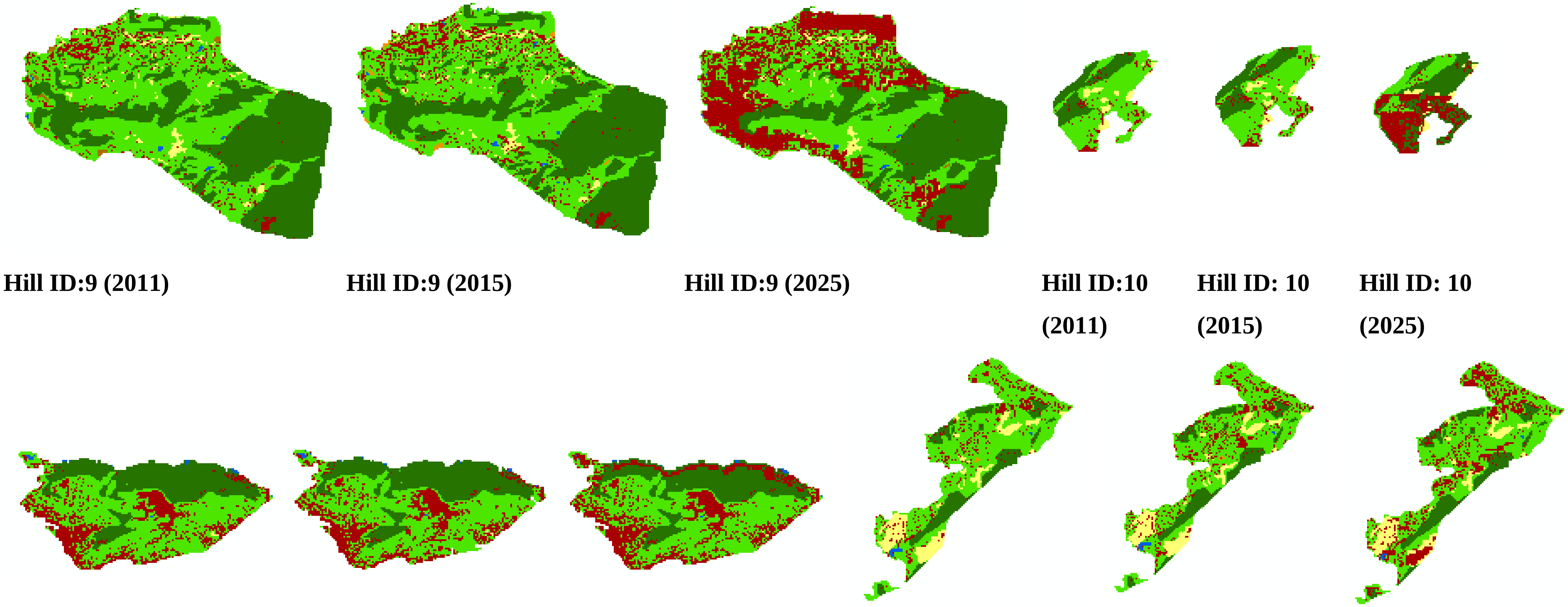

Hill ID:9 (2011) Hill ID:9 (2015) Hill ID:9 (2025) Hill ID:10 (2011) Hill ID: 10 (2015) Hill ID: 10 (2025)

Hill ID:11 (2011) Hill ID:11 (2015) Hill ID:11 (2025) Hill ID:15 (2011) Hill ID:15 (2015) Hill ID:15 (2025)

Fig. 4.3 (c): LULC maps of hills of Guwahati city (Hill ID: 9, 10, 11, 15; Scale= 1: 80000)

: Scrub land : Forest : Marshy land : Bare land : Water bodies : Urban settlement

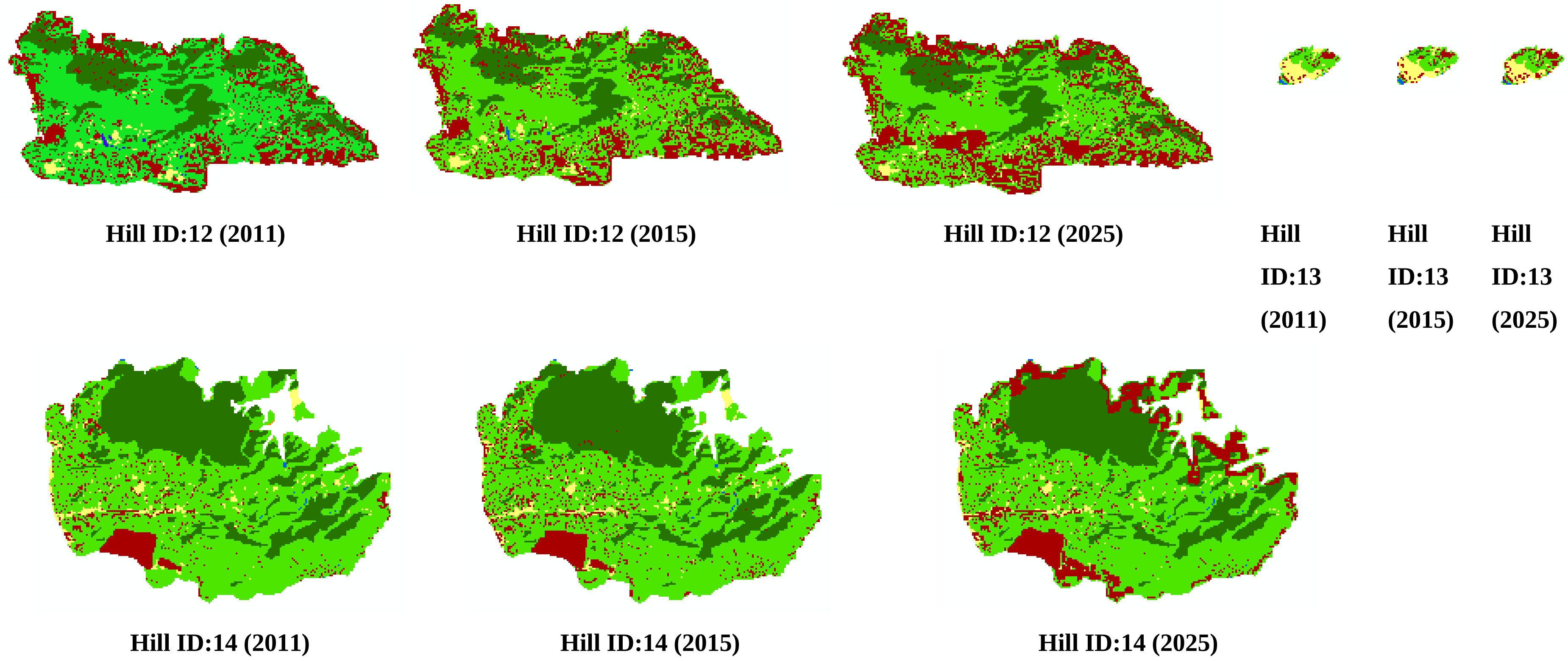

Fig. 4.3 (d): LULC maps of hills of Guwahati city (Hill ID: 12, 13, 14; Scale: 1:80000)

: Scrub land : Forest : Marshy land : Bare land : Water bodies : Urban settlement

Table 4.7: LULC (in sq.km) of 15 hills of Guwahati city in 2011, 2015 and 2025.

	Hill ID:1			Hill ID:2			Hill ID:3			Hill ID:4			Hill ID:5		
LULC (sq km)	**2011**	**2015**	**2025**	**2011**	**2015**	**2025**	**2011**	**2015**	**2025**	**2011**	**2015**	**2025**	**2011**	**2015**	**2025**
Forest	0.9684	0.9509	0.9281	1.9131	1.8989	1.5154	0.1617	0.1607	0.1164	0.0322	0.0316	0.0165	0.0543	0.0538	0.0427
Bare soil	0.0048	0.0026	0.0021	0.3331	0.2326	0.1949	0.1709	0.1696	0.1557	0.0887	0.0878	0.0726	0.0028	0.0027	0.0027
Scrub land	0.9405	0.9173	0.8072	11.6697	11.2936	10.3933	1.2664	1.2232	1.1714	0.1666	0.1485	0.1236	0.1883	0.1845	0.1812
Marshy land	0.0146	0.0130	0.0117	0.0000	0.0000	0.0000	0.0004	0.0004	0.0004	0.0000	0.0000	0.0000	0.0000	0.0000	0.0000
Water bodies	0.0021	0.0021	0.0004	0.0107	0.0105	0.0065	0.0140	0.0140	0.0027	0.0111	0.0098	0.0089	0.0000	0.0000	0.0000
Urban settlement	0.1645	0.2091	0.3455	1.9833	2.4744	3.7998	0.3678	0.4133	0.5346	0.0591	0.0799	0.1361	0.0969	0.1014	0.1158
Total=	2.0950	2.0950	2.0950	15.9100	15.9100	15.9100	1.9812	1.9812	1.9812	0.3576	0.3576	0.3576	0.3424	0.3424	0.3424
	Hill ID:6			**Hill ID:7**			**Hill ID:8**			**Hill ID:9**			**Hill ID:10**		
LULC (sq km)	**2011**	**2015**	**2025**	**2011**	**2015**	**2025**	**2011**	**2015**	**2025**	**2011**	**2015**	**2025**	**2011**	**2015**	**2025**
Forest	1.2123	1.1810	1.0675	1.6351	1.6279	1.4693	0.4476	0.4463	0.4448	2.8494	2.8279	2.3311	0.2458	0.2448	0.1782
Bare soil	0.2821	0.2709	0.2082	0.2079	0.1884	0.1490	0.1851	0.1752	0.1412	0.1633	0.1515	0.1273	0.0582	0.0545	0.0368
Scrub land	3.3531	3.2086	2.9217	6.3772	6.1655	5.7313	1.2151	1.1720	1.0518	3.1352	3.0175	2.4280	0.5674	0.5486	0.3905
Marshy land	0.0001	0.0001	0.0001	0.0000	0.0000	0.0000	0.0376	0.0376	0.0154	0.0360	0.0353	0.0138	0.0000	0.0000	0.0000
Water bodies	0.0006	0.0006	0.0006	0.0193	0.0193	0.0121	0.0063	0.0062	0.0045	0.0180	0.0180	0.0130	0.0000	0.0000	0.0000
Urban settlement	1.6920	1.8791	2.3421	1.4141	1.6526	2.2919	0.1142	0.1686	0.3481	0.4266	0.5784	1.7153	0.0780	0.1014	0.3438
Total=	6.5402	6.5402	6.5402	9.6536	9.6536	9.6536	2.0059	2.0059	2.0059	6.6285	6.6285	6.6285	0.9493	0.9493	0.9493
	Hill ID:11			**Hill ID:12**			**Hill ID:13**			**Hill ID:14**			**Hill ID:15**		
LULC (sq km)	**2011**	**2015**	**2025**	**2011**	**2015**	**2025**	**2011**	**2015**	**2025**	**2011**	**2015**	**2025**	**2011**	**2015**	**2025**
Forest	0.9075	0.9037	0.7853	1.3713	1.3497	1.2302	0.0093	0.0091	0.0051	2.7732	2.7543	2.4768	0.3544	0.3523	0.3414
Bare soil	0.0050	0.0025	0.0020	0.1548	0.1288	0.1081	0.0894	0.0887	0.0764	0.2394	0.2146	0.1935	0.2687	0.2667	0.2132
Scrub land	1.4335	1.3901	1.3800	3.6977	3.6047	3.3108	0.1036	0.0955	0.0894	5.2849	5.1428	4.7924	1.2724	1.1873	1.0920
Marshy land	0.0000	0.0000	0.0000	0.0000	0.0000	0.0000	0.0010	0.0010	0.0010	0.0072	0.0072	0.0068	0.0034	0.0034	0.0027
Water bodies	0.0102	0.0102	0.0065	0.0155	0.0154	0.0017	0.0046	0.0045	0.0037	0.0129	0.0127	0.0107	0.0108	0.0108	0.0054
Urban settlement	0.6890	0.7385	0.8712	1.3850	1.5257	1.9735	0.0349	0.0440	0.0671	0.6092	0.7954	1.4467	0.3117	0.4009	0.5668
Total=	3.0451	3.0451	3.0451	6.6243	6.6243	6.6243	0.2428	0.2428	0.2428	8.9269	8.9269	8.9269	2.2215	2.2215	2.2215

Chapter-5

Effect of projected urban settlement on surface runoff characteristics of the study area

5.1 Introduction

Precipitation, infiltration, runoff, evaporation and transpiration are the most basic components of the hydrologic cycle. Out of these, runoff and infiltration processes are the most affected components by urban settlements. Runoff is that part of the precipitation which is discharged into surface streams. Broadly runoff can be classified as surface runoff, subsurface runoff and base-flow. Surface runoff includes the overland flow resulting from precipitation after satisfying the infiltration or other losses. On the other hand, sub-surface runoff occurs laterally through the unsaturated zone of soil (existing over the water table) due to the infiltration of precipitated water through the soil surface. The base flow is the delayed flow resulting from deep percolation of precipitated water to the water table. From these definitions, it is clear that in all these types of runoff generation, the infiltration capacity of the soil takes a very important role. However, in case of hilly catchments, where land surfaces have steep slopes, overland flow or the surface runoff becomes the major component of runoff. As mentioned earlier, urban settlement enhances the peak of surface runoff by lowering the infiltration capacity of soil to a great extent. Since in this study the target areas are not other than the hills of Guwahati city, so, it has been decided to study the characteristics of peak surface runoff under the impact increasing urban settlement. For the hills of Guwahati city, no runoff records are available. Therefore, in order to study the impact of urban settlements on peak runoff generation from the hills of Guwahati city, Rational Method has been used.

5.2 Determination of peak runoff from hills of Guwahati city

The Rational Method was developed by Kuichling (1889) in order to determine the peak discharge from a small urban watershed. The empirical formula used in this method is,

$$Q = CiA \tag{5.1}$$

where, Q is the peak runoff to be determined, C is the runoff coefficient (dimensionless) defining the ratio of surface runoff depth to the rainfall depth causing that surface runoff from the watershed, i is the rainfall intensity for a specific return period with respect to a duration equal to the time of concentration of the watershed and A is the area of the watershed. The general methodology of the Rational Method is shown in Fig. 5.1. The various assumptions used in the Rational Methods are-

I. This method is suitable for watershed area upto 2.59 sq. km (San Diego County 2003).

II. The time that the water flowing from farthest point of the watershed takes to reach the watershed outlet is called the time of concentration T_c. At this time the discharge becomes peak at the watershed outlet.

III. Rainfall intensity is uniform for the duration equal to the time of concentration T_c.

IV. The return period (frequency) of the peak runoff is same as that of the intensity of rainfall occurring for the duration equal to T_c.

V. The runoff coefficient does not vary with the duration of rainfall.

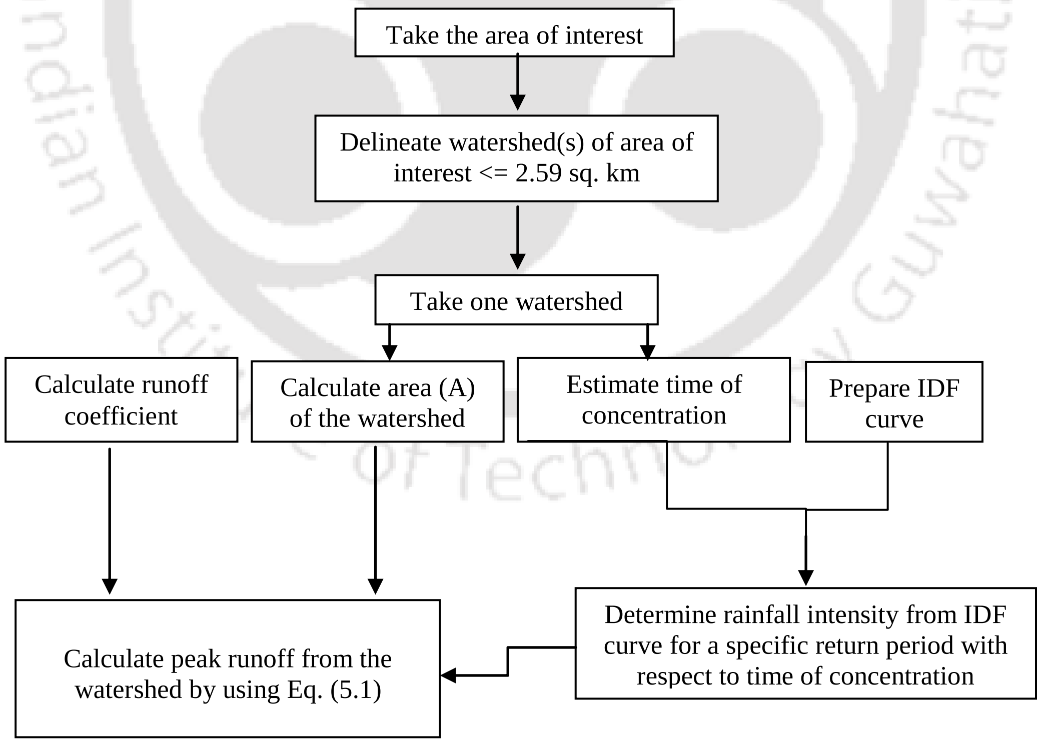

Fig. 5.1: General steps to calculate the peak runoff by Rational Method

5.2.1 Delineation of watersheds of hills of Guwahati city

A watershed is an area which drains rainwater or flows to a common outlet. To know the attributes of a watershed used in the methodology for runoff calculation, first it is essential to delineate the boundary of the watershed. In this study, watershed delineation has been carried out in "Watershed delineator" tool in the ArcSWAT interface of the SWAT model. This tool automatically delineates the watershed by using the "Spatial Analyst" extension functions of ArcGIS (Winchell et al. 2010). However, users can manually edit the various parameters like threshold area of the drainage basin, locations of outlets of watersheds etc. The methodology adopted for watershed delineation in ArcSWAT is given below:

I. Take DEM of the study area.
II. Mark the area covering the target hill of which watersheds are to be delineated.
III. Run ArcSWAT to obtain the DEM-based flow direction and flow accumulation patterns.
IV. Define the threshold area of the watershed. A low threshold value of an area helps to delineate very small watershed.
V. Click to create the streams and outlet. The network of streams and outlets will be displayed on the screen.
VI. Delete all the software generated outlets and add outlets manually to streams in such a way that all the area of the target hill is enclosed by some watershed.
VII. Click to delineate watersheds of the hill.
VIII. Finally, run to calculate sub-basin parameters. It will give the values of various watershed attributes such as area of watershed, length of the longest stream in the watershed, average slope of the watershed etc.

The delineated watersheds of all the 15 hills of Guwahati city are shown in Fig. B.1 to B.14 (Appendix B). Again, Khanapara (Hill ID: 9) and Koinadhara (Hill ID: 15) hills belong to some common watersheds. So, watersheds of these two hills are delineated jointly.

5.2.2 Determination of time of concentration for the watersheds of hills of Guwahati city

In the Rational Method, design rainfall intensity of a specific return period required for the calculation peak discharge is determined from the intensity-duration-frequency

(IDF) curve for rainfall duration equal to the time of concentration. Due to the error in estimation of T_c, a maximum of 75% error in peak runoff calculation can result (Bondelid et al. 1982). Interpreting such importance, researchers have developed different empirical equations of T_c, the applicability of which depends on criteria like type of flow, nature of the catchments etc. Williams (1922) developed an equation for T_c for the watershed area less than 129.5 km^2 (Fang et al. 2008). The necessary experiments related to this equation were carried out in Indian catchments. For some watersheds, where, both the overland and channel flow occur substantially, the total time of concentration is calculated as the sum of overland flow time and channel flow time (San Diego County 2003). However, in the Bransby Williams formula (Williams 1922), the initial overland flow time is already included (ADNRW 2007), and hence, should not be incorporated additionally. Again, this formula is suitable for hilly watersheds (Christchurch City Council 2011). Since watersheds of hills of Guwahati city are having areas less than 129.5 km^2, Bransby Williams formula has been used in this study. Originally, this formula was provided for circular catchments. For the non-circular catchment, T_c increases by L_c/D times, where, L_c is the longest flow channel and D is the equivalent diameter of a circular basin having an area equal to the non-circular watershed area A. The modified formula for 1 for English units is given by T_c (minute) = $21.3 L_c A^{-0.1} S_c^{-0.2}$ (Pilgrim and Cordery 1993), where, L_c is in mi, A is in mi^2 and S_c is in (ft/ft). In SI unit, the same can be rewritten as-

$$T_c \text{ (minute)} = 0.057948\, L_c A^{-0.1} S_c^{-0.2} \tag{5.2}$$

where, L_c is in m, A is in m^2 and S_c is in (m/m). Data regarding the length of the longest flow channel (L_c), watershed area (A) and slope of the longest flow channel (S_c) present in every watershed of hills of Guwahati city have been derived from the attribute tables of the watersheds delineated in ArcSWAT interface.

5.2.3 Intensity duration frequency (IDF) curve for Guwahati city

An IDF curve can be defined as a comprehensive graphical representation of the rainfall intensity of different duration that may occur with a specific frequency. Rainfall duration and intensity are plotted as the abscissa and ordinate, respectively and a set of curves are produced, one for every return period or frequency. In order to calculate the peak discharge by Rational Method, the next step after the calculation of time of concentration is to determine the rainfall intensity that may persist for a duration equal to the time of concentration and those can be obtained from IDF curve. There exist a number of general empirical equations of IDF relationship developed by researchers from different parts of the world (Bernard 1932; Bell 1969; Chen 1983; Gert et al. 1987, Yu and Cheng 1998). In context of Indian basin also, a few general equations of IDF curves are available which are applicable to different regions of India just only by changing the coefficients or parameters involved in the equations (Babu et al. 1979; Kothyari & Garde 1992). These general empirical equations are very useful for regions where rainfall data for a long historical period are not available. However, for a place where local rainfall data are available, it is more meaningful to generate a local IDF curve which will represent the local precipitation events more correctly in comparison to the general empirical IDF equations. Again, Guwahati is a place of very high rainfall events. For such a place, use of an inaccurate IDF curve can produce considerable flaw in hydrologic design or analysis. Therefore, it is very important to use a local IDF curve for Guwahati city. Very few IDF curves are available for Guwahati city. Sarma and Goswami (2006) developed an intensity-duration (ID) curve for Guwahati city by using hourly precipitation data observed at a central place of Guwahati city for the year 2003. This curve gives rainfall intensities with respect to durations. As the curve has been constructed based only on one-year data, it is not capable of giving the rainfall intensities of different return periods. To overcome this restriction, a new set of curves have been developed which will be capable of giving rainfall intensity of any duration with respect to different return periods. For this purpose, 43 years of daily rainfall data from 1969 to 2011 have been collected from Regional Meteorological Centre (RMC), Barjhar. From these, the annual maximums of daily rainfalls have been extracted as shown in Fig. 5.2.

To have maximum daily precipitation for different return period, frequency analysis of the annual maximum precipitation series was performed by five different methods such as Gumbel, Pearson Type III, Log-Pearson Type III, Normal and Log-Normal method. D-index test (USWRC 1981) was performed to find out the most suitable frequency analysis method for estimation of extreme rainfall events of RMC, Barjhar. The D-index (Varma et al. 1989) is given as-

$$\text{D-index} = \frac{1}{\bar{x}}\left(\sum_{i=1}^{6} \text{ABS}\left(x_{i,\text{observed}} - x_{i,\text{computed}}\right)\right) \qquad (5.3)$$

where, $\bar{x}$ is the mean of the observed series. $x_{i,observed}$(i = 1, 2 …6) are the highest six observations in the given data and $x_{i,computed}$ (i = 1, 2 …6) are the computed values corresponding to the return period using the probability distribution. The distribution which gives minimum D-index is considered as the best fit distribution. D-index values obtained against different methods used in this study are displayed in Table 5.1.

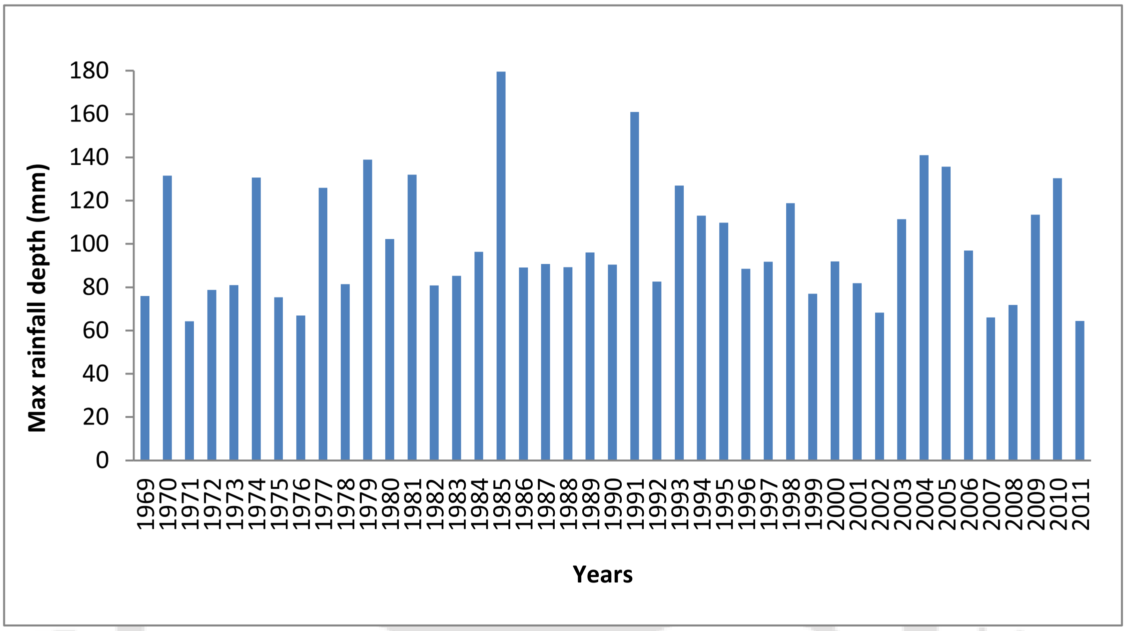

Fig. 5.2: Annual Maximum of daily rainfall data collected from RMC, Barjhar

Table 5.1: D-index values obtained against probability distribution methods for annual maximum of daily rainfall data

Probability Distributions	Gumbel	Normal	Log normal	Pearson Type III	Log Pearson Type III
D-index values	0.3985	0.4844	0.4649	0.3501	0.3490

Based on the D-index test, Log-Pearson Type III distribution was found to be the most suitable for estimation of extreme rainfall events of RMC, Barjhar. Again, to get a short duration rainfall IDF curve, short duration rainfall data are required. Indian Meteorological Department (IMD) has given an empirical reduction formula for the derivation of short duration rainfall values from daily rainfall values. This equation has been successfully applied in many studies (Chowdhury et al. 2007; Rashid et al. 2012; Jalee and Farawn 2013; Nyamathi and Arelt 2013; Bhatt et al. 2014; Rasel and Islam 2015). Here, this IMD empirical reduction formula (Eq. 5.4) has been used to derive short duration design rainfalls from design daily rainfalls obtained from the frequency analysis of collected daily rainfall data.

$$P_t = P_{24}\,(t/24)^{1/3} \qquad (5.4)$$

where, P_t is the required rainfall depth in mm at t-hr duration, P_{24} is the daily rainfall in mm and t is the duration of rainfall in hr for which the rainfall depth is required. From short duration rainfall data, thus derived, rainfall intensities of different return periods have been calculated and IDF curves have been plotted for different return periods like 5, 10, 25, 50, 100 and 200 years (shown in Fig. 5.3). The general form of the equation is $I = a.(t_d)^{-b}$, where t_d is the rainfall duration, 'a' and 'b' are two parameters; 'a' varies with return periods and 'b' remains constant equal to 0.66. The parameter values of the equations of IDF curves for different return periods are shown in Table 5.2.

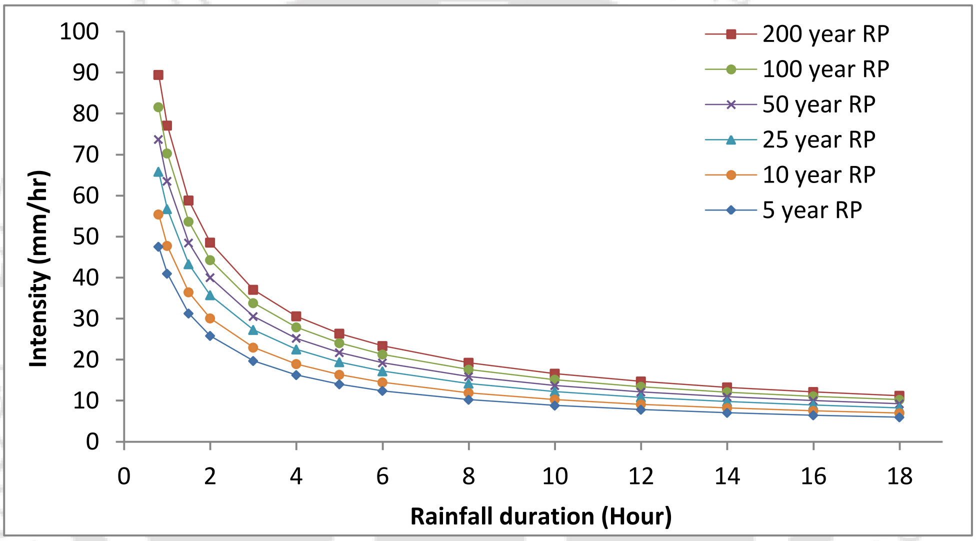

Fig. 5.3: IDF curves of Guwahati city generated by reducing the design daily rainfall of different return periods by IMD empirical reduction formula.

Table 5.2: Parameter values of the equation of the IDF curves for different return periods

Return Period	Parameter 'a'	Parameter 'b'	R-square value
200	77.08	0.66	1
100	70.3	0.66	1
50	63.51	0.66	1
25	56.73	0.66	1
10	47.76	0.66	1
5	40.97	0.66	1

The rainfall distribution in Guwahati city is random in nature (Sarma et al. 2005). When one part of the city faces intense rainstorm, the other parts of the city may experience no or less rainfall. The city being encircled by hills, the orographic effect causes variation of rainfall characteristic within the city. Although RMC, Barjhar is situated only at a distance of about 30 km from the central Guwahati city, rainfall data recorded in Barjhar may not characterize the rainfall behaviour of the whole study area. Hence, based on one-year data of rainfall, a sample test was carried out to check whether the IDF curves (shown in Fig. 5.3) generated with the rainfall data collected in RMC Barjhar are safe for the study area. For this purpose, hourly rainfall data have been taken from MHRD (Ministry of Human Resource Development, India) sponsored project "Urban Flood Hazard Mitigation of Guwahati City by Silt Monitoring and Watershed Modelling" executed in Civil Engineering Department, IIT Guwahati. These hourly rainfall data were recorded for a period of 1 year (from June 2003 to May 2004) in Hatigarh Chariali, a central place of Guwahati city located almost 30 km away from RMC, Barjhar. As per these rainfall data, the maximum and minimum rainfall in the recorded period are 90.25 mm and 0.125 mm, respectively and the numbers of wet days are 136. On the other hand, as per the daily rainfall data collected from RMC Barjhar in the same period, the maximum and minimum rainfall have been obtained as 116.5 mm and 0.1mm, respectively and the numbers of wet days are 148. The monthly average of daily rainfall and the standard deviation and coefficient of variation of the monthly average of daily rainfall are calculated for Hatigarh Chariali and RMC, Barjahr (Fig. 5.4).

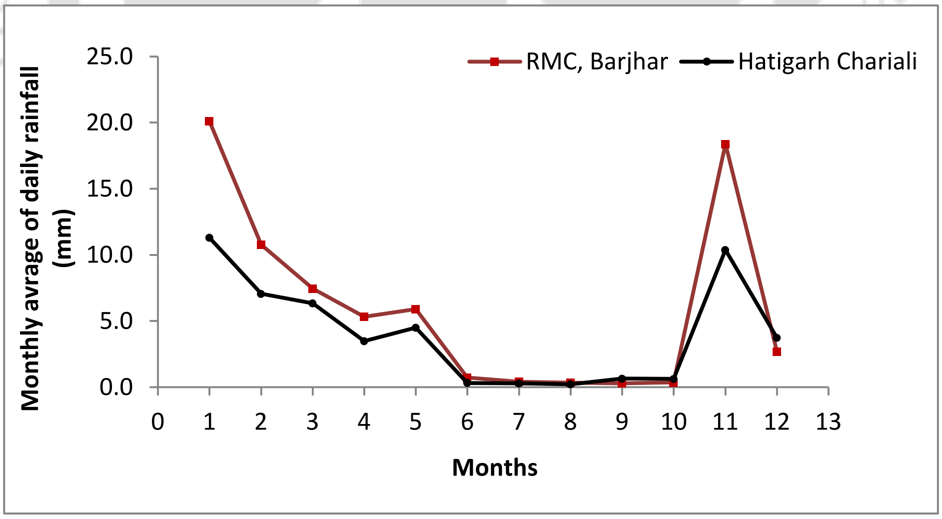

(a)

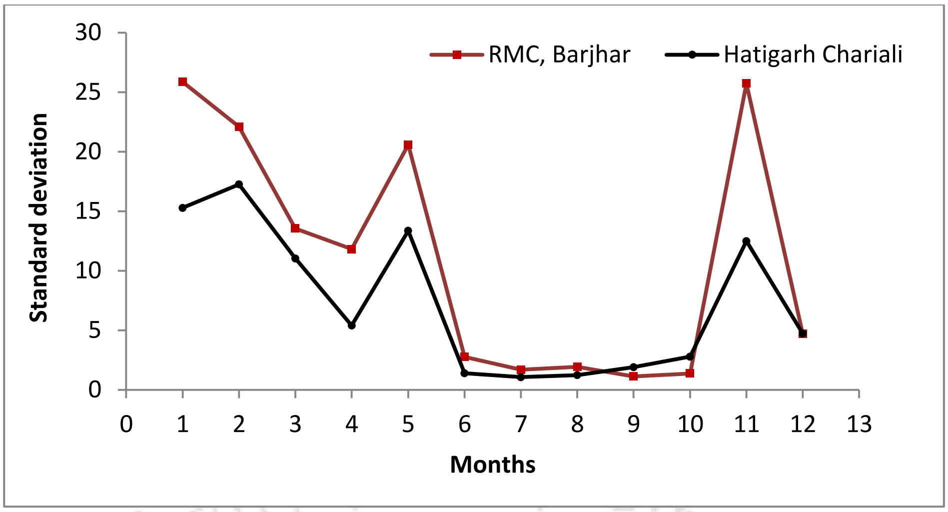

(b)

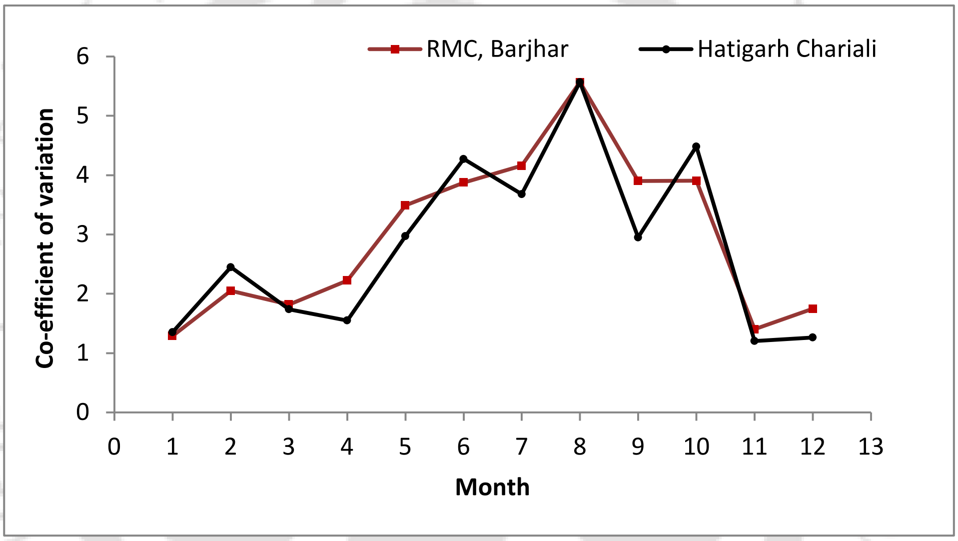

(c)

Fig. 5.4: (a) Monthly average of daily rainfall (b) Standard deviation from monthly average of daily rainfall and (c) Co-efficient of variation of monthly average of daily rainfall in Barjhar and Hatigarh Chariali of Guwahati city.

By comparing these plots, it is clear that though the trend of inter-month variability of average daily rainfall in these two locations is same, Barjhar area which is located at the periphery of the city experiences a little bit higher rainfall than the centre area of Guwahati city. Therefore, rainfall data collected in RMC, Barjhar can be used to represent as the rainfall data of entire Guwahati city since moderately higher rainfall values are considered as conservative for hydraulic design purpose. However, this observation is based only on one-year data of rainfall recorded in core city area of Guwahati city. A more extensive analysis could have been possible to carry out if data were available for a number of years in different locations of Guwahati city. The same hourly rainfall data recorded in Hatigarh Chariali were used by Sarma and Goswami (2006) to form an ID curve of Guwahati city by using a simplified method. To check the reliability of the IDF curves generated by using IMD empirical reduction formula as shown in Fig. 5.3, an ID curve is generated by reducing the maximum daily precipitation 116.5 mm (recorded in RMC, from June 2003 to May 2004) with Eq. (5.4) and compared with the ID curve generated by Sarma and Goswami (2006) (Fig. 5.5).

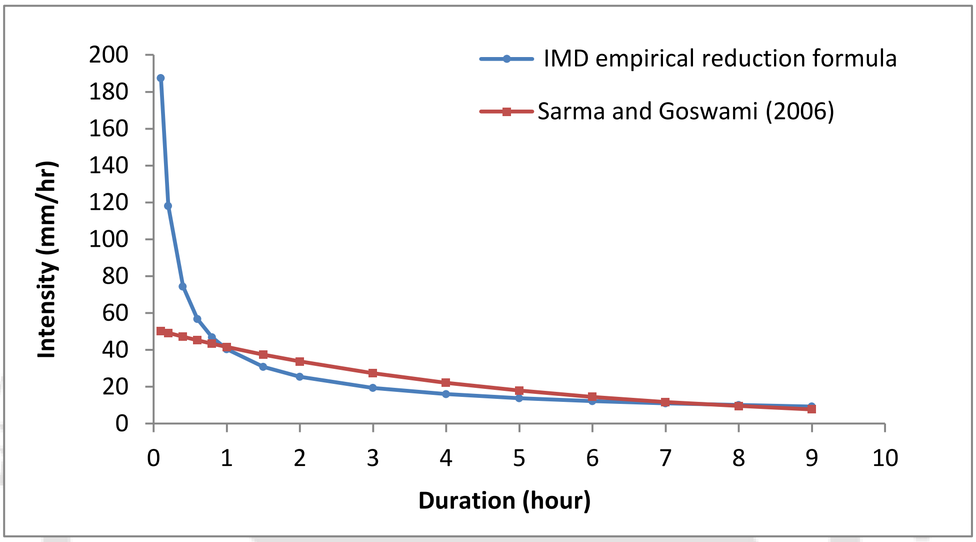

Fig. 5.5: ID curve generated by reducing maximum daily rainfall with IMD empirical reduction formula along with the ID curve generated by Sarma and Goswami (2006).

From Fig. 5.5, it is noticed that ID curve generated by reducing maximum daily rainfall with IMD empirical reduction formula is found to be more conservative for rainfall of durations less than 1 hour and greater than 7 hours. On the other hand, for duration ranging from 1 hour to 7 hours, ID curve generated by Sarma and Goswami (2006) is found to be more conservative. Since, the numbers of watersheds having times of concentration higher than 1 hour are negligible in hills of Guwahati city, hence, it is safe to use the IDF curves shown in Fig 5.3 to determine the maximum average rainfall intensity in the watersheds of this study. However, to be in conservative side, additionally a set of IDF curves has been generated by combining the difference of intensities between the ID curves shown in Fig. 5.5 with the IDF curves shown in Fig. 5.3. The difference in intensities between the ID curves (shown in Fig. 5.5) was modelled by a non-linear relation with respect to time. This non-linear relationship between the difference of rainfall intensities and time is obtained as-

$$\Delta I = -0.085t^4 + 1.622t^3 - 11.08t^2 + 30.08t - 19.10 \tag{5.5}$$

where, ΔI is the rainfall intensities difference in mm/hr between the ID curve generated by Sarma and Goswami (2006) and that by reducing the maximum daily rainfall (recorded in RMC, Barjhar) with IMD empirical reduction formula and't' is the duration of rainfall in hours. The values of 'ΔI' are combined as additive values to the intensities of the different rainfall duration with respect to different return period obtained from the IDF curves of Guwahati city (shown in Fig. 5.3). These newly developed set of IDF curves of Guwahati city are shown in Fig 5.6. The general form of the equations is I= a. $(t_d)^{-b}$, where, t_d is duration of rainfall, 'a' and 'b' are two parameters varying with return periods. The parameters of the equations of safe IDF curves for different return periods are shown in Table 5.3. This new set of IDF equations will be capable of giving the rainfall intensity for any rainfall duration. However, use of very recent data might have generated a new set of IDF curves exceeding the values of "safe" IDF curves shown in Fig. 5.6.

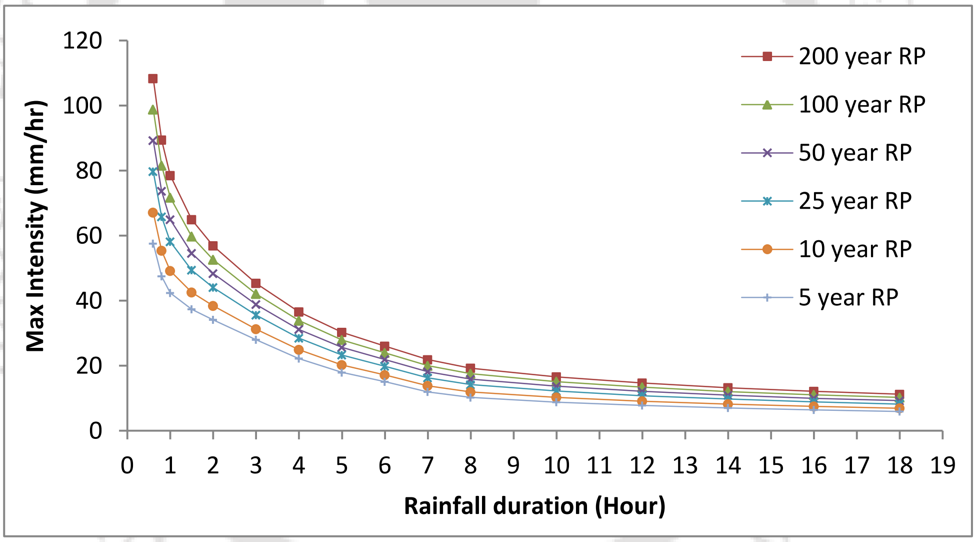

Fig. 5.6: Safe IDF curves of Guwahati city applicable for all rainfall duration

Table 5.3: Parameters of the equation of the safe IDF curves of Guwahati city with respect to different return periods

Return Period	Parameter 'a'	Parameter 'b'	R-square value
200	83.51	0.68	0.99
100	76.70	0.68	0.988
50	69.89	0.68	0.986
25	63.08	0.69	0.983
10	54.06	0.69	0.978
5	47.22	0.69	0.972

5.2.4 Determination of runoff coefficient

Runoff coefficient is the most critical input parameter to the Rational Method. In reality, the value of this parameter depends on various factors such as antecedent moisture content, infiltration capacity, degree of surface undulations, ground slope, soil types, land use land cover (LULC) types etc. (ODOT Highway Division 2014). However, without considering all these factors, some average values of runoff coefficients are considered based on land use land cover types. Again, in case of watersheds having more than one LULC types, a composite runoff coefficient has been determined based on the area shared by different types of LULC present in that watershed. In the watersheds of hills of Guwahati city, basically, six types of LULC have been found. Runoff coefficient values used for these LULC types are shown in Table 5.4. The maximum coverage area including the area for infructural facilities in the urban settlement area is taken as 60% as per the GMDA (2006). Therefore, percent of imperviousness in urban settlement area in a hill is taken as 60% considering the rest 40% area in bare condition. Runoff coefficient for the coverage area is taken as 0.9 (San Diego County 2003; ODOT Highway Division 2014).

Table 5.4: Runoff coefficient values for different surface covers.

LULC	Runoff coefficient C
Bare soil	0.5 (Sarma 2011)
Forest	0.2 (Sarma et al. 2005; Sarma 2011)
Scrub land	0.3 (Sarma 2011)
Marshy land	0
Water bodies	0 (Sarma 2011)
Urban settlement (60% impervious, 40% bare)	0.74 (=0.9x0.60+0.5x0.4)

5.2.5 Calculation of peak discharge for watersheds having area greater than 2.59 sq. km

There are total 6 watersheds having areas greater than 2.59 sq. km in 15 hills of Guwahati city. Those are watersheds with basin ID 53 of Fatasil hill; 2, 5, 6, and 7 of Khanapara-Koinadhara hill and the Garbhanga hill watershed. Peak runoffs from these 6 watersheds have been calculated by using the NRCS TR-55 graphical peak discharge method (SCS 1986). In English system of units, the peak discharge equation used in this method is given by-

$$Q = q_u \times A \times Q_d \times F_p \qquad (5.6)$$

where, Q is the peak discharge (cfs) from the watershed, q_u is the unit peak discharge (csm/in), A is the watershed area (sq. mile), Q_d = runoff depth (in) and F_p is the pond and swamp adjustment factor. To convert the peak dischage value from cfs to cumec, it should be multiplied by a factor of 0.0283. The step by step procedure of the peak discharge calculation by this method has been presented in the Fig. 5.7. The Soil texture class for Fatasil, Khanapara, Koinadhara and Garbhanga hills of Guwahati city is found as Clay loam as given in Das (1992) and soil map of Guwahati city collected from Assam Remote Sensing Application Centre (ARSAC). Accordingly, the Hydrologic Soil Group (HSG) is 'C' (Subramanya 2011). CN values for LULCs, found in the watersheds, are taken from Subramanya (2011) corresponding to the average moisture condition (AMC-II) and HSG-C.

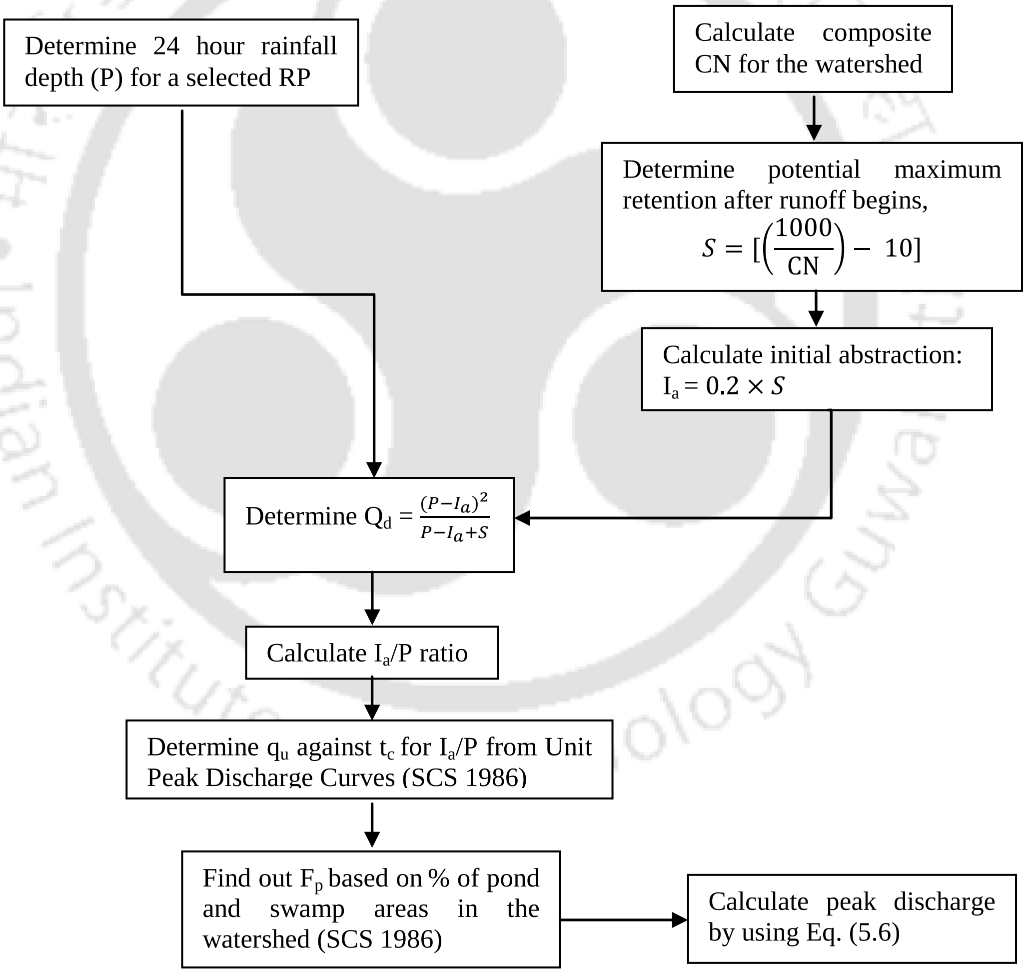

Fig. 5.7: Methodology for peak discharge calculation by NRCS TR-55 graphical peak discharge method

5.3 Results of peak runoff generation

Peak runoff from the watersheds of hills of Guwahati city has been calculated for the years 2011, 2015 and 2025 by using the composite runoff coefficients calculated using the LULC maps generated for the respective years. Again, in the Rational Method it is assumed that return period of peak runoff is same as that of rainfall intensity of duration equal to the time of concentration. Rainfall intensities have been calculated for the return periods 5, 10 and 25 years. Hence, peak discharges have been obtained for the same return periods. A sample calculation of peak discharge has been shown in Appendix B. The peak discharge values for all the watersheds are presented in Table B.1 to Table B.14 (Appendix B). In these Tables, the highest values of rainfall intensities, runoff co-efficients, watershed areas and peak runoffs within every individual hill have been highlighted in blue colour. Again, the watersheds of Fatasil, Khanapara-Koinadhara and Garbhanga hill, whose peak ruoffs were calculated by NRCS TR-55 method, have been highlighted in grey colour.

As watershed area is the significant factor of peak runoff generation; for hills of Guwahati City, higher the watershed area higher the amount of peak runoff. From Table B.1 to B.14 (Appendix B), it is observed that for all the hills except Sonaighuli (Hill ID: 4), the watershed generating the highest peak runoff is same for the years 2011, 2015 and 2025. For Sonaighuli hill, though the watershed with ID 7 is having the largest area, the watershed with ID 18 is producing the highest runoff in 2011 and 2015 due to the quite high runoff coefficients along with its second-highest watershed area in that hill. However, in 2025, the largest watershed with ID 7 is producing the highest runoff due to the projected high increment of urban settlement in the watershed. Again, due to the increase in urban settlement in the watersheds, the runoff coefficients for the same watersheds have different values in the years 2011, 2015 and 2025. Fig. 5.8 and Fig. 5.9 show the total peak runoff with 5 years return period and the average increase in total peak runoff coming from watersheds of individual hills of Guwahati city, respectively. The increases in runoff values in the year 2015 and 2025 have been calculated with respect to runoff values in 2011. It is found that Fatasil (Hill ID 2), Garbhanga (Hill ID 10), Japorigog (Hill ID 7), Khanapara-Koinadhara (combined watersheds, Hill ID 9_15); and Kahilipara (Hill Id 12) are producing comparatively higher runoff. Despite the highest area of Garbhanga hill watershed, Fatasil hill is producing the highest runoff due to the high percentage of urban settlement in it. Again, in 2025, Sonaighuli (Hill ID 4), Chunsali (Hill ID 14) and Khanapara-Koinadhara (combined watersheds, Hill ID 9_15) are the top three hills from the view point of increase in peak runoff due to the projected increase in urban settlement (Fig. 5.9). Despite the highest increase in urban settlement in Garbhanga hill (Hill ID 10) from 2011 to 2025 (from Table 4.6), the watershed of the same does not have a very high increase in peak runoff in comparison to the other watersheds. This is because; in this study, the urban settlement projection has been done only for the hilly areas lying in GMCA and approximately only 2% of the Garbhanga hill watershed area is under GMCA. The remaining portion of the Garbhanga hill watershed is lying in Meghalaya state for which the future LULC of this area is dependent on the development policies of that State. It has been considered that this portion outside GMCA will be having approximately same LULC in 2025. As a result, the increase in peak runoff value from this Garbhanga hill watershed is only with respect to the increase in urban settlement in the 2% watershed area of the hill. From 2011 to 2015, there is an average 2.25% increase in peak runoff from watersheds of hills of Guwahati city, whereas from 2011 to 2025 it is 8.25%.

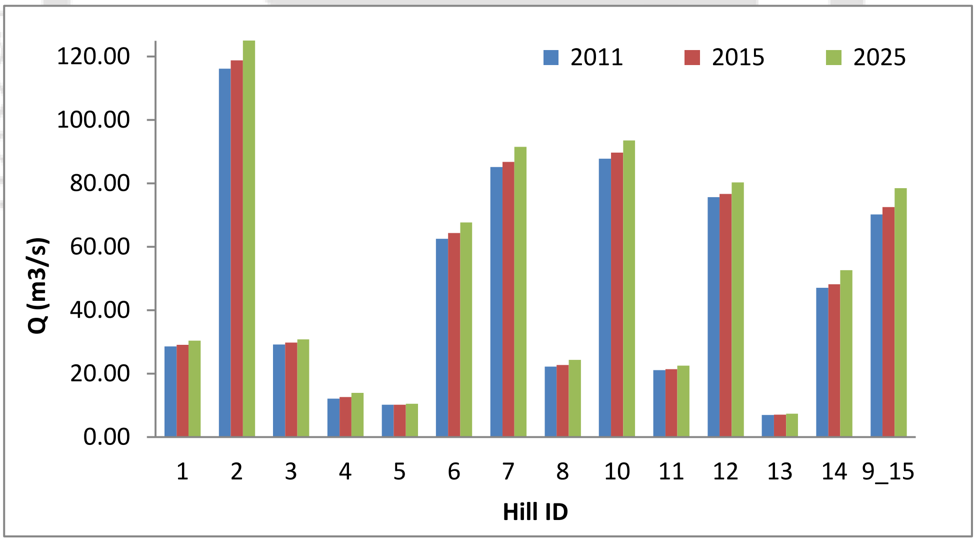

Fig. 5.8: Peak runoffs with 5 year return period coming from the hills of Guwahati city for the years 2011, 2015 and 2025.

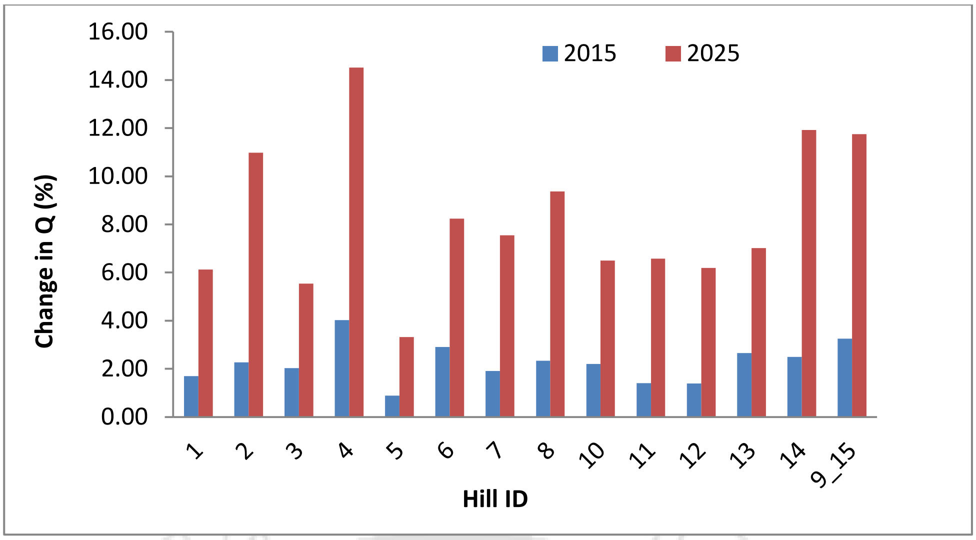

Fig. 5.9: Increase in peak runoffs from the hills of Guwahati city for the years 2015, and 2025 with respect to that in 2011.

5.4 Generation of peak runoff maps

Based on the amount of peak runoff generated, the watersheds of hills of Guwahati city are categorised into 10 classes. These are shown in Table 5.5. Fig. 5.10 shows peak runoff class maps of the hills of Guwahati city for the years 2011, 2015 and 2025, respectively (hills having no change in classes of watersheds are shown once only).

Table 5.5: Classification of watersheds of hills of Guwahati city based on peak runoff generation

Peak Runoff (m^3/s)	Class of watersheds	Assigned colour in map
0-10	Class 1	
10-20	Class 2	
20-30	Class 3	
30-40	Class 4	
40-50	Class 5	
50-60	Class 6	
60-70	Class 7	
70-80	Class 8	
80-90	Class 9	
90-100	Class 10	

5.5 Conclusions

The impact analysis of the projected urban settlement in hills of Guwahati city on peak runoff indicates that the urban flood problem of the city is going to be worsened in future if no proper management actions will be executed. The peak runoff maps developed in this chapter provide a synoptic view of the transition of the class of some watersheds due to the increase in runoff as a result of increasing urban settlement.

These will also help to identify the watersheds of hills requiring watershed management plan in order to minimize peak runoff.

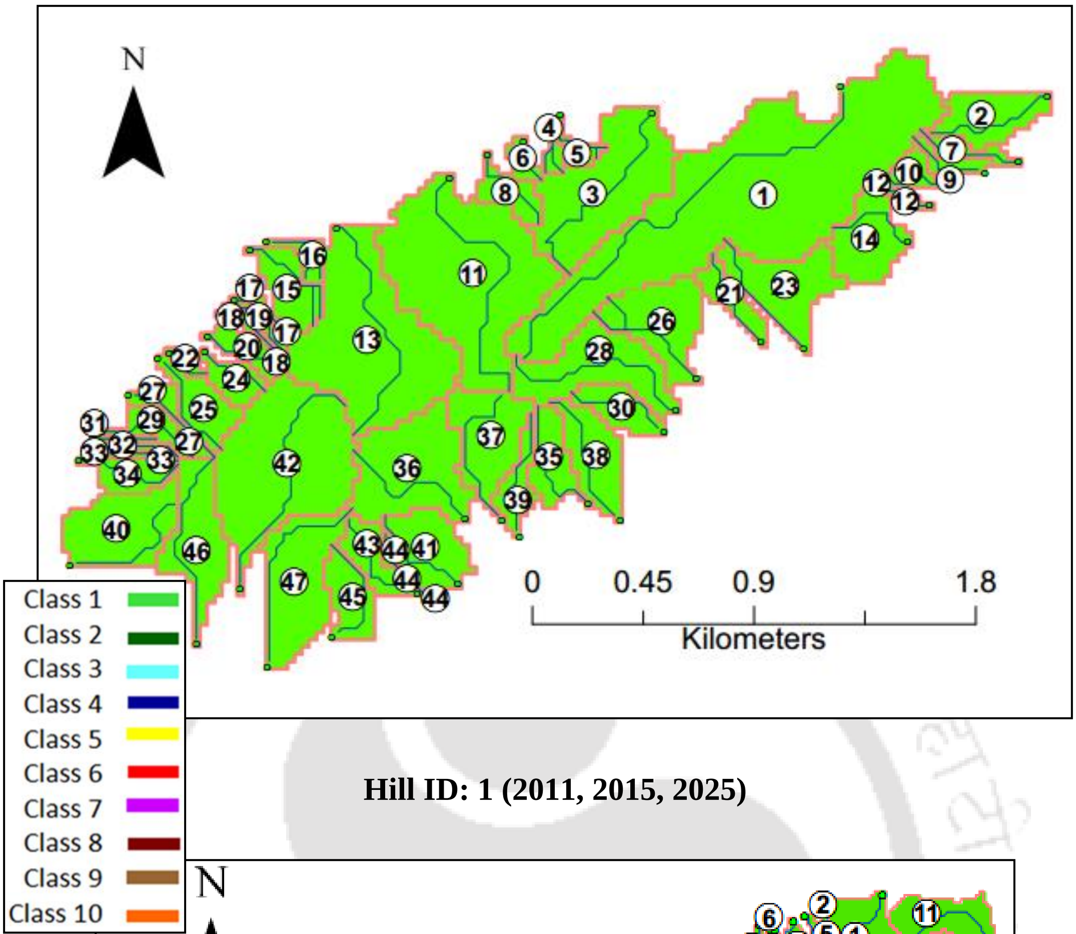

Hill ID: 1 (2011, 2015, 2025)

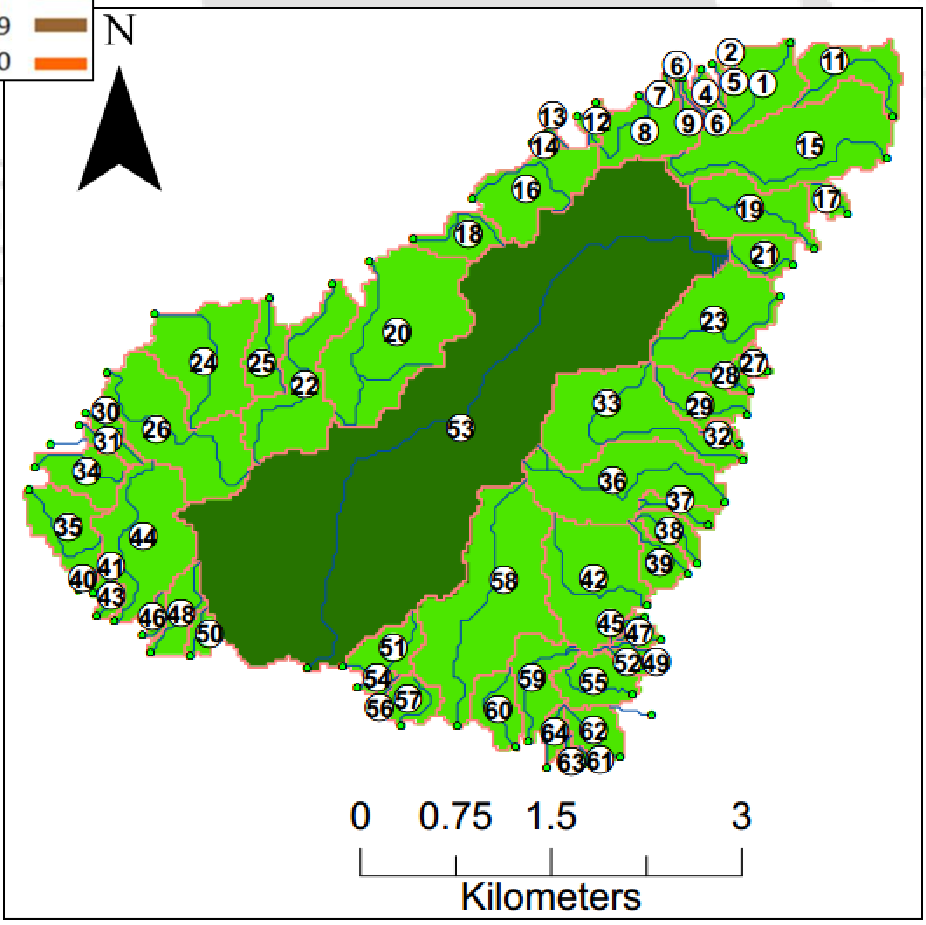

Hill ID: 2 (2011, 2015, 2025)

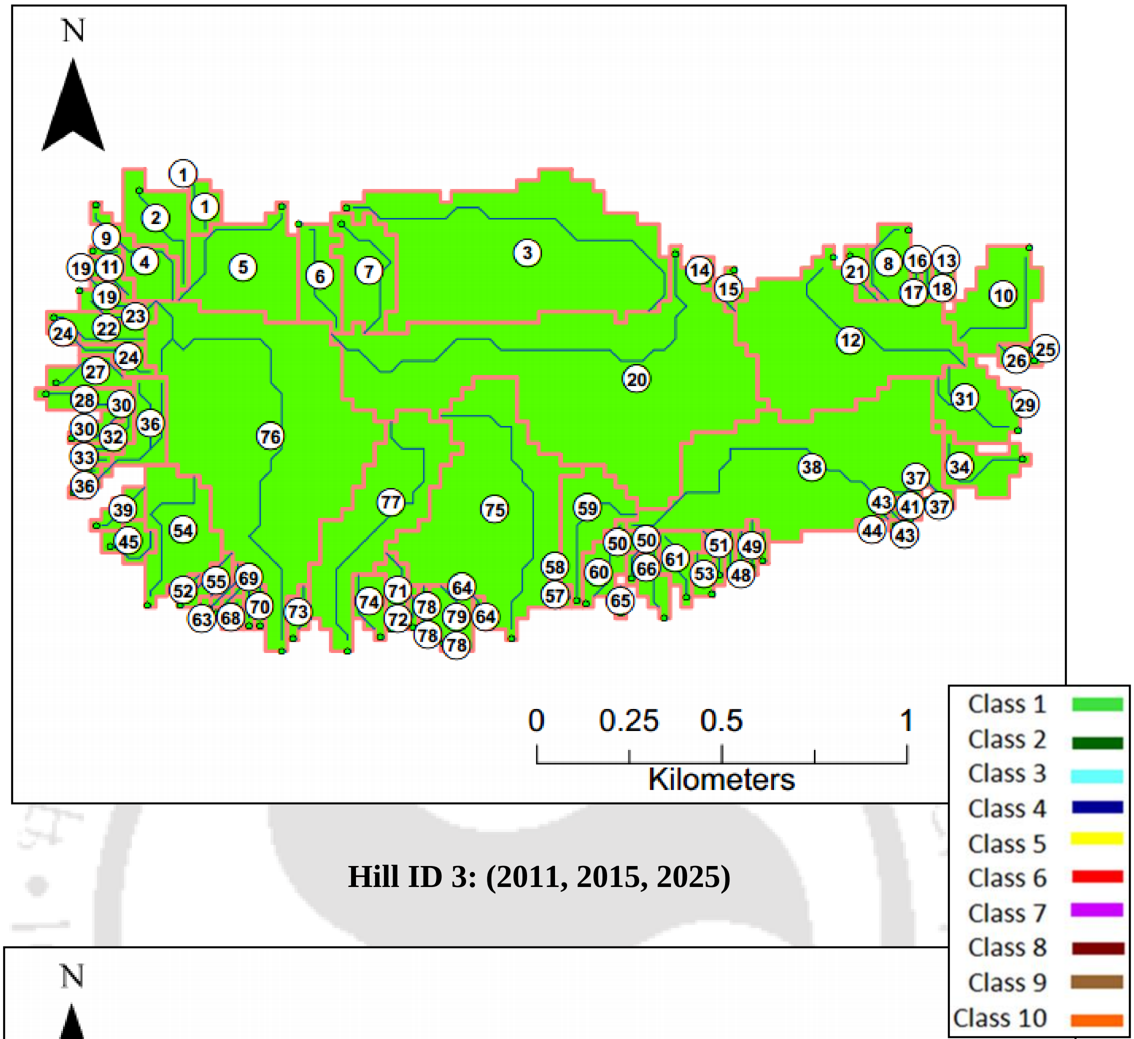

Hill ID 3: (2011, 2015, 2025)

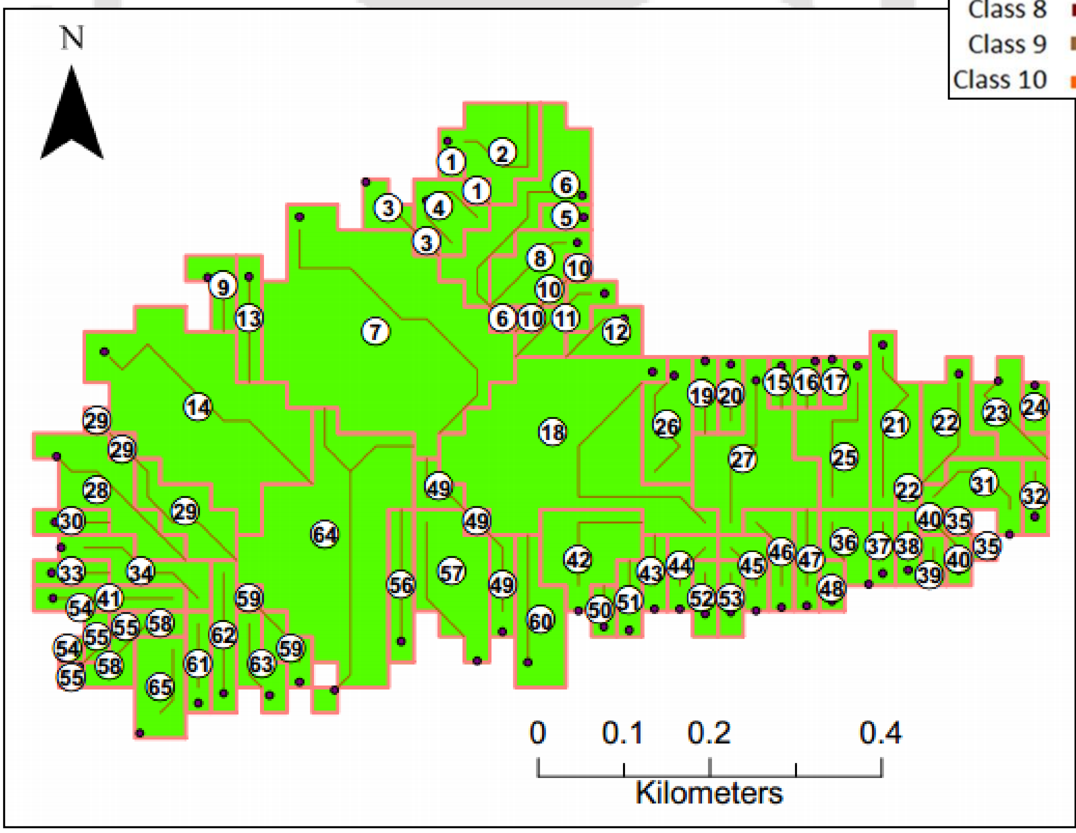

Hill ID: 4 (2011, 2015, 2025)

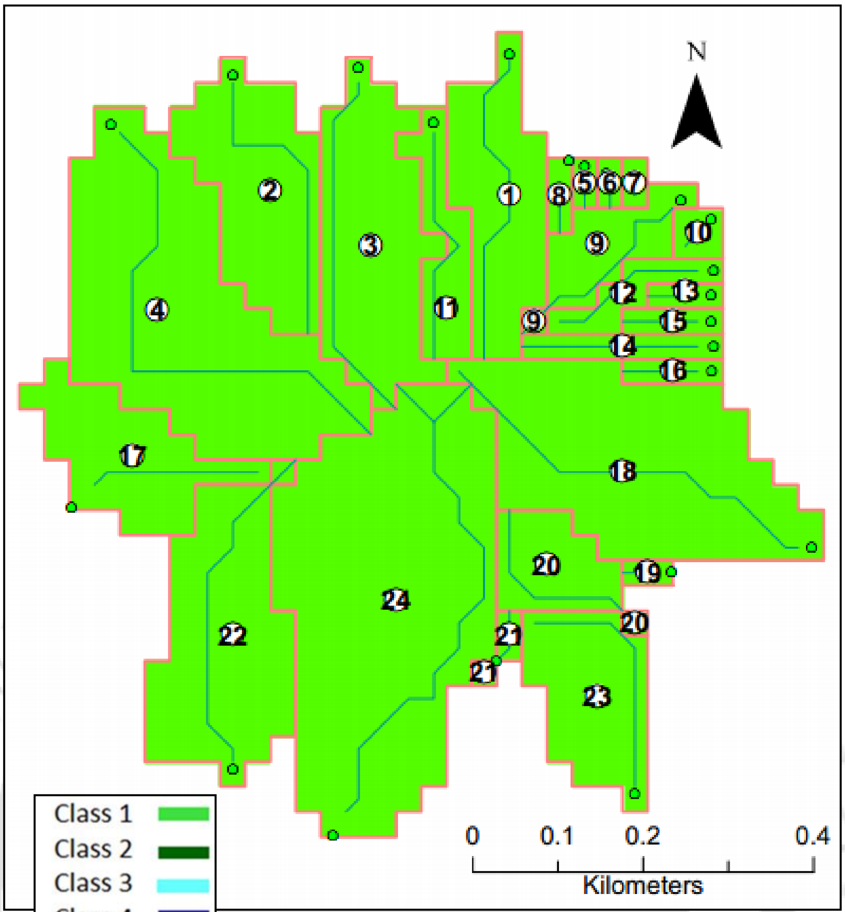

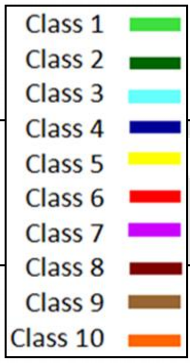

Hill ID: 5 (2011, 2015, 2025)

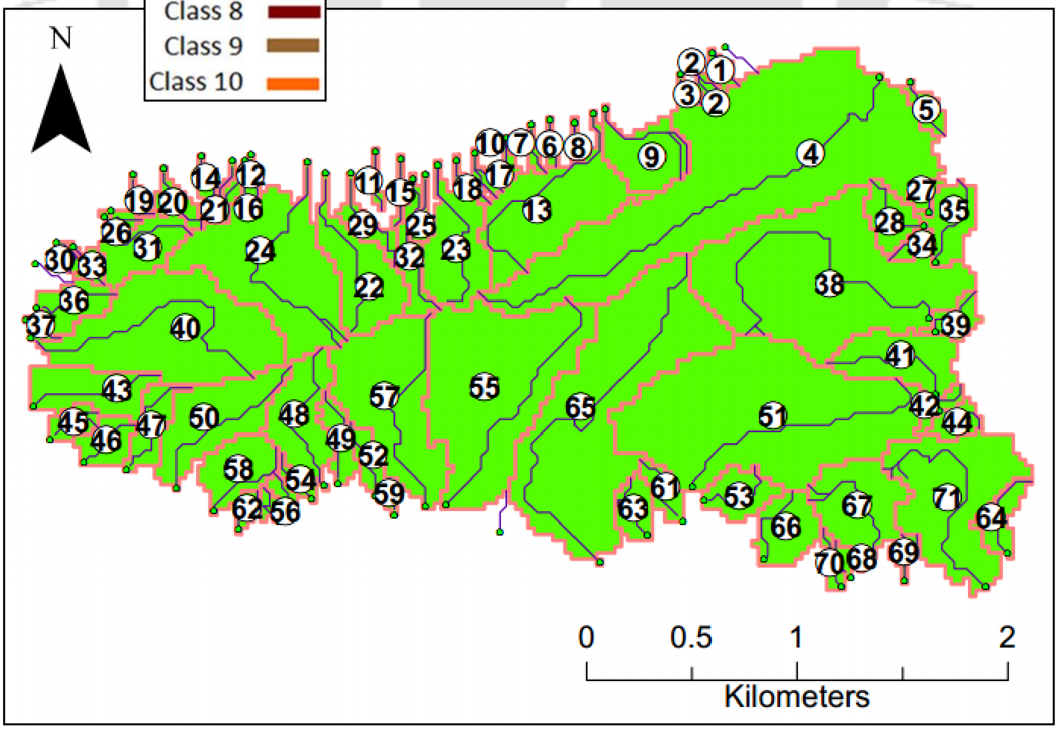

Hill ID: 6 (2011, 2015, 2025)

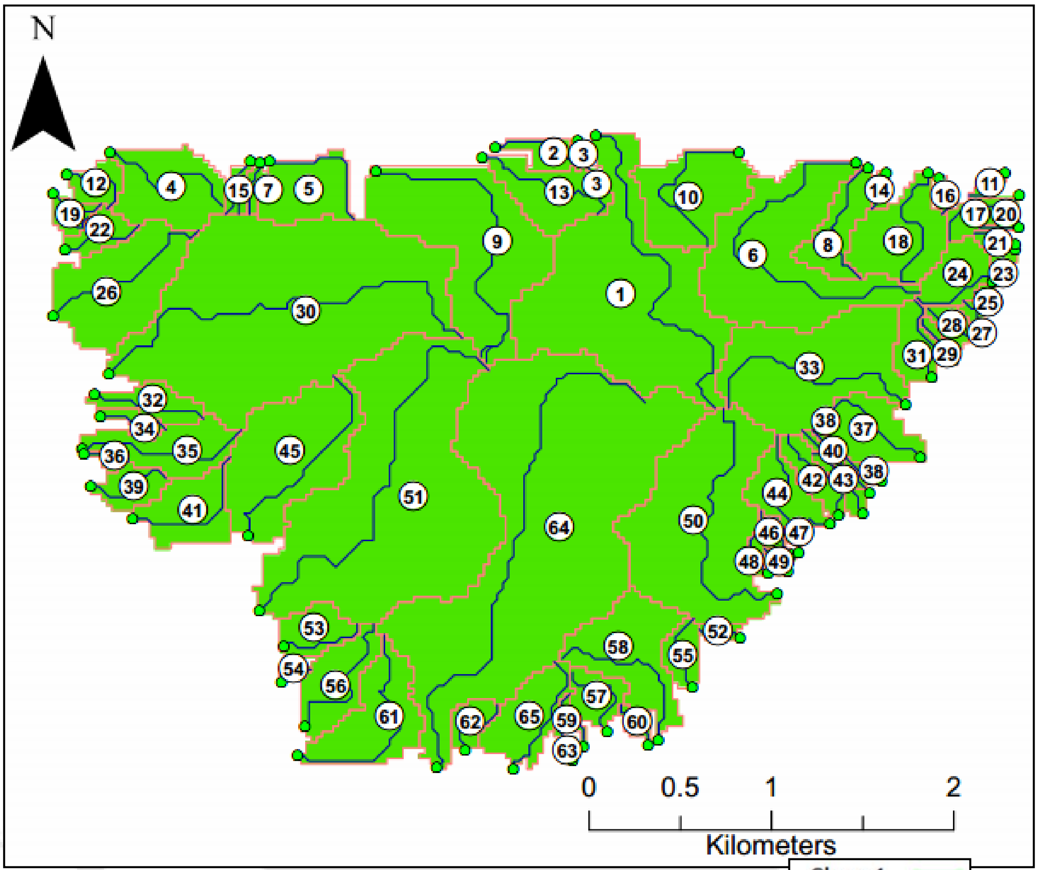

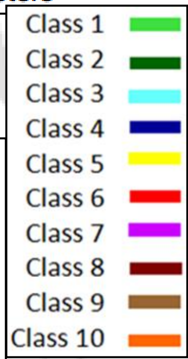

Hill ID: 7 (2011, 2015, 2025)

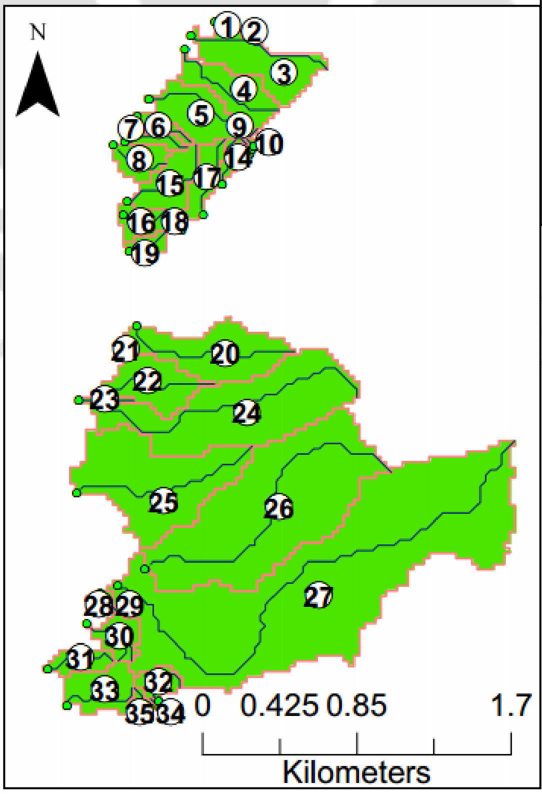

Hill ID: 8 (2011, 2015, 2025)

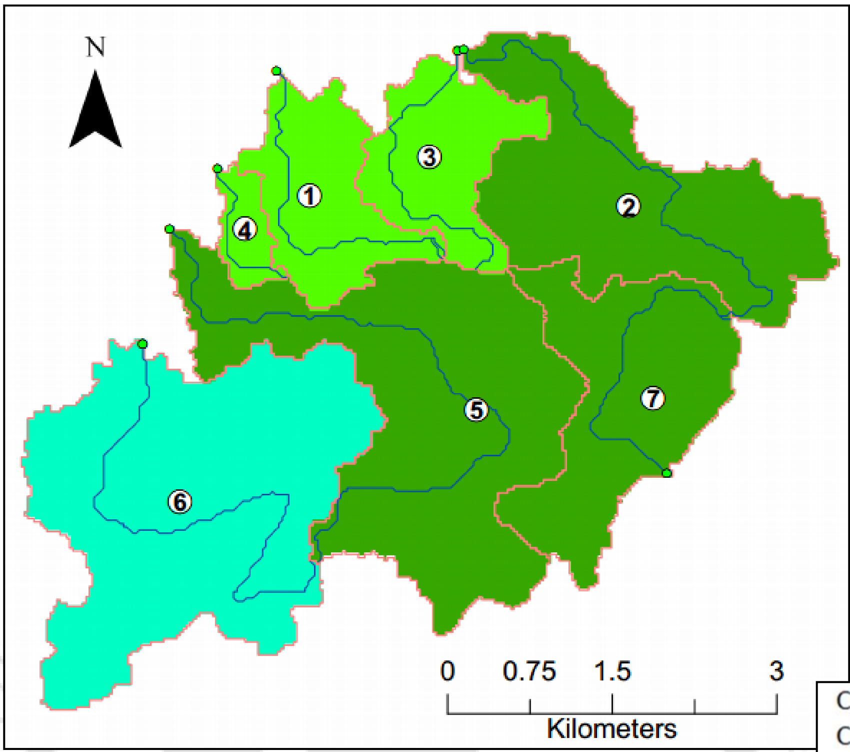

Hill ID: 9_15 (2011, 2015, 2025)

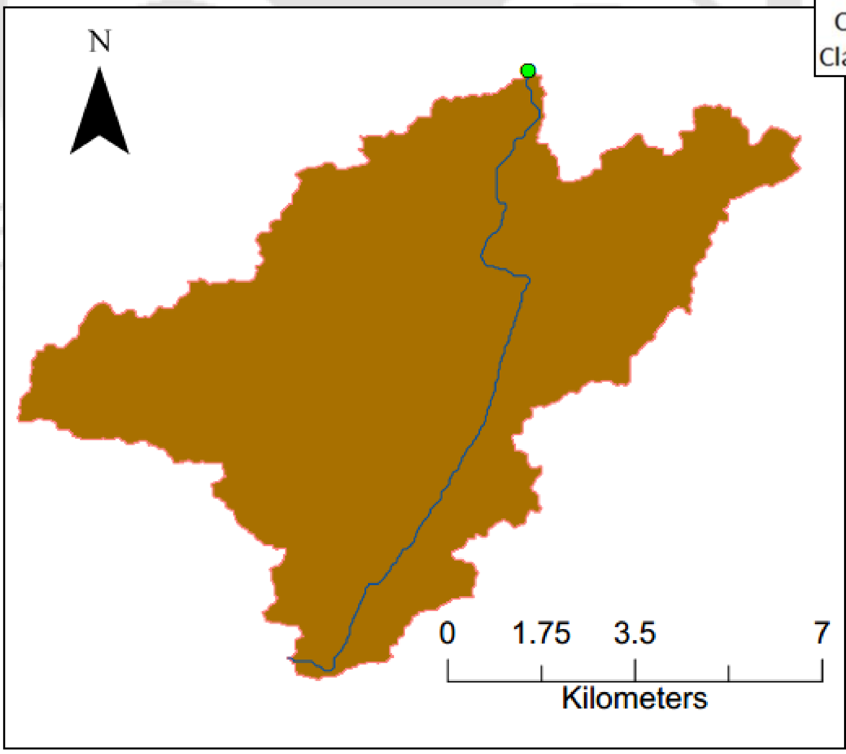

Hill ID: 10 (2011, 2015)

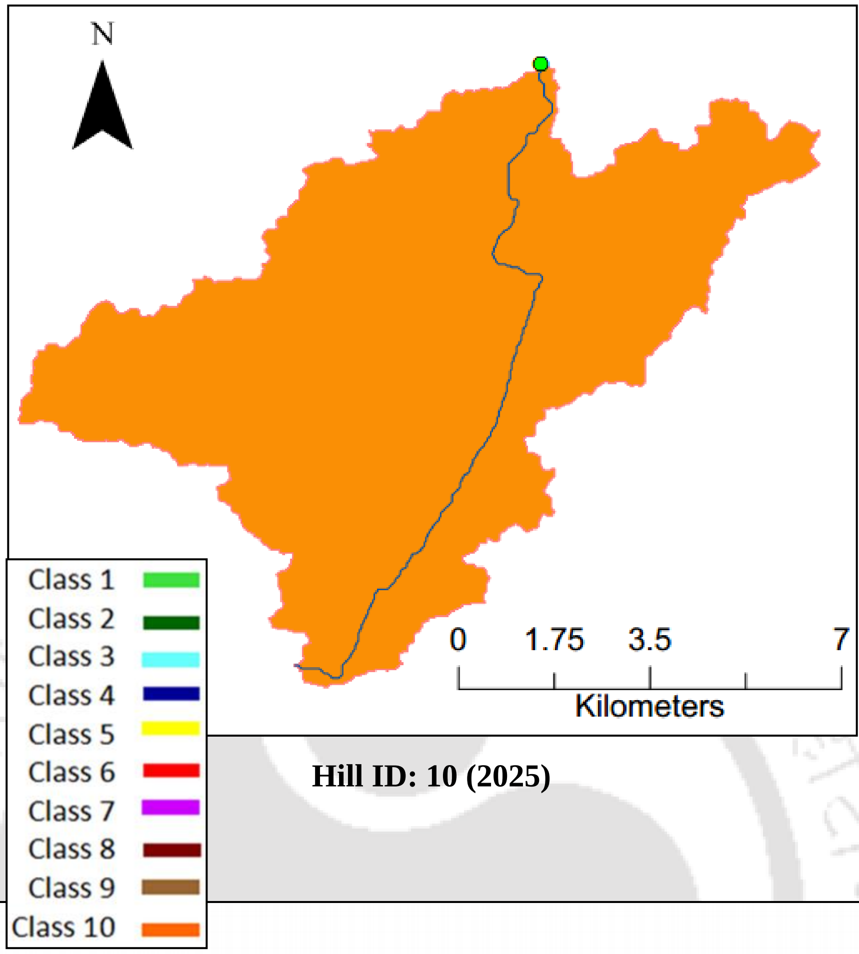

Hill ID: 10 (2025)

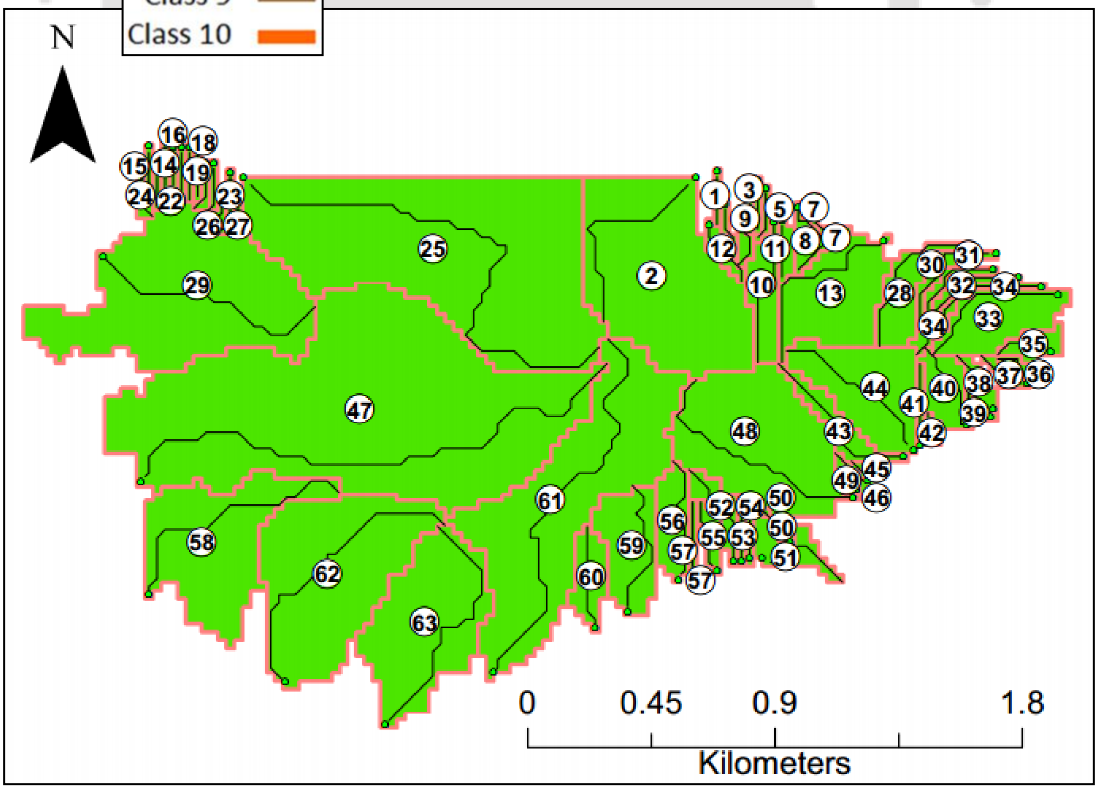

Hill ID: 11 (2011, 2015, 2025)

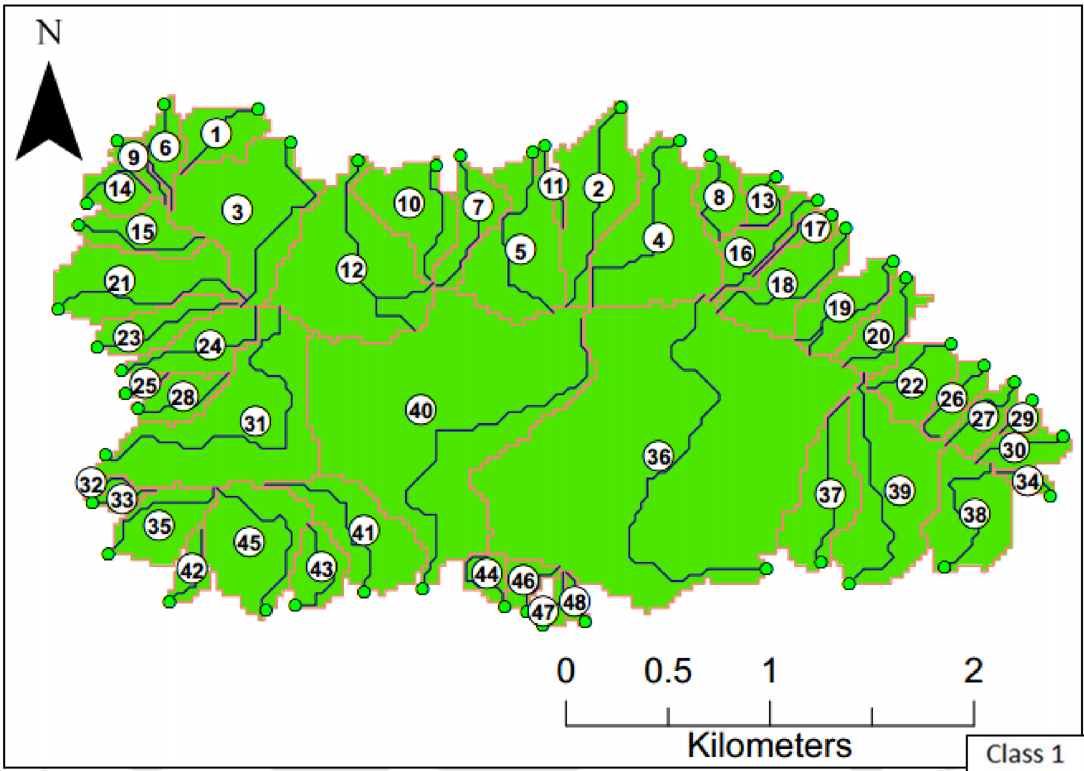

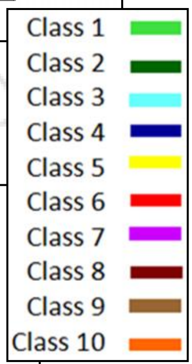

Hill ID: 12 (2011, 2015, 2025)

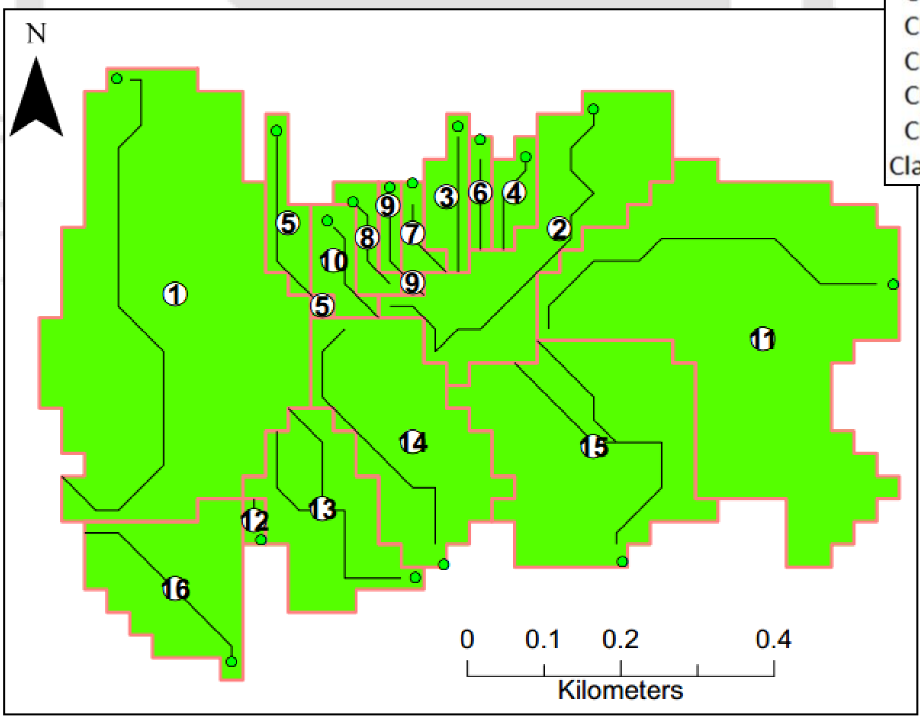

Hill ID: 13 (2011, 2015, 2025)

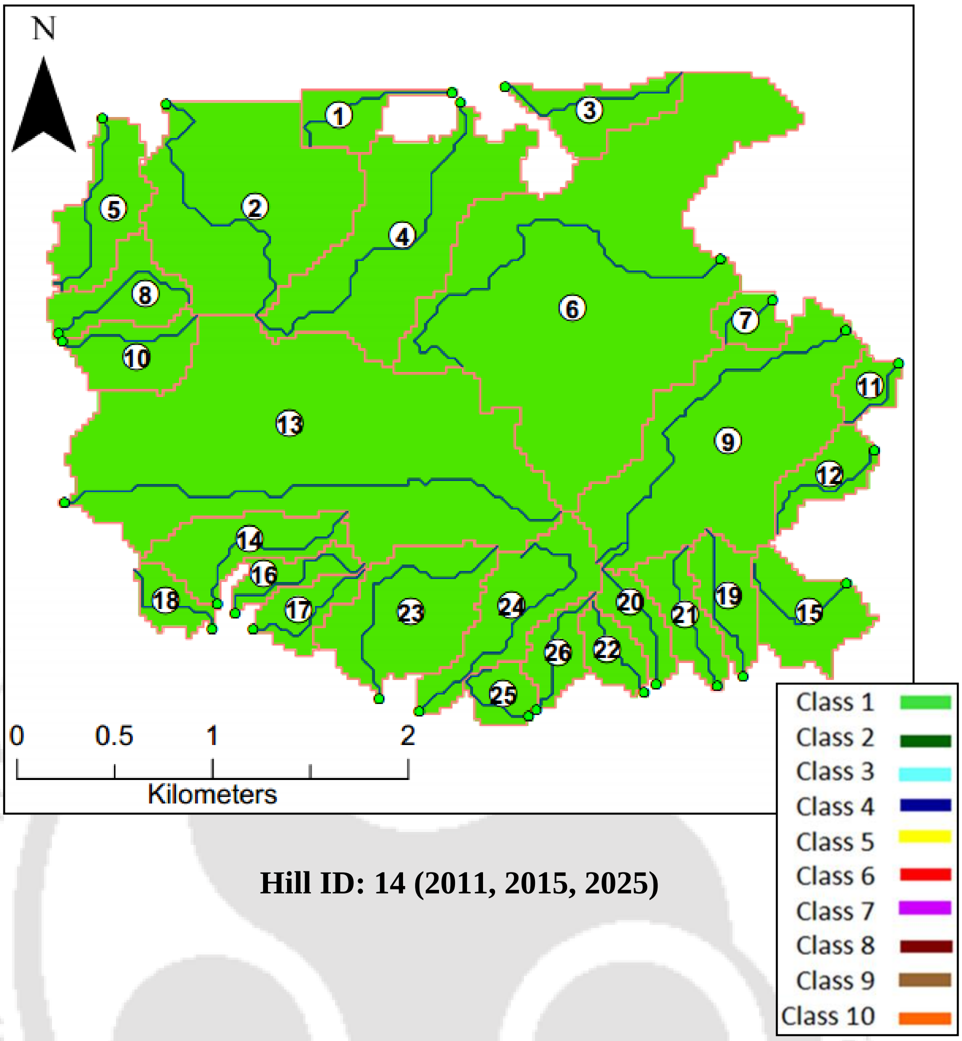

Hill ID: 14 (2011, 2015, 2025)

Fig. 5.10: Peak runoff class maps for watersheds of hills of Guwahati city (∼ : Watershed boundary)

Chapter-6

Effect of projected urban settlement on soil loss from the study area

6.1 Introduction

Steep slopes are more prone to erosion (Duley and Hays 1932, Moore and Burch 1986, Fang et al. 2015). Where removal of the natural land cover is a strong factor of soil detachment, increasing settlements in hills are worsening the soil loss scenario. Sediment delivery ratio which can be defined as the ratio of sediment reached or delivered to the watershed outlet to the total eroded or dislodged soil from that watershed (Fernandez et al. 2003) is generally very high for hilly watersheds. Bare soil particles are detached when they are stricken by raindrops (Singh and Phadke 2006). Steep slopes provide more velocity to runoff which in turn increases the energy of water to detach more soil particles and to carry the sediments with it. All these points exclusively indicate the urgent need of soil loss information such that various management plans can be implemented to tackle the constantly increasing soil erosion hazard with the increase of land degradation process in today's world. According to model projection, within GMCA, in 2025, the average urban settlement in hills of Guwahati city will be 25.45% (in % of hill area), whereas in 2011 it was 14.3%. It is essential to study how this increment of urban settlement in hills of Guwahati city will increase sediment loss in 2025. Hence, RUSLE has been applied for soil loss estimation. In order to interpret the spatial variation of erosion, the model execution has been performed in GIS platform. The detail of estimation is described below.

6.2 Estimation of RUSLE parameters

RUSLE uses the same basic equation of USLE containing six factors. This is given by,

$$A = R \times K \times LS \times C \times P \quad (6.1)$$

where, A is the average annual soil loss per unit area (t $ha^{-1} year^{-1}$), R is the rainfall-runoff erosivity factor (MJ mm ha^{-1} $h^{-1} year^{-1}$); K is the soil erodibility factor (t h MJ^{-1} mm^{-1}); L is the slope length factor; S is the slope steepness factor; C is the cover and management factor; P is the support and conservation practices factor. L, S, C and P factors are dimensionless. Determination of all of these factors are stated below-

(a) Rainfall erosivity factor 'R': Rainfall erosivity factor 'R' stands for the eroding capability of rainfall (Renard et al. 1997). Both due to the impact of raindrops and heavy storm runoff resulting from intense rainfall, soil particles are dislodged which lead to the occurrence of sheet or rill erosion (Biswas and Pani 2015). R factor can be calculated by the equation given by Renard and Freimund (1994). This revised relation was derived based on more data.

$$R=\frac{1}{n}\sum_{j=1}^{n}\left[\sum_{K=1}^{m}(E)_k\,(I_{30})_k\right]_j \qquad (6.2)$$

where, $E=\sum_{r=1}^{m} e_r\,\Delta V_r$ =Total storm kinetic energy in MJ/ha

I_{30} = Maximum 30 minutes rainfall intensity

j = Index for the number of years used to compute the average

k = Index of the number of storms in each year

n = Number of years to obtain average

m = Number of storms in each year

e_r = 0.29 [1- 0.72 exp (-0.05) i_r] = Rainfall energy per unit depth of rainfall per unit area for the r^{th} increment of m numbers of divisions of the storm hydrograph in MJ $ha^{-1}mm^{-1}$.

$i_r=\frac{\Delta V_r}{\Delta t_r}$ = Rainfall intensity for the r^{th} increment in mm h^{-1}.

ΔV_r= Depth of rain falling in the r^{th} increment.

Δt_r = Duration of increment in h (hour).

Sarma et al. (2005) obtained the R factor value for Guwahati city as 9259 MJ.mm ha^{-1} $h^{-1}year^{-1}$. The highest value of R factor in the US is 10000 MJ mm ha^{-1} h^{-1} $year^{-1}$ (Foster et al. 1981). From that point of view, R factor value equal to 9259 MJ mm ha^{-1} h^{-1} $year^{-1}$ is an acceptable value since Guwahati is a place of heavy rainfall (Sarma et al. 2005). In this study, soil loss calculation has been done by taking R= 9259 MJ.mm ha^{-1} $h^{-1}year^{-1}$ (Sarma et al. 2005; Sarma et al. 2013; Sarma et al. 2015).

(b) Soil erodibility factor, K: Soil erodibility factor K indicates the resistance of soil particles against detachment and movement caused by the impact of rainfall and runoff (Renard et al. 1997). It can be defined as the amount of soil loss per unit rainfall erosivity factor from a plot of clean fallow land with a uniform slope of 9% and a slope length of 22.1 m (Weesies 1998, Brady and Weil 2012). K factor can be determined by using soil-erodibility nomograph based on soil texture, composition, organic content and permeability (Wischmeier et al. 1971). In this study, K factor values are taken depending on soil texture class and organic content (2%) as given in Stewart et al. (1975). Necessary unit conversion of K factor has been carried out as per Foster et al. (1981). Soil texture classes for hills of Guwahati city are taken from Das (1992) and also from soil maps of Guwahati city collected from Assam Remote Sensing Application Centre (ARSAC). These soil maps were prepared by using satellite data of years 1993 and 1996; and the SOI (survey of India) map of the year 1995. K factor values for all the hills of Guwahati city are displayed in Table 6.1.

Table 6.1: K factor values for hills of Guwahati city

Hill ID	**Name of hills**	**Soil Type**	**K factor (t h $MJ^{-1}mm^{-1}$) (Stewart et al. (1975)**
1	**University**	Sandy loam	0.031608
2	**Fatasil**	Clay loam	0.032925
3	**Kalapahar**	Sandy loam	0.031608
4	**Sonaighuli**	Sandy loam	0.031608
5	**Sarania**	Clay loam	0.032925
6	**Kharguli**	Clay loam	0.032925
7	**Japorigog**	Clay loam	0.032925
8	**Burhagosain**	Silty clay	0.030291
9	**Khanapara**	Clay loam	0.032925
10	**Garbhanga**	Clay loam	0.032925
11	**Kamakhya**	Sandy loam	0.031608
12	**Kahilipara**	Silty clay	0.030291
13	**Betkuchi**	Sandy loam	0.031608
14	**Chunsali**	Silty clay	0.030291
15	**Koinadhara**	Clay loam	0.032925

(c) Slope length and slope steepness factor, LS: This factor was introduced to account the effect of topography on soil loss (Renard et al. 1997). Slope length is the distance from the starting point of overland flow to the point where deposition starts or runoff goes into a defined channel due to the sufficient decrease of slope and slope steepness means slope gradient (Wishmeier and Smith 1978). Both the quantity and velocity of runoff increase with the increment of slope length and steepness. As a result, soil loss increases. Though originally USLE suggests consideration of an average straight slope, it was found to underestimate the LS factors as it neglects three-dimensional complex form of the topography (Foster and Wishmeier 1974). Use of remote sensing and GIS in the determination of LS factors make possible to consider both the upslope contributing area and the complex three-dimensional form of the topography (Gelagay and Minale 2016). In this study, Eq. (6.3) (Moore and Burch 1986, Desmet and Govers 1996a) has been applied to calculate LS factors in ArcGIS (software) platform. In many studies, this equation has been applied (Moore and Wilson 1992, Mitasova et al. 1999, Gelagay and Minale 2016).

$$LS = \left(\frac{A_c}{22.13}\right)^{0.6} \times \left(\frac{\sin\theta}{0.0896}\right)^{1.3} \tag{6.3}$$

where, A_c and θ are the specific catchment area (m^2) and natural slope angle (degree), respectively. In "Map Algebra" tool of ArcGIS, Eq. (6.3) should be input as-

LS=Power ("Flow accumulation"*cell size/22.13, 0.6)*Power
(Sin("Slope"*0.01745)/0.0896, 1.3) (6.4)

Slope and flow accumulation maps (raster) for the watersheds of 15 hills of Guwahati city have been derived from an SRTM (Shuttle Radar Topography Mission) DEM (Digital Elevation Model) of 1 arc-second resolution.

(d) Cover management factor, C and support practice factor, P: Cover management factor is the ratio of soil loss from a plot of land having a particular land cover condition (natural or artificial) to the soil loss in the condition of continuous tilled fallow on the same soil (Renard et al. 1997). The highest value of cover management factor is '1' assigned to completely bare land and the lowest value '0' is assigned to a very well protected soil. It is the most dynamic factor in RUSLE (Gelagay and Minale 2016). On the other hand, support practice factor (P) is the ratio of soil loss from a plot of land having a specific soil conservation practice to that from straight row cultivation with up and down slope (Pandey et al. 2007). For hills of Guwahati city, there are no support practices. Hence, in this study, P factor is taken as 1. Again, C factor values have been assigned based on land cover types as given in LULC maps (Fig. 4.3). These are shown in Table 6.2. For urban settlement in general located in plain area, C-factor value (C_g) has been assigned by considering 60% of the settlement area being impervious and the remaining 40% being in bare condition [According to Guwahati Metropolitan Development Authority [GMDA] (2006), maximum coverage area of building in a plot of land can be 60% of plot area]. C-factor value for the impervious area is taken as '0' (Sarma 2011).

Table 6.2: Cover management factor (C) values for LULC of hills of Guwahati city

LULC type	C factor
Bare soil	1 (Sarma et al. 2005, Sarma 2011)
Forest	0.01 (Sarma et al. 2005, Gelagay and Minale 2016)
Scrub land	0.014 (Wishmeier and Smith 1978, Gelagay and Minale 2016)
Marshy land	0 (Sarma 2011)
Water bodies	0 (Erdogan et al. 2007, Gelagay and Minale 2016)
Urban settlement in plain area, C_g (60% impervious, 40% bare)	0.4 (=0x0.60+1x0.4)

6.3 Derivation of hill cut factor (H_f)

Residential development in hills is generally associated with hill cutting by the dwellers, which convert a forested stable slope into a steep unstable bare slope. This is very common in hills located near the plain urban areas since inhabitants of such hilly area are generally not indigenous hill tribes. As these dwellers are habituated with the living in plain areas, they often cut the hill slope steeply to have a more plain area for residential purpose. In orthorectified satellite image or in a topographical map, while plain urban settlements are visible as it is, only the projections (horizontal) of the bare steep hill cuts are visible as bare areas within the urban settlement. As a result, this may lead to an underestimation of total soil loss from urban hilly watersheds when urban landuse data in hills are derived from satellite images or maps. This may also cause misinterpretation of sediment delivery ratio defined as the ratio of sediment yield observed at the watershed outlet to total soil loss from the watershed. Hence, in order to take account of the soil loss occurred from the actual steep hill cut area (instead of only the projected area of steep hill cut), this study introduces a new dimensionless factor called "hill cut factor (H_f)", which is incorporated into RUSLE model.

6.3.1 General expression

To derive the mathematical expression of "hill cut factor (H_f)", let us consider a rectangular plot of land (it can also be referred as inhabited urban settlement area) of width 'W' and length 'B' in a hilly watershed. Fig. 6.1(a) shows the schematic diagram of the steep hill cut caused by urban settlement in a hill. Let 'L' is the height (inclined) of the steep hill cut produced due to the considered plot of land, and 'h' and 'm' be the vertical and horizontal projections of 'L' [Fig. 6.1(b)]. The average slope (natural) and average hill cut angle of the hilly portion of the watershed are θ and β, respectively. Here, $(W + L) \times B$ is the actual soil loss risk area (caused by the urban settlement area) comprising plot area $(= W \times B)$ and steep hill cut area $(= L \times B)$ [Fig. 6.1(a)]. In orthorectified satellite images or maps, only the projection of this total urban settlement area (actual soil loss risk area) becomes visible and this projected area is equal to $(W + m) \times B$ [Fig. 6.1(c)].

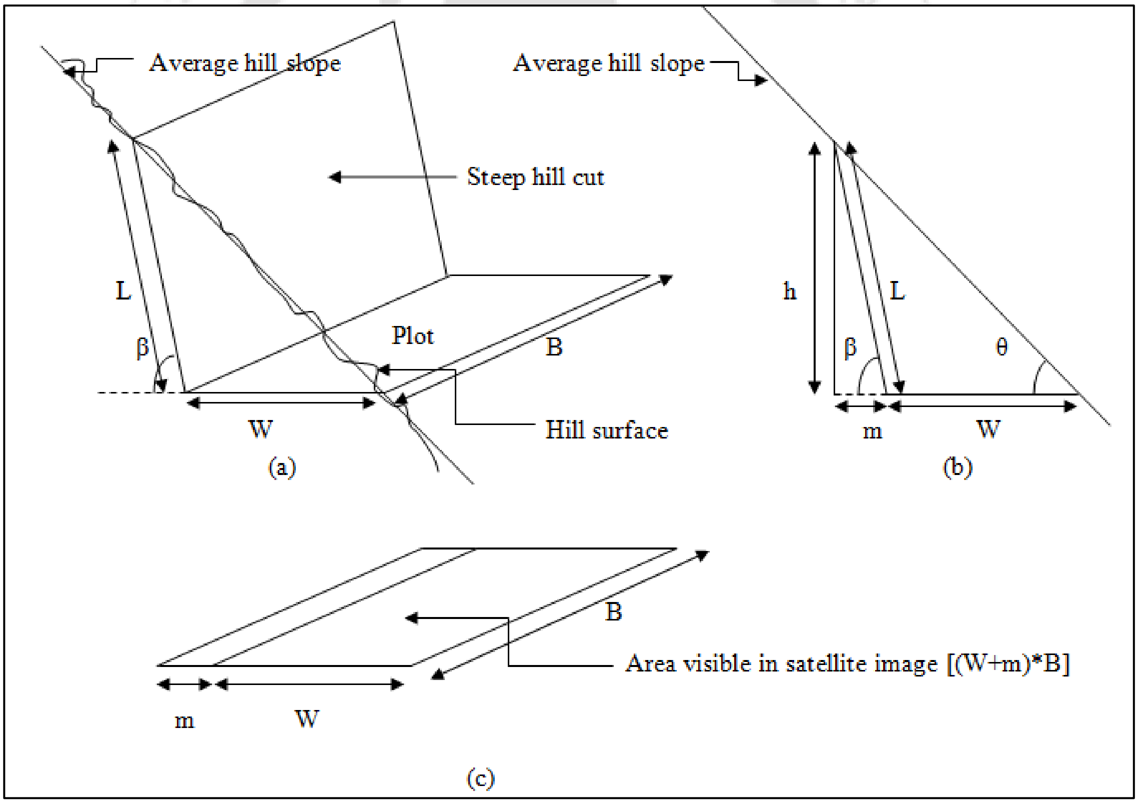

Fig. 6.1: (a) Schematic diagram of steep hill cut caused by urban settlement in hill (b) vertical and horizontal projection of the steep hill cut (c) projected urban settlement area in satellite image.

$$\text{From Fig. 6.1(b), } \frac{h}{m} = \tan\beta \Rightarrow m = h\cot\beta \tag{6.5}$$

$$\text{Again, } \frac{h}{m+W} = \tan\theta \tag{6.6}$$

Substituting Eq. (6.5) in Eq. (6.6),

$$\text{Eq. (6.6)} \Rightarrow \frac{h}{h\ \cot\beta + W} = \tan\theta$$

$$\Rightarrow h = h \cot\beta \tan\theta + W \tan\theta$$

$$\Rightarrow h\,(1 - \cot\beta \tan\theta) = W\tan\theta$$

$$\Rightarrow h = \frac{W \tan\theta}{1 - \cot\beta \tan\theta} \tag{6.7}$$

$$\text{Similarly, } \frac{h}{L} = \sin\beta$$

$$\Rightarrow L = h\ \text{cosec}\beta \tag{6.8}$$

Substituting Eq. (6.7) in Eq. (6.8),

$$\text{Eq. (6.8)} \Rightarrow L = \frac{W \tan\theta\ \text{cosec}\beta}{1 - \cot\beta \tan\theta} \tag{6.9}$$

Therefore, steep hill cut area, which is not visible in the satellite image,

$$A_{hc} = B \times L - B \times m$$

Here,$(B \times m)$ is the projected area of the steep hill cut area $(= L \times B)$.

Hence, the hill cut factor H_f, which is defined as the ratio of the steep hill cut area, not visible in satellite image to the projected settlement area in satellite image or map, can be expressed as,

$$H_f = \frac{B \times L - B \times m}{(W+m) \times B} = \frac{L - m}{W + m} \tag{6.10}$$

Substituting Eq. (6.9) in Eq. (6.10),

$$H_f = \frac{W \tan\theta\ \text{cosec}\beta}{1 - \cot\beta \tan\theta} \times \frac{1}{m+W} - \frac{m}{m+W}$$

$$\Rightarrow H_f = \frac{\sin\theta}{\sin\beta\cos\theta - \cos\beta\sin\theta} \times \frac{W}{m+W} - \frac{m}{m+W}$$

$$\Rightarrow H_f = \frac{\sin\theta}{\sin\,(\beta - \theta)} \times \frac{W}{m+W} - \frac{m}{m+W} \tag{6.11}$$

This H_f is input into the cover management factor of urban settlement and a new cover management factor is obtained, applicable to the urban settlement located in hills only. Due to the inclusion of H_f factor, cover management factor for the urban settlement lying in the hilly portion of the watershed will have a higher value than that for urban settlement, in general, lying in a plain area. Cover management factor for urban settlement in a hill can be expressed as,

$$C_{hu} = C_{add} + C_u$$

where, C_{add} is the cover management factor for hill cut area not visible in satellite image or map, and C_u is the cover management factor for visible urban settlement area of hills in the satellite image. That means the expression of RUSLE for urban settlements located in hills will be,

$$A = R \times K \times LS \times C_{hu} \times P = R \times K \times LS \times (C_{add} + C_u) \times P$$

Additionally, C_{add} depends on the surface condition of the steep hill cuts i.e. whether they are well protected by retaining wall or covered by grass; creeper etc. or they are in bare condition. Hence, C_{add} is given as,

C_{add} = f (H_f, Condition of steep hill cuts associated with urban settlements in hills)

The composite value of C_{add} can be written as,

$$C_{add} = \left(\sum_{i=1}^{n} a_i C_i\right) \times H_f \qquad (6.12)$$

Where, i=1, 2, 3,........, n be types of surface covers.

a_i= Fraction of the total steep hill cut area covered by the i^{th} type of surface cover.

$\sum_{i=1}^{n} a_i = 1$

C_i= Cover management factor of the i^{th} type of surface cover.

Substituting the expression of H_f of Eq. (6.11) in Eq. (6.12),

$$\text{Eq. (6.12)} \Rightarrow C_{add} = \left(\sum_{i=1}^{n} a_i C_i\right) \times \left[\frac{\sin\theta}{\sin(\beta-\theta)} \times \frac{W}{m+W} - \frac{m}{m+W}\right] \qquad (6.13)$$

Similarly, a composite value is also calculated for the cover management factor (C_u) of the urban settlement area visible in the satellite image. Because the projection of the actual soil loss risks area [=(W + m) × B] caused by the urban settlement in hill consists of two types of area:

(1) Projection of the steep hill cut area = m × B.

(2) Projection of the inhabited urban settlement area (or, plot area) =W × B.

Now,

$$\frac{\text{Projection of steep hill cut area}}{\text{Visible urban settlement area in image}} = \frac{m \times B}{(W+m) \times B} = \frac{m}{W+m} = \frac{h\cot\beta}{h\cot\theta} = \frac{\sin\theta\cos\beta}{\sin\beta\cos\theta} \quad (6.14)$$

$$\frac{\text{Projection of plot area}}{\text{Visible urban settlement area in image}} = \frac{W \times B}{(W+m) \times B} = \frac{W}{W+m} = \frac{h\cot\theta - h\cot\beta}{h\cot\theta} = 1 - \frac{\sin\theta\cos\beta}{\sin\beta\cos\theta} \quad (6.15)$$

Therefore,

$$C_u = \underbrace{\frac{m}{W+m} \times \left(\sum_{i=1}^{n} a_i C_i\right)}_{\text{For projection of steep hill cut area}} + \underbrace{\frac{W}{W+m} \times C_g}_{\text{For projection of plot area}} \quad (6.16)$$

where, C_g is the cover management factor for urban settlement located in plain areas. This is also applicable to the inhabited settlement area (or, plot area = W × B) in a hill since before settling in a plot of land, people usually make it plain.

Finally, by adding Eq. (6.13) and Eq. (6.16), the cover management factor for urban settlement located in a hill can be expressed as,

$$C_{hu} = \left(\sum_{i=1}^{n} a_i C_i\right) \times \left[\frac{\sin\theta}{\sin(\beta-\theta)} \times \frac{W}{m+W} - \frac{m}{m+W}\right] + \frac{m}{W+m} \times \left(\sum_{i=1}^{n} a_i C_i\right) + \frac{W}{W+m} \times C_g \quad (6.17)$$

Substituting the expressions of $\frac{m}{W+m}$ and $\frac{W}{W+m}$, respectively from Eq. (6.14) and Eq. (6.15) in Eq. (6.17),

$$\text{Eq. (6.17)} \Rightarrow C_{hu} = \left(\sum_{i=1}^{n} a_i C_i\right) \times \left[\frac{\sin\theta}{\sin\beta\cos\theta}\right] + \left(1 - \frac{\sin\theta\cos\beta}{\sin\beta\cos\theta}\right) \times C_g \quad (6.18)$$

If the projected area of steep hill cuts is very less in comparison to the visible urban settlement area in satellite image [i.e., if $m \times B \ll (m+W) \times B \Rightarrow m \ll (m+W)$], the following two simplifications can be made in Eq. (6.11) and Eq. (6.16),

(i) $\frac{m}{m+W} \ll 1$. Hence, $\frac{m}{m+W}$ term can be considered as negligible [=0].

(ii) $m+W \approx W$ and hence, $\frac{W}{m+W}$ can be taken as 1.

In such a case,

$$\text{Eq. (6.11)} \Rightarrow H_f = \frac{\sin\theta}{\sin(\beta-\theta)} \quad (6.19)$$

$$\text{Eq. (6.16)} \Rightarrow C_{u=} C_g \quad (6.20)$$

Hence, for projected area of steep hill cuts being very less in comparison to the visible urban settlement area in the satellite image, the cover management factor for urban settlement in a hill can be expressed in the following simplified form.

$$C_{hu} = C_{add} + C_u = \left(\sum_{i=1}^{n} a_i C_i\right) \times H_f + C_g = \left(\sum_{i=1}^{n} a_i C_i\right) \times \frac{\sin\theta}{\sin(\beta-\theta)} + C_g \quad (6.21)$$

6.3.2 Model validation

It has already been mentioned that Guwahati is experiencing high sediment loss, beyond its estimated value, because of unplanned residential development in its hilly terrain (Sarma et al. 2013; Sarma et al. 2015). Blockage of drains and culverts due to sediment, brought down from the inhabited hills are exacerbating the urban flash flood problem of Guwahati city (Desai et al. 2014). Hence, hilly watersheds of Guwahati city can be considered as an ideal case-study area in this context. However, observed soil loss data from hilly watersheds of Guwahati city is very scarce. Sarma et al. (2005) observed soil loss at the outlet of a mini-watershed, located in Japorigog hill of Guwahati city for the period from June 2003 to May 2004. In this study, this observed data has been used for validation of the proposed "hill cut factor" incorporated in RUSLE model. The LULC map of the watershed has been prepared by using IKONOS (panchromatic) and LISS III (multispectral) image of capture dates 28th January and 11th December of 2003, respectively. Areas covered by forest, bare land, scrubland and urban settlement in the study watershed are found as 21.5%, 1.8%, 62.35% and 14.35%, respectively. Fig. 6.2 shows the location of the watershed used for validation. Determination and application of H_f factor requires following data-

(a) Average slope of the hilly watershed.

(b) Average hill cut angle.

(c) Data regarding the condition of hill cuts.

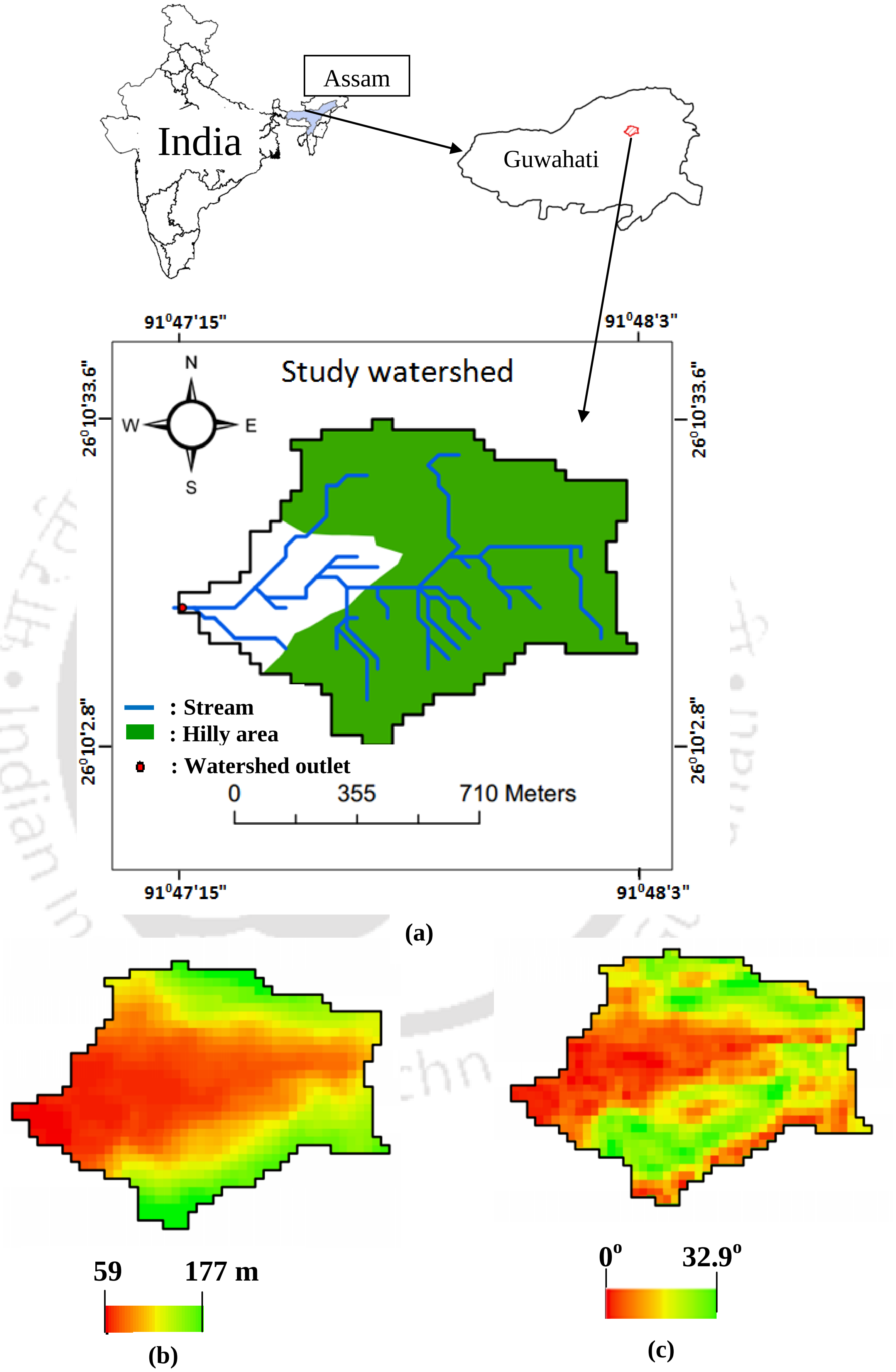

Fig. 6.2: (a) Location (b) elevation map (c) slope map of the study area

In order to have an idea regarding the condition of hill cuts in Guwahati city, a sample field survey was carried out in the Jyotinagar area of the Kharguli hill (Watershed ID: 51 of Hill ID:6). In this survey, total 100 hill cuts were randomly selected to measure the area and angle of hill cuts and also to find the type and approximate quantity of the surface covers of these hill cuts. Some photographs of the field survey are given in Fig. C.1 (Appendix C). It was found that on average only 1% of the total area of hill cuts is protected by retaining wall, 39% area is having grass or creepers and the remaining 60% area is being uncovered or bared. Again, the average gradient of hill cuts was obtained as 70^0. These data represent the vulnerability of widespread sediment loss from the hills of Guwahati city and it has been used to symbolize the present scenario of the entire hills of Guwahati city. These field survey data have been displayed in Table 6.3 and used for calculation of H_f for the considered hilly watershed. By substituting the value of angle β and average slope angle θ of the watershed in Eq. (6.14), it is found that average projected area of the steep hill cut in the watershed is only 0.09 times the urban settlement area visible in the satellite image. That means the projected area of steep hill cut is very less in comparison to the visible urban settlement area in the satellite image and hence, the simplified expression of C_{hu} [Eq. (6.21)] is used for urban settlement in the considered hilly watershed. Soil loss (t ha^{-1} $year^{-1}$) maps are generated for the watershed by multiplying pixel-based values of all the factors of RUSLE in "Map Algebra" tool of ArcGIS software. Two types of raster maps of soil loss rate have been produced- (i) considering H_f (ii) without considering H_f. All the factors of RUSLE other than the C-factor are same for these two scenarios. By taking the arithmetic mean of pixel values of every type of the soil loss raster maps, an average soil loss rate has been calculated. Sarma et al. (2005) measured suspended sediment yield at the outlet of the study watershed and considered an additional 10% of this suspended load as bed load.

Table 6.3: Data used for calculation of H_f and C_{hu} for the hilly watershed.

Types of surface covers in hill cuts (*i*)	a_i (%)	C factor (C_i)	β (degree)	θ (degree)	H_f	C_{hu}
Vegetation (grass, creepers)	39	0.01 (Sarma 2011)	70	14.1725	0.2959	0.5787
Bare (uncovered)	60	1 (Sarma 2011)				
Retaining wall	1	0 (impervious, Sarma 2011)				

By comparing the calculated and observed values (Sarma et al. 2005) of total soil loss from the study watershed in Table 6.4, it is clear that without considering H_f, RUSLE underestimates the total soil loss by almost 28% than the observed one. The mini watershed considered in this study is not having any landslide or gully erosion. Hence, it is clear that this difference of soil loss between the observed and estimated values (without consideration H_f) is not due to some other sources of soil loss like landslides or gully erosion in the watershed. On the other hand, considering H_f, RUSLE has estimated the total soil loss from the watershed with a sediment delivery ratio equal to 0.98. For small hilly watershed located in Guwahati city, Sarma (2011) and Sarma et al. (2013) considered sediment delivery ratio equal to 1. Hence, soil loss estimation from the study watershed by incorporating H_f into RUSLE, which gives a sediment delivery ratio equal to 0.98, is acceptable. However, the hill cut angle β used in the derivation of the hill cut factor of the study area have been calculated as an average of the hill cut angles obtained from a sample field survey. Due to this, at 95% of confidence level, an error margin of (±) 3.02^0 is found for the sample mean of the angle β. Due to this margin of error, the computed value of the total annual soil loss from the study-watershed may vary by (-0.43%) to (+1.2%).

Table 6.4: Calculated and observed values of soil loss from the study watershed

Calculated rate of soil loss (t ha^{-1} year^{-1})		**Watershed Area (ha)**	**Calculated total soil loss (t year^{-1})**		**Observed suspended load (t year^{-1}) (Sarma et al. 2005)**	**Observed total soil loss (t year^{-1}) (Sarma et al. 2005)**
With H_f	**Without H_f**		**With H_f**	**Without H_f**		
239	182	74.47	17798.33	13553.54	15854.81	17440.29

6.3.3 Determination and application of H_f factor to the hills of Guwahati city

The sample field survey data as mentioned in Section 6.3.2 has been used to represent the present scenario of the entire hills of Guwahati city. Apart from this, four other scenarios are also assumed for the hill cuts in order to analyse the variation of sediment loss from hills as a response to conditions of the hill cuts associated with urban settlement in hills. The five different scenarios considered here are-

Scenario 1: Present condition representing average 1% area of hill cuts being protected by retaining wall, 39% area being covered by grass or creepers and the remaining 60% area of hill cut being in bared condition.

Scenario 2: All hill cuts are completely bared (Worst possible scenario).

Scenario 3: All hill cuts are completely protected by retaining wall (best possible scenario).

Scenario 4: All hill cuts are completely covered by grass/creepers.

Scenario 5: Lower 50% area of all the hill cuts being protected by retaining wall and the upper 50% area of all the hill cuts being covered by grass/creepers.

For all the 15 hills of Guwahati city, the average hill cut angle is taken as $\beta=70^0$, as obtained from the sample field survey. Data regarding the average slope of the individual hill of Guwahati city are taken from Table 3.2. From Eq. (6.14), it is found that for the 15 hills of Guwahati city, the average projected area of steep hill cut is 0.08 times the urban settlement area visible in the satellite image. Hence, Eq. (6.21) is used to calculate 'C_{hu}'s for all the hills of Guwahati city for the considered five scenarios. Value of cover management factor for the retaining wall of hill cuts is taken as 0 (since impervious) and for grass or creepers, it is taken as 0.01 (Sarma 2011). From Eq. (6.21) it is clear that when the entire hill cuts are completely protected by retaining wall (Scenario 3), $C_{hu}=C_g=0.4$. This indicates that if the projected area of steep hill cut is very less Scenario 3 is analogous to a scenario where hill cut factor H_f is not considered. Values of the hill cut factor H_f and cover management factor C_{hu} for urban settlement of hills of Guwahati city are shown in Table 6.5.

6.4 Results and Discussions

Maps of soil loss rate (in t ha^{-1} $year^{-1}$) are obtained for all the five assumed scenarios by multiplying raster maps of RUSLE parameters in ArcGIS software. An average rate of soil loss is calculated for every watershed of hills of Guwahati city by taking the arithmetic mean of the pixels values of soil loss rate map for every scenario. Hill wise average rate (t ha^{-1} $year^{-1}$) and the total amount of soil loss (t $year^{-1}$) from watersheds for the years 2011, 2015 and 2025 are given in Table 6.6 and Table 6.7, respectively. Hills with maximum values of rate and the total amount of soil loss are highlighted with blue colour. From Table 6.6, it is found that highest values of soil loss rate (t $ha^{-1}year^{-1}$) are occurring in two different hills depending on the condition of hill cuts represented by scenarios. For scenario 1 and 2, Sarania hill is having the highest soil loss rate as it is the steepest hill producing the highest value of hill cut factor and in these two scenarios, very few hill cuts are protected by retaining wall or covered by grass/ creepers. On the other hand, scenarios 3, 4 and 5 are safe possible scenarios protecting all the steep hill cuts either by retaining wall or by grass/creepers. Hence, in these three scenarios, soil loss rate has not been dominated by hill cut factor but by the amount of urban settlement only. Kahilipara hill is having the highest percentage of urban settlement in the plain portion (not lying in the hilly area) of the watersheds. Consequently, it is having the highest rate of soil loss in scenarios 3, 4 and 5. Again, the total annual soil loss (t yr^{-1}) is being influenced by the total watershed area of the hill. Higher the total watershed area, higher is total annual soil loss from the hill (Table 6.7). Consequently, Garbhanga hill watershed is having the highest annual soil loss.

Table 6.5: Hill cut factor H_f and cover management factor C_{hu} for urban settlement in hill

Hill ID.	Name of hills	Hill cut factor, H_f	Cover management factor for urban settlement in hill, C_{hu}				
			Scenario 1	Scenario 2	Scenario 3	Scenario 4	Scenario 5
1	**University**	0.2866	0.5731	0.6866	0.4	0.40287	0.40143
2	**Fatasil**	0.2674	0.5615	0.6674	0.4	0.40267	0.40134
3	**Kalapahar**	0.1948	0.5177	0.5948	0.4	0.40195	0.40097
4	**Sonaighuli**	0.2365	0.5428	0.6365	0.4	0.40236	0.40118
5	**Sarania**	0.4376	0.6643	0.8376	0.4	0.40438	0.40219
6	**Kharguli**	0.2213	0.5337	0.6213	0.4	0.40221	0.40111
7	**Japorigog**	0.2860	0.5727	0.6860	0.4	0.40286	0.40143
8	**Burhagosain**	0.2840	0.5715	0.6840	0.4	0.40284	0.40142
9	**Khanapara**	0.2944	0.5778	0.6944	0.4	0.40294	0.40147
10	**Garbhanga**	0.2218	0.5340	0.6218	0.4	0.40222	0.40111
11	**Kamakhya**	0.4102	0.6477	0.8102	0.4	0.40410	0.40205
12	**Kahilipara**	0.2711	0.5637	0.6711	0.4	0.40271	0.40136
13	**Betkuchi**	0.2222	0.5342	0.6222	0.4	0.40222	0.40111
14	**Chunsali**	0.2644	0.5597	0.6644	0.4	0.40264	0.40132
15	**Koinadhara**	0.2130	0.5286	0.6130	0.4	0.40213	0.40107

Table 6.6: Hill wise average rate (t ha^{-1} year^{-1}) of soil loss from watersheds for the years 2011, 2015 and 2025.

Hill ID	Hills	Scenario 1			Scenario 2			Scenario 3			Scenario 4			Scenario 5		
		Average soil loss rate (t ha^{-1} year^{-1})														
		2011	2015	2025	2011	2015	2025	2011	2015	2025	2011	2015	2025	2011	2015	2025
1	University	75.29	83.00	101.11	80.21	89.60	111.49	67.57	72.50	111.49	67.92	73.10	85.55	67.79	72.94	85.29
2	Fatasil	287.75	296.57	366.36	313.83	326.42	409.85	247.99	251.07	300.07	248.65	251.82	301.16	248.32	251.44	300.62
3	Kalapahar	195.69	205.76	219.41	207.29	218.97	235.30	177.99	185.62	195.18	178.29	185.96	195.58	178.14	185.79	195.38
4	Sonaighuli	280.06	291.78	313.28	288.51	302.53	330.78	267.18	275.40	286.60	267.40	275.67	287.04	267.29	275.54	286.82
5	Sarania	344.62	360.39	392.41	405.34	425.37	465.82	252.05	261.31	280.48	253.58	262.95	282.34	252.82	262.13	281.41
6	Kharguli	184.17	203.00	238.43	200.38	222.53	264.78	159.45	173.24	198.24	159.86	173.73	198.91	159.66	173.49	198.58
7	Japorigog	236.12	247.37	296.17	256.44	270.36	330.03	205.15	212.32	244.54	205.67	212.91	245.40	205.41	212.62	244.97
8	Burhagosain	150.56	160.74	167.66	152.75	165.81	177.57	147.22	153.00	152.55	147.27	153.13	152.81	147.25	153.06	152.68
10	Garbhanga	135.930	136.465	142.725	136.381	137.048	144.550	135.243	135.576	139.941	135.255	135.591	139.987	135.249	135.584	139.964
11	Kamakhya	244.28	254.20	336.67	281.76	294.48	399.27	187.21	192.44	243.97	188.21	193.40	245.50	187.63	193.30	244.73
12	Kahilipara	326.92	335.10	370.77	352.15	362.16	404.94	288.45	293.86	318.67	289.09	294.54	319.53	288.77	294.20	319.10
13	Betkuchi	191.52	219.19	236.95	196.31	228.75	252.59	184.23	204.63	213.10	184.35	204.87	213.49	184.29	204.75	213.29
14	Chunsali	121.37	133.37	174.10	131.75	146.62	195.21	105.68	113.34	142.18	105.84	113.51	141.91	105.81	113.47	142.45
9+ 15	Khanapara+ Koinadhara	196.08	205.33	264.08	203.13	214.33	286.05	184.54	190.83	230.58	185.49	191.83	231.13	185.40	191.72	230.86

Table 6.7: Hill wise total soil loss (t year^{-1}) from watersheds for the years 2011, 2015 and 2025.

Hill ID	Hills	Scenario 1			Scenario 2			Scenario 3			Scenario 4			Scenario 5		
		Total soil loss (t/yr)														
		2011	2015	2025	2011	2015	2025	2011	2015	2025	2011	2015	2025	2011	2015	2025
1	University	32273	34450	43241	34993	37666	48264	28151	29545	48264	28194	29628	35709	28124	29547	35582
2	Fatasil	529033	568722	704000	572810	624753	787332	462289	483299	576950	463394	484713	579055	462842	484006	578002
3	Kalapahar	55976	58471	64496	59112	62009	69104	51194	53077	57471	51274	53166	57588	51234	53121	57530
4	Sonaighuli	17009	18072	19701	17507	18780	20941	16250	16994	17811	16263	17012	17842	16256	17003	17826
5	Sarania	24426	25166	27375	27677	28623	31409	19470	19894	21225	19552	19982	21327	19511	19938	21276
6	Kharguli	229099	244577	275654	251878	270195	308149	194368	205519	226113	194944	206166	226933	194656	205843	226523
7	Japorigog	327721	352859	416841	358735	389795	468339	280440	296548	338327	281220	297477	339627	280829	297011	338977
8	Burhagosain	84872	89205	106491	87200	92693	114430	81323	83888	94388	81382	83977	94588	81353	83933	94488
10	Garbhanga	981409	985271	1030465	984664	989479	1043646	976447	978854	1010368	976530	978962	1010701	976487	978906	1010535
11	Kamakhya	150329	156760	187940	176259	184616	223932	110820	114271	133324	111486	114951	134228	111123	114490	133776
12	Kahilipara	309098	320278	367219	336391	350570	407500	267486	274095	305806	268175	274860	306823	267830	274478	306315
13	Betkuchi	13509	13904	14012	13692	14162	14442	13232	13510	13357	13236	13517	13368	13234	13513	13362
14	Chunsali	128687	143941	198532	137828	156664	222562	114866	124705	162198	114964	124757	161894	114981	124865	162501
9+ 15	Khanapara+ Koinadhara	648633	675837	797116	664806	697551	846896	622072	640827	721220	624385	643278	722476	624180	643003	721849

Fig. 6.3 compares the change in average rate of soil loss from 2011 to the years 2015 and 2025. In both 2015 and 2025, the highest increase in soil loss rate is observed in Chunsali hill (Hill ID 14) although the total amount of soil loss (Table 6.7) from this hill is relatively low. Again, despite the highest amount of soil loss from the watershed of Garbhanga hill (Hill ID 10), it is having a very low increase in soil loss rate in 2015. It has already been mentioned that approximately 2% of the watershed area of Garbhanga hill lies in GMCA and urban settlement has increased only in that portion. Hence, the change in soil loss is only due to the increase in urban settlement in the area of Garbhanga watershed lying under GMCA in 2015. On the other hand, in 2025, Betkuchi hill (Hill ID 13) is having the lowest increment in soil loss rate. This is because, till 2011, a large percent of Betkuchi hill area was already in bare condition (having RUSLE cover management factor=1). In 2025, some portions of these bare hilly areas are going to be impervious (having RUSLE cover management factor = 0). From 2011 to 2025, the average increase in soil loss is 22.35%, whereas, from 2011 to 2015 it was only 5.34%.

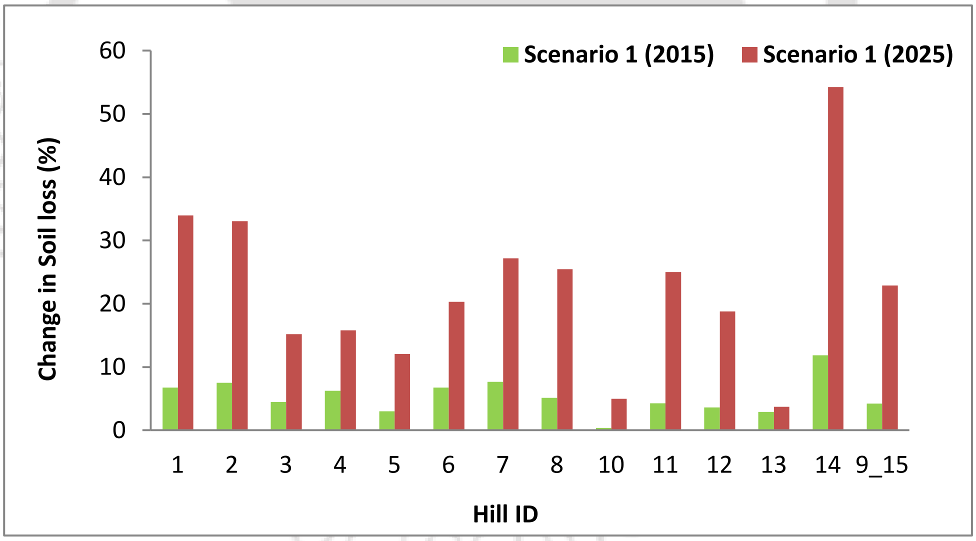

Fig. 6.3: Change in average rate of soil loss from 2011 to 2015 and 2025 under scenario 1

Again, Fig. 6.4 shows how the average rate of soil loss under scenario 1 will change for consideration of the remaining four scenarios. From this figure, it is clear that if all the steep hill cuts will be in worst condition (scenario 2) instead the present condition (scenario 1), there will be a considerable increase (average 8% increase) in soil loss rate for all the hills. On the other hand, soil loss can be significantly decreased by implementing the scenarios 3, 4 and 5. The maximum decrease in soil loss rate can be obtained by replacing the present condition (scenario 1) of the hill cuts with scenario 3. This is as expected since in scenario 3 all hill cuts are well protected by retaining wall. These changes are highest for Sarania hill (Hill ID 5) followed by Kamakhya (Hill ID 11) and Fatasil hill (Hill ID 2) for all the four scenarios i.e. from scenario 2 to 5. On the other hand, lowest changes are observed for Garbhanga hill (Hill ID 10) followed by Burhagosain (Hill ID 8) and Sonaighuli hill (Hill ID 4).

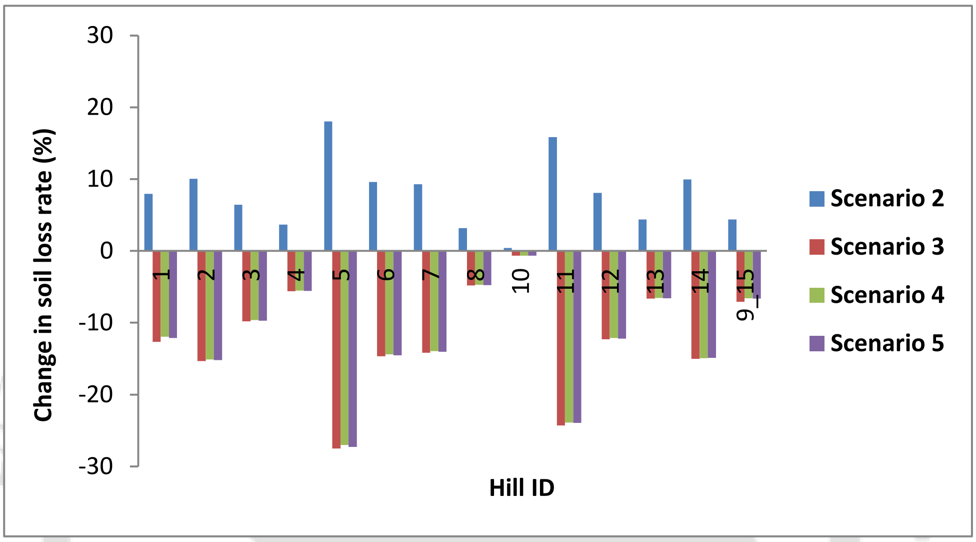

Fig. 6.4: Change in average rate of soil loss in 2015 for replacement of present scenario (Scenario 1) by different scenarios.

Fig. 6.5 shows how the average rate of soil loss will change in 2025 under the five considered scenarios with respect to those in 2015 for scenario 1 representing the present condition. From this figure, it is found that if the present condition (scenario 1) of hill remains same till 2025, the highest and the lowest increase in soil loss rates will be found for Kamakhya (Hill ID 11) and Burhagosain hill (Hill ID 8), respectively. In this case, there will be an average 16% increase in soil loss rate in 2025. However, if all the hill cuts will be in bare condition (Scenario 2), in 2025, the average soil loss rate will increase by almost 28%. Scenarios 3, 4 and 5 are found to be so effective that for some hills like Kalapahar (Hill ID 3), Sonaighuli (Hill ID 4), Sarania (Hill ID 5), Kharguli (Hill ID 6), Japorigog (Hill ID 7), Burhagosain (Hill ID 8), Kamakhya (Hill ID 11), Kahilipara (Hill ID 12) and Betkuchi (Hill ID 13) hill, average soil loss rates even in 2025 can be less than those in 2015 under scenario 1. For all these three scenarios, an overall decrease in soil loss rate is found in 2025.

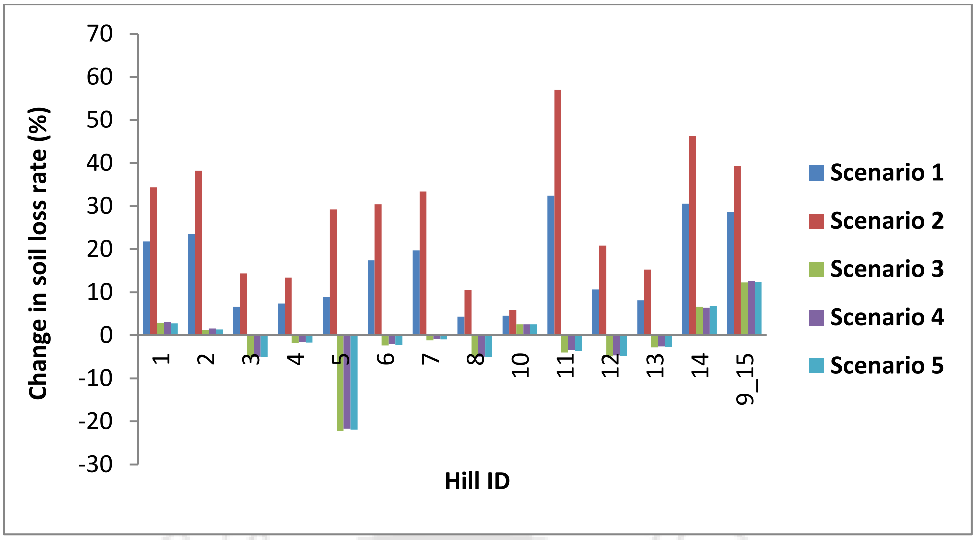

Fig. 6.5: Change in average rate of soil loss from hills in 2025 under different scenarios with respect to those in 2015 under scenario 1.

It has been already mentioned that for hills of Guwahati city Scenario 3 is equivalent to the scenario of soil loss without considering the hill cut factor. In order to show the need of consideration of hill cut factor H_f in the estimation of soil loss from hills, change in soil loss rate between Scenario 1 and Scenario 3 and also the values of soil loss rate for these two scenarios are shown in Fig. 6.6. From this, it is clear that the underestimation of soil loss is resulted from every hill if H_f is not considered. This change in soil rate is highest for Sarania (Hill ID 5) and Kamakhya (Hill ID 11) hill. If H_f factor is not considered, soil loss from hills of Guwahati city will be underestimated by an average value of 12%.

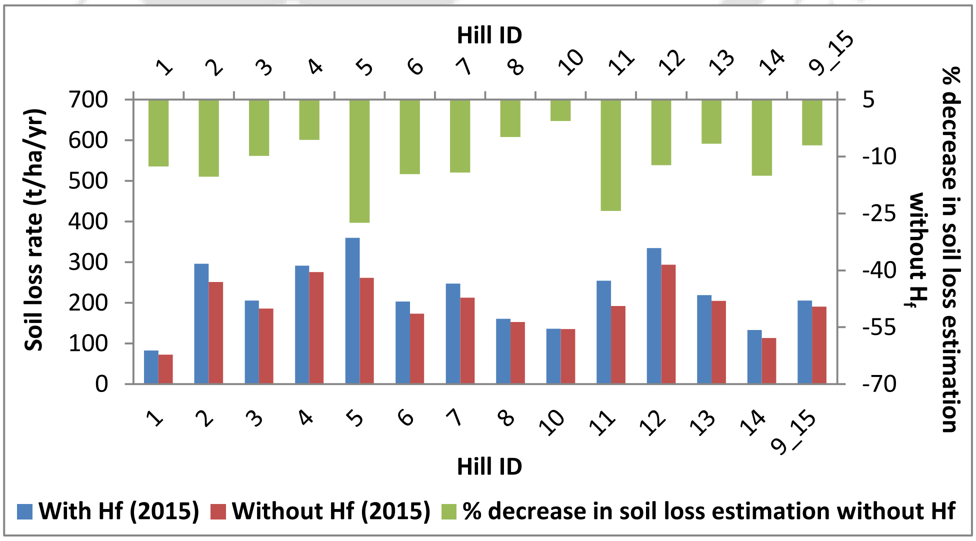

Fig. 6.6: Change in soil loss estimation from hill for non consideration of H_f

In this study, despite the use of distributed value of the C and LS factor, a single R factor value equal to 9259 MJ mm ha^{-1} $h^{-1}year^{-1}$ has been used for the entire study area due to the unavailability of distributed rainfall data. Sarma et al. (2005) calculated this R factor value by using rainfall data of core city area of Guwahati. On the other hand, Das (2017) obtained the R factor as 7924 MJ mm ha^{-1} h^{-1} $year^{-1}$ by using rainfall data of RMC Barjhar. Similarly, based on the variation of soil texture class, the K factor in Guwahati city varies from 0.030291 t h $MJ^{-1}mm^{-1}$ to 0.032925 t h $MJ^{-1}mm^{-1}$. Due to the unavailability of fine-resolution soil texture data, for every hill, only a particular type of soil has been found, whereas, in reality, some variation in soil texture can be there within a single hill. That means for Guwahati city, some uncertainties are associated with the two parameters- R and K factors. Therefore, to have an understanding about the influence of variation of these two parameters on the soil loss computation, a sensitivity analysis has been carried out in the Fatasil hill, which is the largest among all hills within GMCA. For computing soil loss from this hill, to be on the conservative side, we used the value of R as 9259 MJ mm ha^{-1} $h^{-1}year^{-1}$ and based on the soil type, the value of K factor was taken as 0.032925 t h $MJ^{-1}mm^{-1}$. Sensitivity analysis of R and K have been performed within the range (7924, 9259) MJ mm ha^{-1} $h^{-1}year^{-1}$ and (0.030291, 0.032925) t h $MJ^{-1}mm^{-1}$, respectively (Fig. 6.7). Since, RUSLE is a multiplicative equation, the soil loss from Fatasil hill is found to change linearly with the change in the parameter values. It is observed that the soil loss value is more sensitive to the variation of R factor than that of the K factor. Within the considered range, the percentage change in soil loss is 14.42 for unit percent change in R factor; whereas, the same for K factor is only 8. Based on the degree of sensitivity, it is recommended that paramount care should be taken for determining the R factor. In such a case, the use of distributed rainfall data is always preferable since the rainfall distribution of Guwahati city is very erratic in nature.

6.5 Preparation of soil loss vulnerability map

As per the soil loss classes, given by Irvem et al. (2007), every pixel of the raster map of soil loss rate of watersheds of hills of Guwahati city has been classified. Table 6.8 shows the average area (%) of watersheds of hills of Guwahati city lying in different classes of soil loss rates with respect to the years 2015 and 2025 under scenario 1. Area (%) of watersheds of individual hills of Guwahati city lying in different classes of soil loss rates are shown in Table 6.9. By observing the areas lying under different classes in this Table, it is found that in 2025 there is an increase in amount of areas lying in higher soil loss classes and decrease in those lying in lower soil loss classes. Again, the spatial distribution of different soil loss classes in the watersheds of the hills of Guwahati city for the years 2015 and 2025 under scenario 1 are shown in Fig. 6.8. These maps clearly give an idea about the transition of classes of pixels due to the increase of urban settlement. It indicates the soil erosion of hills of Guwahati city is highly sensitive to the increase of urban settlements.

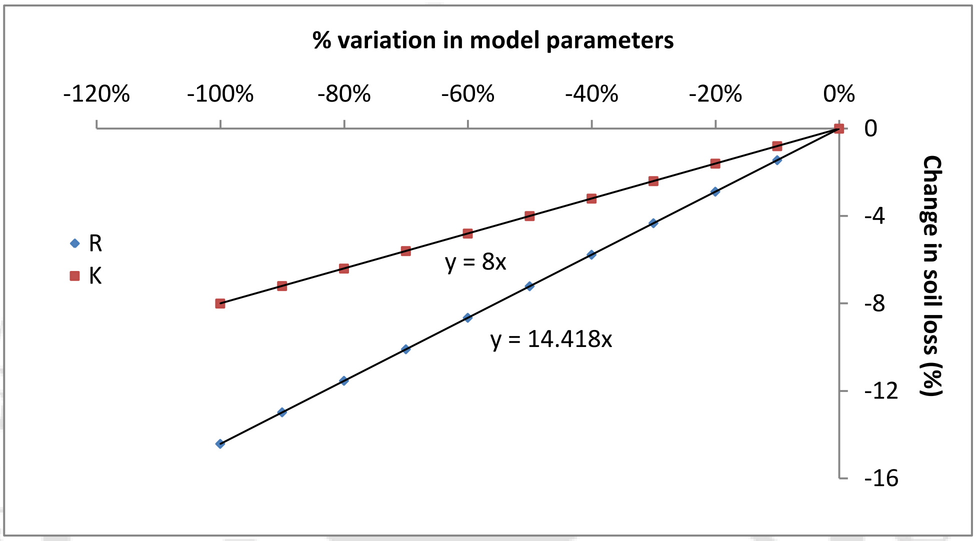

Fig. 6.7: Sensitivity of soil loss from Fatasil hills with respect to variation in R and K factors in RUSLE model.

Table 6.8: Average area (%) of watersheds of hills of Guwahati city lying in different classes of soil loss rates for the years 2015 and 2025 under scenario 1

Soil loss rate (t ha^{-1} yr^{-1})	Class	Assigned colour in map	Average Area (%)	
			2015	2025
<5	Very low		44.36	43.51
5-12	Low		5.46	5.12
12-50	Moderate		23.58	21.99
50-100	Severe		9.08	8.54
100-200	Very severe		4.27	4.34
>200	Extremely severe		13.25	16.52

6.6 Conclusions

The general expression of hill cut factor H_f, developed in this study is applicable to any hilly watershed experiencing urban settlement, although, it has been validated only at a hilly watershed located in Guwahati city. This study indicates that the consideration of the hill cut factor gives better accuracy in soil loss estimation from hilly urban watersheds. Again, it is found due to the increase in urban settlement in 2025, the area under the soil loss categories of "severe" and "extremely severe" will increase. This study has not incorporated the massive amount of sediment loss resulted from potential landslides of the hill cuts with respect to different scenarios. It only considers the soil loss due to rill and inter-rill erosion that may be resulted in the steep hill cuts.

Table 6.9: Area (%) of watersheds of individual hill of Guwahati city lying in different classes of soil loss rates for the years 2015 and 2025 under Scenario 1

Class	Hill ID:1		Hill ID:2		Hill ID:3		Hill ID:4		Hill ID:5		Hill ID:6		Hill ID:7	
	2015	2025	2015	2025	2015	2025	2015	2015	2015	2025	2015	2025	2015	2025
Very low	57.58	57.13	42.10	42.08	44.24	43.68	40.57	40.57	37.60	37.60	41.25	41.02	40.57	40.34
Low	6.71	6.39	6.13	5.95	8.92	8.43	5.49	5.49	1.74	1.74	5.35	5.02	5.49	5.26
Moderate	21.61	20.59	24.29	21.89	23.21	20.96	24.54	24.54	17.54	16.75	23.90	22.25	24.54	22.73
Severe	6.20	6.09	10.39	8.95	5.83	5.02	11.34	11.34	13.90	13.43	7.59	7.10	11.34	10.52
Very severe	2.04	2.29	4.89	4.37	2.21	2.49	5.18	5.18	7.27	6.48	3.77	3.71	5.18	4.71
Ex. severe	5.86	7.49	12.19	16.76	15.59	19.42	12.88	12.88	21.96	24.01	18.14	20.90	12.88	16.44
	Hill ID:8		Hill ID:10		Hill ID:11		Hill ID:12		Hill ID:13		Hill ID:14		Hill ID: 9_15	
Class	41.85	40.14	36.24	36.21	48.20	44.30	39.62	39.01	56.85	57.00	43.34	43.15	47.40	47.11
Very low	4.38	4.12	5.72	5.73	2.23	2.13	5.62	5.13	5.30	5.45	7.28	6.62	5.38	5.14
Low	26.84	26.75	35.41	35.35	20.56	18.38	21.61	20.15	12.52	11.34	30.76	28.09	26.41	24.83
Moderate	12.44	12.70	13.07	13.00	13.89	11.88	10.57	10.01	2.80	2.65	8.62	8.18	8.73	8.18
Severe	6.09	6.62	5.13	5.12	7.27	6.07	6.30	6.13	2.95	2.80	3.43	3.25	3.83	3.65
Very severe	8.41	9.67	4.43	4.59	7.85	17.23	16.29	19.57	19.59	20.77	6.57	10.72	8.26	11.08
Ex. severe	41.85	40.14	36.24	36.21	48.20	44.30	39.62	39.01	56.85	57.00	43.34	43.15	47.40	47.11

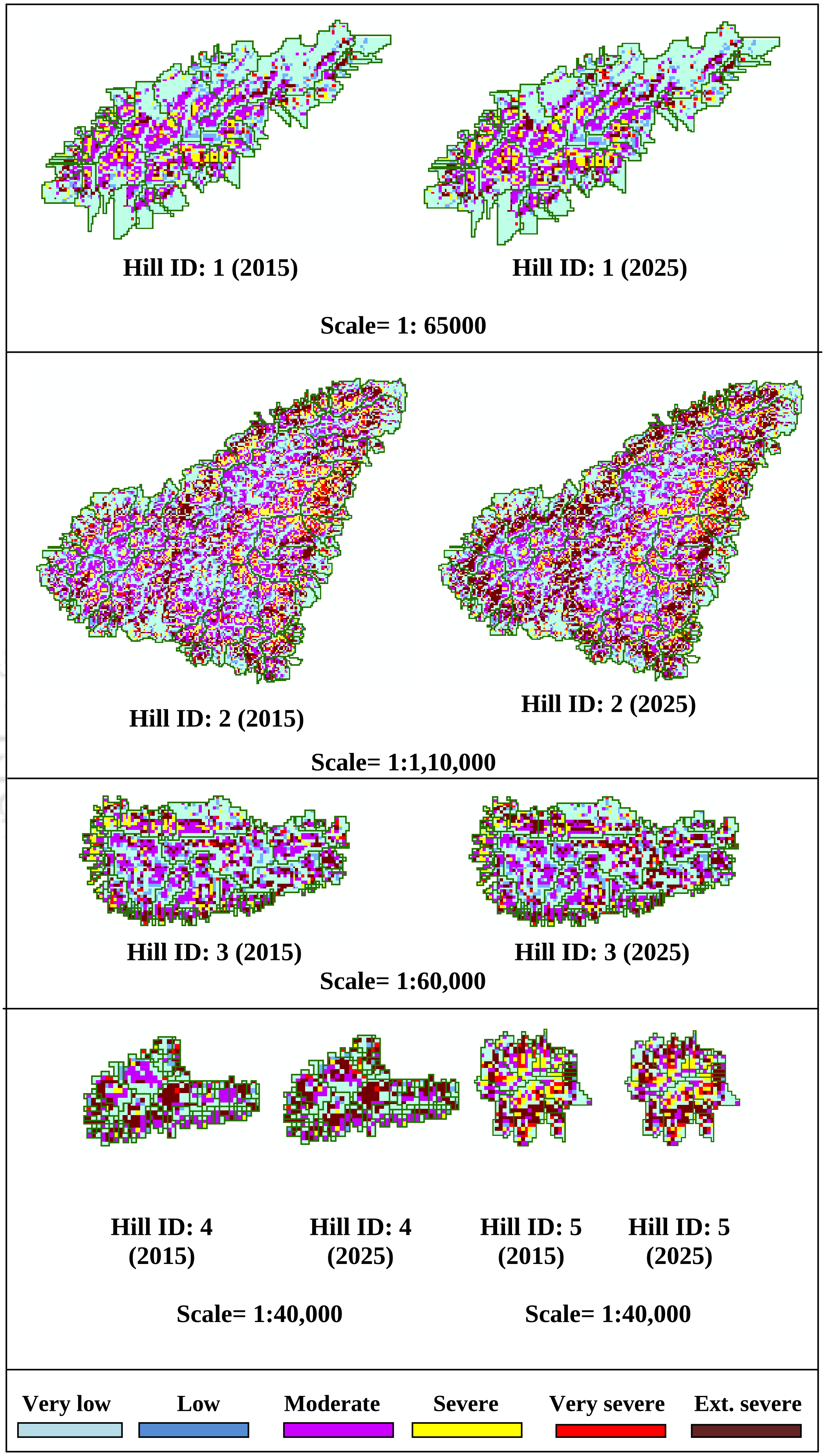
Hill ID: 1 (2015)
Hill ID: 1 (2025)
Scale= 1: 65000
Hill ID: 2 (2015)
Hill ID: 2 (2025)
Scale= 1:1,10,000
Hill ID: 3 (2015)
Hill ID: 3 (2025)
Scale= 1:60,000
Hill ID: 4 (2015)
Hill ID: 4 (2025)
Hill ID: 5 (2015)
Hill ID: 5 (2025)
Scale= 1:40,000
Scale= 1:40,000
Very low
Low
Moderate
Severe
Very severe
Ext. severe

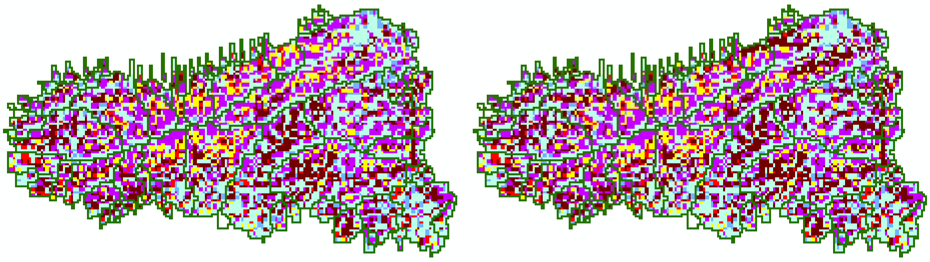

Hill ID: 6 (2015) Hill ID: 6 (2025)

Scale= 1:80,000

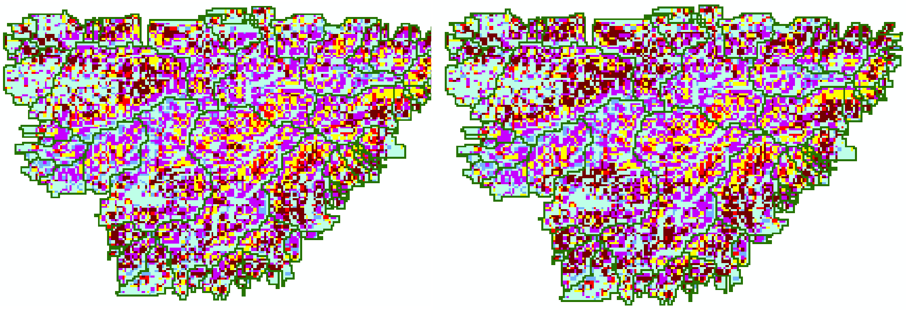

Hill ID: 7 (2015) Hill ID: 7 (2025)

Scale= 1:85,000

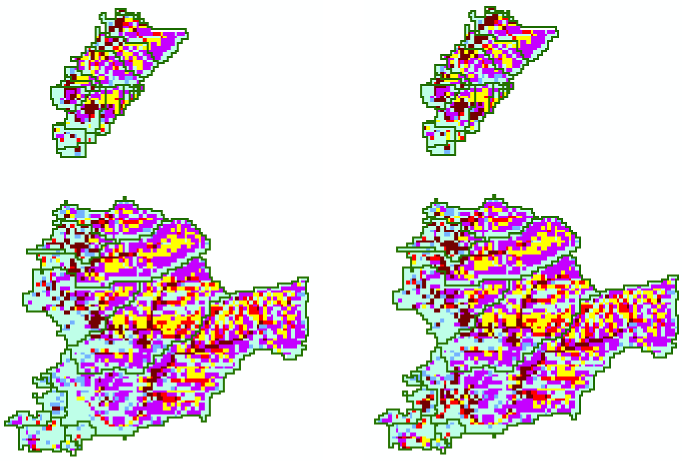

Hill ID: 8 (2015) Hill ID: 8 (2025)

Scale= 1:65,000

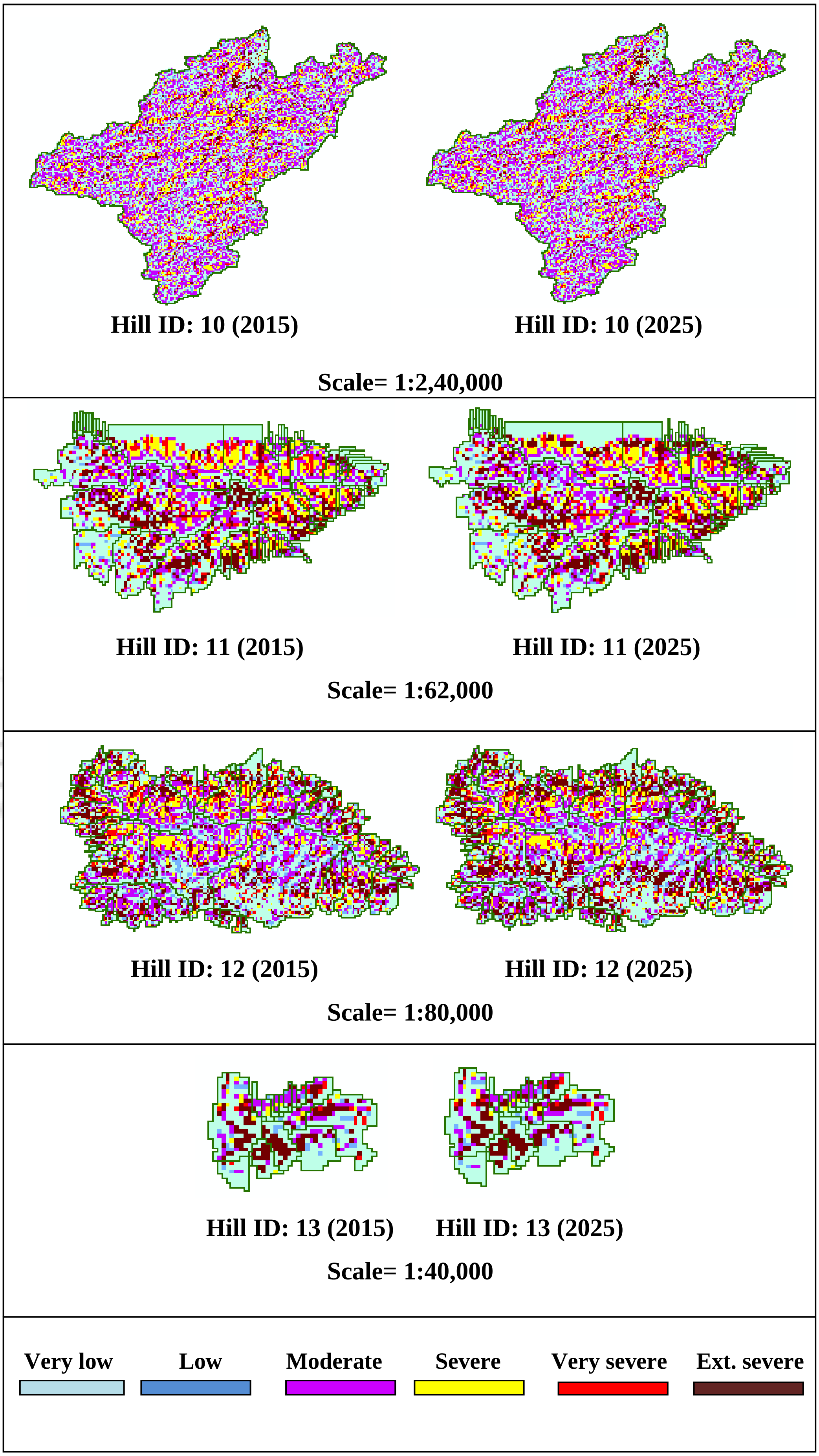
Hill ID: 10 (2015)
Hill ID: 10 (2025)
Scale= 1:2,40,000
Hill ID: 11 (2015)
Hill ID: 11 (2025)
Scale= 1:62,000
Hill ID: 12 (2015)
Hill ID: 12 (2025)
Scale= 1:80,000
Hill ID: 13 (2015)
Hill ID: 13 (2025)
Scale= 1:40,000
Very low
Low
Moderate
Severe
Very severe
Ext. severe

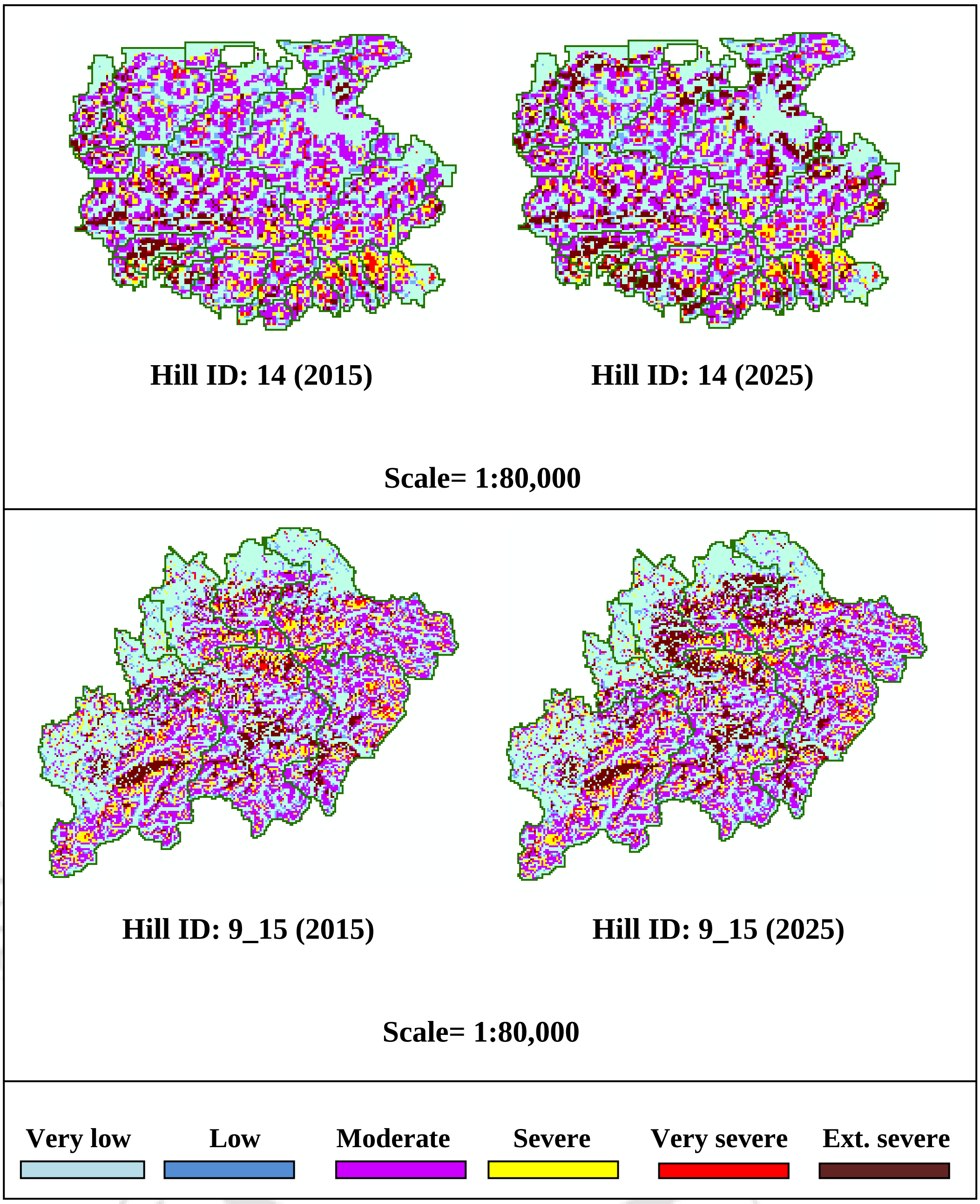

Fig. 6.8: Soil loss vulnerability maps for watersheds of hills of Guwahati city with respect to the years 2015 and 2025 under scenario 1 (~ : Watershed boundary)

Chapter-7

Management practices for controlling sediment and peak runoff

7.1 Introduction

Chapter 5 and Chapter 6 presented the future hydrological scenario of hills of Guwahati city that might result from the unplanned and unscientific growth of urban settlement. Sustainable development of urban land surfaces with Ecological Management Practices (EMPs) is effective for controlling the sediment yield and runoff caused by the conversion of natural land surfaces to urban covers (Sarma 2011). EMPs are the combination of the different structural and vegetative measures like tree/grass plantation, detention and retention ponds, contour terracing, buffer zone with vegetation strip, sediment trap, rainwater harvesting systems, vegetated waterways, perforated covers with pebble and stone etc., which can be used for reducing the ecological disturbances by controlling the sediment and water yield from a degraded watershed (Sarma et al. 2015). For addressing the environmental, economic and social conflict, today's multi-objective environmental as well as water resources problems are mostly solved by using optimization techniques (Guldmann 1986, Gabriel et al. 2006 and Riveira et al. 2008). In exception to the ample application of optimization techniques in allocation of suitable land covers, Sarma et al. (2015) introduced Optimal EMP Model with Linear Programming for Single Ownership (OPTEMP-LS) to determine the optimum allocation of EMPs in a hilly urban watershed to control the sediment and runoff yield from the watershed within a permissible limit but with a minimum possible cost. The model was constrained by several conditions like slope, soil character, land availability, existing land cover type, and ease of maintenance. Sediment yield and discharge constraints were addressed by the RUSLE and Rational Method, respectively. In the model, the entire watershed has been considered under single ownership in terms of a private developer, a society, or the government.

In the previous chapter, it has been well validated that underestimation of soil loss can result from urban hilly watersheds for non-incorporation of the hill cut factor (H_f) into cover management factor of RUSLE. In OPTEMP-LS model, GIS-based

RUSLE was applied to calculate soil loss from an urban hilly watershed and the steep hill cut areas, which are not visible in orthorectified satellite images, were not originally considered in the model. In developing countries like India, due to the poor economic condition, detailed field investigation for determining the optimal EMP areas may not be an easy task. In such a case, a sediment yield control project planned without considering the soil loss taking place from the bare steep hill cuts may lead to misinterpretation of the efficiency of the project and also the total costs of EMPs. Again, as described in section 6.4, amount of soil loss from hilly watersheds of Guwahati city is highly dependent on the surface cover condition of the steep hill cuts. The scenario representing all hill cuts in bare condition, as obvious, generated a higher amount of soil loss in comparison to the scenario representing all hill cuts being protected by retaining wall. Hence, in this chapter, the OPTEMP-LS model has been redefined by incorporating the steep hill cut area not visible in satellite images. Accordingly, some new constraints in relation to the steep hill cuts have been added to the model and the formulation of the model has resulted in an optimum allocation of different EMPs to urban settlements both in the hilly and plain portion of the watershed at a minimum possible cost.

7.2 The revised OPTEMP-LS model

7.2.1 General mathematical formulation

The objective is to minimize the total cost of EMPs required for controlling the annual sediment yield and peak discharge within a sustainable limit from a hilly urban watershed.

7.2.1.1 Objective function

$$\text{Minimize } Z = \sum_{i=1}^{n}(Cq_i + Cm_i)Xp_i + \sum_{j=1}^{q}(Cq_j + Cm_j)Xh_j + \sum_{k=1}^{r}(Cq_k + Cm_k)\,Yh_k \quad (7.1)$$

where, i= 1, 2, 3, ..., n are the EMPs considered for the urban settlement area located in the plain area of the watershed.

j= 1, 2, 3, ..., q are the EMPs considered for the urban settlement area located in the hilly area of the watershed.

k=1, 2, 3, ..., r are the EMPs considered for the steep hill cuts associated with urban settlements in the hilly portion of the watershed.

Cq_i, Cq_j, Cq_k are the construction cost of the i^{th}, j^{th} and k^{th} EMPs, respectively.

Cm_i, Cm_j, Cm_k are the maintenance cost of the i^{th}, j^{th} and k^{th} EMPs, respectively.

Xp_i = Area of the i^{th} EMP applied in the urban settlement area located in the plain area of the watershed (m^2).

Xh_j= Area of the j^{th} EMP applied in the urban settlement area located in the hilly area of the watershed (m^2).

Yh_k= Area of the k^{th} EMP applied in the steep hill cuts of the watershed ((m^2).

7.2.1.2 Constraints

I. Sediment yield constraint: After the application of EMPs, the annual sediment loss from the watershed should be within a permissible limit. The sediment yield from the watershed should not exceed the value of sediment yield from the watershed under natural land cover condition. Again, the lower limit of sediment yield should be determined based on the requirement of the downstream environment. To address this constraint, RUSLE has been used.

The constraint is given by,

$$S_{min} \leq S \leq S_{max}$$

where, S_{min} is the minimum annual sediment yield required from the watershed (t/yr); S_{max} is the maximum annual sediment yield allowed from the watershed (t/yr) and S is the sediment yield after the application of EMPs from the watershed (t/yr). Considering the steep hill cuts which are not visible in orthorectified satellite image, the sediment yield after the application of EMPs from the watershed is given by,

S = Sediment yield from [impervious area in the watershed+ natural land covers in the watershed + EMP areas applied to the bare (uncovered) settlement area in the plain area of the watershed+ remaining bare settlement area in the plain area of the watershed after the application of the EMPs+ EMP areas applied to the bare (uncovered) settlement area in the hilly area of the watershed+ remaining bare settlement area in the hilly area of the watershed after the application of the EMPs+ Existing surface covers (not bare) of the steep hill cuts associated with urban settlements in the hilly area of the watershed+ EMP areas applied to the bare steep hill cuts in the watershed+ remaining bare steep hill cuts in the watershed after the application of EMPs].

Mathematically,

$$S = RKLSP\,[C_c A_c + \sum_{g=1}^{u} C_{Lg} A_{Lg} + \sum_{i=1}^{n} C_{EPi} Xp_i + C_{uc}\left(A_{puc} - \sum_{i=1}^{n} Xp_i\right) + \sum_{j=1}^{q} C_{EHj} Xh_j + C_{uc}\left(A_{huc} - \sum_{j=1}^{q} Xh_j\right) + \sum_{l=1}^{t} C_{LSHl} A_{LSHl} + \sum_{k=1}^{r} C_{ESHk} Yh_k + C_{uc}\left(A_{shuc} - \sum_{k=1}^{r} Yh_k\right)] \quad (7.2)$$

C_c= Cover management factor for impervious area.

A_c= Impervious area in the watershed (m^2) $=A_{ch} + A_{cp}$.

A_{cp}= Impervious area in the plain area of the watershed (m^2).

A_{ch}= Impervious area in the hilly area of the watershed (m^2).

g = 1, 2, 3,....., u are the types of natural land covers in the watershed.

C_{Lg}= Cover management factor for g type of natural land cover in the watershed.

A_{Lg}= Area of g type of natural land covers in the watershed (m^2).

C_{Epi}= Cover management factor for i^{th} type of EMPs applied in the plain area of the watershed.

C_{uc}= Cover management factor for settlement area not having imperviousness i.e. bare/uncovered settlement area in the watershed.

A_{puc}= Settlement area which is not having imperviousness i.e. bare/uncovered area in the settlement area of the plain watershed area (m^2).

C_{EHj}= Cover management factor for j^{th} type of EMPs applied in the settlement area of the hilly portion of the watershed.

A_{huc}= Settlement area which is not having imperviousness i.e. bare/uncovered settlement area in the hilly area of the watershed (m^2).

C_{LSHl}= Cover management factor for l^{th} type of existing surface covers of the steep hill cuts associated with urban settlements in the hilly area of the watershed.

A_{LSHl}= Area of l^{th} type of existing surface covers (not bare) of the steep hill cuts associated with urban settlements in the hilly area of the watershed (m^2).

C_{ESHk}= Cover management factor for k^{th} type of EMPs applied to the bare steep hill cuts associated with urban settlements in the hilly area of the watershed.

A_{shuc}= Area of bare steep hill cuts associated with urban settlements in the hilly area of the watershed (m^2).

In section 6.3.1, it has already been stated that in case of hills, the urban settlement area visible in satellite image (i.e. projected area of the actual soil loss risk area= (W+m) ×B] consists of two types of area: (1) projection of steep hill cut area (= m × B) and (2) projection of inhabited urban settlement area (or, plot area = W × B).

Referring to Fig. 6.1 and from Eq. (6.15),

$$\frac{\text{Projection of plot area}}{\text{Visible urban settlement area in image}} = \frac{W}{W+m} = 1- \frac{\sin\theta\cos\beta}{\sin\beta\cos\theta}$$

=> Inhabited urban settlement area (or, plot area) in the hilly area of the watershed

$$= \frac{W}{W+m} \times U_{sh} = \left(1- \frac{\sin\theta\cos\beta}{\sin\beta\cos\theta}\right) \times U_{sh} \qquad (7.3)$$

$$\text{Therefore, } A_{ch} = p_c \times \left(\frac{W}{W+m}\right) \times U_{sh} = p_c \times \left(1- \frac{\sin\theta\cos\beta}{\sin\beta\cos\theta}\right) \times U_{sh} \qquad (7.4)$$

where, U_{sh}= urban settlement area in the hilly area derived from satellite image (m^2).

p_c = maximum allowable percent coverage of a plot of land. Since the settlement area of the hilly urban watershed contains several residential plots within it, percent coverage of a plot of land can be considered as the percent coverage in the settlement area of the watershed.

Hence, settlement area which is not having imperviousness i.e. bare/uncovered area in the settlement area of the plain watershed area (m^2),

$$A_{puc} = (1 - p_c) \times U_{sp} \tag{7.5}$$

where, U_{sp}= Urban settlement in plain area of the watershed (m^2).

Similarly, settlement area which is not having imperviousness i.e. bare/uncovered settlement area in the hilly area of the watershed (m^2),

$$A_{huc} = (1 - p_c) \times \left(\frac{W}{W+m}\right) \times U_{sh} \tag{7.6}$$

Again, area of bare steep hill cuts associated with urban settlements in the hilly area of the watershed,

A_{shuc} = Steep hill cut area associated with urban settlement in the hill - existing surface covers of the steep hill cuts.

$$=> A_{shuc} = \frac{B \times L}{B \times (m+W)} \times U_{sh} - \sum_{l=1}^{t} A_{LSHl} = \frac{L}{m+W} \times U_{sh} - \sum_{l=1}^{t} A_{LSHl} \tag{7.7}$$

By using Eq. (6.9),

$$A_{shuc} = \frac{W \sin\theta}{\sin\beta\cos\theta - \cos\beta\sin\theta} \times \frac{1}{(m+W)} \times U_{sh} - \sum_{l=1}^{t} A_{LSHl} = \frac{\sin\theta}{\sin(\beta-\theta)} \times \frac{W}{(m+W)} \times U_{sh} - \sum_{l=1}^{t} A_{LSHl} \tag{7.8}$$

II. Peak runoff constraint: After the implementation of EMPs, the peak discharge from the watershed should remain within the permissible limit. This constraint has been addressed by the Rational Method of peak discharge calculation. In Rational Method, the drainage surface area is measured in the horizontal plane (ODOT Highway Division 2014). The amount of rainfall falling over the watershed area will not be affected by the near vertical steep hill cuts. So, in runoff calculation, the effect of steep hill cut has not been considered.

$$Q_{min} \leq Q \leq Q_{max}$$

where, Q_{min} is the minimum peak runoff required from the watershed (m^3/s); Q_{max} is the maximum peak runoff allowed from the watershed (m^3/s) and Q is the peak runoff after the application of EMPs from the watershed (m^3/s).

Q= Peak runoff generated from [impervious area in the watershed+ natural land covers in the watershed + EMP areas applied to the bare (uncovered) settlement area in the plain area of the watershed+ EMP areas applied to the bare (uncovered) settlement area in the hilly area of the watershed+ remaining bare settlement area in the watershed after the application of the EMPs].

Mathematically,

$$Q = [R_{Cc} p_c U_{sw} + \sum_{g=1}^{u} R_{Cg} A_{Lg} + \sum_{i=1}^{n} R_{CEPi} Xp_i + \sum_{j=1}^{q} R_{CEHj} Xh_j + R_{Cuc}\{\left(1 - p_c\right) U_{sw} - \sum_{i=1}^{n} Xp_i - \sum_{j=1}^{q} Xh_j \right)\}] \times I \quad (7.9)$$

where, R_{Cc}= Runoff co-efficient for impervious area.

U_{sw}= Urban settlement in the watershed (m^2).

R_{Cg}= Runoff co-efficient for m type of natural land cover in the watershed.

R_{CEPi}= Runoff co-efficient for i^{th} type of EMPs applied in the plain area of the watershed.

R_{CEHj}= Runoff co-efficient for j^{th} type of EMPs applied in the settlement area of the hilly portion of the watershed.

R_{Cuc}= Runoff co-efficient for settlement area not having imperviousness i.e. bare/uncovered area in the watershed.

I = Rainfall intensity for the time of concentration of the watershed for a selected design storm (m/s).

III. EMP area suitability constraint: The area of an EMP in the watershed cannot exceed the suitable area available in that watershed for that EMP. Again, the available suitable area for that EMP should be greater than a minimum feasible area required for the implementation of that particular EMP.

IV. Maximum area available for EMPs: No EMP can be applied in the allowable coverage (building) area according to the applicable building bye laws. Therefore total EMP area should be less than or equal to the bare settlement area.

$$\sum_{i=1}^{n} Xp_i \leq A_{puc} \quad (7.10)$$

$$\sum_{j=1}^{q} Xh_j \le A_{huc} \tag{7.11}$$

$$\sum_{k=1}^{r} Yh_k \le A_{shuc} \tag{7.12}$$

V. Owner's choice for EMPs: As EMPs will have to be implemented and maintained within the residential area; the planned EMP area must be within the maximum and minimum limit of areas for that particular EMP as per the owner's choice (Sarma et al. 2015). As a hilly urban watershed contains several residential plots within it, a general upper and lower limit of the constraint should be considered for the watershed by combining the limits of the constraint at different plots.

VI. Non negativity constraint: The optimization model cannot generate a negative value of the variables i.e. the areas of the EMPs.

$Xp_i \ge 0$

$Xh_j \ge 0$

$Yh_k \ge 0$

7.2.2 Application of the Model

7.2.2.1 EMP consideration

The mini watershed, mentioned in Section 6.3.2, located in Japorigog hill of Guwahati city has been considered for the application of the optimization model (Fig. 6.2). The watershed, experiencing residential development, contains both hilly and plain area. Hence, by applying the revised OPTEMP-LS model, optimum EMP combinations are to be selected for the plain and hilly area of the watershed and also for the steep hill cuts associated with the urban settlement located in the hilly portion of the watershed. Under the same constraints, optimum EMP combinations are to be found for two LULC scenarios of the watershed: (i) LULC derived from the LISS IV satellite image of 4 December 2015 (ii) LULC derived with reference to the projected urban settlement in 2025 in the hilly area of the watershed. Depending on the availability and ease of execution, various EMPs have been selected. For the urban settlement in the hilly and plain area of the watershed, four types of EMPs have been selected- grass, garden with shrubs or bushy vegetation or vegetables, forest and detention pond. The depth of the detention pond is considered as 1.5 m as given by Sarma et al. (2015). For plain area, the optimal areas of these four EMPs are designated as Xp_1, Xp_2, Xp_3, Xp_4, respectively and the same for the hilly area are represented by Xh_1, Xh_2, Xh_3, Xh_4, respectively. Again, for steep hill cuts associated with urban settlements in the hilly area, selected EMPs are grass and the retaining wall with random rubble masonry, whose optimal areas are given by Yh_1 and Yh_2 correspondingly. The unit costs of EMPs, and their cover management factors and the runoff coefficients have been displayed in Table 7.1. The cover management factor and runoff coefficient for hill cut portion covered with retaining walls have been taken as same as those for impervious surface.

Table 7.1: Unit cost, cover management factors and runoff coefficients of EMPs

EMP	Unit cost* (Rs/m^2)	Runoff coefficient	Cover management factor
Grass	360	0.2 (Sarma et al. 2013)	0.01 (Sarma et al. 2013)
Garden (shrubs)	290	0.3 (Sarma et al. 2015)	0.014 (Wishmeier and Smith 1978, Gelagay and Minale 2016)
Forest	350	0.2 (Sarma et al. 2005)	0.01 (Sarma et al. 2005)
Detention pond	300	0 (Sarma et al. 2015)	0 (Sarma et al. 2015)
Retaining wall	4900	0.9 (San Diego County 2003; ODOT Highway Division 2014).	0 (Sarma 2011)

* Unit cost includes material, construction and maintenance costs per unit area of EMP.

Unit costs of EMPs- grass, garden, forest and detention pond are taken from Sarma et al. (2013) and Sarma et al. (2015), who estimated the costs of EMPs per unit area of the study area based on market rates for the year 2012- 2013. Similarly, the cost of retaining wall per unit area has been derived by using the same schedule of market rates. Although for the theoretical application purpose, here, unit costs have been taken from past literature, it is essential to use the latest available costs for the real field application of the model.

7.2.2.2 Constraints

I. Sediment yield and peak runoff constraint: In the optimization model, the upper limit of the sediment yield is taken as the sediment yield from the watershed under natural landcover condition ($S_{natural}$). Again, the lower limit of sediment yield has been set as zero since the downstream area of the watershed is highly densed urban area and there is no minimum requirement of sediment from the water quality or environmental point of view. On the other hand, the permissible limits of the peak runoff have been taken in such a way that it does not produce flash flood downstream and also the natural drainage condition of the watershed remain same. The lower limit of peak runoff (Q_{min}) from the watershed is assigned as the water flow from the watershed under natural landcover condition ($Q_{natural}$) and the maximum allowable peak discharge (Q_{max}) has been set equal to the safe carrying capacity of the most economic trapezoidal section of a concrete drain (Q_{drain}) designed downstream of the watershed outlet with the available topographical parameters. The safe carrying capacity of the downstream drain section (considering the most economic section criteria) has been obtained as 4 m^3/s designed by using Manning's equation with the available channel bed slope of 0.21%, bottom width of 1.5 m and Manning's roughness coefficient of 0.025. That means for the considered watershed,

$S_{min} = 0$, $S_{max} = S_{natural}$, $Q_{min} = Q_{natural}$, $Q_{max} = Q_{drain}$

The runoff coefficients and cover management factors for the landcovers other than the EMPs, required to put in the Eq. (7.2) and Eq. (7.9), are taken from Table 5.4 and Table 6.2, respectively. The values of other factors of RUSLE like R, K, LS and P are taken as mentioned in Section 6.2. For the watershed, the rainfall intensity I is obtained as 0.00001389 m/s (= 50.013 mm/hr) by using the IDF curves shown in Fig. 5.5 for a design storm of 5 year return period.

II. Maximum area available for EMP: As mentioned earlier, according to GMDA building bye laws (2006), the maximum coverage area of building in a plot of land can be 60% (=p_c) of plot area (Sarma et al. 2013). Therefore, the maximum areas available for the EMPs applicable in urban settlements in the hilly and plain area of the watershed are 40% of the urban settlement area in the hilly and plain area of the watershed, respectively. Again, from the field survey as mentioned in Section 6.3.2, at an average only 1% of the total area of hill cuts is protected by retaining wall, 39% area is having grass or creepers and the remaining 60% of the steep hills cut areas are in bared condition. Therefore, in the steep hill cuts, the maximum area available for installation of EMPs is 60% of the steep hill cut area. Hence,

$$\sum_{i=1}^{4} Xp_i \leq 0.4 \times U_{sp} \qquad \text{[From Eq. (7.5) \& (7.10)]}$$

Again, as mentioned in Section 6.3.2, for the considered watershed, the projected area of steep hill cut is very less in comparison to the visible urban settlement area in the satellite image. Consequently, $\frac{W}{(m+W)} = 1$.

Therefore,

$$\sum_{j=1}^{4} Xh_j \leq 0.4 \times U_{sp} \qquad \text{[From Eq. (7.6) \& (7.11)]}$$

$$\sum_{k=1}^{2} Yh_k \leq 0.6 \times \frac{\sin\theta}{\sin\beta\cos\theta - \cos\beta\sin\theta} \times U_{sh} \qquad \text{[From Eq. (7.8) \& (7.12)]}$$

The values of various parameters related to the constraints of the optimization model are displayed in Table 7.2.

Table 7.2: Parameters related to the constraints of the optimization model.

Watershed Area (ha)	S_{max} (t/yr)	Q_{min} (m^3/s)	Q_{max} (m^3/s)	U_{sp} (m^2)	U_{sh} (m^2)	$\frac{\sin\theta}{\sin(\beta - \theta)}$
74	$S_{natural}$= 2608.79	$Q_{natural}$= 2.979	Q_{drain}= 4	69188	159544 (for 2015) 218148 (for 2025)	0.2959

III. EMP area suitability constraint: The suitability conditions for the considered EMPs (suitable soil type, slope range and elevation) are taken from Sarma (2011) and Sarma et al. (2013). By overlaying the soil map, slope map and DEM of the watershed in ArcGIS, it is found that grass, garden, open mix forest and detention pond are suitable to implement in the bare settlement area of the watershed. However, garden, open mix forest and detention pond is not suitable for the steep hill cuts associated with urban settlement in the hilly area of the watershed. So, for the steep hill cuts, only grass and retaining wall have been considered as the suitable EMPs.

IV. Owner's choice for EMPs: For the study watershed, owner's choices have been considered hypothetically and are presented in Table 7.3.

Table 7.3: Hypothetical owner's choice for EMPs.

EMP	Owner's choice
Grass in bare settlement area	Minimum=10% of bare settlement area, Maximum= Bare settlement area.
Garden (shrubs)	Minimum= 0, Maximum= 50% of bare settlement area
Forest	Minimum= 0, Maximum= 25% of bare settlement area.
Detention pond	Minimum= 0, Maximum= 25% of bare settlement area
Grass in steep hill cut area	Minimum= 0, Maximum= Bare settlement area.
Retaining wall	Minimum= 50% of bare steep hill cut area, Maximum= Bare steep hill cut area.

7.3 Results and discussions

The revised OPTEMP-LS model has been solved by using the Linear Model Solver Tool in Microsoft Excel application. The result shows that for the 2015 LULC scenario, implementation of the considered EMPs makes possible to manage the peak runoff and sediment yield from the watershed within the permissible limits satisfying all the given constraints. However, for the 2025 LULC scenario, due to the projected increase in urban settlement, it is not possible to keep the peak discharge from the watershed within the maximum allowable limit and hence, the model gives an infeasible solution. Sarma et al. (2015) mentioned that installation of rainwater harvesting system (RWH) along with the considered EMPs is a good alternative to bring the peak discharge within the permissible limit. It is found that by adopting roof top rain water harvesting, the runoff coefficient of the built-up area can be reduced by 20% in Guwahati city (Sarma et al. 2006). From last few years, GMDA is giving utmost importance to the adoption rainwater harvesting system and it is now made compulsory in building bye laws of the city. Therefore, it has been considered that till 2025, RWH schemes will be strictly implemented in Guwahati city and consequently, in 2025, the runoff coefficient of the impervious area has been expected to reduce by 20%. Under this consideration, a feasible solution is obtained for the 2025 LULC scenario. The model has been run for both with and without consideration of owner's choice constraints. Table 7.4 and Fig. 7.1 depict that the constraint "owner's choice for EMP" plays a vital role in determining the EMP combination and total costs of implementation. With respect to the 2015 LULC scenario, there is a 178.39% increase in total cost due to the consideration of "owner's choice" constraint. This is because, with consideration owner's choice constraint, the model chooses all types EMP covers. Whereas, without consideration of this constraint (for 2015), it chooses the inexpensive EMPs like garden and detention pond as the optimal EMPs for the bare settlement area of hilly and plain portion of the watershed. On the other hand, for the bare steep hill cut area, "grass" has been chosen as the most optimal EMP as its cost is very less in comparison to another EMP (retaining wall) of steep hill cuts (Fig. 7.1). Another reason for the difference in total costs of these two cases is the owner's willingness to cover a minimum 50% of bare steep hill cut area by retaining wall, whose cost is the highest among all the EMPs. Additionally, owners have shown a little interest for the less expensive EMPs like detention pond and forest. Table 7.4 also shows the increase in the total cost of EMPs with the increase of urban settlement in 2025. For a 36.73% increase in the urban settlement of hilly area of the watershed from 2015 to 2025, there is a 33.44% increase in total cost of EMPs to keep the sediment loss and peak runoff within the permissible limits.

Table 7.4: Results of revised OPTEMP-LS model

Computed parameters	2015		2025	
	With owner's choice	**Without owner's choice**	**With owner's choice**	**Without owner's choice**
Cost (×10^7 Rs)	Total=10.24 Plain= 0.85 Hill= 1.97 Steep hill cut=7.42	Total= 3.68 Plain= 0.80 Hill= 1.88 Steep hill cut=1.00	Total= 13.67 Plain= 0.85 Hill= 2.69 Steep hill cut=10.13	Total= 4.69 Plain= 0.80 Hill= 2.53 Steep hill cut=1.36
Sediment yield (t/yr)	2602.15	2602.15	2602.15	2602.15
Peak runoff (cumec)	4.00	4.00	3.851	3.998

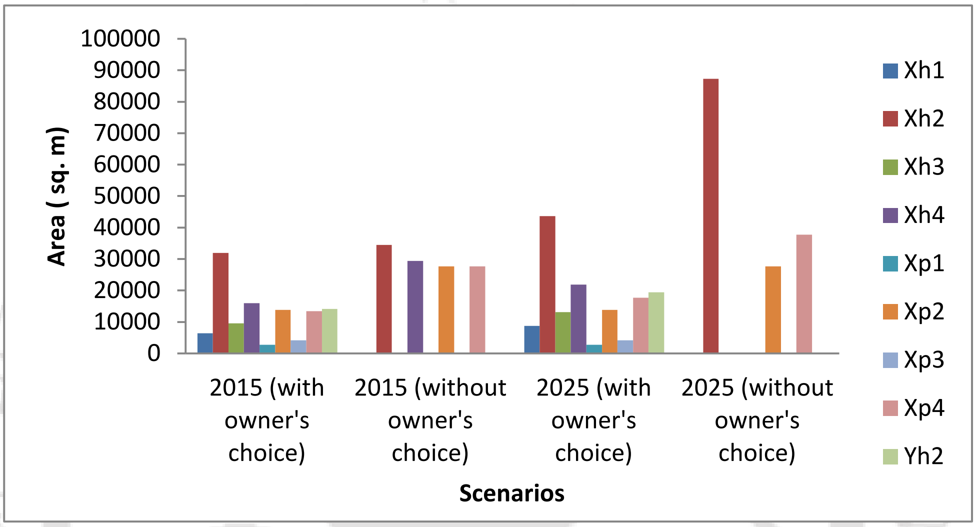

Fig. 7.1: EMP areas for different scenarios

Again, sediment yield and peak runoff under different cases have been compared in Fig. 7.2. After the implementation of EMPs (Case 3), the annual sediment yield from the watershed becomes nearly equal to that in the natural land cover condition (Case1), which is only 7.6% of the sediment yield from the watershed without implementation of EMPs (Case 2). For all the cases of EMPs implementation (i.e. Case 3, Case 4, Case 6 and Case 7) sediment yields from the watershed are same unlike the dissimilar values of peak runoff. It is observed that peak runoff from the watershed has not reduced as much as sediment yield after the implementation of EMPs. It is 91.4% (Case 3) of the peak runoff generated from the watershed without implementation of EMPs (Case 2). This is because, here, the EMPs have been applied in the 40% of the settlement area (Sarma et al. 2015). Though EMPs applied in this 40% area reduces the sediments and peak runoff, the residual 60% of the urban settlement area, which is impervious, produces a high amount of surface runoff but no sediment. As a result, reduction in sediment yield is much higher than that of peak runoff. Again, after the implementation of EMPs, the lower peak runoff values for the 2025 LULC scenario than those for the 2015 LULC scenario indicates that the installation of RWH system along with the other considered EMPs is quite effective in reducing the peak runoff.

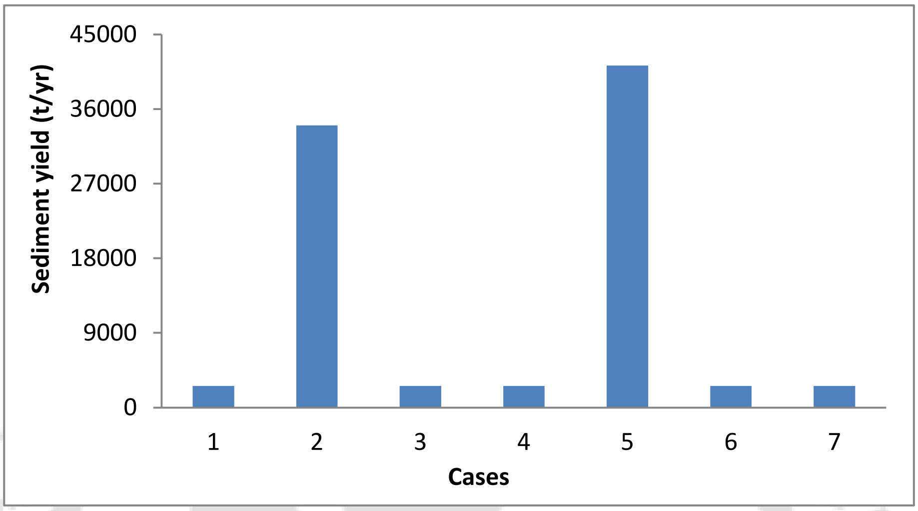

(i)

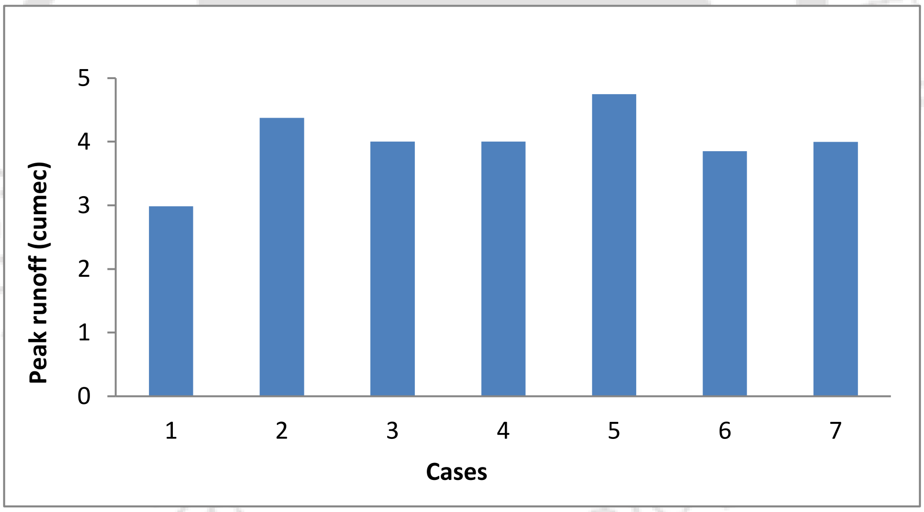

(ii)

Fig. 7.2: Comparison of (i) sediment yield (ii) peak runoff under different cases.

(Case 1: Natural land cover condition, Case 2: Without EMP in 2015 LULC scenario, Case 3: Application of EMP with the owner's choice constraint in 2015 LULC scenario, Case 4: Application of EMP without the owner's choice constraint in 2015 LULC scenario, Case 5: Without EMP in 2025 LULC scenario, Case 6: Application of EMP with the owner's choice constraint in 2025 LULC scenario, Case 7: Application of EMP without the owner's choice constraint in 2025 LULC scenario)

In this study, due to the consideration of soil loss from steep hill cuts, the watershed management (EMP) cost per unit settlement area in the hilly portion of the watershed is quite higher than that in the plain area (Fig. 7.3). Particularly, with consideration of owner's choice constraint in 2015 LULC scenario, the EMP cost per unit settlement area in the hilly portion becomes 4.77 times the unit cost for the plain portion of the watershed and it is 1.55 times without consideration of owner's choice constraint. Therefore, it can be said that a misinterpretation of the total cost of the EMP project can result from the application of OPTEMP-LS model for non-consideration of steep hill cut areas in soil loss estimation.

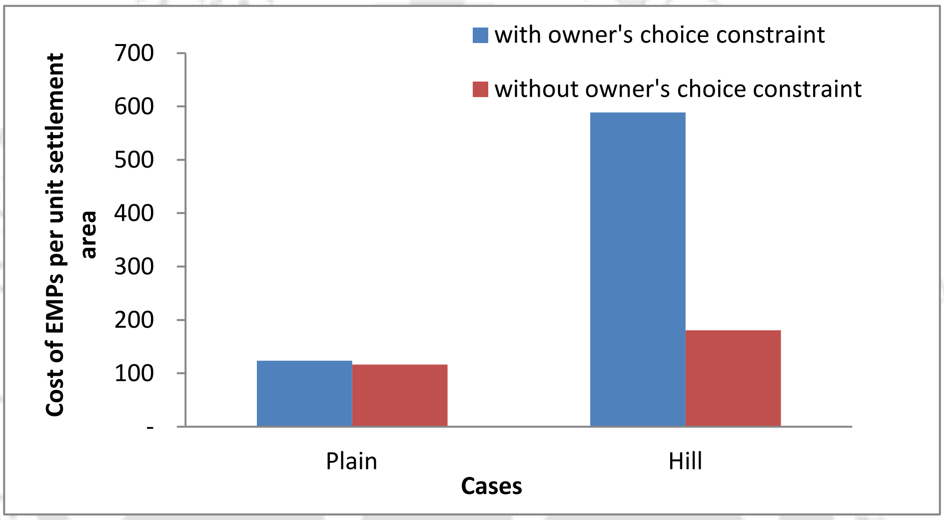

Fig. 7.3: Comparison of EMP costs per unit settlement area (2015) between hilly and plain area of the watershed

7.4 Conclusions

From this chapter, it is well-understood that though the explicit consideration steep hill cuts areas has made the revised OPTEMP-LS model computationally trickier, it has given a more realistic scenario of ecological management practices. Results of this model provide the areas of EMPs to be implemeted in plain, hilly, and also in the steep hill cut area of the watershed. This enables to inspect the management costs of the study watershed individually for these three components of the watershed. The feasible solution of the model indicates that the implementation of EMPs in a similar way for all the 15 hills of Guwahati city will efficiently solve the urban flash flood problem, the most burning urban issue of today's Guwahati.

Chapter-8
Summary and Conclusions

8.1 General

This chapter deals with a comprehensive summary of the study performed in the present research work followed by the major conclusions. The scope of future extension of the research has also been stated in the last section of this chapter.

8.2 Summary

Rapid and unplanned urbanization is transforming the eco-sensitive zones like forests, hills, wetland etc. into hazard-prone areas causing many plausible hazards like landslide, urban flash flood, soil erosion etc. It is a serious issue particularly in developing countries; where nature conservation acts are not rigidly maintained. An efficient management system always asks for an idea of the future situation. For this, it is obligatory to clearly interpret the real processes that attract people to inhabit in eco-sensitive areas. Perceiving this, this study presents a modelling based approach of quantifying urban settlement in eco-sensitive areas. The eco-sensitive hills of Guwahati city in India have been taken as the study area in this research work. Projection of the future urban settlement, analysis of its hydrological impacts and the suggestion of optimal ecological management practices for sustainable development of urban hilly watersheds are the main streams of this research work. Remote sensing and GIS techniques were widely used in the entire study for the purpose of extraction, analysis and management of geospatial data.

Unlike the use of population density and housing density in many existing statistical models for estimation of urban settlement in general, this study uses a list of potential socio-economic, demographic and geographical factors that can influence the urban settlement in the eco-sensitive area. This includes commercial unit density, free space availability, land value in the surrounding plain urban areas, geographical condition of the eco-sensitive area and a favouring index containing miscellaneous favouring conditions for urban settlements like education facilities, tourism activities, economically activeness and the location of the eco-sensitive area with respect to the core city area. The model developed by deriving the statistical relationship between these factors and urban settlement in eco-sensitive areas provides an indirect way of quantifying urban settlement in such area. This model was referred as the model for Assessment of Settlements in Eco-sensitive Area (ASEA). The underlying philosophy of this model is: "Activities and demographic characteristic of a plain urban area, located in close proximity to a particular type of eco-sensitive area, influence the habitation growth in that eco-sensitive area." Applying the proposed model, one can identify the most influencing factors that can compel people to settle in eco-sensitive areas of a city in a developing country. Hence, this type of model can be very useful for environmentalists and urban planners to frame eco-friendly development policy. Application of the model to the hills of Guwahati city reveals that all the considered factors, except the geographical conditions of the eco-sensitive area (i.e. the average elevation and average slope of the hill), influence the urban settlement in those areas of Guwahati. The developed regression model for the hills of Guwahati city is well validated. The sensitivity analysis carried with respect to every individual explanatory variable shows that although commercial unit density and some miscellaneous favouring factors influence the settlement process in hills, the most sensitive parameters are land value and the free space availability in the surrounding area of a hill.

Urban settlement in hills of Guwahati city has been projected to the year 2025 by deriving the future value of various input variables of ASEA model from the "Master Plan for Guwahati Metropolitan Area-2025". As per the model projections, the rate of change in the urban settlement in 2025 will be highest in Garbhanga hill, followed by Khanapara and Burhagosain hills. According to the master plan of the city, the city will shift towards the south and the urban development activities will be more pronounced in the area along the NH-37 highway. Model results are reflecting this shifting of the city. In 2011, the average urban settlement in hills of Guwahati city was 14.3% (in % of hill area), whereas in 2025 it is going to be 25.45%. This type of projection, done on the basis of future socio-economic and, demographic condition derived from the master plan of a city can be used for environmental impact assessment of the plan. Future landuse land cover change data of the hills was generated by spatially distributing the projected urban settlement of a hill in an order of lower elevation grid to higher elevation grid within the hill. Accordingly, the quantities of different LULCs in hills of Guwahati city for the year 2011, 2015 and 2025 (projected) were presented in the study. In 2011, the average urban settlement in hills of Guwahati city was 14.33% (in % of hill area); in 2015 it was 16.97% and in 2025 it is to be 25.45%. In all hills except Sarania and Kamakhya hill, mainly scrublands are going to be converted to urban settlement. On the other hand, in Sarania and Kamakhya hills, mostly forest areas are going to be degraded due to the increase in urban settlement.

In this study, the Rational Method was used to determine the impact of urban settlements on peak runoff generation from the hills of Guwahati city. Watershed of the hills of Guwahati city was delineated by using the ArcSWAT interface of the SWAT model. Times of concentration for those watersheds were calculated by using Bransby Williams equation (Williams 1922). IDF curve, which is an integral element of peak runoff calculation, was developed by using 43 years of daily rainfall data from 1969 to 2011 collected from Regional Meteorological Centre (RMC), Barjhar. Peak runoff values from the watersheds of hills of Guwahati city were calculated for the return periods 100, 50 and 25 years concerning the LULC of the years 2011, 2015 and 2025 (projected). Again, Rational Method is appropriate for drainage area upto 1 sq. mile (San Diego County 2003). Total of 6 hilly watersheds of Guwahati city are having areas greater than 2.59 sq. km. Peak runoffs from these watersheds have been calculated by using the NRCS TR-55 graphical peak discharge method (SCS 1986). From 2011 to 2015, there is an average 2.25% increase in peak runoff from watersheds of hills of Guwahati city, whereas from 2011 to 2025 projected average increase in peak runoff is almost 8.25%. Based on the amount of peak runoff generated, the watersheds of hills of Guwahati city are categorised into 10 classes and peak runoff maps were generated. These figures provide an idea about the transition of runoff class of some watersheds due to the increment in runoff as a result of increasing urban settlement.

The revised universal soil loss equation (RUSLE) was used in GIS platform to predict the increase in soil loss under the impact of urban settlement. Unplanned residential development in hilly areas leads to steep cuts in natural hill-slopes resulting in excessive soil loss. GIS-based RUSLE, applied in such a case, underestimates soil loss since instead of the actual steep area; only the horizontal projection of such near vertical surfaces is visible in orthorectified satellite images. This study introduces a "hill cut factor (H_f)", which is input into the cover management factor of RUSLE model. H_f is defined as the ratio of the steep hill cut area, not visible in satellite imagery, to the area of urban settlement visible in satellite image or map. The H_f-

incorporated soil loss estimation model has been validated with observed soil loss data of a mini hilly urban watershed located in Japorigog hill of Guwahati city. Results reveal that consideration of H_f in GIS-based RUSLE replicates the picture of erosion more accurately and gives a similar result with observed soil loss data. Without consideration H_f, RUSLE underestimates soil loss from the study watershed by almost 28% than the observed value. For visualizing the present scenario of hill cuts in Guwahati city, a sample field survey was performed in the Jyotinagar area of the Kharguli hill by randomly selecting total 100 numbers of hill cuts. It was found that the average steepness of hill cuts is 70^0. At an average only 1% of the total hill cuts area is covered by retaining wall, 39% area is having grass or creepers and the remaining 60% area is uncovered or in bare condition. Apart from the present scenario, four other scenarios were also considered for the hill cuts in order to analyse the variation of sediment loss from hills as a response to conditions of the hill cuts associated with urban settlement in hills of Guwahati city. These scenarios do not consider the substantial amount of sediment loss resulting from the potential landslide of the hill cuts. It only incorporates the soil loss due to rill and inter-rill erosion that may be resulted from the steep hill cuts. Soil loss rate maps were prepared and an average rate of soil loss is calculated for every watershed of hills of Guwahati city by taking the arithmetic mean of the pixels values of soil loss rate maps. Comparing the soil loss rate within the five scenarios, it was found that the highest decrease in soil loss rate can be achieved by replacing the present condition (scenario 1) of the hill cuts with the scenario representing all the hill cuts being protected by retaining walls (scenario 3). As a result of urban settlement increment from 2011 to 2025, there will be an average 22.35% increase in soil loss from the hills of Guwahati, whereas; from 2011 to 2015 it was only 5.34%. Soil loss vulnerability maps were generated for every hill by classifying pixels of the soil loss rate maps as given by Irvem et al. (2007). By observing the areas lying under different classes, it is found that in 2025 there is an increase in amount of areas lying in higher soil loss classes and decrease in those lying in lower soil loss classes.

Finally, as an effective control measure of sediment and peak runoff within a permissible limit but with a minimum possible cost, the optimum allocation of ecological management practices (EMPs) was proposed by redefining the OPTEMP-LS model (Sarma et al. 2015) by incorporating the steep hill area not visible in satellite images. Originally, the steep hill cuts which are not visible in orthorectified satellite image were not considered in the OPTEMP-LS model. Accordingly, some new constraints in relation to the steep hill cuts have been added to the revised model and the formulation of the model has resulted in the optimum allocation of different EMPs to urban settlements both in the hilly and plain portion of the watershed at a minimum possible cost. Like the original OPTEMP-LS model, here also, the sediment yield and peak runoff constraint were addressed by using RUSLE and Rational Method. In addition to this, the maximum area available for EMP, owner's choice, and the EMP area suitability constraints were also included. The revised optimization model was applied to a hilly urban watershed located in Japorigog hill of Guwahati city run for the LULC of both the years 2015 and 2025. Initially, for the LULC of the year 2025, due to the projected increase in urban settlement, the model gave an infeasible solution. However, with the consideration of the strict implementation of rainwater harvesting schemes along with the EMPs in Guwahati city, a feasible solution is obtained for the same 2025 LULC scenario. For a 36.73% increase in urban settlement in the hilly area of the watershed from 2015 to 2025, a 33.44% increase in total cost of EMPs have been obtained to keep the sediment loss and peak runoff within the permissible limits. Again, owner's choice constraint also plays a very important role in determining the total cost of the EMP allocation. Due to the consideration of "owner's choice" constraint, there was a 178.39% increase in total cost.

8.3 Conclusions

The following conclusions can be drawn from the present research work:

1. To choose more eco-friendly and sustainable urban development plans, it is desirable to interpret the factors influencing the urban expansion of a city to its eco-sensitive areas.
2. The ASEA (Assessment of Settlements in Eco-sensitive Area) model, developed in this study by using a wide range of socio-economic, demographic and geographical factors that can influence urban settlement specifically in eco-sensitive areas, can be used to implement policies to discourage settlement in eco-sensitive areas.
3. The multi-linear regression model developed by using ASEA model is capable of giving a good indirect estimate of urban settlement in hills of Guwahati city.

4. The sensitivity analysis of the model parameter indicates that city development plans of Guwahati should give more importance to outward spatial expansion in plain areas with regulated land value to minimize unauthorized settlement in eco-sensitive hilly areas of Guwahati city.
5. As per the future projection of urban settlement in hills of Guwahati city by ASEA model, from 2011 to 2025, an additional 11.12% of the hilly area is going to have urban settlements in Guwahati Municipal Corporation Area. This projection reveals the fact that implementation of the master plan may lead to an increased settlement in the eco-sensitive hilly areas if the nature conservation law will not be follwed strictly in the city.
6. The future LULC maps of hills of Guwahati city can be very useful in the evaluation of the impact of LULC on hydrological alterations of the hilly watersheds of Guwahati city and to plan efficient management actions accordingly.
7. In orthorectified satellite images, only the horizontally projected area is visible. As a result, the amount of steep hill cut area visible in satellite image is less than the actual area of steep hill cuts caused due to the urban settlement in hills. This leads to underestimation of soil loss from urban hilly watersheds when urban settlement data in hills are derived from satellite images or maps. This may also cause misinterpretation of sediment delivery ratio.
8. "Hill cut factor (H_f)" takes account of the soil loss occurring from steep hill cuts. GIS-based estimation of soil loss from urban hilly watersheds with the incorporation of H_f into RUSLE can be very useful in aspects of cost-effectiveness, swiftness and more accuracy for the design of drainage system with proper silt trapping provision.
9. In hills of Guwahati city, the urban settlement increment affects the soil erosion more vigorously than the peak runoff. From 2011 to 2025, for an additional 11.12% of the hilly area being experienced by urban settlement, the projected average increase in peak runoff and soil loss from the hills of Guwahati city are almost 8.25% and 22.35%, respectively.
10. Peak runoff and soil loss vulnerability maps help to identify the watersheds of hills of the city requiring watershed management plan in order to minimize the peak runoff and sediment loss from the hilly watershed.
11. Knowledge of the potential settlement in hills and its plausible hydrological effects can assist the concerned authorities to plan settlement in those areas more

scientifically with the use of Ecological Management Practices (EMPs) to reduce adverse impacts of unplanned settlement.

12. A sediment yield control project planned without considering the soil loss taking place from the bare steep hill cuts may lead to misinterpretation of the efficiency of the project and also the total costs of EMPs. The OPTEMP-LS model revised by the addition of new constraints and unknown variables related to the steep hill cuts gives a more realistic scenario of optimal ecological management practices.

8.4 Future scope of research

The limitations and possible further extension of the present research work are discussed in the following section:

1. Spatial distribution of rainfall in Guwahati city is nonuniform in nature (Sarma et al. 2005). The city is being encircled by hills; the orographic effect causes variation of rainfall characteristic within the city. In the present study, the availability of historical rainfall data only from a single rain-gauge station (i.e. RMC, Barjhar) has constrained to consider a uniform spatial distribution of rainfall throughout the city. The increase of raingauge density in the city with time will help to incorporate the random rainfall distribution in the hydrological analysis of the study.
2. The short duration IDF curves of Guwahati city has been developed by using short duration design rainfalls derived from design daily rainfall using IMD empirical reduction formula. However, RMC Barjhar of late has started disseminating short duration rainfall data. These data can be utilized to verify if the safe IDF curves developed in this study needs any further revision.
3. While applying ASEA model to Guwahati city, it was observed that the land-value of AOI is an important variable for projecting future urban settlements in eco-sensitive areas. Due to the unavailability of systematic record of past land values for the study area, the future value of this factor has been indirectly derived based on the strong co-relation observed between the favouring index and land value of the year 2011. A rigorous study on the factors affecting land values is required to project the future land values of the study area more accurately.
4. Due to the scarcity of observed soil loss data from hilly watersheds of Guwahati city, the applicability of the "hill cut factor" has been evaluated only with respect to

the observed soil loss data of a single watershed. Validation of the factor with more observed soil loss data will help to get insight into the factor more deeply.

5. In this study, it has been assumed that the areal extent of AOI of every hill will remain same in the near future (i.e. 2025). However, for the distant future, there may have changes in the same. Hence, the future projection of urban settlement in eco-sensitive areas with the consideration of potential changes in the areal extent of AOI in the ASEA model can be considered as a future scope of the present study.
6. The future hydrological scenarios of hills of Guwahati city have been conceptualized considering only the future urban-induced LULC scenario of the hills with a stationary climatic condition. Therefore, use of climate change impacted future rainfall data in the hydrological analysis of the study area is another important future extension of this work.

Appendix A

Table A.1: Ward wise population in Guwahati city

Ward No.	Population in 2001	Population in 2011	Population in 2025 (projected)
1	18190	62746	36189
2	13622	19278	48898
3	10258	14229	11100
4	12619	14038	13654
5	7318	12526	19538
6	9071	10171	9815
7	19166	20366	20739
8	9993	7593	10813
9	7272	6746	7868
10	8996	10216	25831
11	12331	18514	24126
12	33846	39995	48572
13	16609	29041	34997
14	21125	17629	22859
15	13535	19228	15194
16	16854	39056	34558
17	10924	21292	67191
18	7394	7431	8000
19	15010	14957	16241
20	11858	11887	12831
21	6572	7718	7111
22	15740	21169	16453
23	11029	10837	11934
24	15963	17830	17272
25	18425	20707	19982
26	10705	10431	17124
27	10725	12008	11605
28	9832	9828	10638
29	8465	6988	9160
30	7564	5688	8184
31	5616	7387	6077
32	10245	10332	11086
33	10531	8368	11395
34	11512	11088	3708
35	11968	11012	12950
36	14986	13966	16216
37	14546	15854	15740
38	8123	8589	10714
39	13257	11574	17185
40	3420	7782	8465

41	20360	21514	24440
42	12181	16649	25642
43	5400	9295	12359
44	15117	15073	16357
45	15642	12537	16925
46	23455	28309	25380
47	7799	9772	13626
48	11622	12686	15873
49	26314	30124	28472
50	10933	14084	13122
51	25989	30057	97435
52	6490	9000	20730
53	8608	14890	19725
54	15347	24226	34330
55	11785	13670	19752
56	19683	26625	40330
57	16143	13359	19026
58	22741	31876	58827
59	18615	25709	58955
60	20456	26951	53598
Total=	8,09,895	10,12,501	13,46,917

Table A.2: Populations in AOI of University hill in 2011 (census) and 2025 (projected)

Ward No.	Fraction of ward area in AOI	Populations in AOI from the wards (2011)	Populations in AOI from the wards (2025)
1	1	62746	83470
2	0.525	10120.95	25671.45
3	0.25	3557.25	2775
5	0.4	5010.4	7815.2
6	0.35	3559.85	3435.25
13	0.03	871.23	1049.91
	Total=	85865.68	1, 24,216.81

Table A.3: Populations in AOI of Fatasil hill in 2011 (census) and 2025 (projected)

Ward No	Fraction of ward area in AOI	Populations in AOI from the wards (2011)	Populations in AOI from the wards (2025)
2	0.25	4819.5	12224.5
5	0.2	2505.2	3907.6
7	0.05	1018.3	1036.95
8	0.7	5315.1	7569.1
9	0.64	4317.44	5035.52
11	0.8	14811.2	19300.8
13	0.62	18005.42	21698.14
14	0.38	6699.02	8686.42
16	0.03	1171.68	1036.74
18	1	7431	8000
19	0.95	14209.15	15428.95
20	0.05	594.35	641.55
28	0.55	5405.4	5850.9
29	1	6988	9160
30	0.18	1023.84	1473.12
	Total=	94315	1,21,050

Table A.4: Populations in AOI of Kalapahar hill in 2011 (census) and 2025 (projected)

Ward No	Fraction of ward area in AOI	Populations in AOI from the wards (2011)	Populations in AOI from the wards (2025)
13	0.055	1597.255	913.495
16	0.3025	11814.44	5098.335
17	0.2	4258.4	2184.8
59	0.32	8226.88	5956.8
60	0.42	11319.42	8591.52
	Total=	22,745	67,194

Table A.5: Populations in AOI of Sonaighuli hill in 2011 (census) and 2025 (projected)

Ward No	Fraction of ward area in AOI	Populations in AOI from the wards (2011)	Populations in AOI from the wards (2025)
13	0.2	5808.2	6999.4
16	0.27	10545.12	9330.66
17	0.12	2555.04	8062.92
	Total=	18908	24393

Table A.6: Populations in AOI of Sarania hill in 2011 (census) and 2025 (projected)

Ward No	Fraction of ward area in AOI	Populations in AOI from the wards (2011)	Populations in AOI from the wards (2025)
26	0.35	3650.85	5993.4
27	0.5	6004	5802.5
28	0.12	1179.36	1276.56
32	1	10332	11086
33	0.38	3179.84	4330.1
35	0.2	2202.4	2590
36	0.85	11871.1	13783.6
39	0.6	6944.4	10311
	Total=	45,364	55,173

Table A.7: Populations in AOI of Kharguli hill in 2011 (census) and 2025 (projected)

Ward No	Fraction of ward area in AOI	Populations in AOI from the wards (2011)	Populations in AOI from the wards (2025)
27	0.04	480.32	464.2
28	0.08	786.24	851.04
30	0.82	4664.16	6710.88
31	1	7387	6077
33	0.62	5188.16	7064.9
34	0.35	3880.8	1297.8
35	0.2	2202.4	2590
37	0.15	2378.1	2361
38	1	8589	10714
40	0.5	3891	4232.5
45	0.192	2407.104	3249.6
48	0.26	3298.36	4126.98
	Total=	45153	49740

Table A.8: Populations in AOI of Japorigog hill in 2011 (census) and 2025 (projected)

Ward No	Fraction of ward area in AOI	Populations in AOI from the wards (2011)	Populations in AOI from the wards (2025)
39	0.25	2893.5	4296.25
40	0.05	389.1	423.25
41	0.65	13984.1	15886
42	0.675	11238.075	17308.35
43	0.1	929.5	1235.9
44	0.65	9797.45	10632.05
45	0.36	4513.32	6093
46	0.09	2547.81	2284.2
48	0.31	3932.66	4920.63
49	0.2	6024.8	5694.4
50	0.22	3098.48	2886.84
51	0.6	18034.2	58461
52	0.05	450	1036.5
53	0.04	595.6	789
57	0.35	4675.65	6659.1
	Total=	83104	1, 38,606

Table A.9: Populations in AOI of Burhagosain hill in 2011(census) and 2025 (projected)

Ward No	Fraction of ward area in AOI	Populations in AOI from the wards (2011)	Populations in AOI from the wards (2025)
46	0.06	1698.54	1522.8
51	0.25	7514.25	24358.75
52	0.52	4680	10779.6
54	0.07	1695.82	2403.1
	Total=	15589	39,064

Table A.10: Populations in AOI of Khanapara hill in 2011 (census) and 2025 (projected)

Ward No	Fraction of ward area in AOI	Populations in AOI from the wards (2011)	Populations in AOI from the wards (2025)
51	0.15	4508.55	14615.25
53	0.624	9291.36	12308.4
54	0.32	7752.32	10985.6
55	0.1	1367	1975.2
57	0.13	1736.67	2473.38
	Total=	24656	42358

Table A.11: Populations in AOI of Garbhanga hill in 2011(census) and 2025(projected)

Ward No	Fraction of ward area in AOI	Populations in AOI from the wards (2011)	Populations in AOI from the wards (2025)
17	0.28	5961.76	18813.48
58	0.18	5737.68	10588.86
60	0.1	2695.1	5359.8
	Total=	14395	34,762

Table A.12: Populations in AOI of Kamakhya hill in 2011(census) and 2025 (projected)

Ward No	Fraction of ward area in AOI	Populations in AOI from the wards (2011)	Populations in AOI from the wards (2025)
3	0.75	10671.75	8325
4	0.95	13336.1	12971.3
5	0.4	5010.4	7815.2
6	0.65	6611.15	6379.75
7	0.0475	967.385	985.1025
8	0.3	2277.9	3243.9
9	0.2	1349.2	1573.6
	Total=	40224	41294

Table A.13: Populations in AOI of Kahilipara hill in 2011 (census) and 2025 (projected)

Ward No	Fraction of ward area in AOI	Populations in AOI from the wards (2011)	Populations in AOI from the wards (2025)
13	0.045	1306.845	1574.865
14	0.62	10929.98	14172.58
15	0.6	11536.8	9116.4
16	0.15	5858.4	5183.7
19	0.05	747.85	812.05
20	0.95	11292.65	12189.45
21	0.4	3087.2	2844.4
24	0.3	5349	5181.6
25	0.8	16565.6	15985.6
26	0.55	5737.05	9418.2
27	0.46	5523.68	5338.3
28	0.25	2457	2659.5
42	0.1	1664.9	2564.2
43	0.9	8365.5	11123.1
57	0.35	4675.65	6659.1
58	0.15	4781.4	8824.05
59	0.68	17482.12	40089.4
60	0.42	11319.42	22511.16
	Total=	128681	1, 76,248

Table A.14: Populations in AOI of Betkuchi hill in 2011 (census) and 2025 (projected)

Ward No	Fraction of ward area in AOI	Populations in AOI from the wards (2011)	Populations in AOI from the wards (2025)
13	0.05	1452.05	1749.85
17	0.3	6387.6	20157.3
	Total=	7840	21907

Table A.15: Populations in AOI of Chunsali hill in 2011 (census) and 2025 (projected)

Ward No	Fraction of ward area in AOI	Populations in AOI from the wards (2011)	Populations in AOI from the wards (2025)
46	0.16	4529.44	6025.44
48	0.12	1522.32	1904.76
	Total=	6052	7930

Table A.16: Populations in AOI of Koinadhara hill in 2011 (census) and 2025 (projected)

Ward No	Fraction of ward area in AOI	Populations in AOI from the wards (2011)	Populations in AOI from the wards (2025)
55	0.72	9842.4	14221.44
56	0.34	9052.5	13712.2
57	0.17	2271.03	3234.42
58	0.5	15938	29413.5
60	0.06	1617.06	3215.88
Total=		38721	63797

Appendix B

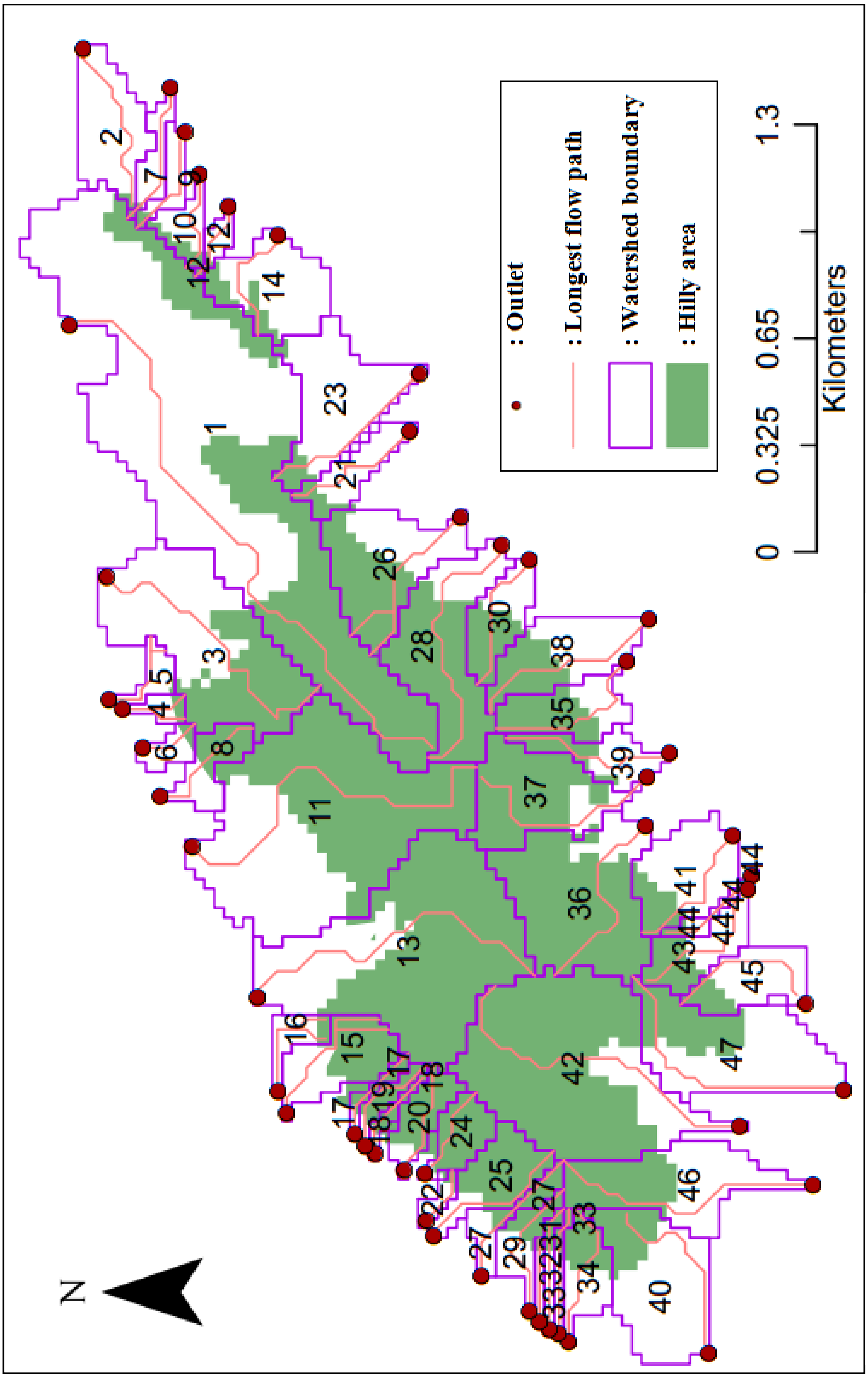

Fig. B.1: Watersheds of University hill (Hill ID: 1)

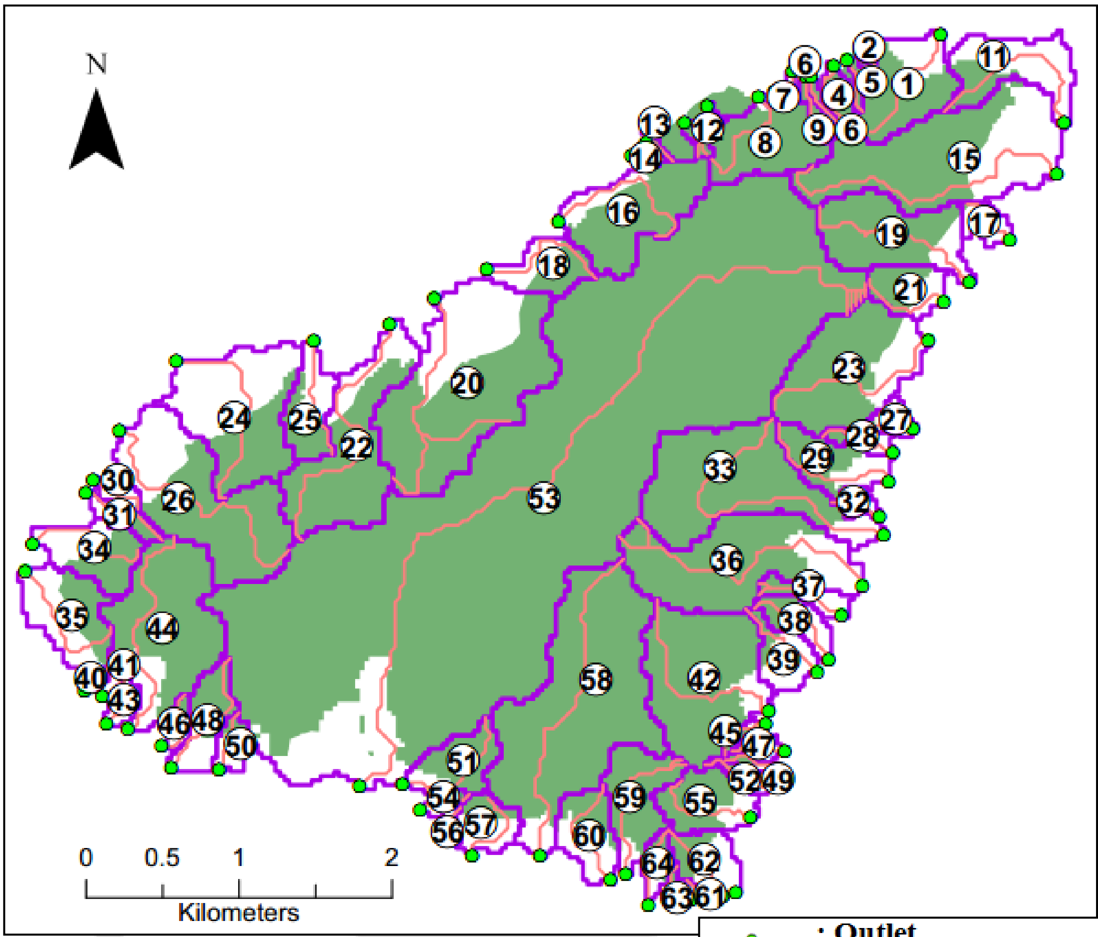

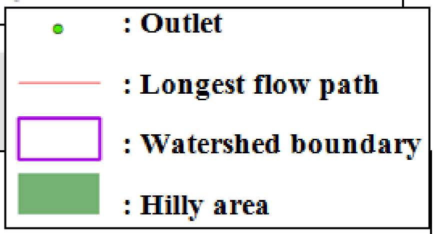

Fig. B.2: Watersheds of Fatasil hill (Hill ID: 2)

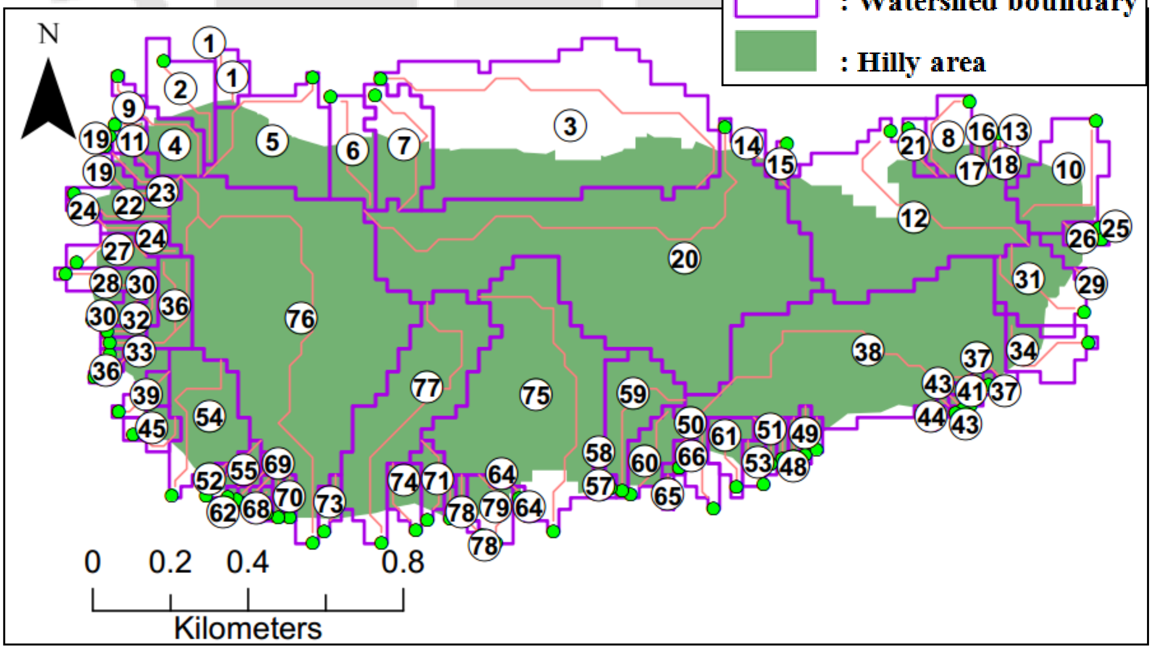

Fig. B.3: Watersheds of Kalapahar Hill (Hill ID: 3)

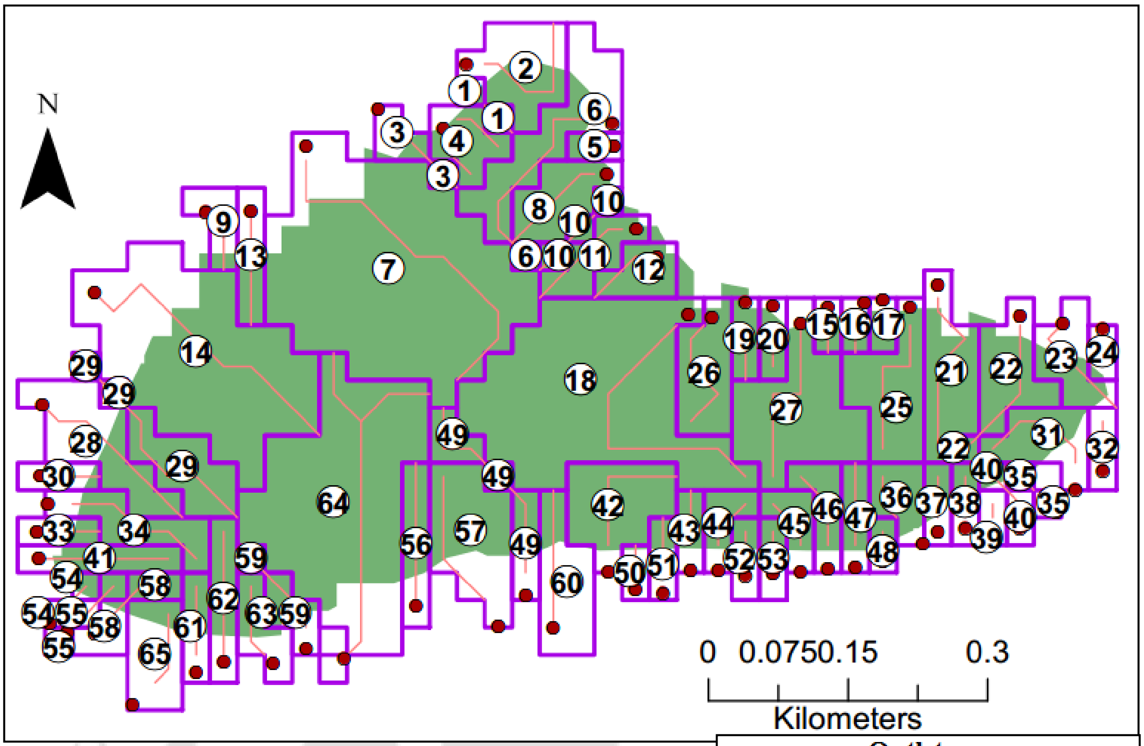

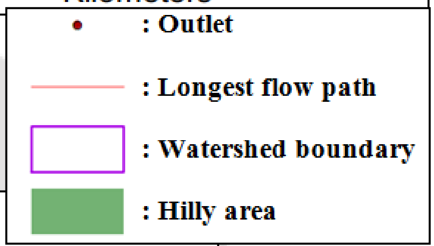

Fig. B.4: Watersheds of Sonaighuli Hill (Hill ID: 4)

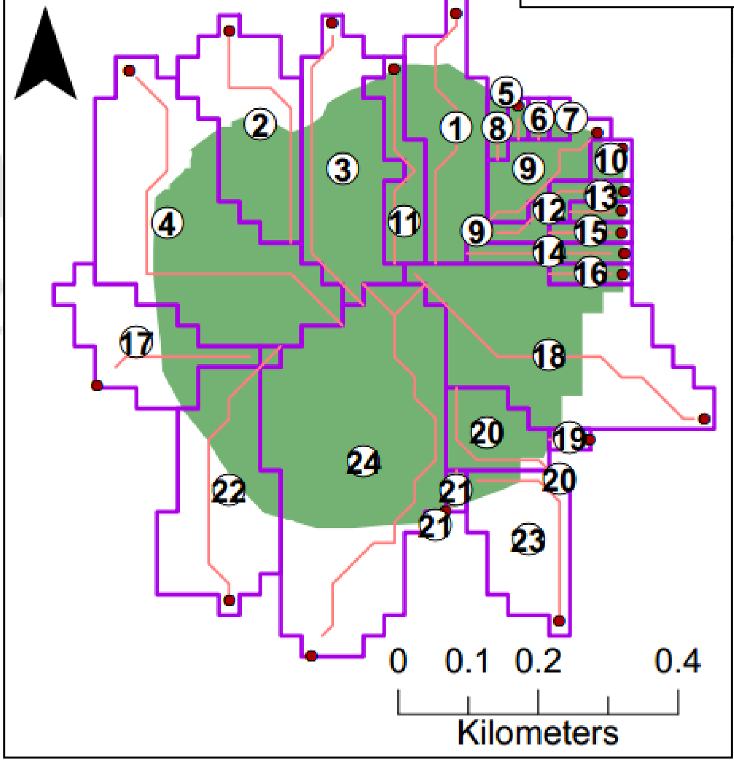

Fig. B.5: Watersheds of Sarania Hill (Hill ID: 5)

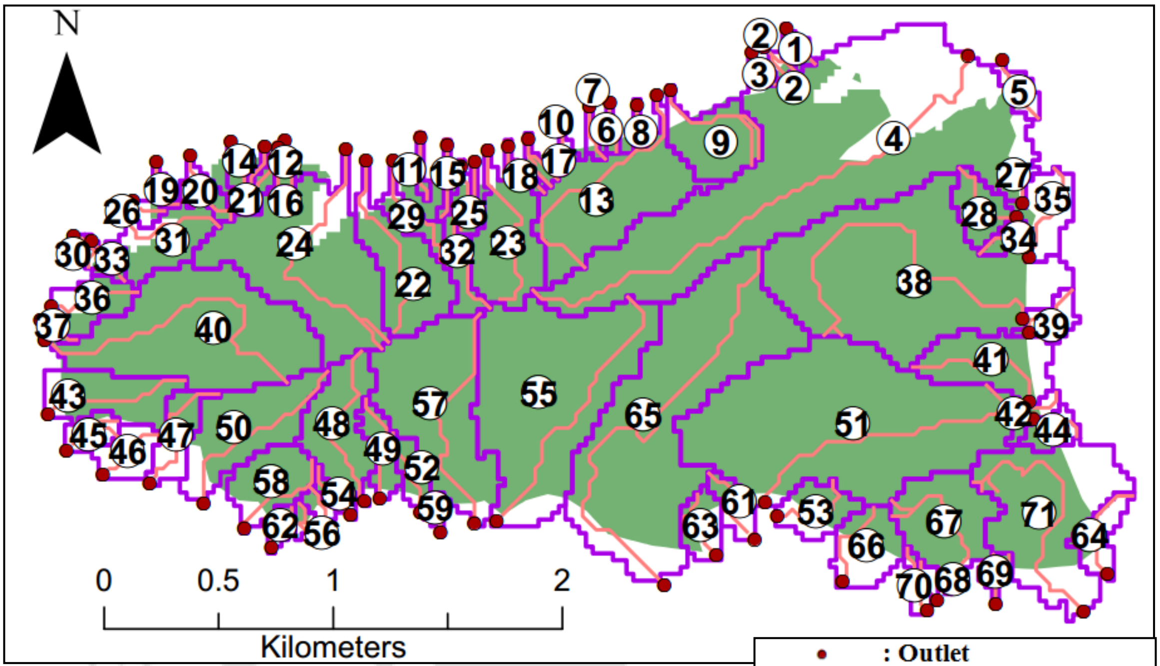

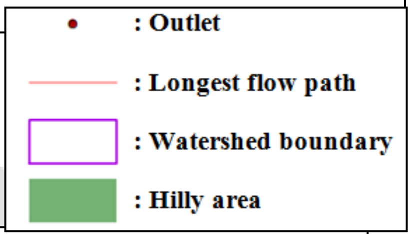

Fig. B.6: Watersheds of Kharguli Hill (Hill ID: 6)

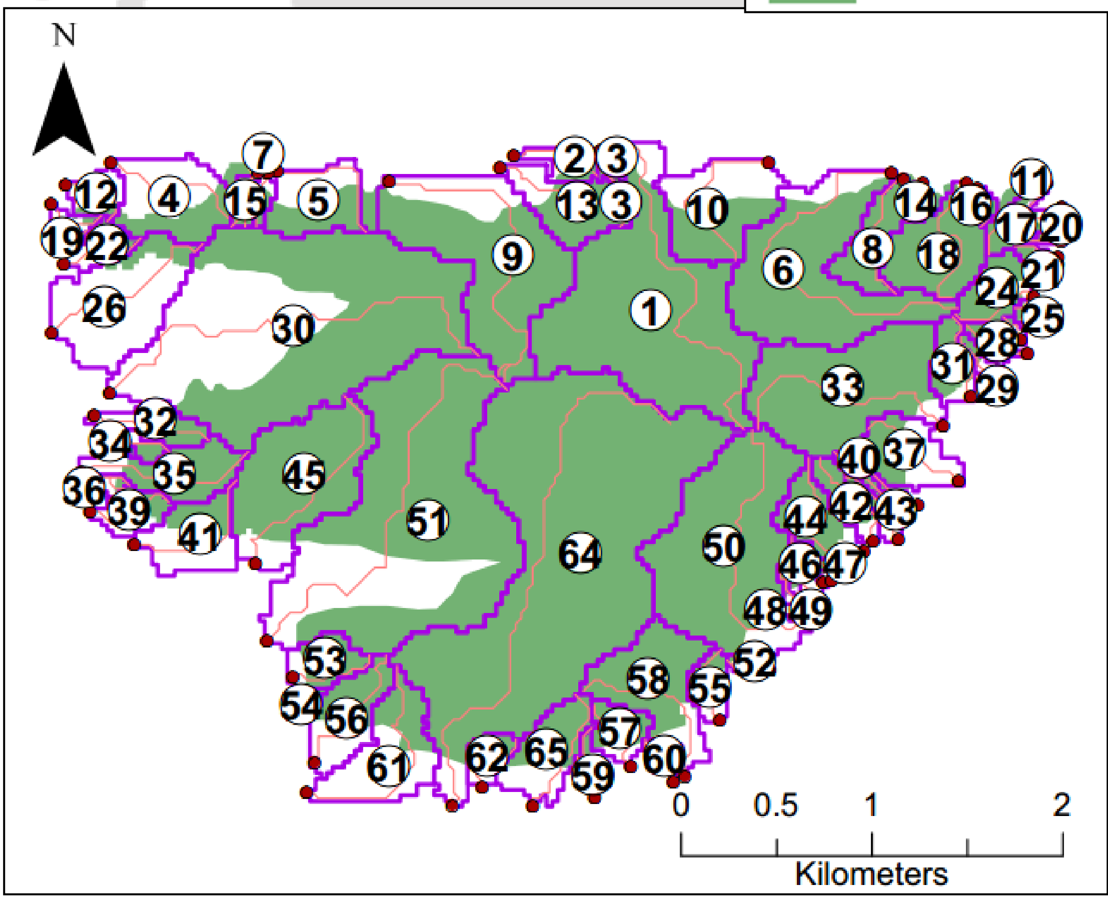

Fig. B.7: Watersheds of Japorigog Hill (Hill ID: 7)

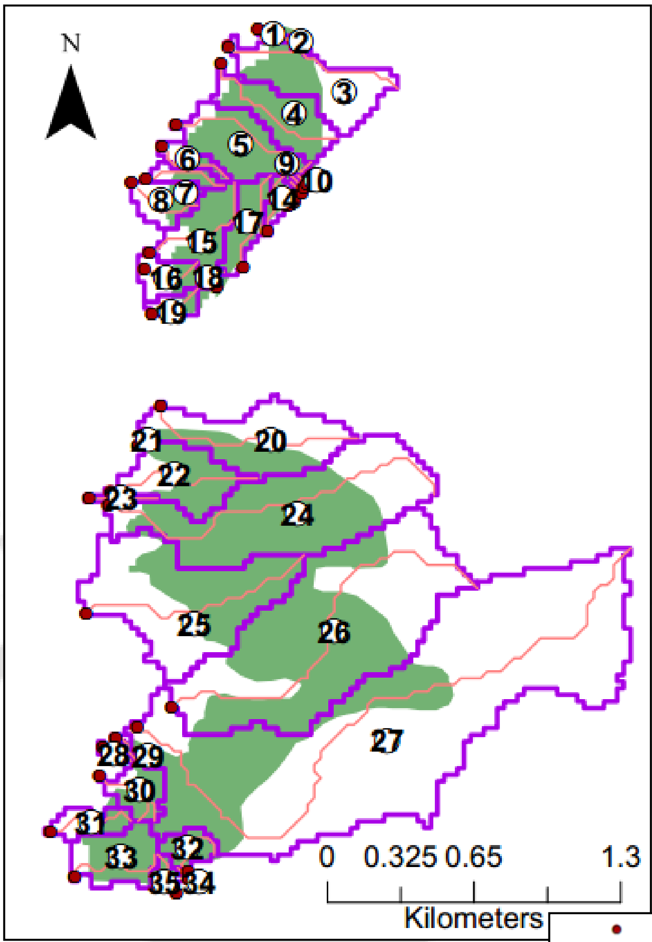

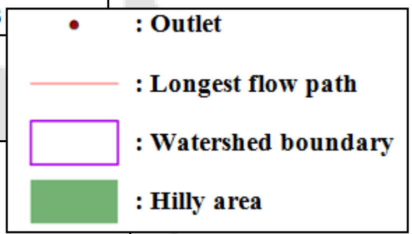

Fig. B.8: Watersheds of Burhagosain hill (Hill ID: 8)

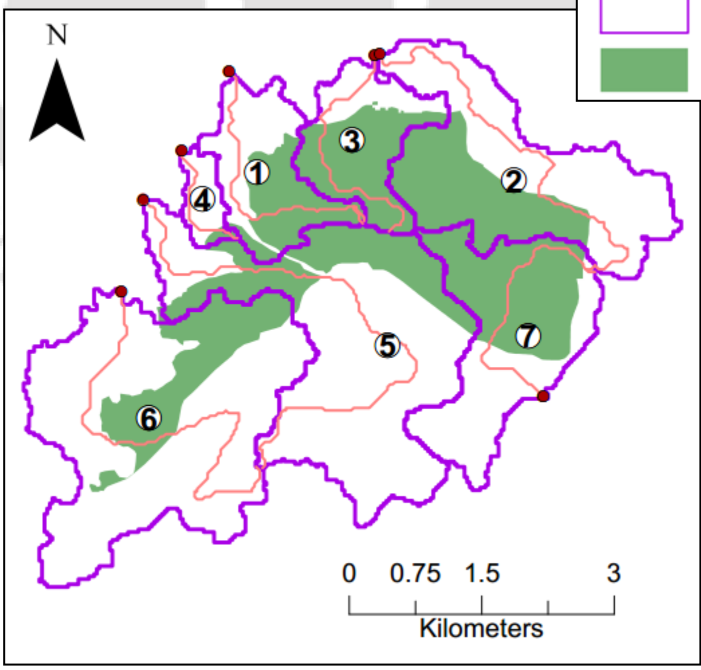

Fig. B.9: Watersheds of Khanapara and Koinadhara hill (Hill ID: 9_15)

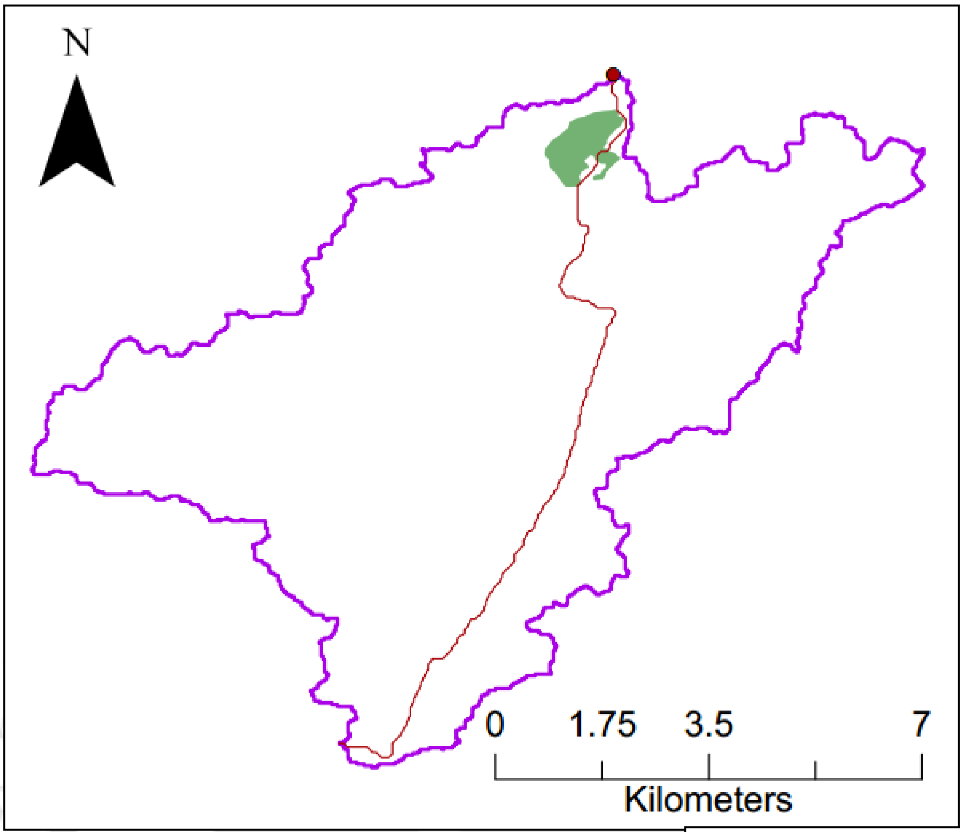

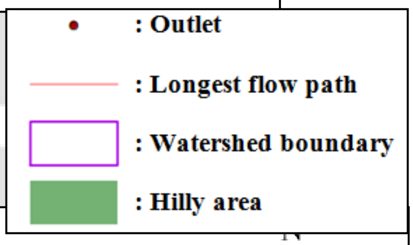

Fig. B.10: Watersheds of Garbhanga Hill (Hill ID: 10)

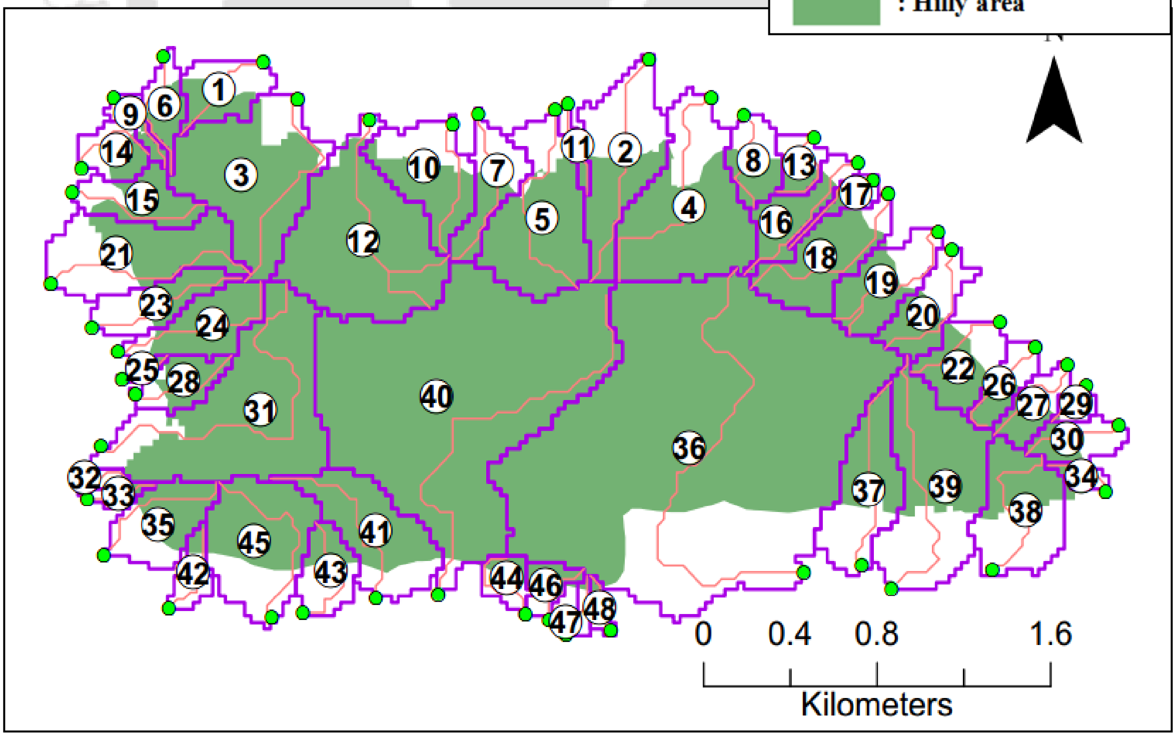

Fig. B.11: Watersheds of Kahilipara Hill (Hill ID: 12)

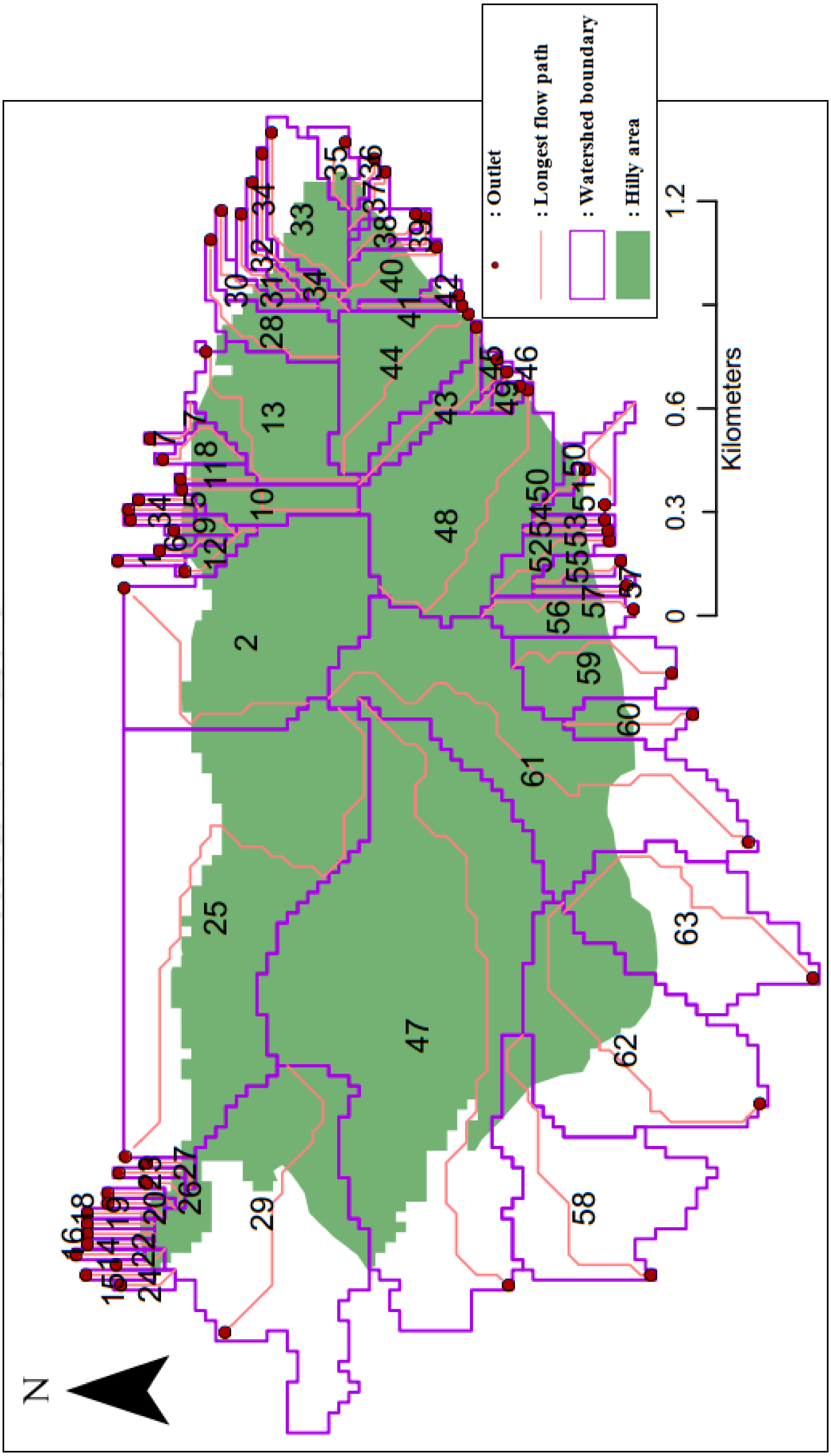

Fig. B.12: Watersheds of Kamakhya hill (Hill ID: 11)

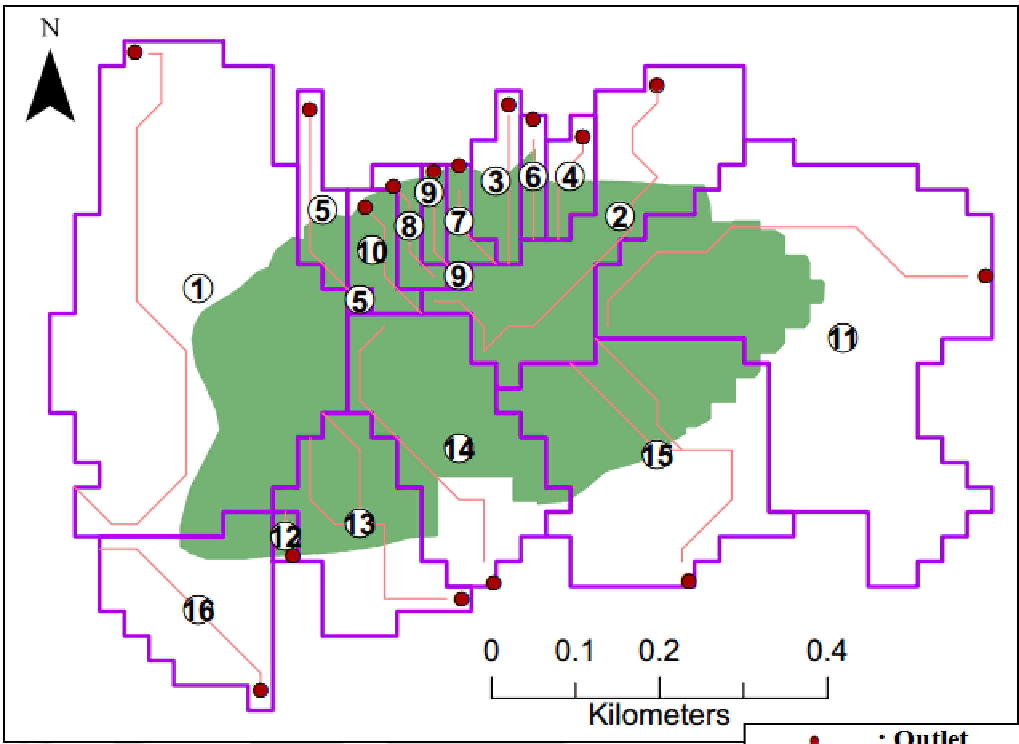

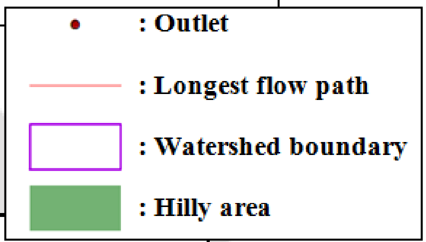

Fig. B.13: Watersheds of Betkuchi Hill (Hill ID: 13)

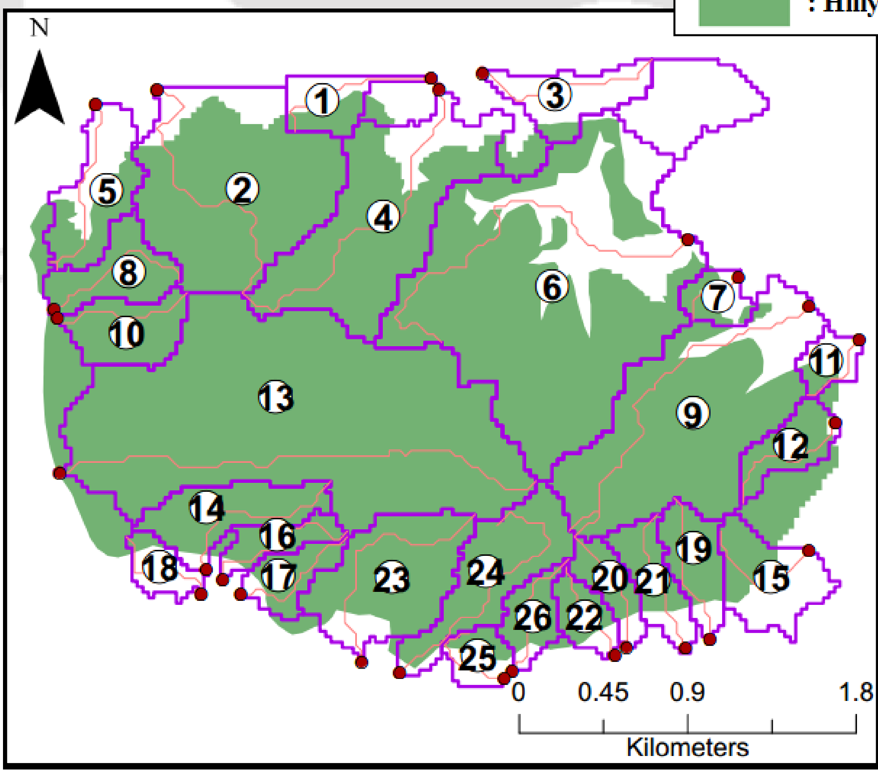

Fig. B.14: Watersheds of Chunsali Hill (Hill ID: 14)

B. Sample calculations of peak runoff

B.1 Peak runoff calculation by Rational Method

Sample watershed= Watershed ID: 1 of University hill (Hill ID: 1)

Composite runoff coefficient for 2025, C = 0.34

Watershed area (A) = 706366.91 sq.m

Length of the longest flow channel (L_c) = 1951.91 m

Slope of the longest flow channel (S_c) = 0.0528 m

By using Eq. (5.2), T_c = 52.98 min = 0.88 hours

From IDF curve of 5 year return period (Fig. 5.6), rainfall intensity, I= 44.48 mm/hr = 1.235×10^{-5} m/s

Therefore, peak runoff with 5 year return period from the considered watershed for the year 2025= 2.95 m^3/s

B.2 Peak runoff calculation by NRCS TR-55 graphical peak discharge method

Sample watershed= Watershed ID: 53 of Fatasil hill (Hill ID: 2)

Composite CN value for 2025= 68.14

For 5 year return period, 24 hours rainfall depth, P = 118.20 mm = 4.65 in

Potential maximum retention after runoff begins, $S = [\left(\frac{1000}{CN}\right) - 10]$= 4.675 in

Initial abstraction I_a=0.2S= 0.935 in

Runoff depth $Q_d = \frac{(P-I_a)^2}{P-I_a+S}$ =1.647 in

Watershed area (A) = 6315443.34 sq.m = 2.438 sq. mile

Length of the longest flow channel (L_c) = 6052.57 m

Slope of the longest flow channel (S_c) = 0.025 m

By using Eq. (5.2), T_c = 153.23 min = 2.55 hours

From unit peak discharge curves (SCS 1986),

q_u= 172 (for T_c = 2.55 hours and I_a/P = 0.2)

Since, percentage of pond and swamp areas in the watershed is zero, F_p= 1

Now, by using Eq. (5.6),

Peak runoff with 5 year return period from the considered watershed of Fatasil hill for the year 2025 = 172× 2.438× 1.647× 1 = 690.88 cfs = 19.56 cumec.

Table B.1: Peak runoff values from watersheds of University hill.

Basin ID	Composite C for the year			Rainfall intensity (x10^{-5} m/s) for RP			Area (sq. m)	Peak Q (m^3/s) in 2011 for RP			Peak Q (m^3/s) in 2015 for RP			Peak Q (m^3/s) in 2025 for RP		
	2011	2015	2025	25 yr	10 yr	5 yr		25 yr	10 yr	5 yr	25 yr	10 yr	5 yr	25 yr	10 yr	5 yr
1	0.32	0.32	0.34	1.71	1.44	1.24	706366.91	3.84	3.23	2.77	3.89	3.28	2.81	4.08	3.43	2.95
2	0.34	0.34	0.35	3.10	2.61	2.24	77613.13	0.83	0.70	0.60	0.83	0.70	0.60	0.83	0.70	0.60
3	0.31	0.31	0.38	2.45	2.06	1.77	215398.30	1.65	1.39	1.19	1.66	1.39	1.20	2.02	1.70	1.46
4	0.36	0.36	0.40	6.10	5.14	4.41	12208.81	0.27	0.23	0.19	0.27	0.23	0.19	0.30	0.25	0.22
5	0.39	0.40	0.40	3.93	3.31	2.84	17441.17	0.27	0.23	0.20	0.27	0.23	0.20	0.27	0.23	0.20
6	0.39	0.39	0.42	6.53	5.50	4.72	16569.11	0.42	0.36	0.31	0.42	0.36	0.31	0.45	0.38	0.33
7	0.38	0.39	0.39	3.42	2.88	2.47	23545.56	0.31	0.26	0.22	0.32	0.27	0.23	0.32	0.27	0.23
8	0.33	0.33	0.42	4.12	3.47	2.97	36626.43	0.50	0.42	0.36	0.50	0.42	0.36	0.64	0.54	0.46
9	0.38	0.38	0.40	4.02	3.39	2.91	19185.29	0.30	0.25	0.21	0.30	0.25	0.21	0.31	0.26	0.22
10	0.44	0.45	0.45	4.95	4.16	3.57	26161.73	0.57	0.48	0.41	0.59	0.49	0.42	0.58	0.49	0.42
11	0.24	0.24	0.26	2.36	1.99	1.71	380217.22	2.17	1.83	1.57	2.18	1.84	1.57	2.36	1.99	1.70
12	0.42	0.43	0.42	5.62	4.73	4.06	12208.81	0.29	0.24	0.21	0.30	0.25	0.21	0.29	0.24	0.21
13	0.23	0.24	0.27	2.60	2.19	1.87	331382.01	1.97	1.66	1.42	2.06	1.73	1.49	2.28	1.92	1.65
14	0.51	0.51	0.52	3.86	3.25	2.79	84589.62	1.67	1.41	1.21	1.68	1.41	1.21	1.70	1.43	1.23
15	0.31	0.32	0.38	4.07	3.43	2.94	64532.29	0.82	0.69	0.59	0.85	0.72	0.62	0.99	0.83	0.71
16	0.44	0.47	0.50	3.96	3.33	2.86	20929.40	0.37	0.31	0.27	0.39	0.33	0.28	0.42	0.35	0.30
17	0.29	0.30	0.32	5.46	4.60	3.94	10464.69	0.16	0.14	0.12	0.17	0.14	0.12	0.19	0.16	0.13
18	0.29	0.31	0.33	5.72	4.81	4.13	9592.63	0.16	0.13	0.12	0.17	0.14	0.12	0.18	0.15	0.13
19	0.24	0.25	0.29	5.02	4.23	3.63	15697.05	0.19	0.16	0.14	0.19	0.16	0.14	0.23	0.19	0.17
20	0.25	0.27	0.27	5.17	4.35	3.73	34882.32	0.44	0.37	0.32	0.48	0.41	0.35	0.48	0.40	0.35
21	0.43	0.43	0.43	3.81	3.21	2.76	39242.61	0.64	0.54	0.46	0.65	0.55	0.47	0.64	0.54	0.46
22	0.40	0.45	0.44	6.30	5.31	4.55	9592.64	0.24	0.20	0.17	0.27	0.23	0.20	0.27	0.22	0.19
23	0.46	0.46	0.46	3.52	2.96	2.54	110751.36	1.78	1.50	1.29	1.78	1.50	1.29	1.79	1.51	1.30
24	0.23	0.24	0.26	5.93	4.99	4.28	34010.26	0.47	0.39	0.34	0.48	0.40	0.34	0.53	0.45	0.38

25	0.29	0.30	0.30	4.36	3.67	3.15	57555.84	0.72	0.61	0.52	0.74	0.63	0.54	0.74	0.62	0.54
26	0.31	0.32	0.32	4.06	3.42	2.93	112495.45	1.42	1.19	1.02	1.45	1.22	1.05	1.45	1.22	1.05
27	0.38	0.40	0.41	4.45	3.75	3.22	27905.86	0.47	0.40	0.34	0.49	0.41	0.35	0.50	0.42	0.36
28	0.30	0.30	0.33	2.89	2.43	2.09	134296.93	1.17	0.98	0.84	1.18	0.99	0.85	1.27	1.07	0.92
29	0.44	0.49	0.49	4.24	3.57	3.06	31394.09	0.59	0.49	0.42	0.65	0.55	0.47	0.65	0.55	0.47
30	0.29	0.29	0.30	4.65	3.92	3.36	47963.19	0.65	0.55	0.47	0.65	0.55	0.47	0.67	0.57	0.49
31	0.40	0.41	0.44	5.04	4.24	3.64	7848.51	0.16	0.13	0.11	0.16	0.14	0.12	0.17	0.15	0.12
32	0.37	0.39	0.38	4.50	3.79	3.25	12208.83	0.20	0.17	0.15	0.22	0.18	0.16	0.21	0.17	0.15
33	0.34	0.35	0.34	4.54	3.82	3.28	11336.74	0.18	0.15	0.13	0.18	0.15	0.13	0.18	0.15	0.13
34	0.42	0.43	0.44	4.18	3.52	3.02	41858.77	0.74	0.62	0.53	0.76	0.64	0.55	0.78	0.65	0.56
35	0.36	0.36	0.37	4.00	3.37	2.89	57555.83	0.82	0.69	0.59	0.83	0.70	0.60	0.85	0.72	0.62
36	0.36	0.36	0.37	3.62	3.05	2.61	174411.57	2.28	1.92	1.64	2.28	1.92	1.64	2.32	1.95	1.68
37	0.33	0.34	0.34	3.59	3.02	2.59	107263.13	1.28	1.07	0.92	1.30	1.10	0.94	1.30	1.09	0.94
38	0.24	0.24	0.24	3.81	3.21	2.75	81973.42	0.75	0.63	0.54	0.75	0.63	0.54	0.75	0.63	0.54
39	0.35	0.36	0.37	3.97	3.34	2.87	41858.77	0.59	0.49	0.42	0.59	0.50	0.43	0.61	0.51	0.44
40	0.40	0.40	0.41	3.30	2.78	2.38	125576.34	1.67	1.41	1.21	1.68	1.41	1.21	1.69	1.42	1.22
41	0.25	0.25	0.25	4.29	3.62	3.10	82845.50	0.87	0.74	0.63	0.88	0.74	0.63	0.87	0.74	0.63
42	0.27	0.28	0.29	2.53	2.13	1.83	298243.80	2.07	1.74	1.50	2.10	1.77	1.52	2.20	1.85	1.59
43	0.26	0.26	0.26	4.08	3.43	2.95	47963.20	0.51	0.43	0.37	0.51	0.43	0.37	0.51	0.43	0.37
44	0.28	0.28	0.28	4.73	3.98	3.42	11336.75	0.15	0.12	0.11	0.15	0.13	0.11	0.15	0.12	0.11
45	0.20	0.20	0.20	3.60	3.03	2.60	55811.68	0.39	0.33	0.28	0.39	0.33	0.28	0.39	0.33	0.28
46	0.31	0.31	0.31	2.87	2.42	2.07	115983.71	1.03	0.87	0.74	1.03	0.87	0.74	1.03	0.87	0.74
47	0.15	0.15	0.15	2.67	2.24	1.92	147377.82	0.58	0.49	0.42	0.59	0.50	0.43	0.60	0.50	0.43

Table B.2: Peak runoff values from watersheds of Fatasil hill.

Basin ID	Composite C (Rational Method) & CN (NRCS-TR55 method) for the year			Rainfall intensity ($x10^{-5}$ m/s) for RP			Area (sq. m)	Peak Q (m3/s) in 2011 for RP			Peak Q (m3/s) in 2015 for RP			Peak Q (m3/s) in 2025 for RP			Method
	2011	2015	2025	25 yr	10 yr	5 yr		25 yr	10 yr	5 yr	25 yr	10 yr	5 yr	25 yr	10 yr	5 yr	
1	0.44	0.44	0.48	3.04	2.56	2.20	327021.72	4.35	3.67	3.14	4.41	3.72	3.19	5.97	5.39	4.82	Rational
2	0.47	0.47	0.61	6.85	5.77	4.95	13080.87	0.42	0.35	0.30	0.42	0.35	0.30	0.68	0.61	0.55	
3	0.64	0.64	0.64	6.11	5.14	4.41	10464.68	0.41	0.35	0.30	0.41	0.35	0.30	0.51	0.46	0.41	
4	0.42	0.42	0.48	4.32	3.64	3.12	63660.23	1.16	0.97	0.84	1.16	0.97	0.84	1.63	1.48	1.32	
5	0.47	0.49	0.54	5.26	4.43	3.80	20057.32	0.49	0.42	0.36	0.52	0.44	0.37	0.71	0.64	0.57	
6	0.60	0.60	0.60	4.77	4.02	3.45	16569.10	0.47	0.40	0.34	0.47	0.40	0.34	0.59	0.53	0.47	
7	0.69	0.71	0.69	6.28	5.29	4.54	13952.93	0.61	0.51	0.44	0.62	0.52	0.45	0.75	0.68	0.61	
8	0.47	0.47	0.50	3.04	2.56	2.20	305220.26	4.35	3.66	3.14	4.36	3.67	3.15	5.76	5.20	4.64	
9	0.39	0.39	0.42	4.58	3.86	3.31	42730.84	0.77	0.65	0.55	0.77	0.65	0.55	1.02	0.92	0.82	
10	0.52	0.52	0.55	8.39	7.06	6.06	13080.87	0.57	0.48	0.41	0.57	0.48	0.41	0.75	0.68	0.61	
11	0.57	0.57	0.58	2.20	1.86	1.59	294755.55	3.68	3.10	2.66	3.68	3.10	2.66	4.63	4.18	3.74	
12	0.63	0.64	0.64	5.00	4.21	3.61	35754.39	1.13	0.95	0.81	1.13	0.96	0.82	1.41	1.28	1.14	
13	0.45	0.50	0.51	7.18	6.04	5.18	13952.93	0.46	0.38	0.33	0.50	0.42	0.36	0.63	0.57	0.51	
14	0.46	0.53	0.53	6.24	5.26	4.51	18313.20	0.53	0.45	0.38	0.60	0.51	0.44	0.74	0.67	0.60	
15	0.44	0.44	0.46	1.59	1.34	1.15	881650.52	6.15	5.18	4.44	6.22	5.23	4.49	14.24	12.86	11.49	
16	0.41	0.41	0.45	2.46	2.07	1.77	426436.31	4.24	3.57	3.06	4.29	3.61	3.10	5.79	5.23	4.67	
17	0.54	0.54	0.54	3.48	2.93	2.51	68892.60	1.29	1.08	0.93	1.29	1.08	0.93	1.61	1.45	1.30	
18	0.38	0.38	0.46	2.64	2.22	1.90	171795.41	1.74	1.46	1.25	1.74	1.46	1.25	2.58	2.33	2.08	
19	0.40	0.40	0.42	2.26	1.91	1.63	404634.83	3.62	3.05	2.62	3.69	3.11	2.67	4.75	4.30	3.84	
20	0.47	0.48	0.53	1.95	1.64	1.41	1016819.51	9.39	7.90	6.78	9.46	7.97	6.84	19.70	17.80	15.90	
21	0.44	0.44	0.45	4.00	3.37	2.89	143889.55	2.52	2.12	1.82	2.55	2.15	1.84	3.24	2.93	2.62	
22	0.35	0.36	0.42	1.72	1.45	1.24	571197.92	3.43	2.89	2.48	3.51	2.96	2.54	5.14	4.64	4.14	
23	0.40	0.41	0.42	2.46	2.07	1.77	569453.82	5.58	4.70	4.03	5.68	4.79	4.11	7.29	6.59	5.89	

24	0.37	0.37	0.43	2.13	1.80	1.54	585150.83	4.57	3.85	3.30	4.60	3.87	3.32	6.68	6.03	5.39	
25	0.33	0.33	0.43	2.95	2.48	2.13	182260.12	1.77	1.49	1.28	1.78	1.50	1.28	2.88	2.60	2.33	
26	0.31	0.32	0.36	1.77	1.49	1.28	710727.18	3.94	3.32	2.85	3.98	3.35	2.87	5.58	5.04	4.50	
27	0.65	0.65	0.67	4.80	4.04	3.46	52323.47	1.62	1.37	1.17	1.64	1.38	1.18	2.07	1.87	1.67	
28	0.39	0.40	0.50	3.88	3.26	2.80	53195.53	0.80	0.67	0.58	0.82	0.69	0.60	1.28	1.16	1.04	
29	0.38	0.39	0.44	2.96	2.50	2.14	200573.33	2.28	1.92	1.65	2.35	1.98	1.70	3.24	2.92	2.61	
30	0.48	0.48	0.49	3.86	3.25	2.79	47091.12	0.88	0.74	0.63	0.88	0.74	0.63	1.10	0.99	0.89	
31	0.38	0.39	0.49	3.43	2.89	2.48	68020.52	0.88	0.74	0.63	0.91	0.77	0.66	1.41	1.27	1.14	
32	0.53	0.53	0.53	3.43	2.89	2.48	40986.72	0.74	0.62	0.53	0.74	0.62	0.53	0.93	0.84	0.75	
33	0.33	0.35	0.35	1.70	1.43	1.23	718575.74	4.02	3.39	2.91	4.28	3.60	3.09	5.34	4.82	4.31	
34	0.30	0.30	0.50	2.88	2.43	2.08	221502.68	1.92	1.62	1.39	1.93	1.62	1.39	3.96	3.58	3.20	
35	0.42	0.42	0.51	2.42	2.04	1.75	291267.34	2.95	2.48	2.13	2.95	2.48	2.13	4.49	4.06	3.62	
36	0.35	0.36	0.38	1.82	1.53	1.31	693286.01	4.37	3.68	3.15	4.48	3.77	3.23	5.88	5.31	4.74	
37	0.41	0.44	0.44	3.45	2.90	2.49	80229.34	1.15	0.97	0.83	1.22	1.03	0.88	1.50	1.36	1.21	
38	0.36	0.36	0.40	3.21	2.70	2.32	110751.33	1.26	1.06	0.91	1.29	1.09	0.93	1.75	1.58	1.41	
39	0.38	0.39	0.41	3.69	3.11	2.67	135168.99	1.91	1.61	1.38	1.93	1.63	1.39	2.56	2.32	2.07	
40	0.50	0.50	0.50	5.09	4.29	3.68	22673.50	0.58	0.49	0.42	0.58	0.49	0.42	0.72	0.65	0.58	
41	0.44	0.45	0.44	4.56	3.84	3.29	20057.33	0.40	0.34	0.29	0.41	0.35	0.30	0.50	0.45	0.40	
42	0.34	0.36	0.41	2.31	1.95	1.67	649683.09	5.14	4.33	3.71	5.45	4.59	3.94	7.55	6.82	6.09	
43	0.36	0.36	0.37	3.48	2.93	2.51	56683.76	0.72	0.61	0.52	0.72	0.61	0.52	0.90	0.82	0.73	
44	0.33	0.34	0.45	1.90	1.60	1.37	637474.32	3.93	3.31	2.84	4.07	3.43	2.94	6.71	6.06	5.42	
45	0.46	0.47	0.46	5.09	4.29	3.68	24417.62	0.58	0.49	0.42	0.58	0.49	0.42	0.72	0.65	0.58	
46	0.43	0.50	0.50	4.13	3.48	2.98	45347.00	0.81	0.68	0.58	0.93	0.78	0.67	1.16	1.05	0.94	
47	0.45	0.45	0.51	5.16	4.34	3.72	40986.72	0.96	0.80	0.69	0.96	0.80	0.69	1.33	1.21	1.08	
48	0.45	0.47	0.48	2.77	2.33	2.00	170923.34	2.15	1.81	1.55	2.20	1.85	1.59	2.83	2.56	2.28	
49	0.47	0.47	0.55	4.98	4.20	3.60	29649.97	0.69	0.58	0.50	0.70	0.59	0.50	1.01	0.92	0.82	
50	0.46	0.46	0.46	4.22	3.56	3.05	64532.29	1.24	1.04	0.90	1.24	1.04	0.90	1.55	1.40	1.25	
51	0.43	0.44	0.47	2.94	2.47	2.12	180515.99	2.29	1.92	1.65	2.32	1.96	1.68	3.10	2.80	2.50	
52	0.49	0.52	0.54	4.17	3.51	3.01	44474.96	0.92	0.77	0.66	0.97	0.82	0.70	1.24	1.12	1.00	

53	66.76	67.46	68.14				6315443.34	35.37	25.19	18.18	36.21	25.89	18.77	37.02	27.03	19.56	NRCS-TR55
54	0.56	0.57	0.58	4.13	3.48	2.98	35754.37	0.83	0.70	0.60	0.84	0.71	0.61	1.06	0.96	0.85	Rational
55	0.45	0.47	0.49	3.25	2.74	2.35	214526.23	3.17	2.67	2.29	3.25	2.73	2.34	4.25	3.84	3.43	
56	0.59	0.61	0.60	4.60	3.87	3.32	18313.21	0.50	0.42	0.36	0.52	0.44	0.37	0.62	0.56	0.50	
57	0.57	0.57	0.58	3.45	2.91	2.49	128192.51	2.52	2.12	1.82	2.52	2.12	1.82	3.16	2.85	2.55	
58	0.33	0.35	0.35	1.67	1.41	1.21	1182510.50	6.60	5.56	4.77	6.82	5.74	4.92	15.17	13.70	12.24	
59	0.40	0.42	0.42	2.67	2.25	1.93	261617.40	2.77	2.34	2.00	2.91	2.45	2.10	3.61	3.26	2.91	
60	0.42	0.43	0.47	2.86	2.41	2.07	186620.37	2.24	1.89	1.62	2.31	1.94	1.67	3.08	2.79	2.49	
61	0.47	0.49	0.47	4.58	3.85	3.30	13080.86	0.28	0.24	0.20	0.29	0.25	0.21	0.35	0.31	0.28	
62	0.48	0.49	0.54	3.27	2.76	2.36	151738.07	2.39	2.01	1.73	2.45	2.06	1.77	3.32	3.00	2.68	
63	0.48	0.48	0.50	4.84	4.08	3.50	20929.38	0.49	0.41	0.35	0.49	0.41	0.35	0.63	0.57	0.51	
64	0.43	0.47	0.52	3.83	3.22	2.76	63660.21	1.05	0.89	0.76	1.16	0.97	0.83	1.58	1.43	1.28	

Table B.3: Peak runoff values from watersheds of Kalapahar hill

Basin ID	Composite C for the year			Rainfall intensity (x10^{-5} m/s) for RP			Area (sq. m)	Peak Q (m3/s) in 2011 for RP			Peak Q (m3/s) in 2015 for RP			Peak Q (m3/s) in 2025 for RP		
	2011	2015	2025	25 yr	10 yr	5 yr		25 yr	10 yr	5 yr	25 yr	10 yr	5 yr	25 yr	10 yr	5 yr
1	0.59	0.60	0.60	7.19	6.06	5.19	12208.81	0.52	0.44	0.38	0.52	0.44	0.38	0.53	0.44	0.38
2	0.54	0.55	0.58	5.70	4.80	4.12	33138.20	1.03	0.87	0.74	1.03	0.87	0.74	1.09	0.92	0.79
3	0.45	0.46	0.48	2.13	1.79	1.54	256385.02	2.46	2.07	1.77	2.50	2.11	1.81	2.60	2.19	1.88
4	0.34	0.34	0.41	5.00	4.21	3.61	25289.68	0.43	0.36	0.31	0.43	0.36	0.31	0.51	0.43	0.37
5	0.38	0.39	0.46	4.71	3.96	3.40	72380.81	1.31	1.10	0.94	1.32	1.11	0.96	1.57	1.32	1.14
6	0.38	0.38	0.46	5.81	4.89	4.20	30522.02	0.67	0.57	0.49	0.68	0.57	0.49	0.81	0.68	0.58
7	0.44	0.45	0.49	4.80	4.04	3.46	44474.95	0.95	0.80	0.68	0.95	0.80	0.69	1.04	0.87	0.75
8	0.28	0.28	0.29	5.74	4.83	4.14	22673.49	0.37	0.31	0.26	0.37	0.31	0.26	0.38	0.32	0.27
9	0.51	0.51	0.51	16.92	14.24	12.22	2616.17	0.23	0.19	0.16	0.23	0.19	0.16	0.23	0.19	0.16
10	0.49	0.49	0.54	4.73	3.98	3.41	51451.42	1.20	1.01	0.86	1.20	1.01	0.87	1.32	1.11	0.95
11	0.31	0.31	0.38	8.83	7.44	6.38	8720.58	0.24	0.20	0.17	0.24	0.20	0.17	0.30	0.25	0.21
12	0.42	0.42	0.45	3.57	3.01	2.58	169179.23	2.51	2.11	1.81	2.55	2.14	1.84	2.71	2.28	1.95
13	0.68	0.70	0.68	17.13	14.42	12.37	1744.12	0.20	0.17	0.15	0.21	0.18	0.15	0.20	0.17	0.15
14	0.48	0.48	0.48	12.67	10.67	9.15	4360.30	0.27	0.22	0.19	0.27	0.22	0.19	0.27	0.22	0.19
15	0.49	0.55	0.49	9.41	7.92	6.80	6104.40	0.28	0.24	0.20	0.31	0.27	0.23	0.28	0.24	0.20
16	0.43	0.43	0.43	14.88	12.53	10.75	2616.18	0.17	0.14	0.12	0.17	0.14	0.12	0.17	0.14	0.12
17	0.55	0.55	0.55	17.85	15.03	12.89	2616.17	0.26	0.22	0.19	0.26	0.22	0.19	0.26	0.22	0.19
18	0.48	0.49	0.48	9.68	8.15	6.99	6104.40	0.28	0.24	0.21	0.29	0.24	0.21	0.28	0.24	0.21
19	0.29	0.29	0.32	8.65	7.28	6.25	6976.47	0.18	0.15	0.13	0.18	0.15	0.13	0.19	0.16	0.14
20	0.40	0.41	0.44	2.14	1.80	1.55	364520.18	3.12	2.63	2.25	3.22	2.71	2.33	3.45	2.90	2.49
21	0.27	0.27	0.27	7.76	6.53	5.60	7848.52	0.17	0.14	0.12	0.17	0.14	0.12	0.17	0.14	0.12
22	0.37	0.38	0.39	6.34	5.34	4.58	15697.05	0.37	0.31	0.26	0.38	0.32	0.27	0.39	0.33	0.28
23	0.34	0.34	0.34	7.14	6.01	5.16	9592.64	0.23	0.20	0.17	0.23	0.20	0.17	0.23	0.20	0.17

24	0.37	0.37	0.37	5.72	4.82	4.13	13952.92	0.29	0.25	0.21	0.30	0.25	0.21	0.29	0.25	0.21
25	0.49	0.49	0.58	19.33	16.28	13.96	2616.17	0.25	0.21	0.18	0.25	0.21	0.18	0.29	0.25	0.21
26	0.55	0.57	0.56	10.54	8.87	7.61	4360.29	0.25	0.21	0.18	0.26	0.22	0.19	0.26	0.22	0.19
27	0.39	0.39	0.39	7.12	6.00	5.15	15697.06	0.43	0.36	0.31	0.44	0.37	0.32	0.43	0.36	0.31
28	0.38	0.41	0.38	6.51	5.48	4.70	13952.92	0.35	0.29	0.25	0.37	0.31	0.27	0.35	0.29	0.25
29	0.56	0.56	0.56	19.06	16.05	13.77	1744.11	0.19	0.16	0.13	0.19	0.16	0.13	0.19	0.16	0.13
30	0.40	0.42	0.40	8.10	6.82	5.85	6976.46	0.23	0.19	0.16	0.24	0.20	0.17	0.23	0.19	0.16
31	0.53	0.55	0.53	5.97	5.03	4.31	40114.67	1.27	1.07	0.92	1.31	1.10	0.95	1.27	1.07	0.92
32	0.33	0.37	0.33	8.57	7.22	6.19	8720.58	0.25	0.21	0.18	0.28	0.23	0.20	0.25	0.21	0.18
33	0.30	0.30	0.30	19.56	16.47	14.12	2616.17	0.15	0.13	0.11	0.15	0.13	0.11	0.15	0.13	0.11
34	0.37	0.38	0.38	4.89	4.11	3.53	26161.74	0.48	0.40	0.34	0.49	0.41	0.35	0.49	0.41	0.35
35	0.38	0.38	0.38	41.01	34.52	29.61	1744.12	0.27	0.23	0.19	0.27	0.23	0.19	0.27	0.23	0.19
36	0.44	0.44	0.44	4.38	3.69	3.16	27905.84	0.53	0.45	0.38	0.53	0.45	0.38	0.53	0.45	0.38
37	0.44	0.44	0.44	14.37	12.10	10.38	1744.12	0.11	0.09	0.08	0.11	0.09	0.08	0.11	0.09	0.08
38	0.43	0.44	0.49	2.28	1.92	1.65	221502.70	2.19	1.85	1.58	2.24	1.89	1.62	2.48	2.08	1.79
39	0.42	0.42	0.42	8.33	7.01	6.02	10464.70	0.36	0.30	0.26	0.37	0.31	0.27	0.36	0.30	0.26
40	0.38	0.39	0.38	13.63	11.47	9.84	1744.12	0.09	0.08	0.07	0.09	0.08	0.07	0.09	0.08	0.07
41	0.46	0.46	0.46	14.00	11.78	10.11	2616.18	0.17	0.14	0.12	0.17	0.14	0.12	0.17	0.14	0.12
42	0.42	0.43	0.42	8.62	7.26	6.23	1744.12	0.06	0.05	0.05	0.06	0.05	0.05	0.06	0.05	0.05
43	0.46	0.47	0.46	9.77	8.23	7.06	2616.17	0.12	0.10	0.09	0.12	0.10	0.09	0.12	0.10	0.09
44	0.40	0.40	0.40	10.84	9.13	7.83	1744.12	0.08	0.06	0.05	0.08	0.06	0.05	0.08	0.06	0.05
45	0.35	0.38	0.35	7.85	6.61	5.67	12208.82	0.34	0.28	0.24	0.37	0.31	0.27	0.34	0.28	0.24
46	0.38	0.39	0.40	12.97	10.92	9.37	2616.17	0.13	0.11	0.09	0.13	0.11	0.10	0.13	0.11	0.10
47	0.37	0.42	0.44	10.62	8.94	7.67	3488.23	0.14	0.12	0.10	0.15	0.13	0.11	0.16	0.14	0.12
48	0.38	0.38	0.44	10.51	8.84	7.59	3488.23	0.14	0.12	0.10	0.14	0.12	0.10	0.16	0.14	0.12
49	0.47	0.47	0.51	8.39	7.07	6.06	4360.30	0.17	0.14	0.12	0.17	0.14	0.12	0.19	0.16	0.14
50	0.40	0.40	0.40	11.26	9.48	8.13	3488.24	0.16	0.13	0.11	0.16	0.13	0.11	0.16	0.13	0.11
51	0.45	0.48	0.49	8.62	7.25	6.22	6104.41	0.24	0.20	0.17	0.25	0.21	0.18	0.26	0.22	0.19
52	0.42	0.42	0.42	17.26	14.53	12.46	1744.12	0.13	0.11	0.09	0.13	0.11	0.09	0.13	0.11	0.09

53	0.38	0.48	0.42	11.43	9.62	8.25	6976.47	0.30	0.25	0.22	0.38	0.32	0.28	0.34	0.28	0.24
54	0.40	0.40	0.41	4.19	3.53	3.03	55811.70	0.94	0.79	0.68	0.94	0.79	0.68	0.95	0.80	0.69
55	0.41	0.43	0.41	7.81	6.57	5.64	8720.58	0.28	0.24	0.20	0.29	0.24	0.21	0.28	0.24	0.20
56	0.51	0.51	0.51	17.26	14.53	12.46	1744.12	0.15	0.13	0.11	0.15	0.13	0.11	0.15	0.13	0.11
57	0.60	0.60	0.60	17.13	14.42	12.37	1744.12	0.18	0.15	0.13	0.18	0.15	0.13	0.18	0.15	0.13
58	0.56	0.56	0.56	9.55	8.04	6.90	2616.17	0.14	0.12	0.10	0.14	0.12	0.10	0.14	0.12	0.10
59	0.44	0.46	0.44	4.47	3.76	3.23	40986.72	0.80	0.67	0.58	0.84	0.70	0.60	0.81	0.68	0.59
60	0.42	0.44	0.43	6.59	5.55	4.76	20929.39	0.58	0.49	0.42	0.60	0.51	0.44	0.60	0.50	0.43
61	0.36	0.39	0.36	7.37	6.20	5.32	15697.04	0.42	0.35	0.30	0.45	0.38	0.32	0.42	0.35	0.30
62	0.37	0.37	0.37	8.02	6.75	5.79	4360.29	0.13	0.11	0.09	0.13	0.11	0.09	0.13	0.11	0.09
63	0.50	0.50	0.50	8.36	7.04	6.04	3488.23	0.15	0.12	0.11	0.15	0.12	0.11	0.15	0.12	0.11
64	0.39	0.39	0.46	11.71	9.86	8.46	3488.23	0.16	0.13	0.11	0.16	0.13	0.11	0.19	0.16	0.14
65	0.43	0.43	0.43	13.47	11.34	9.73	2616.17	0.15	0.13	0.11	0.15	0.13	0.11	0.15	0.13	0.11
66	0.41	0.41	0.41	6.95	5.85	5.02	13080.87	0.38	0.32	0.27	0.38	0.32	0.27	0.38	0.32	0.27
67	0.61	0.61	0.61	14.36	12.09	10.37	2616.17	0.23	0.19	0.17	0.23	0.19	0.17	0.23	0.19	0.17
68	0.51	0.52	0.51	17.13	14.42	12.37	1744.11	0.15	0.13	0.11	0.16	0.13	0.11	0.15	0.13	0.11
69	0.44	0.44	0.44	12.27	10.33	8.86	3488.23	0.19	0.16	0.14	0.19	0.16	0.14	0.19	0.16	0.14
70	0.50	0.53	0.50	10.72	9.03	7.74	3488.24	0.19	0.16	0.14	0.20	0.17	0.14	0.19	0.16	0.14
71	0.40	0.40	0.40	6.71	5.65	4.85	12208.80	0.33	0.27	0.24	0.33	0.28	0.24	0.33	0.27	0.24
72	0.31	0.31	0.36	14.50	12.21	10.47	2616.17	0.12	0.10	0.08	0.12	0.10	0.08	0.13	0.11	0.10
73	0.41	0.41	0.41	9.06	7.63	6.54	6976.47	0.26	0.22	0.19	0.26	0.22	0.19	0.26	0.22	0.19
74	0.35	0.35	0.35	8.09	6.81	5.84	13080.87	0.37	0.31	0.27	0.37	0.31	0.27	0.37	0.31	0.27
75	0.42	0.42	0.43	3.03	2.55	2.19	191852.75	2.43	2.05	1.75	2.46	2.07	1.78	2.50	2.10	1.80
76	0.37	0.38	0.37	2.14	1.80	1.55	328765.84	2.59	2.18	1.87	2.64	2.23	1.91	2.59	2.18	1.87
77	0.37	0.37	0.38	2.95	2.48	2.13	107263.12	1.18	0.99	0.85	1.18	0.99	0.85	1.20	1.01	0.86
78	0.38	0.38	0.43	7.23	6.09	5.22	5232.36	0.14	0.12	0.10	0.14	0.12	0.10	0.16	0.14	0.12
79	0.40	0.40	0.41	7.13	6.01	5.15	16569.10	0.47	0.39	0.34	0.47	0.39	0.34	0.48	0.40	0.35

Table B.4: Peak runoff values from watersheds of Sonaighuli hill

Basin ID	Composite C for the year			Rainfall intensity (x10^{-5} m/s) for RP			Area (sq. m)	Peak Q (m3/s) in 2011 for RP			Peak Q (m3/s) in 2015 for RP			Peak Q (m3/s) in 2025 for RP		
	2011	2015	2025	25 yr	10 yr	5 yr		25 yr	10 yr	5 yr	25 yr	10 yr	5 yr	25 yr	10 yr	5 yr
1	0.54	0.57	0.60	16.22	13.65	11.71	1744.12	0.15	0.13	0.11	0.16	0.14	0.12	0.17	0.14	0.12
2	0.53	0.54	0.55	7.75	6.53	5.60	9592.64	0.39	0.33	0.28	0.40	0.34	0.29	0.41	0.34	0.30
3	0.49	0.53	0.57	11.43	9.63	8.26	3488.23	0.20	0.17	0.14	0.21	0.18	0.15	0.23	0.19	0.16
4	0.46	0.47	0.57	15.72	13.23	11.35	5232.34	0.38	0.32	0.27	0.39	0.32	0.28	0.47	0.40	0.34
5	0.64	0.64	0.64	17.13	14.42	12.37	1744.12	0.19	0.16	0.14	0.19	0.16	0.14	0.19	0.16	0.14
6	0.45	0.47	0.64	5.49	4.62	3.97	13952.93	0.34	0.29	0.25	0.36	0.30	0.26	0.49	0.41	0.35
7	0.32	0.35	0.47	4.64	3.90	3.35	55811.71	0.82	0.69	0.59	0.90	0.76	0.65	1.21	1.02	0.88
8	0.36	0.41	0.55	8.49	7.15	6.13	6976.46	0.21	0.18	0.15	0.24	0.20	0.17	0.33	0.28	0.24
9	0.49	0.49	0.49	11.93	10.05	8.62	3488.23	0.20	0.17	0.15	0.20	0.17	0.15	0.20	0.17	0.15
10	0.44	0.51	0.53	10.54	8.88	7.61	2616.17	0.12	0.10	0.09	0.14	0.12	0.10	0.15	0.12	0.11
11	0.51	0.53	0.55	8.33	7.01	6.02	5232.34	0.22	0.19	0.16	0.23	0.19	0.17	0.24	0.20	0.17
12	0.57	0.59	0.57	11.58	9.75	8.36	4360.28	0.29	0.24	0.21	0.30	0.25	0.22	0.29	0.24	0.21
13	0.38	0.42	0.44	8.74	7.36	6.31	4360.29	0.15	0.12	0.11	0.16	0.13	0.12	0.17	0.14	0.12
14	0.44	0.47	0.47	5.22	4.39	3.77	39242.60	0.90	0.76	0.65	0.96	0.81	0.70	0.97	0.81	0.70
15	0.55	0.55	0.61	21.34	17.97	15.41	1744.12	0.20	0.17	0.15	0.21	0.17	0.15	0.23	0.19	0.16
16	0.50	0.51	0.65	22.31	18.78	16.11	1744.12	0.20	0.17	0.14	0.20	0.17	0.14	0.25	0.21	0.18
17	0.51	0.51	0.51	36.95	31.11	26.69	1744.12	0.33	0.28	0.24	0.33	0.28	0.24	0.33	0.28	0.24
18	0.53	0.55	0.55	4.87	4.10	3.52	42730.84	1.10	0.93	0.80	1.14	0.96	0.82	1.12	0.94	0.81
19	0.52	0.52	0.66	14.36	12.09	10.37	2616.17	0.19	0.16	0.14	0.19	0.16	0.14	0.25	0.21	0.18
20	0.35	0.35	0.48	17.42	14.67	12.58	2616.17	0.16	0.13	0.11	0.16	0.13	0.11	0.22	0.18	0.16
21	0.41	0.42	0.46	7.19	6.05	5.19	9592.63	0.28	0.24	0.20	0.29	0.24	0.21	0.32	0.27	0.23
22	0.50	0.53	0.61	7.99	6.73	5.77	8720.58	0.35	0.30	0.25	0.37	0.31	0.27	0.42	0.36	0.31
23	0.50	0.50	0.54	8.19	6.89	5.91	6104.40	0.25	0.21	0.18	0.25	0.21	0.18	0.27	0.23	0.19
24	0.30	0.30	0.30	35.88	30.21	25.91	1744.11	0.19	0.16	0.14	0.19	0.16	0.14	0.19	0.16	0.14

25	0.32	0.32	0.53	8.11	6.83	5.86	10464.70	0.27	0.23	0.19	0.27	0.23	0.20	0.45	0.38	0.33
26	0.40	0.44	0.53	8.55	7.19	6.17	7848.53	0.27	0.23	0.19	0.30	0.25	0.21	0.36	0.30	0.26
27	0.29	0.31	0.44	7.27	6.12	5.25	16569.11	0.34	0.29	0.25	0.37	0.31	0.27	0.53	0.45	0.39
28	0.52	0.52	0.52	6.79	5.71	4.90	11336.76	0.40	0.34	0.29	0.40	0.34	0.29	0.40	0.34	0.29
29	0.44	0.46	0.47	6.42	5.41	4.64	9592.64	0.27	0.23	0.20	0.28	0.24	0.20	0.29	0.24	0.21
30	0.47	0.47	0.47	12.66	10.66	9.14	2616.17	0.15	0.13	0.11	0.16	0.13	0.11	0.15	0.13	0.11
31	0.36	0.36	0.50	8.74	7.36	6.31	6976.47	0.22	0.18	0.16	0.22	0.18	0.16	0.30	0.25	0.22
32	0.34	0.34	0.34	16.29	13.71	11.76	2616.17	0.14	0.12	0.10	0.14	0.12	0.10	0.14	0.12	0.10
33	0.55	0.55	0.55	14.05	11.83	10.15	2616.17	0.20	0.17	0.15	0.20	0.17	0.15	0.20	0.17	0.15
34	0.44	0.45	0.48	8.18	6.89	5.91	6976.47	0.25	0.21	0.18	0.26	0.22	0.19	0.27	0.23	0.20
35	0.30	0.30	0.30	13.63	11.47	9.84	1744.12	0.07	0.06	0.05	0.07	0.06	0.05	0.07	0.06	0.05
36	0.33	0.33	0.44	16.47	13.87	11.90	4360.30	0.24	0.20	0.17	0.24	0.20	0.17	0.32	0.27	0.23
37	0.33	0.33	0.33	17.42	14.67	12.58	2616.17	0.15	0.13	0.11	0.15	0.13	0.11	0.15	0.13	0.11
38	0.32	0.32	0.32	17.42	14.67	12.58	2616.17	0.15	0.12	0.11	0.15	0.12	0.11	0.15	0.12	0.11
39	0.30	0.30	0.30	17.13	14.42	12.37	1744.12	0.09	0.08	0.06	0.09	0.08	0.06	0.09	0.08	0.06
40	0.30	0.30	0.30	14.87	12.52	10.74	2616.18	0.12	0.10	0.08	0.12	0.10	0.08	0.12	0.10	0.08
41	0.51	0.51	0.55	9.20	7.75	6.65	5232.34	0.24	0.21	0.18	0.24	0.21	0.18	0.27	0.22	0.19
42	0.22	0.33	0.49	7.69	6.48	5.56	10464.70	0.17	0.15	0.13	0.26	0.22	0.19	0.40	0.33	0.29
43	0.41	0.48	0.41	13.47	11.34	9.73	2616.17	0.14	0.12	0.10	0.17	0.14	0.12	0.14	0.12	0.10
44	0.35	0.35	0.35	15.00	12.62	10.83	3488.24	0.18	0.16	0.13	0.19	0.16	0.13	0.18	0.16	0.13
45	0.37	0.37	0.41	15.15	12.76	10.94	3488.24	0.20	0.17	0.14	0.20	0.17	0.14	0.21	0.18	0.15
46	0.31	0.36	0.40	11.51	9.69	8.31	4360.29	0.15	0.13	0.11	0.18	0.15	0.13	0.20	0.17	0.14
47	0.32	0.32	0.43	11.08	9.33	8.00	3488.23	0.12	0.10	0.09	0.12	0.10	0.09	0.17	0.14	0.12
48	0.32	0.32	0.38	17.13	14.42	12.37	1744.11	0.10	0.08	0.07	0.10	0.08	0.07	0.11	0.10	0.08
49	0.47	0.47	0.48	5.95	5.01	4.30	6976.46	0.20	0.17	0.14	0.20	0.17	0.14	0.20	0.17	0.14
50	0.31	0.31	0.31	22.31	18.78	16.11	1744.11	0.12	0.10	0.09	0.12	0.10	0.09	0.12	0.10	0.09
51	0.43	0.43	0.43	14.64	12.32	10.57	2616.17	0.16	0.14	0.12	0.16	0.14	0.12	0.16	0.14	0.12
52	0.31	0.31	0.31	18.04	15.19	13.03	2616.17	0.15	0.12	0.11	0.15	0.12	0.11	0.15	0.12	0.11
53	0.27	0.27	0.27	17.85	15.03	12.89	2616.17	0.13	0.11	0.09	0.13	0.11	0.09	0.13	0.11	0.09

54	0.47	0.47	0.47	29.36	24.72	21.20	1744.12	0.24	0.20	0.17	0.24	0.20	0.17	0.24	0.20	0.17
55	0.38	0.38	0.41	14.41	12.13	10.41	2616.17	0.14	0.12	0.10	0.14	0.12	0.10	0.15	0.13	0.11
56	0.38	0.40	0.42	8.26	6.95	5.97	5232.34	0.17	0.14	0.12	0.17	0.15	0.12	0.18	0.15	0.13
57	0.43	0.43	0.43	8.64	7.27	6.24	12208.82	0.45	0.38	0.33	0.45	0.38	0.33	0.45	0.38	0.33
58	0.49	0.49	0.50	11.55	9.73	8.34	4360.29	0.25	0.21	0.18	0.25	0.21	0.18	0.25	0.21	0.18
59	0.50	0.50	0.50	10.98	9.24	7.93	4360.29	0.24	0.20	0.17	0.24	0.20	0.17	0.24	0.20	0.17
60	0.34	0.40	0.38	8.20	6.91	5.93	8720.57	0.25	0.21	0.18	0.29	0.24	0.21	0.27	0.23	0.20
61	0.51	0.51	0.51	13.23	11.13	9.55	3488.24	0.24	0.20	0.17	0.24	0.20	0.17	0.24	0.20	0.17
62	0.46	0.46	0.46	8.98	7.56	6.49	5232.34	0.22	0.18	0.16	0.22	0.18	0.16	0.22	0.18	0.16
63	0.45	0.46	0.45	12.53	10.55	9.05	4360.28	0.25	0.21	0.18	0.25	0.21	0.18	0.25	0.21	0.18
64	0.38	0.40	0.41	4.94	4.16	3.57	40986.73	0.77	0.65	0.56	0.81	0.68	0.58	0.83	0.70	0.60
65	0.39	0.40	0.39	13.07	11.01	9.44	6976.46	0.35	0.30	0.25	0.36	0.31	0.26	0.35	0.30	0.25

Table B.5: Peak runoff values from watersheds of Sarania hill

Bas-in ID	Composite C for the year			Rainfall intensity ($x10^{-5}$ m/s) for RP			Area (sq. m)	Peak Q (m3/s) in 2011 for RP			Peak Q (m3/s) in 2015 for RP			Peak Q (m3/s) in 2025 for RP		
	2011	2015	2025	25 yr	10 yr	5 yr		25 yr	10 yr	5 yr	25 yr	10 yr	5 yr	25 yr	10 yr	5 yr
1	0.39	0.39	0.42	5.08	4.27	3.67	31394.10	0.62	0.52	0.45	0.62	0.52	0.45	0.67	0.57	0.49
2	0.47	0.47	0.53	4.97	4.18	3.59	36626.43	0.86	0.72	0.62	0.86	0.72	0.62	0.96	0.81	0.69
3	0.40	0.41	0.45	4.80	4.04	3.46	41858.80	0.81	0.68	0.59	0.82	0.69	0.59	0.90	0.76	0.65
4	0.45	0.46	0.48	3.66	3.08	2.65	81101.38	1.35	1.13	0.97	1.36	1.14	0.98	1.44	1.21	1.04
5	0.61	0.61	0.61	21.86	18.41	15.79	1744.11	0.23	0.20	0.17	0.23	0.20	0.17	0.23	0.20	0.17
6	0.56	0.57	0.56	20.72	17.45	14.97	1744.12	0.20	0.17	0.15	0.21	0.17	0.15	0.20	0.17	0.15
7	0.72	0.72	0.72	17.13	14.42	12.37	1744.11	0.21	0.18	0.16	0.21	0.18	0.16	0.21	0.18	0.16
8	0.43	0.46	0.44	16.77	14.12	12.11	2616.17	0.19	0.16	0.14	0.20	0.17	0.14	0.19	0.16	0.14
9	0.36	0.36	0.41	6.68	5.62	4.83	14824.98	0.36	0.30	0.26	0.36	0.30	0.26	0.41	0.34	0.30
10	0.48	0.48	0.48	14.26	12.01	10.30	3488.24	0.24	0.20	0.17	0.24	0.20	0.17	0.24	0.20	0.17
11	0.37	0.37	0.45	6.08	5.12	4.39	13952.92	0.31	0.26	0.22	0.31	0.26	0.22	0.38	0.32	0.27
12	0.41	0.42	0.41	7.96	6.70	5.75	7848.52	0.26	0.22	0.19	0.26	0.22	0.19	0.26	0.22	0.19
13	0.46	0.46	0.46	15.39	12.96	11.12	2616.17	0.18	0.15	0.13	0.18	0.15	0.13	0.18	0.15	0.13
14	0.41	0.44	0.41	7.52	6.33	5.43	6976.48	0.21	0.18	0.15	0.23	0.20	0.17	0.21	0.18	0.15
15	0.54	0.55	0.54	12.39	10.43	8.95	3488.23	0.23	0.20	0.17	0.24	0.20	0.17	0.23	0.20	0.17
16	0.47	0.47	0.47	12.47	10.50	9.01	3488.23	0.21	0.17	0.15	0.21	0.17	0.15	0.21	0.17	0.15
17	0.57	0.57	0.57	7.81	6.57	5.64	27905.85	1.23	1.04	0.89	1.24	1.05	0.90	1.23	1.04	0.89
18	0.43	0.43	0.43	4.54	3.82	3.28	68892.58	1.35	1.14	0.98	1.36	1.14	0.98	1.35	1.14	0.98
19	0.46	0.46	0.46	10.84	9.13	7.83	1744.11	0.09	0.07	0.06	0.09	0.07	0.06	0.09	0.07	0.06
20	0.59	0.59	0.59	6.79	5.72	4.91	15697.04	0.63	0.53	0.45	0.63	0.53	0.45	0.63	0.53	0.45
21	0.68	0.68	0.68	11.37	9.57	8.21	2616.18	0.20	0.17	0.15	0.20	0.17	0.15	0.20	0.17	0.15
22	0.58	0.59	0.58	4.68	3.94	3.38	46219.06	1.26	1.06	0.91	1.27	1.07	0.92	1.26	1.06	0.91
23	0.62	0.62	0.62	4.80	4.04	3.46	26161.73	0.78	0.65	0.56	0.78	0.65	0.56	0.78	0.65	0.56
24	0.50	0.51	0.50	3.76	3.17	2.72	107263.12	2.03	1.71	1.47	2.06	1.73	1.49	2.03	1.71	1.47

Table B.6: Peak runoff values from watersheds of Kharguli hill

Basin ID	Composite C for the year			Rainfall intensity (x10^{-5} m/s) for RP			Area (sq. m)	Peak Q (m3/s) in 2011 for RP			Peak Q (m3/s) in 2015 for RP			Peak Q (m3/s) in 2025 for RP		
	2011	2015	2025	25 yr	10 yr	5 yr		25 yr	10 yr	5 yr	25 yr	10 yr	5 yr	25 yr	10 yr	5 yr
1	0.30	0.30	0.36	6.59	5.55	4.76	17441.16	0.35	0.29	0.25	0.35	0.29	0.25	0.42	0.35	0.30
2	0.30	0.31	0.41	7.95	6.70	5.74	10464.70	0.25	0.21	0.18	0.26	0.22	0.19	0.34	0.29	0.24
3	0.30	0.30	0.30	7.23	6.09	5.22	11336.74	0.25	0.21	0.18	0.25	0.21	0.18	0.25	0.21	0.18
4	0.34	0.35	0.42	1.49	1.25	1.08	1033388.63	5.30	4.46	3.83	5.35	4.50	3.86	6.51	5.48	4.70
5	0.36	0.36	0.37	4.99	4.20	3.60	26161.73	0.46	0.39	0.34	0.46	0.39	0.34	0.48	0.41	0.35
6	0.34	0.39	0.38	6.55	5.51	4.73	10464.71	0.24	0.20	0.17	0.27	0.22	0.19	0.26	0.22	0.19
7	0.31	0.31	0.31	6.20	5.22	4.48	10464.68	0.20	0.17	0.15	0.20	0.17	0.15	0.20	0.17	0.15
8	0.36	0.37	0.36	7.61	6.41	5.50	11336.76	0.31	0.26	0.23	0.32	0.27	0.23	0.31	0.26	0.23
9	0.28	0.29	0.41	3.69	3.11	2.66	108135.17	1.13	0.95	0.81	1.14	0.96	0.82	1.63	1.37	1.17
10	0.30	0.33	0.34	6.84	5.76	4.94	11336.74	0.23	0.19	0.17	0.26	0.22	0.19	0.26	0.22	0.19
11	0.31	0.32	0.36	5.57	4.69	4.02	10464.70	0.18	0.15	0.13	0.19	0.16	0.13	0.21	0.18	0.15
12	0.27	0.37	0.56	7.15	6.02	5.17	10464.69	0.20	0.17	0.14	0.27	0.23	0.20	0.42	0.35	0.30
13	0.30	0.32	0.32	2.47	2.08	1.78	254640.91	1.90	1.60	1.37	1.99	1.68	1.44	1.98	1.67	1.43
14	0.30	0.30	0.46	6.11	5.15	4.42	11336.74	0.21	0.18	0.15	0.21	0.18	0.15	0.32	0.27	0.23
15	0.29	0.30	0.29	5.06	4.26	3.65	11336.74	0.17	0.14	0.12	0.17	0.15	0.13	0.17	0.14	0.12
16	0.30	0.31	0.52	6.78	5.71	4.90	11336.75	0.23	0.19	0.17	0.24	0.20	0.17	0.40	0.34	0.29
17	0.30	0.31	0.34	6.17	5.20	4.46	13080.87	0.25	0.21	0.18	0.25	0.21	0.18	0.28	0.23	0.20
18	0.29	0.35	0.43	5.59	4.71	4.04	13952.94	0.23	0.19	0.16	0.27	0.23	0.20	0.33	0.28	0.24
19	0.32	0.32	0.32	5.63	4.74	4.07	13952.92	0.25	0.21	0.18	0.25	0.21	0.18	0.25	0.21	0.18
20	0.38	0.38	0.41	4.76	4.01	3.44	30522.03	0.55	0.46	0.40	0.55	0.47	0.40	0.59	0.50	0.43
21	0.29	0.29	0.33	5.46	4.59	3.94	19185.27	0.31	0.26	0.22	0.31	0.26	0.22	0.35	0.29	0.25
22	0.27	0.29	0.29	3.09	2.60	2.23	148249.83	1.25	1.06	0.91	1.32	1.11	0.95	1.34	1.13	0.97

23	0.26	0.28	0.28	3.26	2.74	2.35	147377.77	1.26	1.06	0.91	1.32	1.11	0.95	1.36	1.14	0.98
24	0.34	0.37	0.39	2.44	2.05	1.76	373240.80	3.13	2.64	2.26	3.39	2.85	2.45	3.54	2.98	2.56
25	0.27	0.28	0.33	5.54	4.66	4.00	17441.14	0.27	0.22	0.19	0.27	0.23	0.20	0.32	0.27	0.23
26	0.38	0.38	0.38	8.77	7.38	6.33	13080.87	0.44	0.37	0.32	0.44	0.37	0.32	0.44	0.37	0.32
27	0.38	0.39	0.39	6.82	5.75	4.93	17441.15	0.45	0.38	0.33	0.46	0.39	0.33	0.46	0.39	0.33
28	0.40	0.40	0.41	4.42	3.72	3.19	56683.77	1.01	0.85	0.73	1.01	0.85	0.73	1.03	0.87	0.74
29	0.26	0.26	0.33	3.87	3.26	2.79	38370.53	0.39	0.32	0.28	0.39	0.33	0.28	0.49	0.41	0.35
30	0.37	0.38	0.37	7.18	6.04	5.18	12208.81	0.32	0.27	0.23	0.34	0.28	0.24	0.32	0.27	0.23
31	0.38	0.38	0.44	3.62	3.05	2.61	94182.25	1.29	1.09	0.93	1.31	1.10	0.95	1.51	1.27	1.09
32	0.25	0.27	0.27	3.26	2.74	2.35	56683.76	0.46	0.39	0.33	0.50	0.42	0.36	0.50	0.42	0.36
33	0.43	0.43	0.44	5.80	4.88	4.19	20057.34	0.50	0.42	0.36	0.50	0.42	0.36	0.51	0.43	0.37
34	0.48	0.48	0.50	6.51	5.48	4.70	19185.28	0.60	0.50	0.43	0.60	0.50	0.43	0.62	0.52	0.45
35	0.42	0.44	0.43	3.87	3.26	2.80	72380.80	1.18	1.00	0.85	1.25	1.05	0.90	1.20	1.01	0.87
36	0.45	0.46	0.50	4.50	3.79	3.25	61916.11	1.25	1.05	0.90	1.27	1.07	0.92	1.40	1.18	1.01
37	0.58	0.58	0.61	5.45	4.59	3.94	10464.70	0.33	0.28	0.24	0.33	0.28	0.24	0.35	0.29	0.25
38	0.41	0.42	0.44	1.73	1.46	1.25	629625.79	4.49	3.78	3.24	4.54	3.82	3.28	4.78	4.03	3.45
39	0.35	0.38	0.37	5.58	4.70	4.03	34882.32	0.68	0.58	0.49	0.74	0.62	0.53	0.71	0.60	0.52
40	0.42	0.44	0.44	1.99	1.67	1.44	416843.66	3.49	2.93	2.52	3.61	3.04	2.61	3.68	3.10	2.66
41	0.42	0.43	0.43	3.33	2.81	2.41	131680.75	1.84	1.55	1.33	1.91	1.61	1.38	1.91	1.61	1.38
42	0.50	0.51	0.50	5.70	4.80	4.12	24417.62	0.69	0.58	0.50	0.71	0.59	0.51	0.69	0.58	0.50
43	0.53	0.53	0.55	3.39	2.86	2.45	115111.65	2.05	1.73	1.48	2.09	1.76	1.51	2.13	1.80	1.54
44	0.42	0.45	0.49	6.65	5.59	4.80	32266.14	0.90	0.76	0.65	0.97	0.82	0.70	1.06	0.89	0.76
45	0.41	0.41	0.43	5.46	4.60	3.94	31394.08	0.71	0.60	0.51	0.71	0.60	0.51	0.73	0.61	0.53
46	0.57	0.57	0.57	5.27	4.44	3.81	51451.42	1.55	1.31	1.12	1.56	1.31	1.13	1.55	1.31	1.12
47	0.49	0.50	0.50	3.38	2.85	2.44	60172.02	1.00	0.84	0.72	1.01	0.85	0.73	1.01	0.85	0.73
48	0.41	0.43	0.41	3.15	2.66	2.28	136913.08	1.77	1.49	1.28	1.85	1.56	1.34	1.78	1.50	1.29
49	0.47	0.49	0.47	4.30	3.62	3.10	41858.78	0.84	0.71	0.61	0.89	0.75	0.64	0.84	0.71	0.61
50	0.44	0.44	0.45	2.96	2.49	2.14	175283.63	2.26	1.90	1.63	2.31	1.94	1.67	2.34	1.97	1.69
51	0.44	0.45	0.49	2.01	1.69	1.45	711599.26	6.26	5.27	4.52	6.44	5.42	4.65	6.96	5.86	5.03

52	0.53	0.54	0.55	4.43	3.73	3.20	32266.15	0.76	0.64	0.55	0.78	0.66	0.56	0.79	0.67	0.57
53	0.53	0.54	0.54	3.93	3.31	2.84	63660.23	1.31	1.11	0.95	1.35	1.13	0.97	1.35	1.13	0.97
54	0.50	0.50	0.54	5.55	4.68	4.01	19185.27	0.53	0.45	0.39	0.54	0.45	0.39	0.57	0.48	0.41
55	0.42	0.43	0.44	2.24	1.89	1.62	506665.69	4.82	4.05	3.48	4.88	4.11	3.52	5.05	4.25	3.64
56	0.42	0.45	0.42	7.28	6.13	5.26	14824.99	0.45	0.38	0.32	0.49	0.41	0.35	0.45	0.38	0.33
57	0.40	0.41	0.43	2.64	2.22	1.91	306092.30	3.26	2.74	2.35	3.35	2.82	2.42	3.49	2.94	2.52
58	0.45	0.48	0.50	4.16	3.50	3.00	92438.14	1.74	1.47	1.26	1.82	1.54	1.32	1.94	1.63	1.40
59	0.58	0.58	0.58	6.08	5.11	4.39	12208.81	0.43	0.36	0.31	0.43	0.36	0.31	0.43	0.36	0.31
60	0.58	0.62	0.62	6.47	5.44	4.67	11336.76	0.43	0.36	0.31	0.45	0.38	0.33	0.45	0.38	0.33
61	0.65	0.66	0.66	4.40	3.71	3.18	34882.32	1.00	0.84	0.72	1.02	0.86	0.73	1.01	0.85	0.73
62	0.56	0.57	0.60	5.88	4.95	4.25	17441.16	0.58	0.49	0.42	0.58	0.49	0.42	0.62	0.52	0.45
63	0.49	0.53	0.54	4.29	3.61	3.10	47091.14	0.99	0.83	0.72	1.07	0.90	0.77	1.08	0.91	0.78
64	0.52	0.52	0.53	4.01	3.38	2.90	47963.18	0.99	0.84	0.72	0.99	0.84	0.72	1.03	0.86	0.74
65	0.51	0.52	0.52	1.51	1.27	1.09	634858.11	4.88	4.11	3.53	5.00	4.21	3.61	4.99	4.20	3.61
66	0.57	0.58	0.57	4.39	3.69	3.17	85461.69	2.12	1.79	1.53	2.18	1.84	1.58	2.12	1.79	1.53
67	0.49	0.50	0.51	3.03	2.55	2.19	156970.42	2.31	1.95	1.67	2.39	2.01	1.72	2.43	2.04	1.75
68	0.41	0.41	0.41	7.27	6.12	5.25	12208.80	0.36	0.31	0.26	0.37	0.31	0.26	0.36	0.31	0.26
69	0.47	0.48	0.47	5.09	4.29	3.68	18313.22	0.43	0.37	0.31	0.45	0.38	0.33	0.43	0.37	0.31
70	0.43	0.44	0.45	5.11	4.31	3.69	16569.11	0.36	0.31	0.26	0.37	0.31	0.27	0.38	0.32	0.28
71	0.51	0.51	0.55	1.87	1.58	1.35	312196.74	2.97	2.50	2.15	3.00	2.53	2.17	3.22	2.71	2.32

Table B.7: Peak runoff values from watersheds of Japorigog hill

Basin ID	Composite C for the year			Rainfall intensity (x10^{-5} m/s) for RP			Area (Sq. m)	Peak Q (m3/s) in 2011 for RP			Peak Q (m3/s) in 2015 for RP			Peak Q (m3/s) in 2025 for RP		
	2011	2015	2025	25 yr	10 yr	5 yr		25 yr	10 yr	5 yr	25 yr	10 yr	5 yr	25 yr	10 yr	5 yr
1	0.34	0.35	0.35	1.74	1.46	1.26	9,01,707.89	5.28	4.45	3.81	5.43	4.57	3.92	5.44	4.58	3.93
2	0.51	0.51	0.53	3.07	2.59	2.22	50,579.34	0.79	0.66	0.57	0.79	0.66	0.57	0.83	0.70	0.60
3	0.56	0.56	0.56	4.68	3.94	3.38	13,080.87	0.35	0.29	0.25	0.35	0.29	0.25	0.35	0.29	0.25
4	0.54	0.55	0.56	2.85	2.40	2.06	2,26,735.06	3.49	2.94	2.52	3.56	3.00	2.57	3.65	3.07	2.63
5	0.47	0.48	0.53	3.34	2.81	2.41	1,62,202.77	2.55	2.15	1.84	2.59	2.18	1.87	2.86	2.41	2.07
6	0.33	0.34	0.37	1.57	1.33	1.14	5,81,662.59	3.05	2.57	2.20	3.16	2.66	2.28	3.40	2.86	2.46
7	0.43	0.44	0.45	5.82	4.90	4.20	23,545.57	0.59	0.49	0.42	0.60	0.51	0.44	0.62	0.52	0.44
8	0.36	0.38	0.40	3.19	2.68	2.30	1,23,832.23	1.43	1.20	1.03	1.48	1.25	1.07	1.56	1.32	1.13
9	0.40	0.41	0.48	1.77	1.49	1.28	5,89,511.15	4.20	3.53	3.03	4.32	3.63	3.12	5.02	4.23	3.63
10	0.44	0.44	0.49	2.57	2.16	1.86	2,59,873.25	2.94	2.47	2.12	2.96	2.49	2.14	3.29	2.77	2.37
11	0.60	0.60	0.63	5.54	4.66	4.00	17,441.17	0.58	0.49	0.42	0.58	0.49	0.42	0.61	0.51	0.44
12	0.69	0.70	0.69	3.88	3.27	2.80	58,427.88	1.57	1.32	1.13	1.58	1.33	1.14	1.57	1.32	1.13
13	0.46	0.46	0.56	2.39	2.02	1.73	1,70,923.36	1.87	1.57	1.35	1.87	1.57	1.35	2.28	1.92	1.65
14	0.54	0.54	0.59	7.02	5.91	5.07	16,569.11	0.63	0.53	0.46	0.63	0.53	0.46	0.68	0.58	0.49
15	0.39	0.39	0.40	5.51	4.64	3.98	28,777.90	0.61	0.52	0.44	0.62	0.52	0.45	0.64	0.54	0.46
16	0.48	0.48	0.62	6.48	5.46	4.68	18,313.22	0.57	0.48	0.41	0.57	0.48	0.41	0.73	0.62	0.53
17	0.43	0.46	0.51	4.02	3.38	2.90	55,811.69	0.97	0.82	0.70	1.03	0.87	0.74	1.15	0.97	0.83
18	0.36	0.37	0.40	3.03	2.55	2.19	2,15,398.30	2.33	1.96	1.68	2.42	2.04	1.75	2.63	2.22	1.90
19	0.67	0.67	0.67	4.63	3.90	3.35	36,626.42	1.13	0.95	0.82	1.14	0.96	0.82	1.13	0.95	0.82
20	0.50	0.50	0.54	7.02	5.91	5.07	12,208.81	0.43	0.36	0.31	0.43	0.36	0.31	0.46	0.39	0.33
21	0.47	0.47	0.52	6.42	5.40	4.64	18,313.22	0.55	0.46	0.39	0.55	0.46	0.39	0.61	0.51	0.44
22	0.65	0.65	0.65	3.61	3.04	2.61	60,172.01	1.40	1.18	1.01	1.40	1.18	1.01	1.40	1.18	1.01
23	0.59	0.59	0.59	5.77	4.86	4.17	15,697.04	0.54	0.45	0.39	0.54	0.45	0.39	0.54	0.45	0.39

24	0.36	0.36	0.39	4.69	3.95	3.39	1,04,646.96	1.76	1.48	1.27	1.77	1.49	1.28	1.94	1.63	1.40
25	0.58	0.58	0.58	6.93	5.84	5.01	14,824.98	0.60	0.50	0.43	0.60	0.50	0.43	0.60	0.50	0.43
26	0.57	0.57	0.57	2.30	1.94	1.66	3,34,870.22	4.38	3.69	3.16	4.40	3.70	3.18	4.39	3.69	3.17
27	0.45	0.47	0.48	7.85	6.61	5.67	12,208.81	0.43	0.36	0.31	0.45	0.38	0.33	0.46	0.39	0.33
28	0.40	0.40	0.41	5.26	4.43	3.80	40,114.67	0.85	0.71	0.61	0.85	0.71	0.61	0.86	0.72	0.62
29	0.50	0.50	0.54	6.08	5.12	4.39	20,929.39	0.63	0.53	0.46	0.64	0.54	0.46	0.69	0.58	0.50
30	0.44	0.45	0.48	1.45	1.22	1.05	13,94,420.59	8.87	7.47	6.41	9.08	7.64	6.56	9.64	8.12	6.96
31	0.38	0.39	0.46	4.47	3.76	3.23	81,101.39	1.39	1.17	1.00	1.41	1.19	1.02	1.66	1.40	1.20
32	0.40	0.40	0.40	3.40	2.86	2.46	85,461.68	1.16	0.98	0.84	1.17	0.98	0.84	1.17	0.98	0.84
33	0.34	0.35	0.37	2.43	2.04	1.75	4,97,945.04	4.13	3.48	2.99	4.26	3.59	3.08	4.41	3.72	3.19
34	0.41	0.41	0.41	4.11	3.46	2.97	31,394.08	0.53	0.45	0.38	0.53	0.45	0.38	0.53	0.45	0.38
35	0.29	0.29	0.29	2.68	2.26	1.93	1,66,563.06	1.29	1.09	0.93	1.30	1.09	0.94	1.29	1.09	0.93
36	0.37	0.38	0.37	4.93	4.15	3.56	16,569.10	0.30	0.25	0.22	0.31	0.26	0.23	0.30	0.25	0.22
37	0.44	0.44	0.50	3.72	3.14	2.69	1,51,738.11	2.49	2.10	1.80	2.50	2.10	1.80	2.80	2.36	2.03
38	0.41	0.42	0.45	4.19	3.53	3.03	18,313.22	0.31	0.26	0.23	0.32	0.27	0.23	0.34	0.29	0.25
39	0.42	0.42	0.42	3.48	2.93	2.51	72,380.80	1.05	0.88	0.76	1.07	0.90	0.77	1.05	0.88	0.76
40	0.40	0.40	0.43	4.27	3.60	3.08	27,033.80	0.46	0.39	0.33	0.46	0.39	0.33	0.50	0.42	0.36
41	0.42	0.42	0.42	2.90	2.44	2.10	1,60,458.66	1.94	1.63	1.40	1.94	1.63	1.40	1.94	1.63	1.40
42	0.39	0.40	0.40	4.11	3.46	2.97	69,764.63	1.12	0.94	0.81	1.14	0.96	0.82	1.16	0.98	0.84
43	0.51	0.51	0.51	4.49	3.78	3.24	34,010.26	0.78	0.66	0.56	0.78	0.66	0.57	0.78	0.66	0.56
44	0.37	0.38	0.39	3.34	2.82	2.42	1,19,471.95	1.48	1.25	1.07	1.53	1.29	1.11	1.58	1.33	1.14
45	0.25	0.25	0.28	2.41	2.03	1.74	4,26,436.30	2.62	2.21	1.89	2.62	2.21	1.89	2.91	2.45	2.10
46	0.41	0.42	0.49	5.38	4.53	3.89	20,057.34	0.44	0.37	0.32	0.45	0.38	0.32	0.53	0.45	0.38
47	0.41	0.41	0.49	5.59	4.71	4.04	12,208.82	0.28	0.23	0.20	0.28	0.23	0.20	0.33	0.28	0.24
48	0.35	0.35	0.51	5.35	4.50	3.86	14,824.98	0.28	0.24	0.20	0.28	0.24	0.20	0.40	0.34	0.29
49	0.43	0.43	0.48	7.10	5.98	5.13	16,569.10	0.51	0.43	0.37	0.51	0.43	0.37	0.57	0.48	0.41
50	0.39	0.41	0.42	2.12	1.79	1.53	6,75,844.88	5.66	4.76	4.09	5.90	4.96	4.26	6.06	5.10	4.38
51	0.36	0.36	0.39	1.52	1.28	1.10	12,84,541.30	6.96	5.86	5.02	6.99	5.88	5.05	7.67	6.46	5.54
52	0.34	0.35	0.34	6.27	5.28	4.53	19,185.25	0.41	0.35	0.30	0.42	0.35	0.30	0.41	0.35	0.30

53	0.54	0.54	0.56	4.29	3.61	3.10	90,694.03	2.09	1.76	1.51	2.11	1.78	1.53	2.17	1.83	1.57
54	0.50	0.51	0.53	6.60	5.56	4.77	13,952.93	0.46	0.39	0.33	0.47	0.40	0.34	0.49	0.41	0.35
55	0.43	0.43	0.48	4.47	3.77	3.23	61,916.12	1.20	1.01	0.86	1.20	1.01	0.87	1.33	1.12	0.96
56	0.48	0.49	0.50	2.76	2.32	1.99	1,58,714.54	2.09	1.76	1.51	2.15	1.81	1.55	2.21	1.86	1.59
57	0.52	0.53	0.56	3.91	3.30	2.83	76,741.10	1.57	1.32	1.13	1.60	1.35	1.16	1.68	1.41	1.21
58	0.46	0.48	0.48	2.71	2.28	1.95	2,68,593.85	3.32	2.79	2.40	3.45	2.91	2.49	3.52	2.96	2.54
59	0.53	0.53	0.56	4.44	3.74	3.20	17,441.15	0.41	0.34	0.29	0.41	0.35	0.30	0.43	0.37	0.31
60	0.42	0.43	0.42	4.48	3.77	3.23	25,289.67	0.48	0.40	0.35	0.48	0.41	0.35	0.48	0.40	0.35
61	0.51	0.52	0.52	2.14	1.80	1.54	2,36,327.68	2.55	2.15	1.84	2.60	2.19	1.88	2.63	2.22	1.90
62	0.54	0.54	0.54	4.17	3.51	3.01	51,451.44	1.15	0.97	0.83	1.17	0.98	0.84	1.16	0.98	0.84
63	0.56	0.56	0.56	5.20	4.38	3.76	11,336.76	0.33	0.28	0.24	0.33	0.28	0.24	0.33	0.28	0.24
64	0.35	0.36	0.37	1.38	1.16	1.00	17,87,718.64	8.65	7.29	6.25	8.91	7.50	6.44	9.17	7.72	6.62
65	0.51	0.52	0.53	3.26	2.75	2.36	1,57,842.48	2.61	2.20	1.89	2.67	2.25	1.93	2.73	2.30	1.97

Table B.8: Peak runoff values from watersheds of Burhagosain hill

Bas-in ID	Composite C for the year			Rainfall intensity (x10^{-5} m/s) for RP			Area (Sq.m)	Peak Q (m3/s) in 2011 for RP			Peak Q (m3/s) in 2015 for RP			Peak Q (m3/s) in 2025 for RP		
	2011	2015	2025	25 yr	10 yr	5 yr		25 yr	10 yr	5 yr	25 yr	10 yr	5 yr	25 yr	10 yr	5 yr
1	0.39	0.43	0.47	7.31	6.15	5.28	6976.47	0.20	0.17	0.14	0.22	0.19	0.16	0.24	0.20	0.17
2	0.30	0.32	0.30	14.17	11.93	10.23	2616.17	0.11	0.09	0.08	0.12	0.10	0.08	0.11	0.09	0.08
3	0.26	0.27	0.29	3.30	2.78	2.39	142145.44	1.24	1.04	0.89	1.27	1.07	0.92	1.36	1.14	0.98
4	0.27	0.28	0.29	3.56	3.00	2.57	102902.84	0.99	0.83	0.71	1.01	0.85	0.73	1.07	0.90	0.78
5	0.28	0.29	0.32	3.46	2.91	2.50	117727.82	1.15	0.97	0.83	1.18	0.99	0.85	1.29	1.09	0.93
6	0.34	0.36	0.35	5.12	4.31	3.70	23545.56	0.41	0.34	0.29	0.43	0.36	0.31	0.42	0.36	0.31
7	0.28	0.29	0.28	4.97	4.18	3.59	22673.52	0.31	0.26	0.22	0.33	0.28	0.24	0.32	0.27	0.23
8	0.41	0.43	0.43	5.09	4.29	3.68	48835.23	1.01	0.85	0.73	1.07	0.90	0.77	1.06	0.89	0.77
9	0.34	0.34	0.34	8.62	7.26	6.23	1744.12	0.05	0.04	0.04	0.05	0.04	0.04	0.05	0.04	0.04
10	0.34	0.34	0.34	17.06	14.37	12.32	2616.18	0.15	0.13	0.11	0.15	0.13	0.11	0.15	0.13	0.11
11	0.28	0.28	0.28	16.61	13.99	12.00	1744.11	0.08	0.07	0.06	0.08	0.07	0.06	0.08	0.07	0.06
12	0.30	0.30	0.30	43.43	36.56	31.37	1744.11	0.23	0.19	0.16	0.23	0.19	0.16	0.23	0.19	0.16
13	0.30	0.30	0.30	16.55	13.93	11.95	2616.18	0.13	0.11	0.09	0.13	0.11	0.09	0.13	0.11	0.09
14	0.30	0.31	0.30	6.30	5.30	4.55	16569.09	0.31	0.26	0.22	0.32	0.27	0.23	0.31	0.26	0.22
15	0.39	0.42	0.49	3.69	3.11	2.67	83717.56	1.21	1.02	0.88	1.29	1.08	0.93	1.53	1.28	1.10
16	0.42	0.44	0.51	4.46	3.76	3.22	40114.65	0.75	0.63	0.54	0.79	0.66	0.57	0.92	0.77	0.66
17	0.34	0.36	0.41	4.60	3.87	3.32	53195.53	0.82	0.69	0.59	0.87	0.73	0.63	1.01	0.85	0.73
18	0.35	0.45	0.72	9.29	7.82	6.71	8720.58	0.29	0.24	0.21	0.37	0.31	0.26	0.59	0.49	0.42
19	0.36	0.39	0.44	5.03	4.24	3.63	20057.34	0.37	0.31	0.26	0.39	0.33	0.28	0.44	0.37	0.32
20	0.27	0.27	0.27	2.85	2.40	2.06	190980.67	1.47	1.24	1.06	1.47	1.24	1.06	1.50	1.26	1.08
21	0.46	0.46	0.46	12.23	10.29	8.83	3488.23	0.19	0.16	0.14	0.20	0.16	0.14	0.19	0.16	0.14
22	0.46	0.46	0.47	3.28	2.77	2.37	118599.88	1.77	1.49	1.28	1.81	1.52	1.30	1.85	1.56	1.34
23	0.35	0.35	0.39	4.10	3.45	2.96	9592.63	0.14	0.12	0.10	0.14	0.12	0.10	0.15	0.13	0.11

24	0.25	0.26	0.27	1.99	1.68	1.44	425564.26	2.16	1.82	1.56	2.19	1.85	1.58	2.26	1.91	1.64
25	0.34	0.35	0.34	2.78	2.34	2.00	347951.09	3.29	2.77	2.37	3.33	2.81	2.41	3.29	2.77	2.37
26	0.30	0.30	0.30	2.08	1.75	1.51	660147.88	4.07	3.43	2.94	4.09	3.44	2.95	4.11	3.46	2.97
27	0.27	0.27	0.30	1.33	1.12	0.96	1279308.91	4.60	3.87	3.32	4.63	3.90	3.34	5.14	4.33	3.71
28	0.18	0.18	0.18	7.95	6.69	5.74	8720.58	0.12	0.10	0.09	0.13	0.11	0.09	0.12	0.10	0.09
29	0.29	0.29	0.34	7.50	6.31	5.41	5232.34	0.11	0.09	0.08	0.11	0.09	0.08	0.13	0.11	0.10
30	0.27	0.27	0.41	4.22	3.55	3.05	48835.25	0.55	0.46	0.40	0.56	0.47	0.40	0.85	0.72	0.62
31	0.41	0.43	0.46	3.57	3.00	2.58	38370.54	0.56	0.47	0.41	0.59	0.49	0.42	0.63	0.53	0.45
32	0.31	0.31	0.31	4.14	3.49	2.99	33138.22	0.43	0.36	0.31	0.43	0.36	0.31	0.43	0.36	0.31
33	0.40	0.40	0.46	3.35	2.82	2.42	85461.68	1.14	0.96	0.82	1.15	0.97	0.83	1.32	1.11	0.95
34	0.39	0.39	0.39	13.11	11.04	9.47	1744.12	0.09	0.07	0.06	0.09	0.08	0.06	0.09	0.07	0.06
35	0.36	0.36	0.36	6.04	5.08	4.36	13952.93	0.31	0.26	0.22	0.31	0.26	0.22	0.31	0.26	0.22

Table B.9: Peak runoff values from watersheds of Khanapara and Koinadhara hill

Basin ID	Composite C (Rational Method) & CN (NRCS-TR55 method) for the year			Rainfall intensity ($\times 10^{-5}$ m/s) for RP			Area (sq.m)	Peak Q (m3/s) in 2011 for RP			Peak Q (m3/s) in 2015 for RP			Peak Q (m3/s) in 2025 for RP			Method
	2011	2015	2025	25 yr	10 yr	5 yr		25 yr	10 yr	5 yr	25 yr	10 yr	5 yr	25 yr	10 yr	5 yr	
1	0.33	0.34	0.44	1.25	1.06	0.91	1918527.39	8.03	6.76	5.80	8.13	6.84	5.87	10.60	8.92	7.65	Rational
3	0.33	0.33	0.40	1.37	1.15	0.99	1846146.59	8.21	6.91	5.93	8.41	7.08	6.07	9.99	8.41	7.21	
4	0.37	0.37	0.39	1.59	1.34	1.15	445621.573	2.66	2.24	1.92	2.66	2.24	1.92	2.77	2.33	2.00	
2	60.01	60.85	62.07				4441390.87	22.19	15.27	10.19	23.17	15.96	10.78	24.52	17.04	11.62	NRCS-TR55
5	64.46	65.24	66.50				6377359.42	29.31	20.52	14.36	30.13	21.19	15.10	31.86	22.73	16.33	
6	67.21	67.45	67.77				6982567.57	39.70	28.35	20.52	40.01	28.61	20.73	40.44	29.29	21.28	
7	61.78	62.41	62.74		-		3385328.73	24.56	16.76	11.52	25.16	17.44	12.04	25.75	17.69	12.38	

Table B.10: Peak runoff values from watersheds of Garbhanga hill

Basin ID	CN (NRCS-TR55 method) for the year			Area (sq.m)	Peak Q (m3/s) in 2011 for RP			Peak Q (m3/s) in 2015 for RP			Peak Q (m3/s) in 2025 for RP		
	2011	2015	2025		25 yr	10 yr	5 yr	25 yr	10 yr	5 yr	25 yr	10 yr	5 yr
1	61.10	61.50	62.10	72199417.51	191.81	129.16	87.79	194.90	131.61	89.73	199.33	136.48	93.49

Table B.11: Peak runoff values from watersheds of Kamakhya hill

Basin ID	Composite C for the year			Rainfall intensity ($x10^{-5}$ m/s) for RP			Area (Sq. m)	Peak Q (m3/s) in 2011 for RP			Peak Q (m3/s) in 2015 for RP			Peak Q (m3/s) in 2025 for RP		
	2011	2015	2025	25 yr	10 yr	5 yr		25 yr	10 yr	5 yr	25 yr	10 yr	5 yr	25 yr	10 yr	5 yr
1	0.04	0.04	0.04	2.20	1.85	1.59	6104.42	0.01	0.005	0.004	0.01	0.005	0.004	0.01	0.005	0.004
2	0.19	0.19	0.22	2.00	1.68	1.44	338358.46	1.25	1.06	0.91	1.25	1.06	0.91	1.51	1.27	1.09
3	0.06	0.06	0.09	5.24	4.41	3.78	6104.42	0.02	0.01	0.01	0.02	0.01	0.01	0.03	0.03	0.02
4	0.07	0.07	0.10	5.15	4.34	3.72	6104.40	0.02	0.02	0.02	0.02	0.02	0.02	0.03	0.03	0.02
5	0.10	0.10	0.17	4.94	4.16	3.56	6104.40	0.03	0.03	0.02	0.03	0.03	0.02	0.05	0.04	0.04
6	0.13	0.13	0.29	5.75	4.84	4.16	6104.40	0.05	0.04	0.03	0.05	0.04	0.03	0.10	0.09	0.07
7	0.10	0.10	0.13	4.69	3.95	3.39	6976.46	0.03	0.03	0.02	0.03	0.03	0.02	0.04	0.04	0.03
8	0.18	0.18	0.36	3.70	3.12	2.67	18313.22	0.12	0.10	0.09	0.12	0.10	0.09	0.24	0.20	0.18
9	0.16	0.16	0.36	5.16	4.35	3.73	8720.58	0.07	0.06	0.05	0.07	0.06	0.05	0.16	0.14	0.12
10	0.22	0.22	0.26	2.72	2.29	1.96	47963.21	0.29	0.24	0.21	0.29	0.24	0.21	0.33	0.28	0.24
11	0.20	0.20	0.32	5.72	4.82	4.13	12208.80	0.14	0.12	0.10	0.14	0.12	0.10	0.22	0.19	0.16
12	0.20	0.20	0.39	4.59	3.87	3.32	13952.93	0.13	0.11	0.09	0.13	0.11	0.09	0.25	0.21	0.18

13	0.23	0.23	0.31	2.12	1.79	1.53	132552.79	0.63	0.53	0.46	0.63	0.53	0.46	0.86	0.72	0.62
14	0.02	0.02	0.02	2.26	1.90	1.63	6104.42	0.003	0.003	0.002	0.003	0.003	0.002	0.003	0.003	0.002
15	0.07	0.07	0.07	2.18	1.84	1.58	6104.40	0.01	0.01	0.01	0.01	0.01	0.01	0.01	0.01	0.01
16	0.07	0.07	0.08	4.75	4.00	3.43	6104.40	0.02	0.02	0.01	0.02	0.02	0.01	0.02	0.02	0.02
17	0.06	0.06	0.10	4.81	4.05	3.47	6104.40	0.02	0.02	0.01	0.02	0.02	0.01	0.03	0.02	0.02
18	0.05	0.05	0.08	4.89	4.11	3.53	6104.40	0.02	0.01	0.01	0.02	0.01	0.01	0.02	0.02	0.02
19	0.04	0.04	0.04	5.25	4.42	3.79	6104.42	0.01	0.01	0.01	0.01	0.01	0.01	0.01	0.01	0.01
20	0.10	0.10	0.18	5.42	4.56	3.91	6104.40	0.03	0.03	0.03	0.03	0.03	0.03	0.06	0.05	0.04
21	0.15	0.15	0.19	4.66	3.92	3.36	6104.40	0.04	0.03	0.03	0.04	0.03	0.03	0.06	0.05	0.04
22	0.24	0.24	0.24	5.82	4.90	4.20	6104.41	0.08	0.07	0.06	0.08	0.07	0.06	0.08	0.07	0.06
23	0.13	0.13	0.13	4.62	3.89	3.34	6104.42	0.04	0.03	0.03	0.04	0.03	0.03	0.04	0.03	0.03
24	0.32	0.32	0.32	4.40	3.71	3.18	6976.47	0.10	0.08	0.07	0.10	0.08	0.07	0.10	0.08	0.07
25	0.17	0.17	0.21	0.96	0.81	0.70	634858.11	1.05	0.88	0.76	1.07	0.90	0.77	1.30	1.09	0.94
26	0.37	0.37	0.49	6.72	5.66	4.86	6104.40	0.15	0.13	0.11	0.15	0.13	0.11	0.20	0.17	0.14
27	0.37	0.37	0.39	5.14	4.32	3.71	6104.41	0.12	0.10	0.08	0.12	0.10	0.08	0.12	0.10	0.09
28	0.24	0.24	0.27	2.36	1.99	1.71	51451.40	0.29	0.24	0.21	0.29	0.25	0.21	0.33	0.28	0.24
29	0.45	0.45	0.47	1.53	1.29	1.11	383705.48	2.61	2.20	1.89	2.66	2.24	1.92	2.74	2.31	1.98
30	0.19	0.19	0.22	2.59	2.18	1.87	20057.33	0.10	0.08	0.07	0.10	0.08	0.07	0.11	0.10	0.08
31	0.20	0.20	0.20	3.29	2.77	2.38	12208.82	0.08	0.07	0.06	0.08	0.07	0.06	0.08	0.07	0.06
32	0.20	0.23	0.20	2.96	2.49	2.14	14824.98	0.09	0.07	0.06	0.10	0.08	0.07	0.09	0.07	0.06
33	0.32	0.32	0.35	2.40	2.02	1.73	80229.33	0.61	0.51	0.44	0.62	0.52	0.45	0.68	0.57	0.49
34	0.17	0.17	0.19	2.38	2.00	1.72	23545.56	0.10	0.08	0.07	0.10	0.08	0.07	0.11	0.09	0.08
35	0.50	0.50	0.51	4.40	3.71	3.18	20057.32	0.44	0.37	0.32	0.44	0.37	0.32	0.45	0.38	0.32
36	0.47	0.47	0.49	5.50	4.63	3.97	7848.52	0.20	0.17	0.15	0.20	0.17	0.15	0.21	0.18	0.15
37	0.44	0.44	0.50	4.75	4.00	3.43	9592.63	0.20	0.17	0.14	0.20	0.17	0.15	0.23	0.19	0.17
38	0.41	0.41	0.45	4.38	3.69	3.16	15697.04	0.28	0.24	0.20	0.28	0.24	0.21	0.31	0.26	0.22
39	0.41	0.41	0.41	4.61	3.88	3.33	6976.46	0.13	0.11	0.10	0.13	0.11	0.10	0.13	0.11	0.10
40	0.41	0.41	0.42	3.53	2.97	2.55	38370.55	0.55	0.46	0.40	0.56	0.47	0.40	0.57	0.48	0.41
41	0.45	0.45	0.45	4.31	3.63	3.11	8720.60	0.17	0.14	0.12	0.17	0.14	0.12	0.17	0.14	0.12

42	0.58	0.58	0.62	8.00	6.74	5.78	6104.40	0.28	0.24	0.20	0.28	0.24	0.21	0.30	0.26	0.22
43	0.43	0.43	0.43	2.45	2.07	1.77	36626.45	0.38	0.32	0.28	0.39	0.33	0.28	0.38	0.32	0.28
44	0.35	0.35	0.35	2.43	2.04	1.75	125576.31	1.07	0.90	0.77	1.08	0.91	0.78	1.07	0.90	0.77
45	0.59	0.61	0.59	7.19	6.06	5.19	6104.40	0.26	0.22	0.19	0.27	0.22	0.19	0.26	0.22	0.19
46	0.55	0.55	0.55	5.18	4.36	3.74	6104.41	0.17	0.15	0.13	0.17	0.15	0.13	0.17	0.15	0.13
47	0.43	0.43	0.43	0.90	0.76	0.65	470000.00	3.41	2.87	2.46	3.47	2.92	2.51	3.48	2.93	2.51
48	0.42	0.43	0.43	1.75	1.47	1.26	247664.45	1.82	1.53	1.32	1.85	1.56	1.34	1.86	1.57	1.34
49	0.62	0.65	0.62	7.15	6.02	5.16	6104.41	0.27	0.23	0.20	0.28	0.24	0.20	0.27	0.23	0.20
50	0.31	0.32	0.31	6.05	5.09	4.37	6104.40	0.12	0.10	0.08	0.12	0.10	0.08	0.12	0.10	0.08
51	0.43	0.47	0.43	3.13	2.64	2.26	35754.38	0.49	0.41	0.35	0.53	0.45	0.38	0.49	0.41	0.35
52	0.38	0.42	0.38	3.35	2.82	2.42	28777.92	0.37	0.31	0.26	0.41	0.34	0.29	0.37	0.31	0.26
53	0.38	0.38	0.38	4.62	3.89	3.34	7848.51	0.14	0.12	0.10	0.14	0.12	0.10	0.14	0.12	0.10
54	0.43	0.43	0.43	5.10	4.29	3.68	6976.46	0.15	0.13	0.11	0.15	0.13	0.11	0.15	0.13	0.11
55	0.43	0.45	0.43	4.48	3.77	3.23	14824.98	0.29	0.24	0.21	0.30	0.25	0.22	0.29	0.24	0.21
56	0.47	0.47	0.47	2.97	2.50	2.15	45347.01	0.64	0.54	0.46	0.64	0.54	0.46	0.64	0.54	0.46
57	0.47	0.47	0.47	4.28	3.60	3.09	8720.58	0.17	0.15	0.13	0.17	0.15	0.13	0.17	0.15	0.13
58	0.53	0.53	0.53	1.02	0.86	0.74	224990.95	1.21	1.01	0.87	1.21	1.01	0.87	1.21	1.01	0.87
59	0.51	0.52	0.51	2.57	2.17	1.86	84589.62	1.12	0.94	0.81	1.12	0.94	0.81	1.12	0.94	0.81
60	0.54	0.54	0.54	3.25	2.73	2.34	37498.49	0.65	0.55	0.47	0.66	0.55	0.48	0.65	0.55	0.47
61	0.48	0.49	0.48	1.11	0.93	0.80	397658.41	2.10	1.77	1.52	2.15	1.81	1.56	2.10	1.77	1.52
62	0.56	0.57	0.57	1.27	1.07	0.92	299115.86	2.15	1.81	1.55	2.18	1.83	1.57	2.16	1.82	1.56
63	0.53	0.53	0.53	1.43	1.20	1.03	212782.13	1.60	1.35	1.16	1.61	1.35	1.16	1.61	1.35	1.16

Table B.12: Peak runoff values from watersheds of Kahilipara hill

Basin ID	Composite C for the year			Rainfall intensity ($\times 10^{-5}$ m/s) for RP			Area (sq. m)	Peak Q (m3/s) in 2011 for RP			Peak Q (m3/s) in 2015 for RP			Peak Q (m3/s) in 2025 for RP		
	2011	2015	2025	25 yr	10 yr	5 yr		25 yr	10 yr	5 yr	25 yr	10 yr	5 yr	25 yr	10 yr	5 yr
1	0.54	0.54	0.55	4.01	3.38	2.90	95926.38	2.07	1.75	1.50	2.09	1.76	1.51	2.12	1.79	1.53
2	0.46	0.46	0.47	2.77	2.33	2.00	232839.48	2.95	2.49	2.13	2.96	2.49	2.13	3.06	2.58	2.21
3	0.38	0.38	0.42	2.90	2.44	2.09	347079.03	3.80	3.20	2.74	3.86	3.25	2.79	4.20	3.53	3.03
4	0.40	0.41	0.44	2.68	2.26	1.94	348823.14	3.77	3.17	2.72	3.82	3.22	2.76	4.08	3.44	2.95
5	0.36	0.36	0.38	2.94	2.48	2.12	268593.84	2.87	2.41	2.07	2.87	2.42	2.07	3.01	2.54	2.18
6	0.45	0.45	0.51	3.78	3.18	2.73	61916.10	1.05	0.88	0.76	1.05	0.89	0.76	1.20	1.01	0.87
7	0.52	0.52	0.54	3.31	2.79	2.39	102902.81	1.76	1.48	1.27	1.78	1.50	1.28	1.84	1.55	1.33
8	0.49	0.49	0.57	4.08	3.43	2.94	79357.27	1.58	1.33	1.14	1.58	1.33	1.14	1.84	1.55	1.33
9	0.47	0.47	0.49	4.76	4.01	3.44	34010.25	0.76	0.64	0.55	0.76	0.64	0.55	0.79	0.67	0.57
10	0.44	0.44	0.51	3.97	3.34	2.87	170923.36	2.97	2.50	2.15	3.01	2.53	2.17	3.47	2.92	2.50
11	0.60	0.60	0.63	4.41	3.71	3.18	24417.62	0.64	0.54	0.47	0.64	0.54	0.47	0.68	0.57	0.49
12	0.32	0.34	0.34	2.77	2.34	2.00	420331.91	3.79	3.19	2.73	3.97	3.34	2.87	4.00	3.37	2.89
13	0.59	0.59	0.60	4.06	3.42	2.93	47963.20	1.14	0.96	0.83	1.14	0.96	0.83	1.17	0.98	0.84
14	0.58	0.61	0.63	4.58	3.86	3.31	64532.29	1.73	1.45	1.25	1.80	1.51	1.30	1.87	1.57	1.35
15	0.46	0.46	0.48	3.70	3.11	2.67	104646.95	1.79	1.51	1.29	1.79	1.51	1.29	1.84	1.55	1.33
16	0.43	0.45	0.47	3.14	2.65	2.27	96798.42	1.32	1.11	0.95	1.35	1.14	0.98	1.43	1.20	1.03
17	0.58	0.58	0.62	3.84	3.23	2.77	34010.25	0.75	0.63	0.54	0.76	0.64	0.55	0.81	0.68	0.58
18	0.40	0.41	0.41	2.81	2.36	2.03	167435.12	1.89	1.59	1.37	1.93	1.62	1.39	1.93	1.62	1.39
19	0.51	0.52	0.54	3.27	2.76	2.36	132552.81	2.23	1.88	1.61	2.25	1.89	1.62	2.34	1.97	1.69
20	0.55	0.55	0.58	3.45	2.90	2.49	105518.99	1.99	1.68	1.44	2.00	1.68	1.44	2.09	1.76	1.51
21	0.51	0.51	0.51	2.81	2.36	2.03	244176.23	3.51	2.96	2.54	3.52	2.96	2.54	3.52	2.96	2.54
22	0.47	0.48	0.50	4.45	3.74	3.21	115983.69	2.41	2.03	1.74	2.46	2.07	1.78	2.57	2.17	1.86
23	0.50	0.51	0.53	3.50	2.94	2.52	102030.76	1.80	1.51	1.30	1.82	1.53	1.31	1.90	1.60	1.37
24	0.37	0.38	0.39	3.19	2.69	2.31	129936.63	1.55	1.30	1.12	1.57	1.32	1.13	1.64	1.38	1.18

25	0.45	0.45	0.45	4.88	4.11	3.53	11336.76	0.25	0.21	0.18	0.25	0.21	0.18	0.25	0.21	0.18
26	0.56	0.57	0.59	3.86	3.25	2.79	61044.06	1.33	1.12	0.96	1.34	1.13	0.97	1.40	1.18	1.01
27	0.57	0.57	0.57	4.03	3.39	2.91	67148.46	1.54	1.29	1.11	1.54	1.29	1.11	1.54	1.30	1.11
28	0.44	0.45	0.46	4.18	3.52	3.02	74124.92	1.35	1.14	0.98	1.39	1.17	1.00	1.44	1.21	1.04
29	0.66	0.66	0.66	6.22	5.24	4.49	23545.56	0.97	0.82	0.70	0.97	0.82	0.70	0.97	0.82	0.70
30	0.58	0.59	0.61	4.39	3.69	3.17	68892.57	1.76	1.48	1.27	1.77	1.49	1.28	1.84	1.55	1.33
31	0.41	0.42	0.45	1.82	1.53	1.31	497073.00	3.73	3.14	2.69	3.77	3.17	2.72	4.05	3.41	2.92
32	0.60	0.61	0.60	5.01	4.21	3.61	16569.11	0.50	0.42	0.36	0.50	0.42	0.36	0.50	0.42	0.36
33	0.57	0.57	0.57	4.83	4.07	3.49	22673.51	0.62	0.52	0.45	0.62	0.53	0.45	0.62	0.52	0.45
34	0.62	0.63	0.63	5.28	4.44	3.81	24417.62	0.79	0.67	0.57	0.82	0.69	0.59	0.81	0.69	0.59
35	0.47	0.48	0.49	3.40	2.86	2.45	131680.73	2.11	1.78	1.53	2.14	1.80	1.54	2.17	1.83	1.57
36	0.41	0.42	0.45	1.53	1.28	1.10	1796439.27	11.20	9.43	8.09	11.48	9.67	8.29	12.23	10.30	8.83
37	0.57	0.58	0.58	2.85	2.40	2.05	186620.38	3.03	2.55	2.19	3.06	2.58	2.21	3.07	2.58	2.21
38	0.61	0.61	0.61	2.88	2.42	2.08	195340.96	3.44	2.90	2.48	3.45	2.91	2.49	3.45	2.90	2.49
39	0.54	0.55	0.54	2.30	1.94	1.66	344462.87	4.27	3.59	3.08	4.33	3.65	3.13	4.27	3.59	3.08
40	0.33	0.34	0.39	1.80	1.52	1.30	1108385.57	6.64	5.59	4.79	6.83	5.75	4.94	7.82	6.59	5.65
41	0.41	0.42	0.44	2.59	2.18	1.87	205805.66	2.21	1.86	1.59	2.25	1.89	1.62	2.35	1.98	1.70
42	0.51	0.51	0.53	4.50	3.79	3.25	42730.85	0.97	0.82	0.70	0.97	0.82	0.70	1.03	0.86	0.74
43	0.48	0.48	0.49	3.49	2.93	2.52	86333.74	1.45	1.22	1.05	1.46	1.23	1.05	1.47	1.24	1.06
44	0.49	0.49	0.51	3.79	3.19	2.74	43602.89	0.81	0.68	0.59	0.82	0.69	0.59	0.84	0.70	0.60
45	0.46	0.46	0.47	2.76	2.32	1.99	248536.48	3.17	2.67	2.29	3.18	2.68	2.30	3.24	2.73	2.34
46	0.58	0.58	0.58	4.73	3.98	3.41	42730.83	1.16	0.98	0.84	1.17	0.99	0.85	1.17	0.99	0.85
47	0.65	0.65	0.65	5.33	4.49	3.85	20057.32	0.69	0.58	0.50	0.70	0.59	0.51	0.69	0.58	0.50
48	0.58	0.58	0.58	5.27	4.44	3.81	20057.34	0.61	0.51	0.44	0.61	0.51	0.44	0.61	0.51	0.44

Table B.13: Peak runoff values from watersheds of Betkuchi hill

Basin ID	Composite C for the year			Rainfall intensity ($x10^{-5}$ m/s) for RP			Area (Sq. m)	Peak Q (m3/s) in 2011 for RP			Peak Q (m3/s) in 2015 for RP			Peak Q (m3/s) in 2025 for RP		
	2011	2015	2025	25 yr	10 yr	5 yr		25 yr	10 yr	5 yr	25 yr	10 yr	5 yr	25 yr	10 yr	5 yr
1	0.47	0.47	0.48	2.83	2.38	2.04	153482.20	2.04	1.72	1.48	2.05	1.73	1.48	2.10	1.77	1.52
2	0.46	0.48	0.50	3.66	3.09	2.65	53195.53	0.90	0.76	0.65	0.94	0.79	0.68	0.97	0.81	0.70
3	0.36	0.40	0.44	7.70	6.48	5.56	9592.63	0.26	0.22	0.19	0.30	0.25	0.21	0.32	0.27	0.23
4	0.45	0.46	0.52	8.54	7.19	6.17	6976.47	0.27	0.23	0.19	0.28	0.23	0.20	0.31	0.26	0.22
5	0.36	0.37	0.45	6.07	5.11	4.39	10464.69	0.23	0.19	0.17	0.24	0.20	0.17	0.29	0.24	0.21
6	0.37	0.39	0.45	9.49	7.99	6.86	4360.29	0.15	0.13	0.11	0.16	0.14	0.12	0.19	0.16	0.14
7	0.27	0.29	0.34	10.66	8.97	7.70	4360.30	0.13	0.11	0.09	0.13	0.11	0.10	0.16	0.13	0.11
8	0.33	0.41	0.39	10.12	8.52	7.31	6104.40	0.21	0.17	0.15	0.26	0.22	0.18	0.24	0.20	0.17
9	0.34	0.38	0.34	8.96	7.54	6.47	4360.29	0.13	0.11	0.10	0.15	0.12	0.11	0.13	0.11	0.10
10	0.30	0.32	0.44	9.31	7.84	6.73	8720.59	0.24	0.20	0.18	0.26	0.22	0.19	0.36	0.30	0.26
11	0.40	0.40	0.41	3.73	3.14	2.69	136913.09	2.02	1.70	1.46	2.04	1.72	1.47	2.09	1.76	1.51
12	0.50	0.53	0.50	19.95	16.80	14.41	1744.11	0.17	0.15	0.13	0.18	0.15	0.13	0.17	0.15	0.13
13	0.42	0.42	0.42	4.75	4.00	3.43	34882.32	0.69	0.58	0.50	0.70	0.59	0.50	0.70	0.59	0.51
14	0.42	0.43	0.43	4.91	4.13	3.55	49707.29	1.04	0.87	0.75	1.04	0.88	0.75	1.06	0.89	0.76
15	0.24	0.24	0.26	4.48	3.77	3.24	73252.86	0.79	0.66	0.57	0.79	0.67	0.57	0.86	0.72	0.62
16	0.15	0.16	0.16	5.36	4.51	3.87	34010.26	0.28	0.23	0.20	0.30	0.25	0.22	0.28	0.24	0.20

Table B.14 Peak runoff values from watersheds of Chunsali hill

Basin ID	Composite C for the year			Rainfall intensity ($x10^{-5}$ m/s) for RP			Area (sq. m)	Peak Q (m3/s) in 2011 for RP			Peak Q (m3/s) in 2015 for RP			Peak Q (m3/s) in 2025 for RP		
	2011	2015	2025	25 yr	10 yr	5 yr		25 yr	10 yr	5 yr	25 yr	10 yr	5 yr	25 yr	10 yr	5 yr
1	0.12	0.12	0.18	2.43	2.05	1.76	135168.96	0.4	0.337	0.289	0.40	0.34	0.29	0.58	0.49	0.42
2	0.2	0.21	0.26	2.04	1.72	1.47	923509.33	3.784	3.186	2.733	3.89	3.27	2.81	4.83	4.06	3.49
3	0.22	0.22	0.24	2.45	2.06	1.77	197957.14	1.054	0.887	0.761	1.06	0.89	0.76	1.14	0.96	0.82
4	0.19	0.2	0.26	1.81	1.52	1.31	782235.93	2.735	2.303	1.976	2.78	2.34	2.01	3.67	3.09	2.65
5	0.28	0.29	0.3	2.52	2.12	1.82	268593.83	1.869	1.573	1.35	1.96	1.65	1.42	2.02	1.70	1.46
6	0.23	0.23	0.29	1.53	1.29	1.11	2111252.2	7.499	6.313	5.416	7.52	6.33	5.43	9.32	7.84	6.73
7	0.25	0.27	0.44	4.88	4.1	3.52	89821.977	1.11	0.934	0.802	1.16	0.98	0.84	1.93	1.63	1.40
8	0.36	0.38	0.36	2.9	2.44	2.1	201445.36	2.125	1.789	1.535	2.25	1.89	1.63	2.13	1.80	1.54
9	0.24	0.25	0.27	1.75	1.47	1.26	1025540.1	4.313	3.631	3.115	4.42	3.72	3.20	4.83	4.06	3.49
10	0.31	0.34	0.31	3.3	2.78	2.38	200573.31	2.069	1.742	1.495	2.23	1.87	1.61	2.07	1.74	1.49
11	0.21	0.21	0.28	4.51	3.8	3.26	80229.334	0.745	0.627	0.538	0.76	0.64	0.55	1.00	0.84	0.72
12	0.33	0.34	0.34	3.24	2.73	2.34	140401.32	1.512	1.273	1.092	1.54	1.30	1.11	1.55	1.31	1.12
13	0.34	0.36	0.35	1.45	1.22	1.05	2033639	10.02	8.435	7.236	10.48	8.82	7.57	10.18	8.57	7.35
14	0.54	0.54	0.55	2.38	2	1.72	258129.16	3.315	2.791	2.394	3.32	2.79	2.40	3.38	2.84	2.44
15	0.38	0.38	0.4	3.67	3.09	2.65	243304.16	3.371	2.838	2.435	3.39	2.85	2.44	3.56	3.00	2.57
16	0.57	0.58	0.58	2.52	2.12	1.82	103774.89	1.493	1.257	1.078	1.51	1.27	1.09	1.52	1.28	1.10
17	0.49	0.51	0.57	2.91	2.45	2.11	125576.33	1.781	1.499	1.286	1.85	1.56	1.34	2.07	1.74	1.49
18	0.54	0.54	0.55	3.15	2.65	2.28	91566.066	1.571	1.322	1.134	1.57	1.32	1.13	1.58	1.33	1.14
19	0.32	0.33	0.32	3.2	2.69	2.31	166563.05	1.725	1.452	1.246	1.75	1.48	1.27	1.73	1.45	1.25
20	0.32	0.33	0.33	3.7	3.12	2.67	115983.7	1.374	1.157	0.992	1.41	1.19	1.02	1.43	1.21	1.04
21	0.34	0.35	0.34	3.15	2.65	2.27	158714.54	1.706	1.436	1.232	1.76	1.48	1.27	1.72	1.45	1.24

22	0.33	0.34	0.36	4.12	3.47	2.97	102902.83	1.414	1.19	1.021	1.44	1.21	1.04	1.54	1.30	1.11
23	0.34	0.35	0.4	2.29	1.93	1.66	447365.68	3.485	2.934	2.517	3.57	3.00	2.58	4.14	3.48	2.99
24	0.29	0.3	0.32	2.07	1.74	1.5	349695.21	2.119	1.784	1.531	2.14	1.80	1.54	2.30	1.93	1.66
25	0.38	0.38	0.41	3.56	3	2.57	94182.253	1.274	1.072	0.92	1.28	1.08	0.93	1.38	1.16	1.00
26	0.31	0.32	0.32	3.33	2.8	2.4	119471.93	1.244	1.047	0.899	1.29	1.09	0.93	1.27	1.07	0.92

Appendix C

Fig. C.1: Photographs of field survey

References

Acharjee, S., Goswami, U., & Saikia, R. (2013). Visual change detection study of some of the urban areas of Assam, India using Remote Sensing. *International Journal of Geomatics and Geosciences*, *3*(3), 500.

Acreman, M. C., & Sinclair, C. D. (1986). Classification of drainage basins according to their physical characteristics; an application for flood frequency analysis in Scotland. *Journal of Hydrology*, *84*(3), 365-380.

Ajibola, M. O., Adewale, B. A., & Ijasan, K. C. (2012). Effects of urbanisation on Lagos wetlands. *International Journal of Business and Social Science*, *3*(17), 310-318.

Alley, W. M., & Veenhuis, J. E. (1983). Effective impervious area in urban runoff modeling. *Journal of Hydraulic Engineering*, *109*(2), 313-319.

Amoako, C., & Cobbinah, P. B. (2011). Slum improvement in the Kumasi metropolis, Ghana: A review of approaches and results. *Journal of Sustainable Development in Africa*, *13*(8), 150-170.

Amoateng, P., B Cobbinah, P., & Owusu-Adade, K. (2013). Managing physical development in peri-urban areas of Kumasi, Ghana: A case of Abuakwa. *Journal of Urban and Environmental Engineering*, *7*(1).

Anbazhagan, S., Ramasamy, S. M., & Gupta, S. D. (2005). Remote sensing and GIS for artificial recharge study, runoff estimation and planning in Ayyar basin, Tamil Nadu, India. *Environmental Geology*, *48*(2), 158-170.

Arnold Jr, C. L., & Gibbons, C. J. (1996). Impervious surface coverage: the emergence of a key environmental indicator. *Journal of the American planning Association*, *62*(2), 243-258.

Arnold, J. G., Srinivasan, R., Muttiah, R. S., & Williams, J. R. (1998). Large area hydrologic modeling and assessment part I: model development. *JAWRA Journal of the American Water Resources Association*, *34*(1), 73-89.

Aswathy S.S., & Sindhu, P. (2013). Effect of urbanization on soil erosion. *International Journal of Innovative Research in Science, Engineering and Technology*, 2(1), 75-81.

ADNRW (Australian Department of Natural Resources and Water) (2007). *Queensland urban drainage manual, 2e*. Brisbane, Australia: ADNRW.

Babu, R., Tejwani, K. G., Agarwal, M. C., & Bhushan, L. S. (1979). *Rainfall Intensity Duration Returne Period Equation and Nomographs of India*. Central soil and water conservation & traing Institute.

Bahadur, K. K. (2009). Mapping soil erosion susceptibility using remote sensing and GIS: a case of the Upper Nam Wa Watershed, Nan Province, Thailand. *Environmental geology*, *57*(3), 695-705.

Barrett, M. E. (1999). *Complying with the Edwards Aquifer Rules: technical guidance on best management practices*. Texas Natural Resource Conservation Commission.

Barron, O. V., Donn, M. J., & Barr, A. D. (2013). Urbanisation and shallow groundwater: predicting changes in catchment hydrological responses. *Water resources management*, *27*(1), 95-115.

Beasley, D. B., Huggins, L. F., & Monke, A. (1980). ANSWERS: A model for watershed planning. *Transactions of the ASAE*, *23*(4), 938-0944.

Beighley, R. E., Kargar, M., & He, Y. (2009). Effects of impervious area estimation methods on simulated peak discharges. *Journal of Hydrologic Engineering*, *14*(4), 388-398.

Bell, F. C. (1969). Generalized rainfall-duration-frequency relationships. *Journal of the Hydraulics Division*.

Bernard, M. M. (1932). Formulas for rainfall intensities of long duration. *Transactions of the American Society of Civil Engineers*, *96*(1), 592-606.

Beven, K. J. (1990). A discussion of distributed hydrological modelling. In *Distributed hydrological modelling* (pp. 255-278). Springer Netherlands.

Beven, K. J. (2000). Uniqueness of place and process representations in hydrological modelling. *Hydrology and Earth System Sciences Discussions*, *4*(2), 203-213.

Bhatt, J. V., Gandhi, H. M., & Gohil, K. V. (2014). Generation of intensity duration frequency curve using daily rainfall data for different return period. *Journal of International Academic Research for Multidisciplinary*, 2(2), 717-722.

Bhattarai, R., & Dutta, D. (2007). Estimation of soil erosion and sediment yield using GIS at catchment scale. *Water Resources Management*, *21*(10), 1635-1647.

Bierwagen, B. G., Theobald, D. M., Pyke, C. R., Choate, A., Groth, P., Thomas, J. V., & Morefield, P. (2010). National housing and impervious surface scenarios for integrated climate impact assessments. *Proceedings of the National Academy of Sciences*, *107*(49), 20887-20892.

Bird, S., Harrison, J., Exum, L., Alberty, S., & Perkins, C. (2002). *Screening to identify and prevent urban storm water problems: Estimating impervious area accurately and inexpensively*. US Environmental Protection Agency, Office of Research and Development.

Biswas, S. S., & Pani, P. (2015). Estimation of soil erosion using RUSLE and GIS techniques: a case study of Barakar River basin, Jharkhand, India. *Modeling Earth Systems and Environment*, *1*(4), 42.

Bondelid, T. R., McCuen, R. H., & Jackson, T. J. (1982). Sensitivity of SCS models to curve number variation. *JAWRA Journal of the American Water Resources Association*, *18*(1), 111-116.

Borthakur, M., & Nath, B. K. (2012). A study of changing urban landscape and heat island phenomenon in Guwahati metropolitan area. *International Journal of Scientific and Research Publications*, *2*(11), 1-6.

Boyd, M. J., Bufill, M. C., & Knee, R. M. (1993). Pervious and impervious runoff in urban catchments. *Hydrological Sciences Journal*, *38*(6), 463-478.

Brady, N. C. and Weil, R. C. (2012). The nature and properties of soils. *Pearson education*, New Delhi.

Brockerhoff, M. (2000). *An urbanizing world*. Population Reference Bureau.

Brun, S. E., & Band, L. E. (2000). Simulating runoff behavior in an urbanizing watershed. *Computers, Environment and Urban Systems*, *24*(1), 5-22.

Burns, D., Vitvar, T., McDonnell, J., Hassett, J., Duncan, J., & Kendall, C. (2005). Effects of suburban development on runoff generation in the Croton River basin, New York, USA. *Journal of Hydrology*, *311*(1), 266-281.

Caldwell, P. V., Sun, G., McNulty, S. G., Cohen, E. C., & Myers, J. M. (2012). Impacts of impervious cover, water withdrawals, and climate change on river flows in the conterminous US. *Hydrology and Earth System Sciences*, *16*(8), 2839.

Chabaeva, A. A., Civco, D. L., & Prisloe, S. (2004). Development of a population density and land use based regression model to calculate the amount of imperviousness. In *Proceedings of ASPRS annual conference*. Denver, Colorado.

Chabaeva, A., Civco, D. L., & Hurd, J. D. (2009). Assessment of impervious surface estimation techniques. *Journal of Hydrologic Engineering*, *14*(4), 377-387.

Chen, C. L. (1983). Rainfall intensity-duration-frequency formulas. *Journal of Hydraulic Engineering*, *109*(12), 1603-1621.

Chen, J., Hill, A. A., & Urbano, L. D. (2009). A GIS-based model for urban flood inundation. *Journal of Hydrology*, *373*(1), 184-192.

Cheng, Q., Ko, C., Yuan, Y., Ge, Y., & Zhang, S. (2006). GIS modeling for predicting river runoff volume in ungauged drainages in the Greater Toronto Area, Canada. *Computers & geosciences*, *32*(8), 1108-1119.

Chowdhury, R. K., Alam, J. B., Das, P., & Alam, M. M. (2007). Short duration rainfall estimation of Sylhet: IMD and USWB method.

Christchurch City Council (2011). *Waterways, Wetlands and Drainage Guide: Rainfall and runoff, Chapter 21, Part B.* Christchurch, New Zealand, Christchurch City Council, 21-1–21-15.
(https://www.ccc.govt.nz/assets/Documents/Environment/Water/waterwaysguide/21.RainfallAndRunoff.pdf)

Clarke, K. C., & Gaydos, L. J. (1998). Loose-coupling a cellular automaton model and GIS: long-term urban growth prediction for San Francisco and Washington/Baltimore. *International journal of geographical information science*, *12*(7), 699-714.

Cobbinah, P. B., & Darkwah, R. M. (2016). African urbanism: the geography of urban greenery. In *Urban Forum*(Vol. 27, No. 2, pp. 149-165). Springer Netherlands.

Cobbinah, P. B., Erdiaw-Kwasie, M. O., & Amoateng, P. (2015). Africa's urbanisation: Implications for sustainable development. *Cities*, *47*, 62-72.

Dabral, P. P., Baithuri, N., & Pandey, A. (2008). Soil erosion assessment in a hilly catchment of North Eastern India using USLE, GIS and remote sensing. *Water Resources Management*, *22*(12), 1783-1798.

Dams, J., Dujardin, J., Reggers, R., Bashir, I., Canters, F., & Batelaan, O. (2013). Mapping impervious surface change from remote sensing for hydrological modeling. *Journal of Hydrology*, *485*, 84-95.

Darkwah, R. M., & Cobbinah, P. B. (2014). Stewardship of urban greenery in an era of global urbanisation. *International Journal of Environmental, Ecological, Geological and Geophysical Engineering*, *8*(10), 671-674.

Das, N. (1992). *An investigation of soil characteristics of the Greater Guwahati landslide areas.* M.E. Dissertation, Department of Civil Engineering, Assam Engineering College, Guwahati.

Das, T. (2017). *Catchment degradation due to overland water erosion.* M. Tech. dissertation, IIT Guwahati, India.

De Graaff, J. (1996). *The price of soil erosion; an economic evaluation of soil conservation and watershed development*(No. 3). sn].

De Roo, A. P. J., Wesseling, C. G., & Ritsema, C. J. (1996). LISEM: A single-event physically based hydrological and soil erosion model for drainage basins. I: theory, input and output. *Hydrological processes*, *10*(8), 1107-1117.

De Winnaar, G., Jewitt, G. P. W., & Horan, M. (2007). A GIS-based approach for identifying potential runoff harvesting sites in the Thukela River basin, South Africa. *Physics and Chemistry of the Earth, Parts A/B/C*, *32*(15), 1058-1067.

Deng, J. S., Wang, K., Hong, Y., & Qi, J. G. (2009). Spatio-temporal dynamics and evolution of land use change and landscape pattern in response to rapid urbanization. *Landscape and urban planning*, *92*(3-4), 187-198.

Desai, R., Mahadevia, D., & Mishra, A. (2016). City profile: Guwahati (CUE Working Paper 24). Centre for Urban Equity (CUE), Ahmedabad. https://cept.ac.in/UserFiles/File/CUE/Working%20Papers/Revised%20New/24%20City%20Profile%20Guwahat.pdf

Desmet, P. J. J., & Govers, G. (1996). A GIS procedure for automatically calculating the USLE LS factor on topographically complex landscape units. *Journal of soil and water conservation*, *51*(5), 427-433.

Dhorde, A. A., Dhorde, A., & Joshi, G. (2012). Population calibrated land cover impervious surface coefficients for Upper Bhima basin. *Intl. j. Geomatics and geosciences*, *2*(4), 1027-1047.

Duley, F. L., & Hays, O. E. (1932). *The effect of the degree of slope on run-off an soil erosion*. US Department of Agriculture.

Dumitru, T. R. O. A. N. C. A. (2012). The impact of tourism development on urban environment. *Studies in Business & Economics*, *7*(3), 160-164.

EPA (1983). *Results of the Nationwide Urban Runoff Program*. Environmental Protection Agency NTIS Access No. PB84-18552, Washington D.C

EPA (2004). *The Use of Best Management Practices (BMPs) in Urban Watersheds*. Report of United States Environmental Protection Agency, Office of Research and Development Washington DC 20460, EPA/600/R-04/184.

Erdogan, E. H., Erpul, G., & Bayramin, İ. (2007). Use of USLE/GIS methodology for predicting soil loss in a semiarid agricultural watershed. *Environmental monitoring and assessment*, *131*(1), 153-161.

European Environment Agency. (2002). Toward an urban atlas: Assessment of spatial data on 25 European cities and urban areas. Copenhagen: Environmental Issue Rep. 30, EEA.

Exum, L. R., Bird, S. L., Harrison, J., & Perkins, C. A. (2005). *Estimating and projecting impervious cover in the southeastern United States*. Athens: Ecosystems Research Division, National Exposure Research Laboratory, U.S. EPA.

Ezra, P. (2006). *Variations in Land Values in Jos.* B.SC Dissertation, Department of Geography and Planning of Jos.

Fang, H., Sun, L., & Tang, Z. (2015). Effects of rainfall and slope on runoff, soil erosion and rill development: an experimental study using two loess soils. *Hydrological processes*, *29*(11), 2649-2658.

Fang, X., Thompson, D. B., Cleveland, T. G., Pradhan, P., & Malla, R. (2008). Time of concentration estimated using watershed parameters determined by automated and manual methods. *Journal of Irrigation and Drainage Engineering*, *134*(2), 202-211.

Fernandez, C., Wu, J. Q., McCool, D. K., & Stöckle, C. O. (2003). Estimating water erosion and sediment yield with GIS, RUSLE, and SEDD. *Journal of Soil and Water Conservation*, *58*(3), 128-136.

Ferro, V., & Porto, P. (2000). Sediment delivery distributed (SEDD) model. *Journal of hydrologic engineering*, *5*(4), 411-422.

Fistikoglu, O., & Harmancioglu, N. B. (2002). Integration of GIS with USLE in assessment of soil erosion. *Water Resources Management*, *16*(6), 447-467.

Flinker, P. (2010). The Need to Reduce Impervious Cover to Prevent Flooding and Protect Water Quality. *AICP Dodson Associates, LTD.*

Foster, G. R., & Wischmeier, W. (1974). Evaluating irregular slopes for soil loss prediction. *Transactions of the ASAE, 17*(2), 305-0309.

Foster, G. R., McCool, D. K., Renard, K. G., & Moldenhauer, W. C. (1981). Conversion of the universal soil loss equation to SI metric units. *Journal of Soil and Water Conservation*, *36*(6), 355-359.

Gabriel, S. A., Faria, J. A., & Moglen, G. E. (2006). A multiobjective optimization approach to smart growth in land development. *Socio-Economic Planning Sciences*, *40*(3), 212-248.

Gadgil, M., Daniels, R. R., Ganeshaiah, K. N., Prasad, S. N., Murthy, M. S. R., Jha, C. S., ... & Subramanian, K. A. (2011). Mapping ecologically sensitive, significant and salient areas of Western Ghats: proposed protocols and methodology. *Current Science*, *100*(2), 175-182.

Ganasri, B. P., & Ramesh, H. (2016). Assessment of soil erosion by RUSLE model using remote sensing and GIS-A case study of Nethravathi Basin. *Geoscience Frontiers*, *7*(6), 953-961.

Gangodagamage, C. (2001, November). Hydrological modeling using remote sensing and GIS. In *Paper presented at the 22nd Asian Conference on Remote Sensing* (Vol. 5, p. 9).

Gelagay, H. S., & Minale, A. S. (2016). Soil loss estimation using GIS and Remote sensing techniques: A case of Koga watershed, Northwestern Ethiopia. *International Soil and Water Conservation Research*, *4*(2), 126-136.

Gert, A., Wall, D. J., White, E.L. & Dunn, C.N. (1987). Regional rainfall intensity - duration-frequency curves for Pennsylvania. *Water Resources Bulletin*, 23(3), 479-486.

Gharabaghi, B., Rudra, R. P., & Goel, P. K. (2006). Effectiveness of vegetative filter strips in removal of sediments from overland flow. *Water Quality Research Journal of Canada*, *41*(3), 275-282.

Ghosh, S., & Guchhait, S. K. (2012). Soil loss estimation through USLE and MMF methods in the lateritic tracts of eastern plateau fringe of Rajmahal Traps, India. *Ethiopian Journal of Environmental Studies and Management*, *5*(4), 529-541.

GMDA (2006). Building By-Laws for Guwahati Metropolitan Area. Guwahati Metropolitan Development Authority, Guwahati.

GMDA. (2009). Master plan of Guwahati metropolitan area 2025. Guwahati Metropolitan Development Authority, Guwahati. http://www.gmda.co.in/master_plan.php as browsed on 28th October 2015.

Goetz, S. J., Jantz, C. A., & Sun, M. (2011). Forecasting future land use and its hydrologic implications: A case study of the Upper Delaware River watershed. *Watershed Science Bulletin*, *2*(2), 18-26.

Graham, P. H., Costello, L. S., & Mallon, H. J. (1974). Estimation of imperviousness and specific curb length for forecasting stormwater quality and quantity. *Journal (Water Pollution Control Federation)*, 717-725.

Guldmann, J. M. (1986). A structural framework for the design of integrated environmental and land-use planning optimization models. *Mathematical Modelling*, *7*(1), 61-81.

Gwenzi, W., & Nyamadzawo, G. (2014). Hydrological impacts of urbanization and urban roof water harvesting in water-limited catchments: a review. *Environmental Processes*, *1*(4), 573-593.

Haith, D. A., & Shoenaker, L. L. (1987). Generalized watershed loading functions for stream flow nutrients. *JAWRA Journal of the American Water Resources Association*, *23*(3), 471-478.

Han, W. S., & Burian, S. J. (2009). Determining effective impervious area for urban hydrologic modeling. *Journal of Hydrologic Engineering*, *14*(2), 111-120.

He, C. (2003). Integration of geographic information systems and simulation model for watershed management. *Environmental Modelling & Software*, *18*(8), 809-813.

Henderson, V. (2003). The urbanization process and economic growth: The so-what question. *Journal of Economic growth*, *8*(1), 47-71.

Ibrahim, M. B. (2009). Rainwater harvesting for urban areas: a success story from Gadarif city in central Sudan. *Water resources management*, *23*(13), 2727-2736.

Ichimura, M. (2003, January). Urbanization, urban environment and land use: challenges and opportunities. In Asia-Pacific Forum for Environment and Development, Expert Meeting 23 January 2003, Guilin, People's Republic of China.

Irvem, A., Topaloğlu, F., & Uygur, V. (2007). Estimating spatial distribution of soil loss over Seyhan River Basin in Turkey. Journal of Hydrology, 336(1), 30-37.

Jain, S. K., Singh, R. D., Jain, M. K., & Lohani, A. K. (2005). Delineation of flood-prone areas using remote sensing techniques. *Water Resources Management*, *19*(4), 333-347.

Jalee, L. A., & Farawn, M. A. (2014). Developing Rainfall Intensity-Duration-Freqency Relationship For Basrah City. *Kufa journal of Engineering*, *5*(1), 105-112.

Jayaraman, V., Chandrasekhar, M. G., & Rao, U. R. (1997). Managing the natural disasters from space technology inputs. *Acta Astronautica*, *40*(2), 291-325.

Jedwab, R., Christiaensen, L., & Gindelsky, M. (2015). Demography, urbanization and development: Rural push, urban pull and… urban push?. *Journal of Urban Economics*.

Ji, M., & Jensen, J. R. (1999). Effectiveness of subpixel analysis in detecting and quantifying urban imperviousness from Landsat Thematic Mapper imagery. *Geocarto International*, *14*(4), 33-41.

Jim, C. Y. (2004). Green-space preservation and allocation for sustainable greening of compact cities. *Cities*, *21*(4), 311-320.

Kang, I. S., Park, J. I., & Singh, V. P. (1998). Effect of urbanization on runoff characteristics of the On-Cheon Stream watershed in Pusan, Korea. *Hydrological Processes*, *12*(2), 351-363.

Kauffman, G. J., Belden, A. C., Vonck, K. J., & Homsey, A. R. (2009). Link between impervious cover and base flow in the White Clay Creek Wild and Scenic watershed in Delaware. *Journal of Hydrologic Engineering*, *14*(4), 324-334.

Kauffman, G. J., Belden, A. C., Vonck, K. J., & Homsey, A. R. (2009). Link between impervious cover and base flow in the White Clay Creek Wild and Scenic watershed in Delaware. *Journal of Hydrologic Engineering*, *14*(4), 324-334.

Klein, R. D. (1979). Urbanization and stream quality impairment. *JAWRA Journal of the American Water Resources Association*, *15*(4), 948-963.

Knisel, W. G. (1980). CREAMS: a field scale model for Chemicals, Runoff, and Erosion from Agricultural Management Systems [USA]. *United States. Dept. of Agriculture. Conservation research report (USA).*

Kok, N., Monkkonen, P., & Quigley, J. M. (2014). Land use regulations and the value of land and housing: An intra-metropolitan analysis. *Journal of Urban Economics*, *81*, 136-148.

Kolowe, P. (2014). The Determinants of Urban Land and Property Values: The Case of Rwanda. Master's Theses. 87. https://repository.usfca.edu/thes/87

Kosmas, C., Danalatos, N., Cammeraat, L. H., Chabart, M., Diamantopoulos, J., Farand, R., Gutierrez, L., Jacob, A., Marques, H., Martinez-Fernandez, J., & Mizara, A. (1997). The effect of land use on runoff and soil erosion rates under Mediterranean conditions. *Catena*, *29*(1), 45-59.

Kothyari, U. C. (1996). Erosion and sedimentation problems in India. *IAHS Publications-Series of Proceedings and Reports-Intern Assoc Hydrological Sciences*, *236*, 531-540.

Kothyari, U. C., & Garde, R. J. (1992). Rainfall intensity-duration-frequency formula for India. *Journal of Hydraulic Engineering*, *118*(2), 323-336.

Kuichling, E. (1889). The relation between the rainfall and the discharge of sewers in populous districts. *Transactions of the American Society of Civil Engineers*, *20*(1), 1-56.

Laenen, A. (1983). *Storm runoff as related to urbanization based on data collected in Salem and Portland, and generalized for the Willamette Valley, Oregon* (pp. 83-4143). Denver: US Geological Survey.

Lech-hab, K. B. H., Issa, L. K., Raissouni, A., El Arrim, A., Tribak, A. A., & Moussadek, R. (2015). Effects of Vegetation Cover and Land Use Changes on Soil

Erosion in Kalaya Watershed (North Western Morocco). *International Journal of Geosciences*, *6*(12), 1353.

Lee, J. G., & Heaney, J. P. (2003). Estimation of urban imperviousness and its impacts on storm water systems. *Journal of Water Resources Planning and Management*, *129*(5), 419-426.

Lee, L. (1979). Factors Affecting Land Use Change at the Urban-Rural Fringe. *Growth and Change*, *10*(4), 25-31.

Li, Z., Deng, X., Wu, F., & Hasan, S. S. (2015). Scenario analysis for water resources in response to land use change in the middle and upper reaches of the Heihe River Basin. *Sustainability*, *7*(3), 3086-3108.

Lim, K. J., Sagong, M., Engel, B. A., Tang, Z., Choi, J., & Kim, K. S. (2005). GIS-based sediment assessment tool. *Catena*, *64*(1), 61-80.

Liu, S., & Gu, G. (2017). Improving the Impervious Surface Estimation from Hyperspectral Images Using a Spectral-Spatial Feature Sparse Representation and Post-Processing Approach. *Remote Sensing*, *9*(5), 456.

Liu, Y., Lv, X., Qin, X., Guo, H., Yu, Y., Wang, J., & Mao, G. (2007). An integrated GIS-based analysis system for land-use management of lake areas in urban fringe. *Landscape and urban planning*, *82*(4), 233-246.

Liu, Y., Nie, L., Wang, F., & Nies, Z. (2015). The impact of tourism development on local residents in Bama, Guangxi, China. *Tourism Economics*, *21*(6), 1133-1148.

Long, H., Liu, Y., Hou, X., Li, T., & Li, Y. (2014). Effects of land use transitions due to rapid urbanization on ecosystem services: Implications for urban planning in the new developing area of China. *Habitat International*, *44*, 536-544.

Lu, L., Guo, H., & Martino, P. (2017). Remote Sensing of Urbanization Dynamics along the Belt and Road. *Bulletin of Chinese Academy of Sciences*, *32*(Z1), 74-81.

Martens, L. A. (1966). Flood inundation and effects of urbanization in metropolitan Charlotte [North Carolina]: US Geol. *Survey open-file rept*, *54*.

McCuen, R. H. (2005). *Hydrologic analysis and design*. 3rd Ed, Prentice-Hall, Englewood Cliffs, N.J.

McDonald, R. I., Forman, R. T., & Kareiva, P. (2010). Open space loss and land inequality in United States' cities, 1990–2000. *PLoS One*, *5*(3), e9509.

Megic, B. J., MacIntyre, D. F., Smith, D., Aikens, A. W., & Beatham, C. The Effects of Urbanization on Water Supply.

Mekonnen, M., Keesstra, S. D., Baartman, J. E., Ritsema, C. J., & Melesse, A. M. (2015). Evaluating sediment storage dams: structural off-site sediment trapping measures in Northwest Ethiopia. *Cuadernos de Investigación Geográfica*, *41*(1).

Melesse, A. M., & Shih, S. F. (2002). Spatially distributed storm runoff depth estimation using Landsat images and GIS. *Computers and Electronics in Agriculture*, *37*(1), 173-183.

Mensah, C. A. (2014). Urban green spaces in Africa: nature and challenges. *International Journal of Ecosystem*, *4*(1), 1-11.

Menzel, L., Koch, J., Onigkeit, J., & Schaldach, R. (2009). Modelling the effects of land-use and land-cover change on water availability in the Jordan River region. *Advances in Geosciences*, *21*, 73.

Merz, R., Blöschl, G., & Parajka, J. D. (2006). Regionalization methods in rainfall-runoff modelling using large catchment samples. *IAHS publication*, *307*, 117.

Miller, J. D., & Grebby, S. (2014). Mapping long-term temporal change in imperviousness using topographic maps. *International Journal of Applied Earth Observation and Geoinformation*, *30*, 9-20.

Minton, G. R. & Benedict, A. H. (1999). Treatment of Construction Site Stormwater." In *Proceeding of the 1999 International Water Resources Engineering Conference*, ASCE, Seattle, WA.

Mitasova, H., Mitas, L., Brown, W. M., & Johnston, D. M. (1999). Terrain modeling and soil erosion simulations for Fort Hood and Fort Polk test areas. *Geographic Modeling and Systems Laboratory, University of Illinois at Urbana-Champaign*.

Mohan, M., Pathan, S. K., Narendrareddy, K., Kandya, A., & Pandey, S. (2011). Dynamics of urbanization and its impact on land-use/land-cover: a case study of megacity Delhi. *Journal of Environmental Protection*, *2*(09), 1274.

Moore, I. D., & Burch, G. J. (1986). Physical basis of the length-slope factor in the Universal Soil Loss Equation. *Soil Science Society of America Journal*, *50*(5), 1294-1298.

Moore, I. D., & Wilson, J. P. (1992). Length-slope factors for the Revised Universal Soil Loss Equation: Simplified method of estimation. *Journal of soil and water conservation*, *47*(5), 423-428.

Moore, I. D., Grayson, R. B., & Ladson, A. R. (1991). Digital terrain modelling: a review of hydrological, geomorphological, and biological applications. *Hydrological processes*, *5*(1), 3-30.

Morgan, R. P. C. (2001). A simple approach to soil loss prediction: a revised Morgan–Morgan–Finney model. *Catena*, *44*(4), 305-322.

Morgan, R. P. C. (2009). *Soil erosion and conservation*. John Wiley & Sons.

Morgan, R. P. C., & Duzant, J. H. (2008). Modified MMF (Morgan–Morgan–Finney) model for evaluating effects of crops and vegetation cover on soil erosion. *Earth Surface Processes and Landforms*, *33*(1), 90-106.

Morgan, R. P. C., Morgan, D. D. V., & Finney, H. J. (1984). A predictive model for the assessment of soil erosion risk. *Journal of agricultural engineering research*, *30*, 245-253.

Morgan, R. P. C., Quinton, J. N., Smith, R. E., Govers, G., Poesen, J. W. A., Auerswald, K., ... & Styczen, M. E. (1998). The European Soil Erosion Model (EUROSEM): a dynamic approach for predicting sediment transport from fields and small catchments. *Earth surface processes and landforms*, *23*(6), 527-544.

Mosley, M. P. (1981). Delimitation of New Zealand hydrologic regions. *Journal of Hydrology*, *49*(1-2), 173-192.

Mundia, C. N., & Aniya, M. (2006). Dynamics of landuse/cover changes and degradation of Nairobi City, Kenya. *Land Degradation & Development*, *17*(1), 97-108.

Narayana, D. V., & Babu, R. (1983). Estimation of soil erosion in India. *Journal of Irrigation and Drainage Engineering*, *109*(4), 419-434.

Nearing, M. A., Ascough, L. D., & Chaves, H. M. L. (1989). WEPP model sensitivity analysis. *Water erosion prediction project landscape profi le model documentation. NSERL Report*, (2).

Nelson, E. J., & Booth, D. B. (2002). Sediment sources in an urbanizing, mixed land-use watershed. *Journal of Hydrology*, *264*(1), 51-68.

Ng, H. Y. F., & Marsalek, J. (1989). Simulation of the effects of urbanization on basin streamflow. *JAWRA Journal of the American Water Resources Association*, *25*(1), 117-124.

Nyamathi, S. J., & Arelt, A. (2013). Modelling of short duration rainfall IDF equation for Bangalore city. *Research and Reviews: Journal of Engineering and Technology*, 2(3), 80-86.

ODOT Highway Division. (2014). Hydraulics Design Manual: Appendix F- Rational Method. Oregon Department of Transportation, Geo-Environmental Section, 7-F-1–7-F-14. https://www.oregon.gov/ODOT/HWY/GEOENVIRONMENTAL/docs/Hydraulics/Hydraulics%20Manual/CHAPTER_07_appendix_F.pdf

Otis, T. (2012). Evaluating SLEUTH Model Accuracy at Different Geographic Scales Around National Parks.

Oueslati, W., Alvanides, S., & Garrod, G. (2015). Determinants of urban sprawl in European cities. *Urban Studies*, *52*(9), 1594-1614.

Pandey, A., Chowdary, V. M., & Mal, B. C. (2007). Identification of critical erosion prone areas in the small agricultural watershed using USLE, GIS and remote sensing. *Water resources management*, *21*(4), 729-746.

Pilgrim, D. H., & Cordery, I. (1993). Flood runoff. *Handbook of hydrology*, *9*, 1-42.

Piman, T., & Babel, M. S. (2012). Prediction of rainfall-runoff in an ungauged basin: Case study in the mountainous region of northern Thailand. *Journal of Hydrologic Engineering*, *18*(2), 285-296.

Post, D. A., Jones, J. A., & Grant, G. E. (1998). An improved methodology for predicting the daily hydrologic response of ungauged catchments. *Environmental modelling & software*, *13*(3), 395-403.

Preston, S. H. (1979). Urban growth in developing countries: A demographic reappraisal. *Population and Development Review*, 195-215.

Rahman, G., Alam, D., & Islam, S. (2008, September). City growth with urban sprawl and problems of management for sustainable urbanisation. In *International Society of City and Regional Planners (ISOCARP) Congress, Hague*.

Ramachandra, T. V., & Mujumdar, P. P. (2009). Urban floods: case study of Bangalore. *Disaster and Development*, *3*(2).

Ramlal, B., & Baban, S. M. (2008). Developing a GIS based integrated approach to flood management in Trinidad, West Indies. *Journal of environmental management*, *88*(4), 1131-1140.

Rasel, M. M. & Islam, M. M. (2015). Generation of rainfall intensity-duration-frequency relationship for North-Western region in Bangladesh. *IOSR Journal of Environmental Science, Toxicology and Food Technology*, 9(9), 41-47.

Rashid, M. M., Faruque, S. B., & Alam, J. B. (2012). Modelling of short duration rainfall intensity duration Frequency (SDRIDF) equation for Sylhet City in Bangladesh. *ARPN Journal of Science and Technology*, *2*(2), 92-95.

Regmi, R. R., & Saha, S. K. (2015). Impact assessment of land use land cover change on soil erosion status in Phewa Lake watershed of Nepal. *International Journal of Current Engineering and Technology*, *5*, 1708-1717.

Renard, K. G. (1997). Predicting soil erosion by water: a guide to conservation planning with the revised universal soil loss equation (RUSLE). *Agricultural Handbook 703,* USDA-ARS.

Renard, K. G., & Freimund, J. R. (1994). Using monthly precipitation data to estimate the R-factor in the revised USLE. *Journal of hydrology*, *157*(1-4), 287-306.

Renard, K. G., Foster, G. R., Weesies, G. A., & Porter, J. P. (1991). RUSLE: Revised universal soil loss equation. *Journal of soil and Water Conservation*, *46*(1), 30-33.

Riveira ,I. S. , Marcos ,B. M., Rafael, C.M. and David,M. B. (2008). Algorithm based on simulated annealing for land-use allocation. *Computers & Geosciences*, *34*(3), 259-268.

Sadeghi, S. H. R., Jalili, K., & Nikkami, D. (2009). Land use optimization in watershed scale. *Land Use Policy*, *26*(2), 186-193.

Sahoo, S. N., & Sreeja, P. (2011). Indirect Determination of Effective Impervious Area (EIA) of an Urban City of North East India. In *World Environmental and Water Resources Congress 2011: Bearing Knowledge for Sustainability* (pp. 742-750).

Sajjad, H., & Iqbal, M. (2012). Impact of urbanization on land use/land cover of Dudhganga watershed of Kashmir Valley, India. *International Journal of Urban Sciences*, *16*(3), 321-339.

San Diego County (2003). San Diego County Hydrology Manual. San Diego County Department of Public Works, Flood Control Section. http://www.sandiegocounty.gov/dpw/floodcontrol/floodcontrolpdf/hydro-hydrologymanual.pdf

Santillan, J. R., Makinanob, M. M., & Paringit, E. C. (2010). Integrating remote sensing, GIS and hydrologic models for predicting land cover change impacts on surface runoff and sediment yield in a critical watershed in Mindanao, Philippines. *Remote Sensing and Spatial Information Science*, *38*(8), 6.

Sarma, A. K., & Goswami, P. (2006). Developing intensity duration curve with limited rainfall data. *Predictions in ungauged basins for sustainable water resource planning and management. Jain Brothers, New Delhi*, 187-194.

Sarma, A. K., Chandramouli, V., Singh, B., Goswami, P., & Rajbongshi, N. (2005). Urban flood hazard mitigation of Guwahati city by silt monitoring and watershed modeling. Report submitted to ministry of human resources department (MHRD) by Department of Civil Engineering, IIT Guwahati.

Sarma, A.K., Giraud G. and Baishya, M.D. (2006). Rainwater Harvesting for Urban Flood Peak Reduction, My Green Earth. Journal of Society for Socio Economic Awareness and Environment Protection, 3(2), 14-21.

Sarma, B. (2011). Optimal ecological management practices for controlling sediment and water yield from a hilly urban system within sustainable limit (Doctoral dissertation), IIT Guwahati, India.

Sarma, B., Sarma, A. K., & Singh, V. P. (2013). Optimal ecological management practices (EMPs) for minimizing the impact of climate change and watershed degradation due to urbanization. *Water resources management*, *27*(11), 4069-4082.

Sarma, B., Sarma, A. K., Mahanta, C., & Singh, V. P. (2015). Optimal ecological management practices for controlling sediment yield and peak discharge from hilly urban areas. *Journal of Hydrologic Engineering*, *20*(10), 04015005.

Schueler, T. R., Kumble, P. A., & Heraty, M. A. (1992). *A current assessment of urban best management practices*. United States Environmental Protection Agency, Office of Wetlands, Oceans, and Watersheds, Assessment & Watershed Protection Division.

Shammaa, Y., & Zhu, D. Z. (2001). Techniques for controlling total suspended solids in stormwater runoff. *Canadian Water Resources Journal*, *26*(3), 359-375.

Shammaa, Y., Zhu, D. Z., Gyürék, L. L., & Labatiuk, C. W. (2002). Effectiveness of dry ponds for stormwater total suspended solids removal. *Canadian Journal of Civil Engineering*, *29*(2), 316-324.

Sharma, A., Tiwari, K. N., & Bhadoria, P. B. S. (2011). Effect of land use land cover change on soil erosion potential in an agricultural watershed. *Environmental Monitoring and Assessment*, *173*(1-4), 789-801.

Sharma, B., Tyagi, S., Singh, P., Dobhal, R., & Jaiswal, V. (2015). Application of remote sensing and gis in hydrological studies in india: an overview. *National Academy Science Letters*, *38*(1), 1-8.

Shiono, T., Haraguchi, N., Miyamoto, K., Shinogi, Y., Miyamoto, T., & Kameyama, K. (2008). Evaluation of strips of centipede grass for sediment load reduction. *Water Science and Technology*, *58*(12), 2347-2352.

Shuster, W. D., Bonta, J., Thurston, H., Warnemuende, E., & Smith, D. R. (2005). Impacts of impervious surface on watershed hydrology: A review. *Urban Water Journal*, *2*(4), 263-275.

Simanton, J. R., Osborn, H. B., & Renard, K. G. (1980, April). Application of the USLE to southwestern rangelands. In *Hydrology and Water Resources in Arizona and the Southwest*. Arizona-Nevada Academy of Science.

Singh, L. K., Jha, M. K., & Chowdary, V. M. (2017). Multi-criteria analysis and GIS modeling for identifying prospective water harvesting and artificial recharge sites for sustainable water supply. *Journal of Cleaner Production*, *142*, 1436-1456.

Singh, R., & Phadke, V. S. (2006). Assessing soil loss by water erosion in Jamni River Basin, Bundelkhand region, India, adopting universal soil loss equation using GIS. *Current Science*, 1431-1435.

Sleavin, W. J., Civco, D. L., Prisloe, S., & Giannotti, L. (2000, May). Measuring impervious surfaces for non-point source pollution modeling. In *Proceedings of the ASPRS 2000 Annual Convention* (pp. 22-26).

Smith, H. J. (1999). Application of empirical soil loss models in southern Africa: A review. *South African Journal of Plant and Soil*, *16*(3), 158-163.

Soil Conservation Service. (1986). Urban Hydrology for Small Watersheds. Technical Release 55, Washington, D.C.

Stankowski, S. J. (1972). Population density as an indirect indicator of urban and suburban land-surface modifications. *US Geological Survey Professional Paper*, *800*, 219-224.

Stewart, B. A., Woolhiser, D. A., Wischmeier, W. H., Caro, J. H., & Frere, M. H. (1975). Control of Water Pollution from Cropland, Volume 1--A Manual for Guideline Development.

Su, S., Ma, X., & Xiao, R. (2014). Agricultural landscape pattern changes in response to urbanization at ecoregional scale. *Ecological indicators*, *40*, 10-18.

Subramanya, K. (2011). *Engineering Hydrology, 3e*. Tata McGraw-Hill Education.

Sultana, M. S., Islam, G. T., & Islam, Z. (2009). Pre-and post-urban wetland area in Dhaka City, Bangladesh: a remote sensing and GIS analysis. *Journal of Water Resource and Protection*, *1*(06), 414.

Sutherland, R. C. (1995). Methodology for estimating the effective impervious area of urban watersheds. *Watershed Protection Techniques*, *2*(1), 282-284.

Syahli, F. (2015). *The Impact of Land Use Change on Soil Erosion in Serayu Watershed*. University of Twente Faculty of Geo-Information and Earth Observation (ITC).

Taebi, A., & Droste, R. L. (2004). Pollution loads in urban runoff and sanitary wastewater. *Science of the total Environment*, *327*(1), 175-184.

Tan, P. Y., Wang, J., & Sia, A. (2013). Perspectives on five decades of the urban greening of Singapore. *Cities*, *32*, 24-32.

Theobald, D. M. (2005). Landscape patterns of exurban growth in the USA from 1980 to 2020. Ecology and Society, 10(1), 32. https://www.ecologyandsociety.org/vol10/iss1/art32/.

Theobald, D. M., Goetz, S. J., Norman, J. B., & Jantz, P. (2009). Watersheds at risk to increased impervious surface cover in the conterminous United States. *Journal of Hydrologic Engineering*, *14*(4), 362-368.

Thompson, D. B. (2006). The Rational Method. *David B. Thompson Civil Engineering Department Texas Tech University. pp*, 1-7.

Topcu, M., & Kubat, A. S. (2009, June). The analysis of urban features that affect land values in residential areas. In *Proceedings of the 7th International Space Syntax Symposium, Stockholm, Sweden* (pp. 8-11).

Tyagi, J. V., Mishra, S. K., Singh, R., & Singh, V. P. (2008). SCS-CN based time-distributed sediment yield model. *Journal of hydrology*, *352*(3), 388-403.

UNDESA/PD. (2012). *World urbanization prospects, the 2011 revision.* Final Report with Annex Tables. New York, NY: United Nations Department of Economic and Social Affairs.

UNDESA/PD. (2014). *World urbanization prospects: The 2014 revision, highlights (ST/ESA/SER. A/352).* Department of Economic and Social Affairs. Population Division, New York: United Nations.

United Nations. (2001). *The components of urban growth in developing countries (ESA/P/WP.169).* Newyork, United Nations.

United Nations. (2013b). *World economic and social survey: sustainable development challenges (E/2013/50/Rev. 1 ST/ESA/344).* UNDESA, Newyork.

United States Water Resources Council. (1981). *Guidelines for determining flood flow frequency*. Bulletin No. 17B, Washington, DC.

Vandewiele, G. L., & Elias, A. (1995). Monthly water balance of ungauged catchments obtained by geographical regionalization. *Journal of hydrology*, *170*(1-4), 277-291.

Varma, C. V. J., Saxena, K. R., & Rao, M. K. (1989). *River behaviour management and training.* Central Board of Irrigation and Power, New Delhi, India.

Veldkamp, A., & Fresco, L. O. (1996). CLUE: a conceptual model to study the conversion of land use and its effects. *Ecological modelling*, *85*(2-3), 253-270.

Verburg, P. H., Soepboer, W., Veldkamp, A., Limpiada, R., Espaldon, V., & Mastura, S. S. (2002). Modeling the spatial dynamics of regional land use: the CLUE-S model. *Environmental management*, *30*(3), 391-405.

Wagner, P. D., Kumar, S., & Schneider, K. (2013). An assessment of land use change impacts on the water resources of the Mula and Mutha Rivers catchment upstream of Pune, India. *Hydrology and Earth System Sciences*, *17*(6), 2233-2246.

Wang, X., Yu, S., & Huang, G. H. (2004). Land allocation based on integrated GIS-optimization modeling at a watershed level. *Landscape and Urban Planning*, *66*(2), 61-74.

Weesies, G. A. (1998). K factor. Soil erodibility. Guidelines for the use of the Revised Universal Soil Loss Equation (RUSLE), version, 1.

Weng, Q. (2012). Remote sensing of impervious surfaces in the urban areas: Requirements, methods, and trends. *Remote Sensing of Environment*, *117*, 34-49.

Weng, Y. C. (2007). Spatiotemporal changes of landscape pattern in response to urbanization. *Landscape and urban planning*, *81*(4), 341-353.

Wenger, S. (1999). A review of the scientific literature on riparian buffer width, extent and vegetation.

Williams, G. B. (1922). Flood discharges and the dimensions of spillways in India. *Engineering (London)*, *134*(9), 321-322.

Williams, J. R. (1975). Sediment routing for agricultural watersheds. *JAWRA Journal of the American Water Resources Association*, *11*(5), 965-974.

Williams, J. R., Jones, C. A., & Dyke, P. T. (1984, March). The EPIC model and its application. In *Proc. Int. Symp. on minimum data sets for agrotechnology transfer* (pp. 111-121).

Winchell, M., Srinivasan, R., Di Luzio, M., & Arnold, J. (2010). ArcSWAT interface for SWAT 2009. *User's guide*, 1-490.

Wischmeier, W. H., & Smith, D. D. (1961). A universal equation for predicting rainfall erosion losses–An aid to conservation farming in humid regions. *US Dept. of Agric., Agr. Res. Serv. ARS Special Report*, 22-66.

Wischmeier, W. H., & Smith, D. D. (1978). Predicting rainfall erosion losses-a guide to conservation planning. *U.S. Department of Agriculture Handbook No.537.*

Wischmeier, W. H., Johnson, C. B. & Cross, B. V. (1971). A soil erodibility nomograph for farmland and construction sites. *Journal of Soil and Water Conservation*, 26, 189-192.

Young, R. A., Onstad, C. A., Bosch, D. D., & Anderson, W. P. (1989). AGNPS: A nonpoint-source pollution model for evaluating agricultural watersheds. *Journal of soil and water conservation*, *44*(2), 168-173.

Yu, P. S., & Cheng, C. J. (1998). Incorporating uncertainty analysis into a regional IDF formula. *Hydrological processes*, *12*(5), 713-726.

Yuksel, A., Akay, A. E., Reis, M., & Gundogan, R. (2007, March). Using the WEPP model to predict sediment yield in a sample watershed in Kahramanmaras region. In *International Congress River Basin Management* (Vol. 2, pp. 11-22).

Xu, H. Q., Wang, X. Q., & Xiao, G. R. (2000). A remote sensing and GIS integrated study on urbanization with its impact on arable lands: Fuqing City, Fujian Province, China. *Land Degradation & Development*, *11*(4), 301-314.

Zhang, Y., Degroote, J., Wolter, C., & Sugumaran, R. (2009). Integration of Modified Universal Soil Loss Equation (MUSLE) into a GIS framework to assess soil erosion risk. *Land Degradation & Development*, *20*(1), 84-91.

Zhou, Y., Wang, Y., Gold, A. J., August, P. V., & Boving, T. B. (2014). Assessing impact of urban impervious surface on watershed hydrology using distributed object-oriented simulation and spatial regression. *GeoJournal*, *79*(2), 155-166.

List of Publications

Journal publications:

1. **Patowary, S.** and Sarma, A. K. (2018). "Model-based analysis of urban settlement process in eco-sensitive area of developing country: a study with special reference to hills of an Indian city". *Environment, Development and Sustainability*, Springer, *20*(4), 1777-1795. DOI 10.1007/s10668-017-9965-1

2. **Patowary, S.** and Sarma, A. K. (2018) "GIS-based estimation of soil loss from hilly urban area incorporating hill cut factor into RUSLE". *Water Resources Management*, Springer, *32*(10), 3535–3547. DOI 10.1007/s11269-018-2006-5

3. **Patowary, S.** and Sarma, A. K. "Projection of urban settlement in eco-sensitive hilly areas and its impact on peak runoff". *Environment, Development and Sustainability*, Springer (under review).

4. **Patowary, S.** and Sarma, A. K. "A revision of OPTEMP-LS model for selecting optimal EMP combination for minimizing sediment and water yield from hilly urban watersheds." *Water Resources Management*, Springer (under review).

Conference publications:

1. **Patowary, S.** and Sarma, A. K. "Safe IDF Curves From Daily Rainfall Data For Guwahati City". *Proceedings of National Conference on Water Resources and Flood Management with Special Reference to Flood Modelling*, 14th-15th Oct, 2016, Gujarat, India.

2. **Patowary, S.**, Hazarika J. & Sarma A. K. "Potential Impact of Climate Change on Rainfall Intensity-Duration-Frequency Curves of Guwahati city". *Proceedings of CESDOC-2016, 1st International Conference on Civil Engineering for Sustainable Development-Opportunities and Challenges*, 19th-21st Dec, 2016, AEC, Guwahati, India.

3. Sarma A.K, Sarma B., Hazarika J., **Patowary S.** "Ecological Management Practices: A Participatory Approach for Sustainable Urban Development". *The Thirteenth International Conference on Technology, Knowledge and Society*, 26-28th May, 2017, University of Toronto, Canada.

4. **Patowary, S.**, Hazarika J. & Sarma A. K. "Potential Impact of Climate Change on Rainfall Extremes for Urban Drainage Management". *Proceedings of Urbanization Challenges in Emerging Economies (Moving Towards Resilient Sustainable Cities and Infrastructure)*, ASCE, 12th – 14th Dec, 2017, New Delhi, India.

5. **Patowary, S.**, Das, T. & Sarma A. K. "Effect Of Urban Settlement on Soil Loss From Hilly Urban Watershed". *Proceedings of 22^{nd} International Conference on Hydraulics, Water Resources and Coastal Engineering*, Hydro 2017, 21^{st} - 23^{rd} Dec, 2017, Gujarat, India.

6. **Patowary, S.** and Sarma, A. K. "A study of soil loss behaviour of hilly urban watershed of Guwahati city for various surface cover scenarios of steep hill cuts". (Abstract submitted to *2nd International Conference on Civil Engineering for Sustainable Development-Opportunities and Challenges*, to be held on 18^{th}-19^{th} Dec, 2018, AEC, Guwahati, India.)